

**Effect of modulation of auxin response on clubroot development caused by
Plasmodiophora brassicae in Arabidopsis**

by

Shengjuan Li

A thesis submitted in partial fulfillment of the requirements for the degree of

Master of Science

in

Plant Science

Department of Agricultural, Food and Nutritional Science

University of Alberta

© Shengjuan Li, 2024

Abstract

Clubroot disease caused by the obligate biotrophic protist *Plasmodiophora brassicae*, is a serious soilborne disease in Brassicaceae species including cruciferous crops such as canola and the genetic model species *Arabidopsis*. This disease, identified by the formation of sizable root galls, is accompanied by alterations in the plant's source-sink relations and hormonal balance, leading to stunting of above-ground growth and reduction in yields in crop plants. The plant hormone auxin is believed to be among the hormones utilized by the clubroot pathogen in gall development; therefore, it may be possible to suppress gall development due to *P. brassicae* by modulating auxin signaling in the plant host. In this study, *Arabidopsis* auxin receptor double mutant (*tir1afb2*) and quadruple mutant (*tir1afb245*) lines were assessed for their ability to suppress clubroot disease progression. The WT line displayed the most significant disease symptoms when inoculated with *P. brassicae* [Disease Index (DI) = 90.3 %], with the auxin receptor mutants exhibiting less severe disease symptoms [*tir1afb2*, DI = 67.7 %; *tir1afb245*, DI = 45.0 % at 32 days after inoculation (DAI)]. Less severe clubroot disease symptoms were also observed in all three separately generated *tir1afb2* double mutant lines compared to the WT line, further confirming a reduction in clubroot progression in the *tir1afb2* lines. Additional confirmation that reduced auxin response was associated with reduced clubroot disease progression was obtained by measuring the fresh weights of the root-shoot transition region among the lines tested. Root-shoot transition region fresh weights were less (reduced galling) in the auxin receptor mutant lines than the WT line.

The transcript abundance of auxin-response gene expression markers, *AtARF3*, *AtARF19*, *AtGH3.3* and *AtGH3.17*, decreased with loss of auxin response (WT > *tir1afb2C* ≥ *tir1afb245*) at 21 DAI, confirming reduced auxin signaling in the auxin receptor mutant lines when inoculated

with *P. brassicae*. The transcript abundance of *AtPR5*, a defense gene marker, was higher in the *tir1afb2C* and *tir1afb245* lines compared to their non-inoculated controls at 21 DAI with *P. brassicae*, but not in the WT line, suggesting that plant defense genes are stimulated in the auxin receptor mutant lines when challenged with *P. brassicae* infection.

Another possible approach to modify auxin response in the root is to transform Arabidopsis with an auxin receptor that does not naturally occur in this species. Using this approach, auxin receptor mutants expressing *PsAFB6*, which codes for a pea (*Pisum sativum*) auxin receptor that does not occur in Brassicaceae species including Arabidopsis, were also assessed for their ability to suppress clubroot disease progression. When *PsAFB6* was expressed in auxin receptor *tir1afb2* and *tir1afb245* mutant backgrounds, there was a trend to reduce *P. brassicae*-induced disease development. In clubroot inoculated plants, expression of *PsAFB6* in the *tir1afb2* auxin receptor mutant background decreased the transcript abundance of the *Aux/IAA* genes (*AtIAA9*, *AtIAA16*, and *AtIAA19*), *ARF* genes (*AtARF3*, *AtARF5*, and *AtARF19*), and *GH3* genes (*AtGH3.3* and *AtGH3.17*) (Figure 3.21), suggesting that expression of *PsAFB6* reduced auxin response in this line, consistent with results of the auxin-inhibition root growth assays. In summary, reduction in auxin response reduced the progression of clubroot symptoms in Arabidopsis, supporting the hypothesis that auxin is utilized by the clubroot pathogen in gall development.

Preface

All the experiments in this thesis were conceptualized and designed by Dr. Jocelyn Ozga. I grew plants for all experiments, prepared experimental designs for implementation, prepared and quantified clubroot spore suspensions, performed all clubroot inoculations for experiments, part of team in harvesting all tissues for experiments with Drs. Bin Shan and Harleen Kaur, created and characterized the two new auxin receptor mutant lines, performed the auxin-inhibition root growth assays, performed the ANOVA analyses, and prepared the figures in OriginLab software. Dr. Harleen Kaur created the phylogenetic tree and helped me in refining the experimental design, harvesting of root tissues, and techniques for creating and characterizing the double mutant lines, performing auxin-inhibition root growth assays, standardising the method for quantifying clubroot disease ratings, preparing the figures in Originlab software and performing statistics using the R program. For qRT-PCR assays, total RNA extractions and designing of Taq-Man primers and probes were performed by Dr. Harleen Kaur, and qRT-PCR assays were performed by me (*PsAFB6* and *AtARF19*) and the assays for the remaining genes were performed by Dr. Harleen Kaur. Data analyses were completed with the help of Drs. Harleen Kaur and Jocelyn Ozga and data interpretation by Dr. Jocelyn Ozga.

Acknowledgements

I would like to express my deepest gratitude to my supervisor, Dr. Jocelyn Ozga, for giving me the opportunity to do my MSc study with her. Her unwavering support, invaluable guidance, and insightful feedback throughout the entire research process played a crucial role in shaping the direction and quality of this thesis. Her encouragement and support also helped me go through COVID time and complete my studies successfully. I am also indebted to the members of my thesis committee, Dr. Guanqun (Gavin) Chen and Dr. Charitha P. A. Jayasinghe, for their constructive criticism and valuable suggestions that significantly contributed to the refinement of this work. They also gave me valuable suggestions and helps before I went to Canada to pursue my MSc degree.

I would like to give my special thanks to the lab members in Dr. Ozga/Reinecke's lab. I thank Dr. Harleen Kuar for helping me in each experiment. Her generosity and willingness to offer me hand-by-hand guidance significantly contributed to the success of each experiment. Her expertise, patience, and encouragement were invaluable throughout this research journey. I am sincerely grateful for her unwavering support and help in my research and also in my daily life. I thank Dr. Bin Shan for her help with my experiments and daily life. Those days working with her became the most unforgettable and precious days in my three-year study life. I thank Hui (David) Liu for his advice on experiments and studies. The engaging discussions he provided, especially during the challenging phases of this research continuously kept me motivated. The days when we were teaching assistants together were also a wonderful memory. I also want to express my appreciation to Duncan Giebelhaus for his coffee chats and for sharing the experience of studying the RENR statistics class.

Furthermore, I extend my gratitude to the University of Alberta's staff from various groups for their unwavering support during my MSc program. Special thanks go to Ms. Kelley Dunfield, Shay Missiaen, and Dr. Andrea Botero, the Plant Growth Facility Lead/Assist, for their excellent management of essential equipment crucial to my experiments. Additionally, I appreciate the collective efforts of the staff in the Department of Agricultural, Food & Nutritional Science and the Faculty of Graduate Studies and Research. Their contributions, from organizing workshops to sharing scientific knowledge, have been integral to my academic journey, providing comprehensive support in all aspects.

Last but not least, I am thankful to my family and friends for their understanding, patience, and unwavering belief in my abilities. Your love and support have been my anchor throughout this academic endeavor. My parents (Li Li & Guijie Sun) and my sister (Qi Li), whose endless patience, understanding, and words of encouragement have been a guiding light, propelling me forward during moments of doubt. Your belief in the importance of education has been a guiding light, and I am truly fortunate to have you as my parents. I thank Qinqin Zhou for sharing her experience, offering a listening ear, and giving me advice whenever I feel anxious about my studies and the future. I also thank my amazing roommates, Xiaoyu Wang and Yiyang Wu. Thank you for being not just roommates but friends and supporters. Your willingness to share the ups and downs, late-night discussions, and occasional shared meals brought comfort during stressful times. Finally, I want to thank all my friends in China who talked to me regardless of the time and were willing to help no matter how busy they were.

Table of Contents

List of Tables.....	X
List of Figures.....	XV
List of Abbreviations.....	XX
Chapter 1: Literature review.....	1
1.1 CLUBROOT DISEASE IN BRASSICA	1
1.1.1 <i>P. brassicae</i> life cycle.....	1
1.1.2 <i>P. brassicae</i> host range.....	3
1.1.3 <i>P. brassicae</i> host symptoms	4
1.1.4 <i>P. brassicae</i> disease management	4
1.1.4.1 <i>Cultural strategy</i>	4
1.1.4.2 <i>Biological control</i>	5
1.1.4.3 <i>Chemical control</i>	5
1.1.4.4 <i>Genetic resistance</i>	6
1.2 AUXIN IN PLANT-PATHOGEN INTERACTION	7
1.3 AUXIN SIGNALING PROCESS IN PLANTS	11
1.3.1 <i>TIR1/AFB</i> auxin receptor gene family.....	13
1.3.2 <i>Aux/IAA</i> transcriptional repressor gene family.....	14
1.3.3 <i>ARF</i> transcription factor gene family	16
1.3.4 Gretchen Hagen3 (GH3) protein family.....	19
1.4 ROLES OF AUXIN RESPONSE DURING CLUBROOT DEVELOPMENT	20
1.4.1 <i>TIR1/AFB</i> family genes	20
1.4.2 <i>Aux/IAA</i> family genes	21
1.4.3 <i>ARF</i> family genes	22
1.4.4 Gretchen Hagen3 (GH3) protein family.....	23
1.5 ROLES OF SALICYLIC ACID (SA) AND JASMONIC ACID (JA) RESPONSE DURING CLUBROOT DEVELOPMENT	24
1.6 HYPOTHESIS TO BE TESTED	28
1.7 RESEARCH OBJECTIVES	28
Chapter 2: Effect of pea <i>PsAFB6</i> auxin receptor on auxin-induced root inhibition in <i>PsAFB6</i>-transformed <i>Arabidopsis</i> auxin receptor mutant lines	30
2.1 INTRODUCTION.....	30
2.2 MATERIALS AND METHODS	32
2.2.1 Plant materials	32
2.2.2 <i>Arabidopsis</i> root growth assays.....	33
2.2.3 RNA extraction and Taqman qRT-PCR assays.....	36
2.2.4 Statistical analyses.....	40
2.3 RESULTS.....	41
2.3.1 <i>PsAFB6</i> quantification using qRT-PCR assays in roots and shoots of <i>Arabidopsis</i> transgenic lines used for root growth assays	41
2.3.2 <i>PsAFB6</i> expression reduced the auxin response in <i>Arabidopsis</i> root growth assays...	43
2.4 DISCUSSION	47

2.4.1 <i>PsAFB6</i> is expressed in the roots and shoots of Arabidopsis transgenic lines.....	47
2.4.2 The <i>PsAFB6</i> auxin receptor does not complement <i>AtTIR1</i> or <i>AtAFB2</i> in Arabidopsis auxin root growth assays	47
2.4.3 The <i>PsAFB6</i> auxin receptor does not complement <i>AtTIR1/AtAFB2</i> effects on lateral root density in Arabidopsis roots.....	49

Chapter 3: The effect of auxin receptor modification on clubroot development in

Arabidopsis.....	50
3.1 INTRODUCTION.....	50
3.2 MATERIALS AND METHODS	56
3.2.1 Plant material.....	56
3.2.2 Creation of additional non-transgenic Arabidopsis <i>tir1-10 afb2-3</i> double mutant lines	56
3.2.3 Peat-based medium growth system for performing clubroot-inoculation assays with Arabidopsis auxin receptor mutants and mutants-expressing <i>PsAFB6</i>	60
3.2.3.1 <i>Seed germination</i>	60
3.2.3.2 <i>Pathogen material and inoculum preparation</i>	61
3.2.3.3 <i>Clubroot Inoculations</i>	61
3.2.3.4 <i>Digitized clubroot disease rating</i>	62
3.2.3.5 <i>Root-shoot transition region fresh weight analysis in Arabidopsis plants</i>	63
3.2.4 RNA extraction and Taqman qRT-PCR assays.....	64
3.2.5 Statistical analyses.....	66
3.3 RESULTS.....	68
3.3.1 Two new lines of auxin receptor double mutants were generated when <i>tir1-10</i> was the female parent	68
3.3.2 <i>PsAFB6</i> quantification using qRT-PCR assays in roots of clubroot-inoculated and non-inoculated Arabidopsis transgenic lines.....	69
3.3.3 Clubroot disease index calculation indicates reducing auxin response reduces disease progression.....	71
3.3.4 Frequency distribution of disease severity in clubroot-inoculated Arabidopsis lines ..	75
3.3.5 Average fresh weights of the root-shoot transition region are consistent with the DI ratings in response to <i>P. brassicae</i> inoculation	80
3.3.6 qRT-PCR quantification of hormone-related genes in the clubroot-inoculated and non-inoculated roots of transgenic lines at 21 DAI	83
3.4 DISCUSSION	93
3.4.1 Reduction in auxin signaling reduced <i>P. brassicae</i> -induced disease development in Arabidopsis.....	93
3.4.2 <i>PsAFB6</i> expression in auxin receptor <i>tir1afb2</i> and <i>tir1afb245</i> mutant backgrounds lead to a trend to reduce <i>P. brassicae</i> -induced disease development.....	94
3.4.3 Plant hormone-related gene expression in Arabidopsis roots of <i>tir1afb2</i> and <i>tir1afb245</i> lines in response to clubroot pathogen inoculation at 21 DAI	95
3.4.4 Plant hormone-related gene expression in Arabidopsis roots of WT, <i>tir1afb2</i> and <i>tir1afb245</i> lines in response to clubroot pathogen inoculation at 21 DAI.....	99
3.4.5 Effect of reduced auxin response on plant hormone-related gene expression in Arabidopsis roots in clubroot-inoculated lines at 21 DAI.....	102

3.4.6 Plant hormone-related gene expression in Arabidopsis roots of non-inoculated and clubroot-inoculated <i>PsAFB6</i> -expressing <i>tir1afb2</i> and <i>tir1afb245</i> lines harvested at the 21 DAI time point.....	104
3.5 CONCLUSION.....	107
Chapter 4: General conclusions and future perspectives.....	108
4.1 GENERAL CONCLUSIONS.....	108
4.2 FUTURE PERSPECTIVES.....	109
References.....	111
APPENDIX A.....	130
APPENDIX B.....	140

List of Tables

Tables	Page
2.1	Taqman primers and probes used for quantification of gene expression in root and shoot tissues of seedlings from the root growth assays by qRT-PCR and their PCR efficiencies and r^2 values.....40
3.1	Taqman primers and probes used for quantification of gene expression by qRT-PCR assays in root tissues of non-inoculated control and 21d- <i>P. brassicae</i> -inoculated Arabidopsis Columbia wild-type (WT), auxin receptor <i>tir1afb2C</i> double and <i>tir1afb245</i> quadruple mutant lines, and mutant lines expressing <i>PsAFB6</i> (<i>PsAFB6/+ 4-8 tir1afb2</i> and <i>PsAFB6/+ 3-2 tir1afb245</i>), and their PCR efficiencies and r^2 values.....65
A1	The probability, degrees of freedom and F values for the relative transcript abundance of <i>PsAFB6</i> in the shoot tissues of ten-day-old seedlings of the Arabidopsis <i>PsAFB6</i> -expressing lines (<i>PsAFB6/+ 4-8 tir1afb2</i> vs. <i>PsAFB6/+ 3-3 tir1afb2</i> vs. <i>PsAFB6/+ 1-6 tir1afb245</i> vs. <i>PsAFB6/+ 3-2 tir1afb245</i> vs. <i>PsAFB6/+ 5-9 tir1afb245</i>) in one-way ANOVA analysis followed by mean separation using LSD post-hoc test performed on data presented in Figure 2.1 and Appendix Figure A3.....136
A2	The probability, degrees of freedom and F values on the lateral root density for treatments (Control vs. 2,4-D), lines (WT vs. <i>tir1afb2</i> vs. <i>tir1afb245</i>) and treatments x lines interaction in two-way ANOVA analysis followed by mean separation using LSD post-hoc test performed on data presented in Figure 2.3A.....137
A3	The probability, degrees of freedom and F values on the lateral root density for treatments (Control vs. 2,4-D), lines (WT vs. <i>tir1afb2</i> vs. <i>PsAFB6/+ 4-8 tir1afb2</i> vs. <i>PsAFB6/+ 3-3 tir1afb2</i>) and treatments x lines interaction in two-way ANOVA analysis followed by mean separation using LSD post-hoc test performed on data presented in Figure 2.3B.....138
A4	The probability, degrees of freedom and F values on the lateral root density for treatments (Control vs. 2,4-D), lines (<i>tir1afb245</i> vs. <i>PsAFB6/+ 1-6 tir1afb245</i> vs. <i>PsAFB6/+ 3-2 tir1afb245</i> vs. <i>PsAFB6/+ 5-9 tir1afb245</i>) and treatments x lines interaction in two-way ANOVA analysis followed by mean separation using LSD post-hoc test performed on data presented in Figure 2.3C.....139

B1	Primers used for PCR verification of auxin receptor <i>tir1-10</i> and <i>afb2-3</i> T-DNA insertions in Arabidopsis homozygous <i>tir1afb2</i> double mutant lines.....	162
B2	The probability (P), degrees of freedom and F values for the relative transcript abundance of <i>PsAFB6</i> for comparisons among treatments (non-inoculated and clubroot-inoculated) and lines (<i>PsAFB6/+ 4-8 tir1afb2</i> , and <i>PsAFB6/+ 3-2 tir1afb245</i>), and the treatment x line interaction in the root tissue of 21 DAI seedlings using a two-way ANOVA analysis followed by mean separation using LSD post-hoc test (data presented in Figure 3.4)...	163
B3	The probability (P), degrees of freedom and F values for clubroot disease index (DI) at 32 DAI for comparisons among lines (Set 1: WT, <i>tir1afb2C</i> , <i>tir1afb245</i> , <i>PsAFB6/+ 1-6 tir1afb245</i> , <i>PsAFB6/+ 3-2 tir1afb245</i> , and <i>PsAFB6/+ 5-9 tir1afb245</i>) using a one-way ANOVA analysis followed by mean separation using LSD post-hoc test (data presented in Figure 3.5A).....	164
B4	The probability (P), degrees of freedom and F values for clubroot disease index (DI) at 32 DAI for comparisons among lines (Set 2: WT, <i>tir1afb2C</i> , <i>tir1afb2A2</i> , and <i>tir1afb2D1</i>) using a one-way ANOVA analysis followed by mean separation using LSD post-hoc test (data presented in Figure 3.5B).....	165
B5	The probability (P), degrees of freedom and F values for clubroot disease index (DI) at 32 DAI for comparisons among lines (Set 3: WT, <i>tir1afb2C</i> , <i>PsAFB6/+ 4-8 tir1afb2</i> , and <i>PsAFB6/+ 3-3 tir1afb2</i>) using a one-way ANOVA analysis followed by mean separation using LSD post-hoc test (data presented in Figure 3.5C).....	166
B6	The probability (P), degrees of freedom and F values on the average fresh weight of the root-shoot transition region at 32 DAI for comparisons among treatments (non-inoculated and clubroot-inoculated) and lines (Set 1: WT, <i>tir1afb2C</i> , <i>tir1afb245</i> , <i>PsAFB6/+ 1-6 tir1afb245</i> , <i>PsAFB6/+ 3-2 tir1afb245</i> , and <i>PsAFB6/+ 5-9 tir1afb245</i>) and the treatment x line interaction using a two-way ANOVA analysis followed by mean separation using LSD post-hoc test (data presented in Figure 3. 12A).....	167
B7	The probability (P), degrees of freedom and F values on the average fresh weight of the root-shoot transition region at 32 DAI for comparisons among treatments (non-inoculated and clubroot-inoculated) and lines (Set 2: WT, <i>tir1afb2C</i> , <i>tir1afb2A2</i> , and <i>tir1afb2D1</i>), and the treatment x line interaction using a two-way ANOVA analysis followed by mean separation using LSD post-hoc test (data presented in Figure 3.12B).....	168

B8	The probability (P), degrees of freedom and F values on the average fresh weight of the root-shoot transition region at 32 DAI for comparisons among treatments (non-inoculated and clubroot-inoculated) and lines (WT, <i>tir1afb2C</i> , <i>PsAFB6/+ 4-8 tir1afb2</i> , and <i>PsAFB6/+ 3-3 tir1afb2</i>), and the treatment x line interaction using a two-way ANOVA analysis followed by mean separation using LSD post-hoc test (data presented in Figure 3.12C).....	169
B9	The probability (P), degrees of freedom and F values for the relative transcript abundance of <i>AtIAA9</i> in the root tissue of 21 DAI seedlings for comparisons among treatments (non-inoculated and clubroot-inoculated) and lines (WT, <i>tir1afb2C</i> , <i>tir1afb245</i> , <i>PsAFB6/+ 4-8 tir1afb2</i> , and <i>PsAFB6/+ 3-2 tir1afb245</i>), and the treatment x line interaction using a two-way ANOVA analysis followed by mean separation using LSD post-hoc test (data presented in Figure 3.13A).....	170
B10	The probability (P), degrees of freedom and F values for the relative transcript abundance of <i>AtIAA16</i> in the root tissue of 21 DAI seedlings for comparisons among treatments (non-inoculated and clubroot-inoculated) and lines (WT, <i>tir1afb2C</i> , <i>tir1afb245</i> , <i>PsAFB6/+ 4-8 tir1afb2</i> , and <i>PsAFB6/+ 3-2 tir1afb245</i>), and the treatment x line interaction using a two-way ANOVA analysis followed by mean separation using LSD post-hoc test (data presented in Figure 3.13B).....	171
B11	The probability (P), degrees of freedom and F values for the relative transcript abundance of <i>AtIAA19</i> in the root tissue of 21 DAI seedlings for comparisons among treatments (non-inoculated and clubroot-inoculated) and lines (WT, <i>tir1afb2C</i> , <i>tir1afb245</i> , <i>PsAFB6/+ 4-8 tir1afb2</i> , and <i>PsAFB6/+ 3-2 tir1afb245</i>), and the treatment x line interaction using a two-way ANOVA analysis followed by mean separation using LSD post-hoc test (data presented in Figure 3.13C).....	172
B12	The probability (P), degrees of freedom and F values for the relative transcript abundance of <i>AtARF3</i> in the root tissue of 21 DAI seedlings for comparisons among treatments (non-inoculated and clubroot-inoculated) and lines (WT, <i>tir1afb2C</i> , <i>tir1afb245</i> , <i>PsAFB6/+ 4-8 tir1afb2</i> , and <i>PsAFB6/+ 3-2 tir1afb245</i>), and the treatment x line interaction using a two-way ANOVA analysis followed by mean separation using LSD post-hoc test (data presented in Figure 3.14A).....	173

B13	The probability (P), degrees of freedom and F values for the relative transcript abundance of <i>AtARF5</i> in the root tissue of 21 DAI seedlings for comparisons among treatments (non-inoculated and clubroot-inoculated) and lines (WT, <i>tir1afb2C</i> , <i>tir1afb245</i> , <i>PsAFB6/+ 4-8 tir1afb2</i> , and <i>PsAFB6/+ 3-2 tir1afb245</i>), and the treatment x line interaction using a two-way ANOVA analysis followed by mean separation using LSD post-hoc test (data presented in Figure 3.14B).....	174
B14	The probability (P), degrees of freedom and F values for the relative transcript abundance of <i>AtARF19</i> in the root tissue of 21 DAI seedlings for comparisons among treatments (non-inoculated and clubroot-inoculated) and lines (WT, <i>tir1afb2C</i> , <i>tir1afb245</i> , <i>PsAFB6/+ 4-8 tir1afb2</i> , and <i>PsAFB6/+ 3-2 tir1afb245</i>), and the treatment x line interaction using a two-way ANOVA analysis followed by mean separation using LSD post-hoc test (data presented in Figure 3.14C).....	175
B15	The probability (P), degrees of freedom and F values for the relative transcript abundance of <i>AtGH3.3</i> in the root tissue of 21 DAI seedlings for comparisons among treatments (non-inoculated and clubroot-inoculated) and lines (WT, <i>tir1afb2C</i> , <i>tir1afb245</i> , <i>PsAFB6/+ 4-8 tir1afb2</i> , and <i>PsAFB6/+ 3-2 tir1afb245</i>), and the treatment x line interaction using a two-way ANOVA analysis followed by mean separation using LSD post-hoc test (data presented in Figure 3.15A).....	176
B16	The probability (P), degrees of freedom and F values for the relative transcript abundance of <i>AtGH3.17</i> in the root tissue of 21 DAI seedlings for comparisons among treatments (non-inoculated and clubroot-inoculated) and lines (WT, <i>tir1afb2C</i> , <i>tir1afb245</i> , <i>PsAFB6/+ 4-8 tir1afb2</i> , and <i>PsAFB6/+ 3-2 tir1afb245</i>), and the treatment x line interaction using a two-way ANOVA analysis followed by mean separation using LSD post-hoc test (data presented in Figure 3.15B).....	177
B17	The probability (P), degrees of freedom and F values for the relative transcript abundance of <i>AtICS1</i> in the root tissue of 21 DAI seedlings for comparisons among treatments (non-inoculated and clubroot-inoculated) and lines (WT, <i>tir1afb2C</i> , <i>tir1afb245</i> , <i>PsAFB6/+ 4-8 tir1afb2</i> , and <i>PsAFB6/+ 3-2 tir1afb245</i>), and the treatment x line interaction using a two-way ANOVA analysis followed by mean separation using LSD post-hoc test (data presented in Figure 3.16A).....	178

B18 The probability (P), degrees of freedom and F values for the relative transcript abundance of *AtPR5* in the root tissue of 21 DAI seedlings for comparisons among treatments (non-inoculated and clubroot-inoculated) and lines (WT, *tir1afb2C*, *tir1afb245*, *PsAFB6/+ 4-8 tir1afb2*, and *PsAFB6/+ 3-2 tir1afb245*), and the treatment x line interaction using a two-way ANOVA analysis followed by mean separation using LSD post-hoc test (data presented in Figure 3.16B).....179

List of Figures

Figure	Page
1.1	The life cycle of <i>Plasmodiophora brassicae</i>2
1.2	Trp-dependent IAA biosynthesis and auxin conjugation pathways.....10
1.3	Mechanism of auxin perception and response through the TIR1/AFB-mediated pathway.....12
1.4	Pathogen-induced SA biosynthesis in Arabidopsis.....28
2.1	Transcript abundance of <i>PsAFB6</i> in root and shoot tissues of Arabidopsis <i>tir1afb2</i> double and <i>tir1afb245</i> quadruple mutants and mutants expressing <i>PsAFB6</i>42
2.2	The effect of 2,4-D on root elongation of Arabidopsis <i>tir1afb2</i> double and quadruple mutants and mutants expressing <i>PsAFB6</i>43
2.3	The effect of 2,4-D on lateral root density of Arabidopsis <i>tir1afb2</i> double and <i>tir1afb245</i> quadruple mutants and mutants expressing <i>PsAFB6</i>45
3.1	A diagram of auxin response and defense response marker genes used for gene expression analysis in Arabidopsis roots in response to clubroot pathogen inoculation...54
3.2	Representative microscopic images of the disease rating scale for clubroot symptoms on root-shoot transition zone of Arabidopsis.....63
3.3	Molecular characterization of auxin receptor <i>tir1-10 afb2-3</i> T-DNA insertion in double mutant lines in Columbia-wild type (WT) background.....68
3.4	Transcript abundance of <i>PsAFB6</i> in clubroot-inoculated and non-inoculated root tissue of Arabidopsis <i>tir1afb2C</i> double mutant, <i>tir1afb245</i> quadruple mutant, and mutants expressing <i>PsAFB6</i> at 21 DAI.....69
3.5	Clubroot disease severity index (DI) of Arabidopsis auxin receptor <i>tir1afb2</i> double and <i>tir1afb245</i> quadruple mutants and mutants expressing <i>PsAFB6</i> caused by <i>P. brassicae</i> at 32 DAI.....71
3.6	Representative microscopic images of the root-shoot transition region of clubroot-inoculated and non-inoculated Arabidopsis Columbia wild-type (WT), auxin receptor <i>tir1afb2</i> double and <i>tir1afb245</i> quadruple mutant lines, and <i>PsAFB6</i> -expressing quadruple mutant lines at 32 DAI.....73

3.7	Representative microscopic images of the root-shoot transition region of clubroot-inoculated and non-inoculated Arabidopsis Columbia wild-type (WT), auxin receptor <i>tir1afb2</i> double mutant lines at 32 DAI.....	73
3.8	Representative microscopic images of the root-shoot transition region of clubroot-inoculated and non-inoculated Arabidopsis Columbia wild-type (WT), auxin receptor <i>tir1afb2</i> double mutant and double mutant lines expressing <i>PsAFB6</i> at 32 DAI.....	74
3.9	The frequency distribution of disease severity in <i>P. brassicae</i> -inoculated Arabidopsis WT, <i>tir1afb2</i> and <i>tir1afb245</i> mutant lines, and mutant lines expressing <i>PsAFB6</i> at 32 DAI..	75
3.10	Frequency distribution of disease severity in <i>P. brassicae</i> -inoculated Arabidopsis <i>tir1afb2</i> mutant lines at 32 DAI.....	77
3.11	Frequency distribution of disease severity in <i>P. brassicae</i> -inoculated Arabidopsis <i>tir1afb2</i> mutant line and mutant lines expressing <i>PsAFB6</i> at 32 DAI.....	78
3.12	Root-shoot transition region fresh weights of clubroot-inoculated and non-inoculated Arabidopsis WT, <i>tir1afb2</i> and <i>tir1afb245</i> mutant lines, and mutants expressing <i>PsAFB6</i> at 32 DAI. Plants (48-day-old) with 16 days of seedling growth prior to clubroot-inoculation followed by 32 days of growth after clubroot-inoculation in the peat-based medium were assessed.....	80
3.13	Transcript abundance of <i>AtIAA9</i> , <i>AtIAA16</i> , and <i>AtIAA19</i> in clubroot-inoculated and non-inoculated root tissue of Arabidopsis WT, <i>tir1afb2</i> double mutant, <i>tir1afb245</i> quadruple mutant, and mutants expressing <i>PsAFB6</i> at 21 DAI.....	83
3.14	Transcript abundance of <i>AtARF3</i> , <i>AtARF5</i> , and <i>AtARF19</i> in clubroot-inoculated and non-inoculated root tissue of Arabidopsis WT, <i>tir1afb2</i> double mutant, <i>tir1afb245</i> quadruple mutant, and mutants expressing <i>PsAFB6</i> at 21 DAI.....	86
3.15	Transcript abundance of <i>AtGH3.3</i> and <i>AtGH3.17</i> in clubroot-inoculated and non-inoculated root tissue of Arabidopsis WT, <i>tir1afb2</i> double mutant, <i>tir1afb245</i> quadruple mutant, and mutants expressing <i>PsAFB6</i> at 21 DAI.....	88
3.16	Transcript abundance of <i>AtICS1</i> and <i>AtPR5</i> in clubroot-inoculated and non-inoculated root tissue of Arabidopsis WT, <i>tir1afb2</i> double mutant, <i>tir1afb245</i> quadruple mutant, and mutants expressing <i>PsAFB6</i> at 21 DAI.....	91

3.17	Expression profiles of auxin metabolism and signaling genes and genes associated with SA biosynthesis and defense signaling in Arabidopsis roots of non-inoculated control <i>tir1afb2C</i> and <i>tir1afb245</i> lines harvested at the 21 DAI time point.....	98
3.18	Expression profiles of auxin metabolism and signaling genes and genes associated with SA biosynthesis and defense signaling in Arabidopsis roots of clubroot-inoculated WT, <i>tir1afb2C</i> and <i>tir1afb245</i> lines harvested at the 21 DAI.....	101
3.19	Expression profiles of auxin metabolism and signaling genes and genes associated with SA biosynthesis and defense signaling in Arabidopsis roots of clubroot-inoculated <i>tir1afb2C</i> and <i>tir1afb245</i> lines compared to the WT line harvested at the 21 DAI.....	103
3.20	Expression profiles of auxin metabolism and signaling genes and genes associated with SA biosynthesis and defense signaling in Arabidopsis roots of non-inoculated <i>PsAFB6/+ 4-8 tir1afb2</i> and <i>PsAFB6/+ 3-2 tir1afb245</i> lines compared to their respective auxin receptor mutant backgrounds at the 21 DAI experimental time point.....	104
3.21	Expression profiles of auxin metabolism and signaling genes and genes associated with SA biosynthesis and defense signaling in Arabidopsis roots of clubroot-inoculated <i>PsAFB6/+ 4-8 tir1afb2</i> and <i>PsAFB6/+ 3-2 tir1afb245</i> lines compared to their respective mutant backgrounds at the 21 DAI time point.....	106
A1	Diagrams of the <i>AtTIR1</i> , <i>AtAFB2</i> , <i>AtAFB4</i> and <i>AtAFB5</i> auxin receptor T-DNA insertion sites.....	130
A2	Overview of the root growth assays.....	131
A3	<i>PsAFB6</i> transcript abundance in root and shoot tissues of Arabidopsis <i>tir1afb2</i> double and <i>tir1afb245</i> quadruple mutants expressing <i>PsAFB6</i>	133
A4	A phylogenetic tree and amino acid percent global similarities and identities showing the association of <i>Pisum sativum</i> auxin receptor <i>PsAFB6</i> with Transport Inhibitor Response 1 and Auxin-Signaling F-box (TIR1/AFB) proteins from <i>Arabidopsis thaliana</i> (At)...	134
B1	The procedure of creation of auxin receptor <i>tir1afb2A2</i> and <i>tir1afb2D1</i> double mutant lines.....	140
B2	The procedure of clubroot inoculation assays.....	142
B3	The schematic representation of the improved Neubauer counting chamber within the hemocytometer for estimating the clubroot resting spore concentration.....	144

B4	The complete coding sequence of the auxin receptor <i>PsAFB6</i> (KY829119) from <i>P. sativum</i> L. cv. I3 (Alaska-type).....	146
B5	The complete coding sequence of gene encoding auxin/indole-3-acetic acid 9 protein (<i>AtAux/IAA9</i> ; At5g65670) retrieved from <i>Arabidopsis thaliana</i> genome annotation version TAIR10 (https://www.arabidopsis.org/).....	147
B6	The complete coding sequence of gene encoding auxin/indole-3-acetic acid 16 protein (<i>AtAuxIAA16</i> ; At3g04730) retrieved from <i>Arabidopsis thaliana</i> genome annotation version TAIR10 (https://www.arabidopsis.org/).....	148
B7	The complete coding sequence of gene encoding auxin/indole-3-acetic acid 19 protein (<i>AtAux/IAA19</i> ; At3g15540) retrieved from <i>Arabidopsis thaliana</i> genome annotation version TAIR10 (https://www.arabidopsis.org/).....	148
B8	The complete coding sequence of gene encoding auxin response factor 3 (<i>AtARF3</i> ; At2g33860.1) retrieved from <i>Arabidopsis thaliana</i> genome annotation version TAIR10 (https://www.arabidopsis.org/).....	150
B9	The complete coding sequence of gene encoding auxin response factor 5 (<i>AtARF5</i> ; At1g19850) retrieved from <i>Arabidopsis thaliana</i> genome annotation version TAIR10 (https://www.arabidopsis.org/).....	152
B10	The complete coding sequence of gene encoding auxin response factor 19 (<i>AtARF19</i> ; At1g19220) retrieved from <i>Arabidopsis thaliana</i> genome annotation version TAIR10 (https://www.arabidopsis.org/).....	154
B11	The complete coding sequence of gene encoding Gretchen Hagen 3.3 acyl acid amido synthetase (<i>AtGH3.3</i> ; At2g23170) retrieved from <i>Arabidopsis thaliana</i> genome annotation version TAIR10 (https://www.arabidopsis.org/).....	155
B12	The complete coding sequence of gene encoding Gretchen Hagen 3.3 acyl acid amido synthetase (<i>AtGH3.17</i> ; At1g28130) retrieved from <i>Arabidopsis thaliana</i> genome annotation version TAIR10 (https://www.arabidopsis.org/).....	157
B13	The complete coding sequence of gene encoding isochorismate synthase 1 (<i>AtICS1</i> ; At1g74710) retrieved from <i>Arabidopsis thaliana</i> genome annotation version TAIR10 (https://www.arabidopsis.org/).....	158

B14	The complete coding sequence of the pathogenesis related 5 (<i>AtPR5</i> ; At1g75040) retrieved from <i>Arabidopsis thaliana</i> genome annotation version TAIR10 (https://www.arabidopsis.org/).....	159
B15	The complete coding sequence of the PROTEIN PHOSPHATASE 2A SUBUNIT A3 (<i>AtPP2AA3</i> ; AT1G13320) retrieved from <i>Arabidopsis thaliana</i> genome annotation version TAIR10 (https://www.arabidopsis.org/).....	160

List of Abbreviations

Abbreviations	Definition
ABA	Abscisic acid
ABRE	Abscisic acid (ABA) response element
AD	Activation domain
AMI1	Amidase1
ANOVA	Analysis of Variance
AO	Aldehyde oxidase
AREs	Auxin response elements
ARF	Auxin response factor
AuxREs	Auxin response elements
AUX/IAA	Auxin/Indole-3-acetic Acid
AVE Ct	Average of Ct values
BL	Brassinosteroids
BRX	Brevixradix
CBF1	CRT binding factor1
CK	Cytokinins
COI1	Coronatine-insensitive 1
CR	Clubroot-resistant
CTD	Carboxy-terminal dimerization
CUL1	CULLIN 1
DAI	Day after inoculation
DAMPs	Damage-associated molecular patterns
DBD	DNA binding domain
DI	Disease Index
Di19	Drought-induced 19
DREB2A	Dehydration responsive element binding factor 2A
EAR	Ethylene response factor (ERF)-associated amphiphilic repression
EDS5	Enhanced disease susceptibility 5
EIN3/EIL1	Ethylene 3/Ethylene insensitive 3 like 1
ERF	Ethylene response factor

ETI	Effector-triggered immunity
FMOs	Flavin monooxygenase-like proteins
GA	Gibberellins
GH3	Gretchen Hagen 3
GRX480	Glutaredoxin 480
HDACs	Histone deacetylases
IAA	Indole-3-acetic acid
IAAld	Indole-3-acetaldehyde
IAM	Indole-3-acetamide
IAN	Indole-3-acetonitrile
IAOx	Indole-3-acetaldoxime
IBFQ	Iowa black fluorescent quencher
ICS1	Isochorismate synthase 1
IPA	Indole-3-pyruvic acid
JA	Jasmonic acid
JAZ	Jasmonate ZIM-domain
JAZ1-JAZ3	Jasmonate Zim-Domain
LBD16/ASL18	Lateral organ boundaries-domain16/asymmetric leaves2-like18
LiCl	Lithium chloride
LRRs	Leucine rich repeats
LSD	Least Significant Difference
miRNAs	MicroRNAs
MS	Murashige and Skoog
MYC2	Jasmonate Insensitive 1, Jin1
M/PAMPs	Microbe/pathogen-associated molecular patterns
NIT1	Nitrilase
NPR1	Non expressor of pathogenesis-related gene 1
ORA59	Octadecanoid-Responsive Arabidopsis 59
OXR2	Oxidation Resistant 2
PAA	Phenylacetic acid
PBS3	avrPphB susceptible 3

PP2AA3	Protein phosphatase 2A subunit A3
ppm	Parts per million
PR	Pathogenesis-related
PRRs	Pattern recognition receptors
PTI	PAMP-triggered immunity
qRT-PCR	Quantitative reverse transcription polymerase chain reaction
RD	Repression domain
ROS	Reactive oxygen species
SA	Salicylic acid
SAR	Systemic acquired resistance
SCF	Skip-Cullin-F-box
SE	Standard error
SISA	Sequence identity and similarity
TAA1	Tryptophan aminotransferase of Arabidopsis 1
TARs	TAA1-related proteins
TCP20	Teosinte branched1/cycloidea/proliferating cell factor 20
TGA	TGACG-binding
TIR1/AFB	Transport inhibitor response 1/Auxin signaling F-box protein
TPL	TOPLESS
TPR	TPL/ TOPLESS-related
Trp	Tryptophan
WRI1	Wrinkled1
WRKY70	WRKY DNA-binding protein 70
WT	Wild-type
YUC	YUCCA
ZEN	N, N-diethyl-4-(4-nitronaphthalen-1-ylazo)-phenylamine
$\beta\alpha\alpha$	Beta-alpha-alpha
2,4-D	2,4-dichlorophenoxyacetic acid
4-Cl-IAA	Chlorinated auxin 4-chloroindole-3-acetic acid
6-FAM	6-carboxyfluorescein

Chapter 1: Literature review

1.1 CLUBROOT DISEASE IN BRASSICA

The clubroot disease in Brassicaceae is caused by the obligate biotrophic protist *Plasmodiophora brassicae* Woronin. It is wide spread throughout the world wherever Brassica crops are grown and can cause 30 %-100 % of yield loss and declines of 4.7 %-6.1 % in oil content for canola (Hwang et al., 2012). However, as a non-axenic, microscopic, single-celled, soilborne microbe, the study and the control of the pathogen was greatly hampered. Recently, the release of the whole genome sequence of the pathogen indicates that the study of the pathogen has reached into the genomics era (Rolfe et al., 2016; Schwelm et al., 2016; Daval et al., 2019). ‘Omic’ approaches such as genomics, proteomics, transcriptomics and metabolomics analyses hold promise to greatly improve the understanding of the mechanisms of *P. brassicae* pathogenesis and lead to the development of novel sources of resistance and other control measures. In this part of the review, clubroot disease will be generally introduced, including the study on the current progress of life cycle, host range, disease symptoms, and disease management strategies.

1.1.1 *P. brassicae* life cycle

Since the clubroot pathogen cannot be cultivated outside its host, there are still some aspects of its life cycle that are not completely understood. Generally, the *P. brassicae* life cycle is divided into three stages: survival in the soil as resting spores, root hair infection and cortical infection (Kageyama and Asano, 2009). Some researchers combined the first two stages and divide the life cycle into two main phases: (i) the primary infection and (ii) the secondary infection (Dixon, 2006; Javed et al., 2023; Figure 1.1). Regardless of the classification, the life cycle starts with the resting spores. The resting spores are extremely robust, well-protected, and long-lived, and remain viable under different environmental conditions (Zahr et al., 2021). The mechanism that stimulates the germination of resting spores remains unknown. Studies suggest that the release of calcium ions and the changes in soil microbiome can influence the germination of immature young spores (Yano et al., 1991; Kageyama and Asano, 2009; Wang et al., 2023). Host or nonhost root exudates can also trigger its germination (Dixon, 2006; Dixon,

2009a). After germination, an oval-shaped, biflagellate primary zoospore is released and it moves through the soil moisture films until it reaches the surfaces of roots. By penetrating the cell wall of root hairs or epidermal cells, the primary infection phase or root hair infection stage officially starts (Liu et al., 2020). Then the zoospores grow into an uninucleate primary plasmodium, followed by a multinucleate plasmodium and finally cleaving into zoosporangia. Each zoosporangium contains 4-16 secondary zoospores which are released into the lumen of root hairs or epidermal cells or soil (Hwang et al., 2012; Javed et al., 2023). The secondary zoospores performed a conjugation in the root epidermal cell and formed a diploid uninucleate zygote, resulting in the initiating of the secondary infection phase or cortical infection stage. The invasion of the cortical tissue led to the formation of a uninucleate secondary plasmodium and finally a multinucleate secondary plasmodium. At this stage, cellular hypertrophy and hyperplasia cause abnormal gall formation on the host roots, which is a typical disease symptom that causes severe yield and quality loss (Gahatraj et al., 2019). Finally, uninucleate resting spores form from the secondary plasmodium and are released into the soil as the tissue decomposes. As previously stated, some detailed processes of this life cycle are still not fully understood including the relationship between primary and secondary infection process, the karyogamy of secondary zoospores, how the secondary zoospores become resting spores, as well as how the pathogen is restricted to the root and hypocotyl of the host plant (Ludwig-Müller, 2022; Javed et al., 2023).

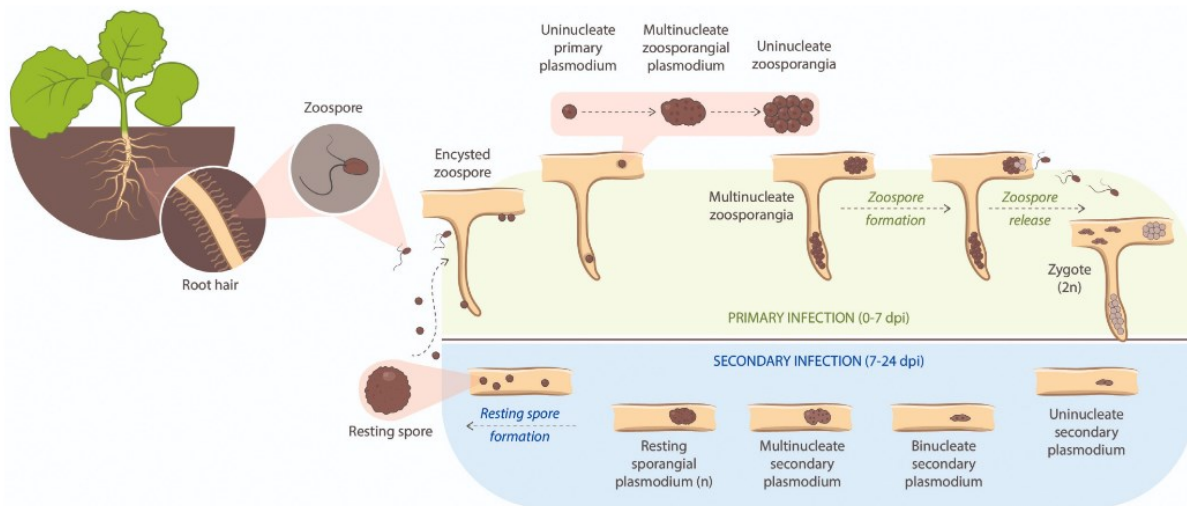


Figure 1.1 The life cycle of *Plasmodiophora brassicae*. The life cycle of *P. brassicae* involves two distinct stages: primary infection in the host's root hairs and epidermal cells (depicted in the top panel in yellow) and secondary infection in the cortical tissues (represented in the bottom panel in blue). Primary infection begins with the germination of resting spores forming primary zoospores in the soil. These zoospores, after encysting, penetrate the host cell wall, resulting in the formation of an uninucleate primary plasmodium within the root hairs. Then a multinucleate zoosporangial plasmodium is generated, followed by the development of an uninucleate zoosporangial cluster. Within each multinucleate zoosporangium, uninucleate secondary zoospores are produced and released into the lumen of root hairs or epidermal cells. The cycle concludes with the conjugation of two haploid uninucleate secondary zoospores in the root epidermal cell, giving rise to a diploid uninucleate zygote. Secondary infection begins with the formation of an uninucleate secondary plasmodium in the cortical cell, which progresses to a binucleate and then a multinucleate secondary plasmodium. Finally, a haploid multinucleate resting sporangial plasmodium is formed, from which haploid uninucleate resting spores are generated by splitting. Figure from Javed et al. (2023), based on Liu et al. (2020), with permission.

1.1.2 *P. brassicae* host range

There are approximately 350 genera and 3700 species in the Brassicaceae family (Howard et al., 2010) and all are the potential host for *P. brassicae*. Within this family, both root hair and cortical infection of the life cycle can be completed (Dixon, 2009b). Some studies found that the root hair or epidermal cell infection can also occur in non-cruciferous hosts such as ryegrass (*Lolium perenne*), spinach (*Spinacia oleracea*) and spring cereals (Bhattacharya and Dixon, 2010; Gahatraj et al., 2019). In addition, the germination of resting spores was reported to be stimulated by non-host plant species including winter rye, leek, red clover, and perennial ryegrass (Friberg et al., 2005; Hwang et al., 2015). Even though the primary or secondary infection phase cannot be completed in these plant species, they can be used as bait or trap crops for the practical management of clubroot disease (Javed et al., 2023).

1.1.3 *P. brassicae* host symptoms

The above-ground symptoms can be reduced aerial plant growth, flagging of leaves, young leaves turning pale green and then yellow, premature seed ripening and production of shriveled seeds, and wilting and stunting of the whole plant (Hwang et al., 2014). However, these symptoms can be confused with water or nutrient deficiency or other diseases and only above-ground symptoms are not sufficient to determine whether the plants are clubroot infected or not. When infection is severe, club-shaped root galls can be seen after the plant is dug from the soil.

The severity of the disease depends on many factors, including susceptibility of the host, virulence and abundance of the pathogen, as well as environmental factors such as temperature, soil pH, soil type, soil moisture (Dixon, 2009a; Gahatraj et al., 2019). It is easy to understand that the more susceptible a host and more virulent a pathotype, the more likely severe disease symptoms will develop. Temperature, soil pH, soil type, and soil moisture can also affect every stage of clubroot development. Studies suggest that *P. brassicae* cortical infection optimally occurs around 25°C (Sharma et al., 2011). Additionally, alkaline soil and a higher amount of soil organic matter caused reduction in clubroot severity (Dixon, 2009a). Soil moisture is a dominant environmental factor since it affects the germination of resting spores and the movement of zoospores in the soil. Although infection can occur at low soil moisture, the most favorable soil moisture for clubroot gall development is 60-70 % (Hamilton and Crete, 2010).

1.1.4 *P. brassicae* disease management

Clubroot disease is almost impossible to eradicate once a field gets infested. Therefore, the prevention of *P. brassicae* field infection is paramount. However, once a field gets infested, the best management practice to reduce disease incidence and severity is to integrate individual control measures into a management strategy. Available control measures including cultural strategy, biological control, chemical control, and genetic resistance (Donald and Porter, 2009; Strelkov et al., 2011). A summary of the most commonly used practices are as follows:

1.1.4.1 Cultural strategy

While clubroot zoospore motility is limited, pathogen spread over long distances occurs through infected plant materials, transplant trays, farm machinery, tools and field equipment. Therefore, to prevent the spread of resting spores to a pathogen-free field, sanitation of field

equipment and machinery that could be contaminated with clubroot-infested soil is an important process for clubroot disease management (Howard et al., 2010). Another cultural strategy is crop rotation which is an effective method to reduce the inoculum load of *P. brassicae* in the soil. Studies suggest that at least 2 years of rotations with non-host crops can reduce resting spore load in the field and facilitate obtaining maximum yield (Peng et al., 2014; Hwang et al., 2019). Spore density of the pathogen can also be reduced by soil amendments. Changing soil pH to 7.0 or higher with lime-based products such as lime and wood ash is frequently used when the inoculum levels are relatively low (Donald and Porter, 2009; Howard et al., 2010; Gahatraj et al., 2019). In addition, the combination of lime with one or two soil amendments such as boron, calcium nitrate, calcium cyanamide, metham sodium, and calcium carbonate has been identified as a cost-effective cultural strategy for managing clubroot disease (Donald et al., 2006; Donald and Porter, 2009).

As mentioned above, bait or decoy crops can stimulate the germination of resting spores without being infected; therefore, they can be used as a reliable method to reduce inoculum density in clubroot-infected fields. Moreover, disruption of the pathogens' favorite environmental conditions can prevent dissemination of the pathogen. Therefore, scheduling the sowing date properly and improve drainage conditions can minimize the risk of disease build-up (Javed et al., 2023).

1.1.4.2 *Biological control*

As an environmentally friendly tool to manage clubroot disease, the use of soil microorganisms, also called biological agents or bio-fungicides, has caught attention of clubroot researchers. Although the mechanisms of how these micro-organisms control clubroot spread and promote plant growth remain largely unknown, *Trichoderma* spp., *Bacillus* spp., *Pseudomonas* spp., *Acremonium alternatum*, *Heteroconium chaetospora*, and *Gliocladium catenulatum*, are the potential biological agents against clubroot (Donald and Porter, 2009; Howard et al., 2010; Gahatraj et al., 2019; Javed et al., 2023).

1.1.4.3 *Chemical control*

Chemical application such as fungicides and fumigants has been part of clubroot management strategies since 1980s (Doyle and Clancy, 1987). The commonly used synthetic fungicides and fumigants such as fluazinam, cyazofamid, pentachloronitrobenzene, sodium methyldithiocarbamate, carbendazim, mancozeb, azoxystrobin, and difenoconazole, are effective

in clubroot control (Donald and Porter, 2009; Kowata-Dresch and May-De Mio, 2012; Gahatraj et al., 2019). However, the high cost for growers and the prohibition of using some of these chemicals in some countries minimizes their use, and it is recommended to combine other management strategies to control the clubroot disease.

1.1.4.4 *Genetic resistance*

Genetic resistance to clubroot can be the most effective and environmentally friendly solution for the long-term management of the disease. It can vary from broad-spectrum resistance to highly specific resistance, also called pathotype-specific resistance (Diederichsen and Sacristan, 1996). To date, most clubroot-resistant Brassica crop cultivars are generally race or pathotype-specific. When a cultivar with single-gene resistance is grown in a field with a mixture of several pathotypes, a strong selection pressure for pathogen genotypes that are able to overcome or breakdown this resistance is likely to occur (Diederichsen et al., 2009). This breakdown phenomenon may occur, particularly in heavily infested fields, due to the short-term continuous cropping following the introduction of clubroot-resistant (CR) cultivars (Leboldus et al., 2012; Tanaka and Ito, 2013). This could potentially be attributed to the selective propagation of pathogenic genotypes on the cultivars. Under the selection pressure of newly introduced CR cultivars, less prominent pathogenic genotypes of *P. brassicae*, which are initially concealed within the variable population structure on field-grown host plants, emerge and dominate (Tanaka and Ito, 2013). A similar scenario was obtained under experimental conditions. Five cycles of infection from a spore population or a single-spore isolate of the pathogen (SACAN03) were performed on resistant, moderately resistant, and susceptible canola cultivars. An increase in the disease index for both resistant and moderately resistant cultivars was observed after the first cycle of inoculation with the single-spore isolate or the spore population of *P. brassicae*, suggesting the ability of both single-spore isolates and populations of *P. brassicae* to rapidly erode the resistance inherent in the two canola genotypes (Leboldus et al., 2012).

Therefore, identification and functional characterization of broad-spectrum resistance to clubroot in Brassica crops will be an important area of study for clubroot researchers. In conclusion, successful control of clubroot disease requires integrated management strategies that are cost-effective.

1.2 AUXIN IN PLANT-PATHOGEN INTERACTION

Plants and pathogens have interacted for growth and survival throughout their evolutionary history. The plant growth hormone auxin is a master regulator of plant developmental processes and it is also involved in plant-pathogen interactions (Kunkel and Harper, 2018). In clubroot disease progression, plant-derived auxin is implicated in the cell division and elongation process that leads to the hyperplasia and hypertrophy of infected roots (Ludwig-Müller et al., 2009). However, due to the complicated processes of auxin perception, signaling, transport and crosstalk with other plant hormone networks, the role of auxin in plant-pathogen interactions remains poorly understood, especially for the biotrophic pathogens like *P. brassicae* which acquire nutrients from the live host tissue.

Before discussing the role of auxin during plant-pathogen interactions, it is important to review the current concepts of how the plant immune system recognize a harmful microbe. First, pattern recognition receptors (PRRs), which are typically found on the plasma membrane of cells, detect the presence of conserved microbial elicitors, also known as microbe/pathogen-associated molecular patterns (M/PAMPs) (Jones and Dang, 2006). This initial recognition leads to part of a basal resistance called PAMP-triggered immunity (PTI), which acts as a first barrier to prevent the infection of non-host pathogens (Göhre and Robatzek, 2008).

However, PTI can be easily suppressed by virulent pathogens that can infect susceptible hosts. To overcome PTI, virulent pathogens have developed specific effector molecules that can penetrate the host cell. The effector molecules are subsequently recognized by resistance (R)-gene products, which trigger a potent immune response known as effector-triggered immunity (ETI) (Hammond-Kosack and Parker, 2003). ETI typically involves a local death program called hypersensitive response which helps limit pathogen invasion (Hammond-Kosack and Parker, 2003; Göhre and Robatzek, 2008). These two layers of immune systems are generally capable of perceiving and restricting most of the invading pathogens and is known as basal resistance (Jones and Dang, 2006). Basal resistance does not provide complete protection against pathogens; instead, it limits their virulence. It can be described as a response triggered by virulent pathogens in susceptible hosts, or as the remaining level of PTI (and weak ETI) in a susceptible interaction, wherein various immune responses of PTI are suppressed by effectors (Göhre and Robatzek, 2008).

Even with the immune barriers mediated by the host, virulent pathogens can still cause infections in susceptible host plants and the host plant hormone auxin can be manipulated by pathogens to propagate (Naseem et al., 2015). Pathogens can modulate auxin homeostasis, biosynthesis, signaling, and transport in their plant host by secreting virulence factors. These disturbances contribute to colonization events, allowing the pathogen to acquire the necessary water and nutrients from the host to support its growth (Spaepen and Vanderleyden, 2011; Naseem et al., 2015; Kunkel and Harper, 2018). For clubroot disease, it has been suggested that *P. brassicae* stimulates the accumulation of IAA in the infected roots in a sink-dependent manner (Ludwig-Müller and Schuller, 2008; Ludwig-Müller et al., 2009). It is proposed that the host auxin biosynthetic pathways can be modulated by the pathogen, resulting in a re-direction of water or nutrient flow towards the infected roots (Ludwig-Müller et al., 2009). The de novo biosynthesis of IAA in plants occurs via the tryptophan (Trp)-dependent pathway or by a Trp-independent pathway, with most occurring through the Trp-dependent pathway (Zhao, 2012; Zhao, 2014) (Figure 1.2). Trp-dependent IAA biosynthesis includes a series of enzymatic reactions that convert tryptophan into IAA. The indole-3-pyruvic acid (IPA) pathway is the major pathway in plants, and additionally the indole-3-acetaldoxime (IAOx) pathway occurs in certain species including members of the Brassicaceae family. In the IPA pathway, TRYPTOPHAN AMINOTRANSFERASE OF ARABIDOPSIS1 (TAA1) and TAA1-RELATED proteins (TARs) convert tryptophan into IPA, which is then converted into IAA by enzymes from the YUCCA (YUC) family. The IAOx pathway involves the conversion of tryptophan into IAOx by CYP79B2 and CYP79B3. IAOx, through a number of steps, is metabolized to glucobrassicin which can be subsequently hydrolyzed by myrosinase and result in the formation of indole-3-acetonitrile (IAN). Plant nitrilases have the ability to convert IAN into IAA, while AMIDASE1 (AMI1) facilitates the conversion of indole-3-acetamide (IAM) into IAA (Bajguz and Piotrowska, 2009; Zhao, 2014; Malka and Cheng, 2017).

Several genes coding for key enzymes involved in either the IPA or IAOx pathway of IAA biosynthesis and their enzyme activities were found to be differentially regulated during clubroot formation. Nitrilase activity was increased in the roots of turnip (*B. campestris* L.) at 38 days after inoculation (DAI), when the level of IAA was also increased five-fold over healthy roots, suggesting the elevated IAA concentration after *P. brassicae* infection was possibly due to IAA synthesis via pathways involving nitrilase (Ugajin et al., 2003). Other studies also found

induced expression of genes encoding nitrilase at various stages of infection (14, 28, 35 DAI) in *A. thaliana* and *B. rapa* (Siemens et al., 2006; Ishikawa et al., 2007; Robin et al., 2020). A nitrilase (*NIT1*) mutant (*nit1*) displays smaller root galls with fewer pathogen structures, along with reduced free IAA levels in the clubbed roots of infected plants (Grsic-Rausch et al., 2000; Neuhaus et al., 2000). These finds indicate that in general the increased production of IAA through the nitrilase pathway likely influences gall formation during the later phase of infection. Myrosinase activity was also up-regulated at 4 DAI in *P. brassicae*-infected *A. thaliana* roots (Devos et al., 2006). Aldehyde oxidase (AO), which is involved in IAA biosynthesis through the IAOx and TAM pathways, is presumed to be responsible for the conversion of indole-3-acetaldehyde (IAAld) to IAA. Rapid induction of *BnAAO4* was observed in the roots of *B. napus* at 3 DAI (Xu et al., 2016). In addition, the expression of *BnFMO5*, a member of the Yucca-encoded flavin monooxygenase-like proteins (FMOs), was induced at 3–10 DAI in *P. brassicae*-inoculated *B. napus* roots (Xu et al., 2016). These results suggest the involvement of these enzymes in the early stages of clubroot infection.

An additional pathway for the biosynthesis of IAA is the hydrolysis of free IAA from inactive conjugates. The reverse reaction from free IAA to auxin conjugates can be catalyzed by the IAA amino acid conjugate synthetases (GH3) (Ludwig-Müller et al., 2009). Several members of the *GH3* family involved in IAA-amino acid conjugate formation were significantly up-regulated during clubroot infection, and it was suggested that the up-regulation may be due to the initiation of a detoxification reaction by the host plant against high levels of auxin in the root galls (Jahn et al., 2013; Robin et al., 2020). The modulation of free-IAA pools in root galls also indicates that auxin signaling and transport are potentially modified by the pathogen. The role of auxin signaling in clubroot development will be discussed in detail in the following sections. For auxin transport, IAA transport is necessary for accurate plasmodial development. The inhibition of host auxin transport at the onset of infection led to a decrease in clubroot development and a lower presence of IAA in plasmodia (Devos and Prinsen, 2006). Furthermore, there was a notable increase in the expression of polar auxin transport genes and proteins during clubroot infection (Robin et al., 2020). Taken together, these findings indicate that auxin transport is essential for early clubroot symptom development. With the availability of transgenic or mutant plant lines modified in various parts of the auxin synthesis and response pathways, it is possible to further understand the role of auxin during clubroot disease development even though

sometimes the mutation can be compensated by other parallel pathways that are present (Ludwig-Müller and Schuller, 2008).

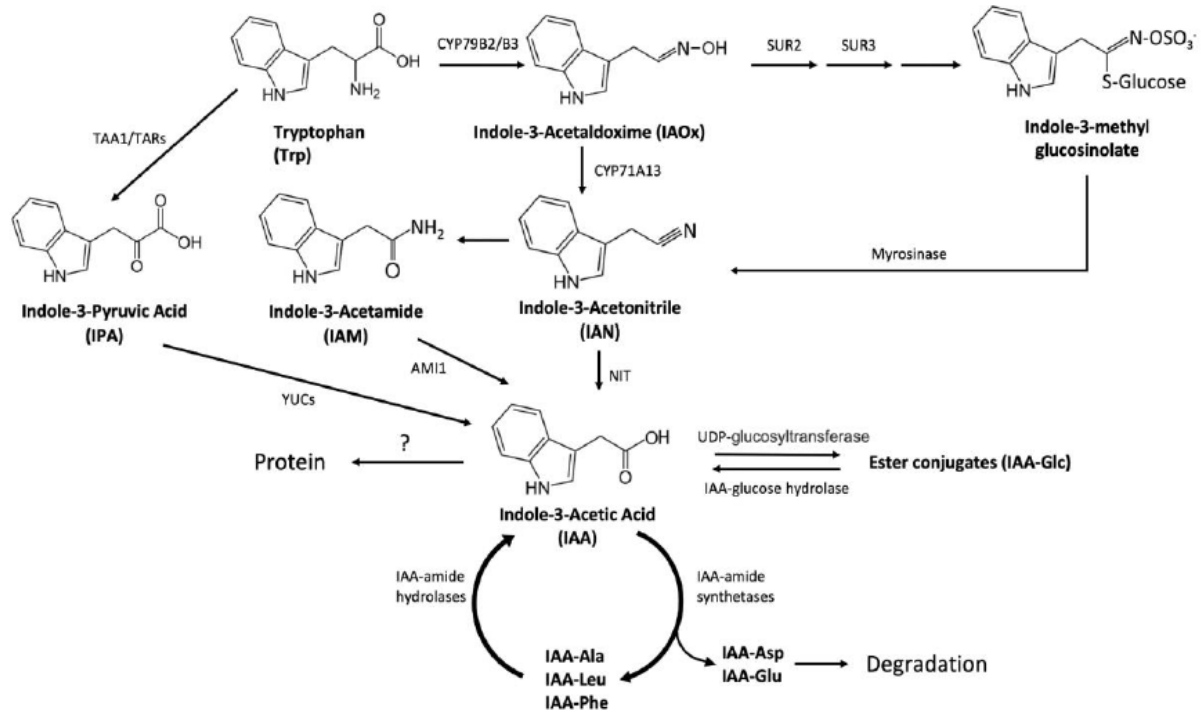


Figure 1.2 Trp-dependent IAA biosynthesis and auxin conjugation pathways. The Trp-dependent IAA biosynthesis and conjugation pathways requires multiple enzymatic reactions. The upper section illustrates the different pathways of auxin biosynthesis from Trp, while the lower section depicts the various auxin conjugation pathways. For IAA biosynthesis, the IPA pathway involves TAA1 and TARs converting Trp to IPA, which is subsequently converted to IAA by YUC family enzymes. In the IAOx pathway, CYP79B2 and CYP79B3 convert Trp to IAOx, primarily leading to the production of indole-3-methyl glucosinolate (glucobrassicin). Glucobrassicin can be hydrolyzed by myrosinase to form IAN, which can then be converted to IAA by plant nitrilases. Additionally, IAM can be converted to IAA by AMI1. The IAA conjugation pathway involves the formation of sugar conjugates (IAA-glucose), amino acid conjugates (IAA-Ala, IAA-Leu, IAA-Phe, IAA-Asp, IAA-Glu), and protein conjugates. Figure from Liu (2023) with permission, based on Zhao (2014), Malka and Cheng (2017), and Bajguz and Piotrowska (2009).

1.3 AUXIN SIGNALING PROCESS IN PLANTS

Nuclear auxin signal perception and the resulting changes in gene expression are carried out by three core auxin signaling protein families: the F-box TRANSPORT INHIBITOR RESPONSE 1/AUXIN SIGNALING F-BOX PROTEIN (TIR1/AFB) auxin receptors, the Auxin/INDOLE-3-ACETIC ACID (Aux/IAA) transcriptional repressors, and the AUXIN RESPONSE FACTOR (ARF) transcription factors (Salehin et al., 2015; Lavy and Estelle, 2016). The TIR1/AFB proteins are subunits of a ubiquitin protein ligase E3 complex called SCF^{TIR1/AFB} (SKP-Cullin-F box [SCF]-type E3 ligase) (Wang and Estelle, 2014; Salehin et al., 2015). When the auxin level in a cell is low, Aux/IAA repressors bind with ARFs, which recruit TOPLESS (TPL) co-repressors to the chromatin, leading to the repression of auxin responsive gene expression. When the auxin level in a cell is elevated, auxin promotes an interaction between the F-box of TIR1/AFBs and Aux/IAA repressors, resulting in SCF^{TIR1/AFB} mediated ubiquitination of Aux/IAAs and degradation by the 26S proteasome complex. Therefore, the ARF transcription factors are released and activate expression of auxin response genes (Figure 1.3). Auxin binding does not appear to cause a notable change in the conformation of TIR1/AFB (coded by 6 genes in Arabidopsis); instead, it functions as a ‘molecular glue’ to stabilize the interaction between TIR1/AFB and the Aux/IAA protein (coded by 29 genes in Arabidopsis) therefore, these two protein families act as co-receptors for auxin [reviewed in Hagen (2015)].

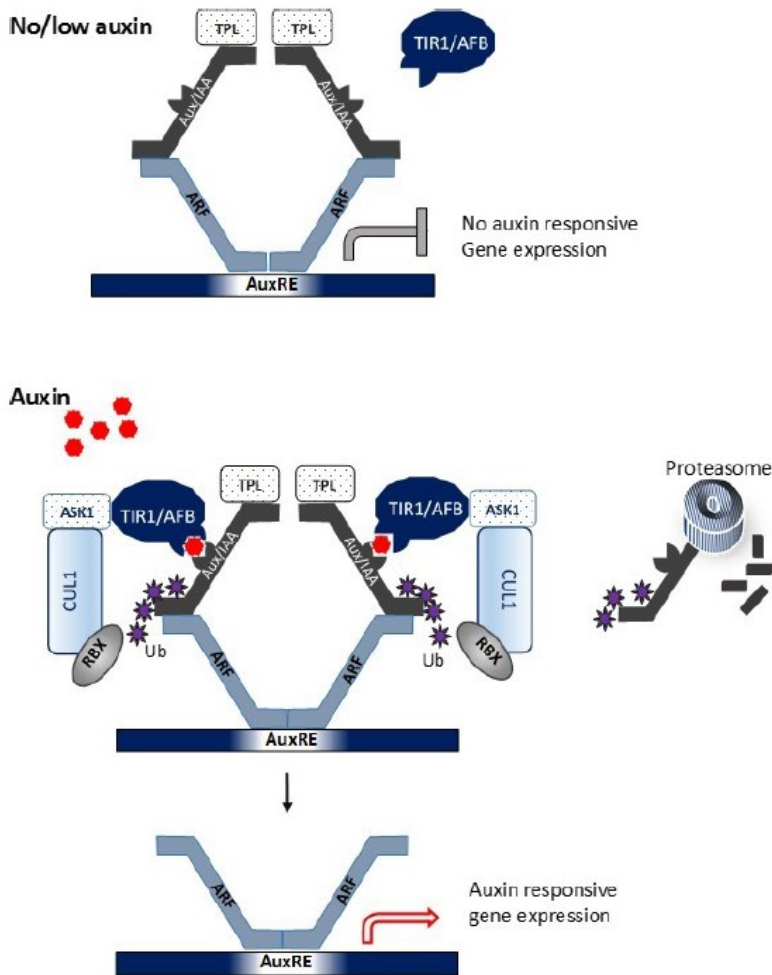


Figure 1.3 Mechanism of auxin perception and response through the TIR1/AFB-mediated pathway. At low levels of auxin, Aux/IAA proteins associate with ARF proteins, repressing transcription of auxin-regulated genes. At high auxin levels, auxin acts as ‘a molecular glue’, binding TIR1 and Aux/IAA proteins together, leading to poly-ubiquitination of the Aux/IAs and their degradation in the 26S proteasome. The released ARFs allows the transcription of auxin responsive genes. Figure from Jayasinghege (2017) with permission, based on Wang and Estelle (2014) and Salehin et al. (2015).

1.3.1 *TIR1/AFB* auxin receptor gene family

Phylogenetic analysis showed that the TIR1/AFB auxin-receptor protein family is conserved across land plants and the family was divided into four clades: TIR1, AFB2, AFB4, and AFB6 (Parry et al., 2009). Arabidopsis contains three TIR1/AFB clades with two alleles per clade (AtTIR1 and AtAFB1; AtAFB2 and AtAFB3; AtAFB4 and AtAFB5; Parry et al., 2009), while pea (*Pisum sativum* L.) contains TIR1/AFB gene members from four clades (TIR1a and TIR1b; AFB2; AFB4; AFB6; Jayasinghe et al., 2019). Their function as auxin receptors was identified based on the structure and their role in regulating auxin response. TIR1/AFB proteins consist of a C-terminal F-box domain and a N-terminal Leucine Rich Repeats (LRRs) domain (Powers and Strader, 2020). The F-box domain is where the TIR1/AFB protein bind to CULLIN1 (CUL1) in the ubiquitin ligase complex. The LRRs domain's upper surface contains a single pocket, in which auxin directly binds to it and stimulates interaction between SCF^{TIR1/AFB} and the Aux/IAA substrate (Tan et al., 2007). Although all the auxin receptors can bind with auxin, genetic analysis suggested that TIR1/AFB receptors have both overlapping and specialized functions (Mockaitis and Estelle, 2008; Parry et al., 2009; Prigge et al., 2016; Prigge et al., 2020). For example, the loss of a single functional member of TIR1 through AFB3 only has a minor impact on plant growth and auxin response. However, the combination of *tir1* and *afb1-3* mutations results in a significant reduction in auxin response and various developmental abnormalities associated with auxin (Dharmasiri et al., 2005b). When all six TIR1/AFB proteins are lost in Arabidopsis, it causes early embryo defects that eventually leads to seed abortion (Prigge et al., 2020). These results suggested extensive functional overlap or functional redundancy among the *TIR1/AFB* genes. Additional studies indicate that various TIR1/AFBs also demonstrate distinct properties. Phenotypes of single mutants showed that TIR1 appears to make the largest contribution followed by AFB2. Genetic analysis of various combinations of *tir1*, *afb1*, *afb2*, and *afb3* mutants in Arabidopsis found that TIR1 and AFB2 play a more substantial role in regulating auxin response in the roots compared to AFB1 or AFB3 (Parry et al., 2009). However, rapid root growth inhibition assay showed that the *afb1-3* mutant is almost completely resistant to auxin, suggesting that AFB1 plays a dominant role for this rapid, nongenomic auxin inhibition of root growth. AFB1 was also found to be responsible for regulating the initial phase of the root gravitropic response (Prigge et al., 2020). The function of AFB4 and AFB5 are less known, but the resistance of *afb4* and *afb5* mutants to the synthetic

auxin picloram suggested that both AFB4 and AFB5 are selective for the picloram family of auxinic herbicides (Prigge et al., 2016). The *afb4-8* and *afb5-5* single mutants exhibit heightened rosette branching compared to the WT, and the *afb4-8 afb5-5* double mutants display even further increased branching relative to their respective single mutants, indicating the involvement of AFB4 and AFB5 in shoot branching regulation (Ligerot et al., 2017).

1.3.2 *Aux/IAA* transcriptional repressor gene family

The Arabidopsis genome contains 29 *Aux/IAA* genes that are divided into genes that code for canonical and non-canonical Aux/IAA proteins according to their conserved domains (Sato and Yamamoto, 2008; Waseem et al., 2018). Aux/IAA proteins with four highly conserved domains (I, II, III, IV) are known as the canonical Aux/IAAs, while those lacking at least one conserved domain are regarded as non-canonical Aux/IAAs (Shi et al., 2020). The repression domain, known as Domain I, contains an ethylene response factor (ERF)-associated amphiphilic repression (EAR) motif "LxLxL" or "(L/F) DLN (L/F) xP", and recruits the corepressor TPL/TPL-RELATED PROTEIN (Ke et al., 2015; Plant et al., 2021). This interaction leads to the recruitment of HISTONE DEACETYLASEs (HDACs), including the well-known HDA19, which ultimately triggers chromatin condensation and represses the expression of ARF target genes (Chapman and Estelle, 2009). Mutations in domain I can lead to complete loss of repression, suggesting the important role of this domain in auxin response (Tiwari et al., 2001). Domain II carries a highly conserved 13-amino acid degron motif (Gly-Trp-Pro-Pro-Val; GWPPV) that interacts with SCF^{TIR1/AFB} to mediate Aux/IAA degradation (Ramos et al., 2022). The degradation rates or the half-life of Aux/IAAs is primarily determined by the property of domain II, ranging from 10 minutes to several hours (Dreher et al., 2006). Mutations in this domain often lead to a longer half-life and decreased auxin responsiveness by abolishing its interaction with the SCF complex (Tiwari et al., 2001; Dharmasiri et al., 2005a; Kepinski and Leyser, 2005). Among the 29 Aux/IAA proteins, 5 of them lack domain II (IAA20, IAA30, IAA32, IAA33 and IAA34), which are considered as non-canonical Aux/IAA proteins (Sato and Yamamoto, 2008). Because these non-canonical Aux/IAAs lack the conserved degron sequence that binds with auxin receptors, their protein stability is highly increased (Sato and Yamamoto, 2008) and these types of proteins seem important for organ morphogenesis, since IAA20 and IAA30 were required for the proper vascular patterning, IAA32 and IAA34 participated in

regulating differential growth of the apical hook, and IAA33 was reported to control root distal stem cell identity (Müller et al., 2016; Cao et al., 2019; Lv et al., 2020). Although the canonical auxin signaling pathway is very important for plant growth and development, recent studies also suggest that non-canonical Aux/IAAs work together with the canonical Aux/IAAs to integrate the auxin pathway with multiple signaling cascades and further modulate growth and development (Lv et al., 2020; Shi et al., 2020).

The PB1 domain, which consists of Domains III and IV, is responsible for the formation of dimers between Aux/IAA and ARF proteins (Luo et al., 2018; Waseem et al., 2018; Shi et al., 2020). These interactions, which can be homo- or hetero-binding, inhibit ARF function and lead to the repression of auxin-responsive transcription (Piya et al., 2014). Domain III is believed to play a more critical role in dimer formation due to its beta-alpha-alpha ($\beta\alpha\alpha$)-fold structure (Morgan et al., 1999). On the other hand, Domain IV also contributes to dimer formation by containing a conserved "GDVP" motif that promotes electrostatic protein interactions (Guilfoyle and Hagen, 2012). In addition to dimerization, Aux/IAA multimerization is essential for efficient recruitment of the TPL/TPR co-repressor. Studies have shown that the binding affinity of TPL/TOPLESS-related (TPR) increases in the presence of oligomerized EAR-motif containing repressors (Ke et al., 2015). Although how the different Aux/IAAs regulate the large and dynamic range of auxin responses has yet to be elucidated, it has been suggested that sequence variation within domains among different members of the Aux/IAA family may regulate interaction specificity leading to variation in auxin response (Luo et al., 2018; Powers and Strader, 2020).

Aux/IAA proteins are involved in many aspects of plant growth and development including embryo axis formation, response to light, embryonic patterning, hypocotyl elongation, gravitropism, and leaf morphology, vasculature, and lateral root formation (Luo et al., 2018). However, plants deficient in any one of the 12 *Aux/IAA* genes examined showed no visible developmental defects compared with the wild type, suggesting a high level of redundancy in function (Overvoorde et al., 2005). Even when closely related *Aux/IAA* genes such as *iaa8-1*, *iaa9-1*, or *iaa5-1*, *iaa6-1*, *iaa19-1* are mutated in combination (double or triple mutant combinations), the resulting plants still exhibit wild-type phenotypes (Overvoorde et al., 2005). These results suggested that loss-of-function mutation cannot provide an accurate understanding of the normal function of *Aux/IAA* genes since the mutations have minor effects on plant growth

and development. On the contrary, the gain-of-function mutations sometimes can result in distinct gain-of-function phenotypes, especially domain II mutations of various Aux/IAA proteins (Liscum and Reed, 2002; Mockaitis and Estelle, 2008; Rinaldi et al., 2012). For example, putative null mutations of *iaa3/shy2* and *iaa7/axr2* cause mild elongation of hypocotyls, whereas the strong gain-of-function mutations of *shy2-2* and *axr2-1* cause very short hypocotyls (Tian and Reed, 1999; Nagpal et al., 2000). The notable gain-of-function phenotypes do provide useful insight into the auxin-mediated developmental processes that Aux/IAA proteins can regulate. A gain-of-function mutation in *IAA18* causes aberrant cotyledon placement in embryos, suggesting that IAA18 can regulate embryonic apical patterning (Ploense et al., 2009). *Iaa12/bdl-1* mutant fail to initiate the root meristem during early embryogenesis (Hamann et al., 1999; Hamann et al., 2002), and *iaa7/axr2-1* and *iaa17/axr3-1* mutants cause changed gene expression pattern in the root meristem (Rouse et al., 1998; Sabatini et al., 1999). These results suggested that *Aux/IAA* genes are involved in regulating tissue patterning. Second, *iaa7/axr2-1*, *iaa14/slr-1* and *iaa17/axr3-1* mutants have short root hairs (Rouse et al., 1998; Nagpal et al., 2000; Guseman et al., 2015); *iaa8-1*, *iaa15-ox*, and *iaa16-1* mutants have less number of lateral roots (Arase et al., 2012; Rinaldi et al., 2012; Kim et al., 2020); *msg2/iaa19*, *shy2/iaa3*, and *shy1/iaa6* gain-of-function mutants exhibited short hypocotyls and up-curved leaves (Kim et al., 1996; Tian and Reed, 1999; Tatematsu et al., 2004), suggesting that Aux/IAA proteins regulate cell enlargement and cell division in various growing tissues. For the non-canonical Aux/IAA proteins, the lack of domain II results in much higher stability than that of the canonical Aux/IAA proteins, making it an interesting opportunity to understand the molecular function in plant growth and development. For example, overexpression of *IAA20*, *IAA30* and *IAA31* can cause auxin-related aberrant phenotypes, with *IAA20* overexpression showing the most severe defects including modified gravitropic growth in the hypocotyl and root, malformed vasculature of cotyledons and the collapse of root apical meristem that stops primary root growth (Sato and Yamamoto, 2008). These results suggest that non-canonical Aux/IAA proteins also play a significant role in hypocotyl, cotyledon and root formation.

1.3.3 *ARF* transcription factor gene family

ARFs are plant-specific transcriptional regulators that play a key role in regulating the expression of auxin-responsive genes (Chandler, 2016; Cancé et al., 2022). They interact

specifically with TGTCTC auxin response elements (AuxREs) located in the promoters of these genes and work in conjunction with Aux/IAA repressors, which dimerize with ARF activators in an auxin-dependent manner (Roosjen et al., 2018). Like Aux/IAAs, the ARF proteins also contains four domains. Domain I is a highly-conserved B3-type DNA binding domain (DBD), which located at the N-terminus of the protein with a sequence of about 350 amino acids (Cancé et al., 2022). The ARF-B3s bind to 6-bp sequences referred to as AuxREs, which were initially discovered as TGTCTC sequences located in the promoters of auxin responsive genes. Thus, the DNA binding properties of ARF-DBDs plays a crucial role in determining which genes are regulated by auxin (Li et al., 2016). The middle region of ARF protein known as Domain II can serve as either an activation domain (AD) or a repression domain (RD), which ultimately determines whether the ARF protein functions as a transcriptional activator or repressor (Roosjen et al., 2018). In Arabidopsis, ARFs that act as activators (ARF5/6/7/8/19) typically contain a high proportion of glutamine, while ARFs that act as repressors are characterized by an abundance of serine, threonine, and proline. This classification has been utilized to categorize ARFs in different plant species (Chandler, 2016). Domains III and IV are collectively referred to as the PB1 domain, or the carboxy-terminal dimerization (CTD) domain. This domain is responsible for facilitating the formation of homodimers or heterodimers with Aux/IAAs or other ARFs (Guilfoyle and Hagen, 2007). Arabidopsis has 22 full-length *ARF* genes, as well as one partial-length gene (*ARF23*) that contains a stop codon within its DBD. In addition, ARF3, 13, and 17 lack the conserved PB1 found in most ARFs, but these proteins do control auxin-dependent development, suggesting that these ARFs have alternative or other auxin-sensing pathway to regulate auxin responsive genes expression (Simonini et al., 2016; Cancé et al., 2022).

Like Aux/IAA proteins, ARFs also showed widespread functional redundancy. T-DNA insertion mutation analysis of 18 out of 23 *ARF* family members revealed clear phenotypes only for *arf2*, *arf3*, *arf5*, *arf7* and *arf8* mutants. Notably, *arf3-1* and *arf3-2* mutants display atypical gynoecium and floral patterning defects, characterized by an elevated number of sepals and carpals, and the *arf5-1* mutant fails to form a root meristem and normal cotyledons (Okushima et al., 2005). In Arabidopsis, phenotypic analysis indicated that specific phylogenetically-related pairs of ARFs act redundantly in a characteristically developmental manner (Okushima et al., 2005). For example, single mutants of *arf2* exhibit delayed flowering, leaf senescence, floral

abscission, and silique ripening. These phenotypes are further intensified in *arf1arf2* double mutants (Ellis et al., 2005; Okushima et al., 2005). The defects in embryo patterning and vasculature observed in *arf5* mutants are amplified in *arf5arf7* double mutants (Hardtke et al., 2004). Based on the observed phenotypes of individual *arf7* and *arf19* mutants, it is evident that ARF7 primarily governs the regulation of auxin-dependent differential growth in hypocotyls, while ARF19 plays a partial role in mediating auxin signaling in roots. However, in the *arf7arf19* double mutant, their phenotypes become significantly intensified, which exhibits pronounced auxin-related characteristics, including severely impaired lateral root formation, compromised gravitropic responses in both hypocotyls and roots, reduced organ size, and enhanced apical dominance in the aerial parts of the plant (Okushima et al., 2005; Wilmoth et al., 2005). These results also suggested that ARFs proteins play a crucial role in governing all facets of plant growth and development, such as root and leaf development, flower maturation, fruit ripening, senescence, etc. Other transcriptional factors may also be involved, working collaboratively with ARFs at various plant stages to regulate plant growth. For example, microRNA160 regulates root cap cell formation in Arabidopsis by targeting *AtARF10* and *AtARF16* (Wang et al., 2005). The positive regulators *AtARF6* and *AtARF8* and the negative regulator *AtARF17* regulate each other's expression at both transcriptional and posttranscriptional levels by modulating miR160 and miR167 availability, thus controlling the formation of adventitious roots (Gutierrez et al., 2009). *Monopteros/AtARF5* regulates the initiation of embryonic roots by controlling a mobile transcription factor, and it is probable that it plays a redundant role in the regulation of lateral root formation through transcriptional activating the downstream target genes of *AtARF7/19* (Schlereth et al., 2010). Understanding of ARF regulatory mechanisms and their role during plant growth and development has improved in the last 20 years, but much is still not known. Functioning through nuclear auxin signaling only applies to activating ARFs, as there is little evidence indicating that repressor ARFs, which make up most of the Arabidopsis ARF family, form heterodimers with Aux/IAA repressors (Vernoux et al., 2011; Chandler, 2016). Therefore, understanding the mechanisms by which repressor ARFs regulate gene repression, as well as the ways in which other transcription factors and signaling proteins interact with ARF proteins, would be of significant interest. Furthermore, knowledge of ARFs in plant species other than the model plant Arabidopsis is limited.

1.3.4 Gretchen Hagen3 (GH3) protein family

One of the most important ways to control phytohormonal homeostasis is through hormone conjugation. Conjugated hormones serve two primary functions: either as a storage form, where the phytohormone is released through enzymatic hydrolysis when needed, or as a form that will be further metabolized to a non-bioactive product (Piotrowska and Bajguz, 2011). There are two types of phytohormone conjugates based on the type of bond involved. The first type is ester conjugates, where the hormone is linked to a sugar or alcohol through an ester linkage. The second type is amide conjugates, where the hormone is bonded to an amino acid, peptide, or poly-peptide through an amide bond (Ludwig-Müller, 2011). GH3 amido synthetases (catalyze the biosynthesis of phytohormone-amino acid conjugates through the formation of an amide bond between the carboxyl group of hormones and the amino group of an amino acid), are proposed to play important roles in phytohormone homeostasis (Guo et al., 2022; Jez, 2022; Wojtaczka et al., 2022). In Arabidopsis, 19 *GH3* genes, along with additional partial genes encoding an amino-terminal residues of a protein, have been identified (Hagen and Guilfoyle, 2002; Wang et al., 2008). While there are different classifications of the GH3 family based on various criteria, it is generally divided into three groups based on phylogenetic relationships, gene structure and protein function (Okrent and Wildermuth, 2011). Group I consists of GH3.10 and GH3.11. The largest group II has eight members, including GH3.1, GH3.2, GH3.3, GH3.4, GH3.5, GH3.6, GH3.9, and GH3.17. It has been confirmed that all group II GH3 proteins possess the ability to conjugate auxin to amino acids (Westfall et al., 2012). Group III contains nine members, including GH3.7, GH3.8, GH3.12, GH3.13, GH3.14, GH3.15, GH3.16, GH3.18, GH3.19. The functions of the majority of GH3 proteins within this group remain largely unknown. Group II *GH3* genes can be further subdivided into three sub-groups based on phylogenetic relationships. Within each sub-group, *GH3* genes show closer relationships to other members of the same sub-group rather than to members from different sub-groups (Guo et al., 2022).

The genetic redundancy among the *GH3* genes in Arabidopsis has posed challenges for the genetic dissection of the functions of each *GH3*. Single loss-of-function mutants of *gh3.17* in Arabidopsis exhibit only minor phenotypic changes including longer hypocotyls compared with WT (Zheng et al., 2016). The *gh3.5 gh3.6* double mutants closely resemble the WT Arabidopsis except that the double mutants had more lateral roots (Guo et al., 2022). In this study,

gh3(1/2/3/4) and *gh3(5/6/9/17)* quadruple knockout mutants were also generated. Both quadruple mutants developed more lateral roots than WT, but *gh3(1/2/3/4)* had slightly longer primary roots while the primary roots of *gh3(5/6/9/17)* were only half the length of those of WT plants (Guo et al., 2022). Arabidopsis plants with inactivation of all group II *GH3* genes (*gh3* octuple mutants) exhibit significant phenotypes associated with auxin over-accumulation. When grown in light, the *gh3* octuple mutants display short primary roots, elongated lateral roots, dense and elongated root hairs, and elongated petioles. In dark-grown *gh3* octuple seedlings, the hypocotyls were noticeably shorter. Importantly, both IAA-Asp and IAA-Glu conjugates were undetectable in the *gh3* octuple mutants, indicating that these *GH3* genes are primary contributors to the synthesis of these IAA conjugates (Guo et al., 2022). In order to determine the specific functions of individual *GH3* genes, several *gh3* septuple mutants were compared to the *gh3* octuple mutants. The results revealed that GH3.17 primarily regulates root elongation, while GH3.9 predominantly controls fertility in Arabidopsis (Guo et al., 2022).

1.4 ROLES OF AUXIN DURING CLUBROOT DEVELOPMENT

1.4.1 *TIR1/AFB* family genes

Auxin has been implicated in development of stem/root hyperplasia and hypertrophy during the secondary phase of clubroot in Brassica species (Ludwig-Müller et al., 2009). However, understanding the specific mechanisms of how the pathogen modifies the host's auxin biosynthesis, signaling and transport pathway to bring the hyperplasia and hypertrophy requires more research. As a central component of auxin signaling, few studies have conducted research on the role of auxin receptors in clubroot disease. In recent years, studies have suggested that auxin receptors are involved in the process of clubroot formation (Ludwig-Müller, 2014). In two-week-old seedlings of *B. juncea* var. *tumida*, RT-qPCR analysis found that the expression of *BjuTIR1A* and *BjuAFB3B* was markedly induced by *P. brassicae* treatment 6 to 72 hours after inoculation (Cai et al., 2019). In Arabidopsis (Col-0), a significant increase in the expression of *TIR1* and *AFB1* genes was observed at 24 and 28 DAI using RT-qPCR and microarray analyses. Conversely, a decrease in *AFB2* transcript was observed at 10, 21, and 28 DAI (Jahn et al., 2013). These data suggest that *P. brassicae* infection can modify auxin receptor gene transcription in Brassica species roots. T-DNA insertion single mutants *tir1*, *afb1*, and the double mutant *afb1 afb2* were tested for disease severity 28 DAI after *P. brassicae* inoculation (Jahn et

al., 2013). At a lower spore inoculum density (10^4 spores/mL), all mutant lines exhibited an increase in disease index (higher susceptibility) compared to the WT line. It should be noted that *TIR1* and *AFB2* are main auxin receptor genes involved in auxin responses in Arabidopsis roots, so it would be useful to test the *tir1 afb2* double mutant lines for susceptibility to *P. brassicae*.

1.4.2 *Aux/IAA* family genes

Aux/IAA proteins typically exhibit a size range of 20 to 35 kDa. They have a short lifespan and are primarily found in the nucleus (Abel et al., 1994). Once auxin-induced degradation of *Aux/IAAs* occurs to derepress the transcription of auxin responsive genes, the transcription of *Aux/IAA* genes is quickly induced by auxin (Hagen, 2015) via the presence of TGTCTC auxin response promoter elements or AuxREs in the *Aux/IAA* genes. This activation occurs as early as 2 to 5 minutes after the application of auxin, leading to a rapid increase in their mRNA and protein (Hagen and Guilfoyle, 2002; Hagen, 2015).

Studies assessing gene expression changes in Brassicaceae plant hosts have found that a number of *Aux/IAAs* exhibit modified gene expression during various stages of clubroot disease progression (Siemens et al., 2006; Jahn et al., 2013; Robin et al., 2020; Zhou et al., 2020; Wei et al., 2021). In the roots of Chinese cabbage (*Brassica rapa*), the up-regulation of *IAA2* (2.4-fold), *IAA3* (1.6-fold), and *IAA5* (2.8-fold) was observed at 14 DAI during the secondary infection phase of *P. brassicae* (Robin et al., 2020). In Arabidopsis, *IAA7* was up-regulated at 17, 21, and 24 DAI in the *P. brassicae*-infected roots, while *IAA28* was always down-regulated in this time frame (Jahn et al., 2013). In addition, the comparison between *P. brassicae*-resistant and -susceptible cultivars makes it much clearer to understand the differential regulation of host *Aux/IAA* in response to the pathogen. According to the transcriptomic data analysis of the Zhou et al. (2020) study completed in the Ozga lab (unpublished data), gene expression was down-regulated for *IAA2* and *IAA3* at 7 DAI, and *IAA16* and *IAA18*, at 7 and 14 DAI with *P. brassicae* in the pathogen-resistant rutabaga cultivar (*Brassica napus subsp. rapifera*), while being either minimally affected or up-regulated in the susceptible rutabaga cultivar. In contrast, *IAA26*, and *IAA30* expression was up-regulated at 7 DAI, *IAA13* at 7 and 14 DAI, *IAA 19* at 14 DAI, and *IAA9* at 7, 14, and 21 DAI with *P. brassicae* in the pathogen-resistant rutabaga cultivar but either minimally affected or down-regulated in the susceptible rutabaga cultivar. Among these differentially regulated *Aux/IAAs*, *IAA3*, *IAA16*, *IAA18*, and *IAA19*, have been previously

reported as negative regulators of lateral root formation (Tatematsu et al., 2004; Uehara et al., 2008; Goh et al., 2012; Rinaldi et al., 2012), suggesting that the resistance might be build-up through modification of the expression of genes that code for these Aux/IAs during clubroot disease development. Mutation analysis of *axr3-1* found that the auxin-resistant and the no root hair mutant *axr3-1* exhibited partial resistance to clubroot compared to the wild-type (Alix et al., 2007). The *AXR3* gene encodes protein *IAA17* and the *axr3-1* mutation results in increased stability of *IAA17*, leading to its accumulation at high levels. Expression of *IAA17* was down-regulated at 7, 14, and 21 DAI with *P. brassicae* in the pathogen-resistant and susceptible cultivars assessed in the Zhou et al. (2020) transcriptomic database (Ozga lab, unpublished data). Other mutants in auxin response (*axr1*, *axr2*) did not show clear effects concerning a higher tolerance against clubroot (Siemens et al., 2002). The different results might be due to the functional redundancy of Aux/IAs and the present of the parallel pathways in the host plant. Therefore, the role of Aux/IAs during clubroot development needs to be further explored.

1.4.3 ARF family genes

The expression levels of both activator and repressor ARFs can be changed in host plants after infection with *P. brassicae*. *ARF5* gene expression showed down-regulation in the infected roots of Arabidopsis at 14, 17, and 21 DAI, and *ARF7* a slight down-regulation at 14 and 17 DAI, while *ARF8* showed a slight transcriptional up-regulation at 17 DAI (Jahn et al., 2013). *ARF5* and *ARF7* partially overlap in their function as positive regulators of lateral root formation (Hardtke et al., 2004). Jahn et al. (2013) suggested that a reduction in their expression levels could indicate a disruption of the organized tissue layers of roots and a reduction of lateral roots in favor of undifferentiated gall formation. Transcriptome analysis of Arabidopsis roots also revealed that *ARF3* and *ARF8* gene expression was elevated at 10 and 23 DAI with *P. brassicae* compared to the control, whereas *ARF7* expression was reduced at these time points (Siemens et al., 2006). Expression trends in the rutabaga transcriptome (Zhou et al., 2020) show that *ARF3* and *ARF19* at 14 and 21 DAI with *P. brassicae*, and *ARF5* at 14 DAI, are up-regulated or up-regulated to a greater extent in the roots of the susceptible cultivar compared to the resistant cultivar (Ozga lab, unpublished). The genes of other repressor ARFs, such as *ARF11*, which negatively regulate primary root growth, and *ARF2*, which inhibit cell division and organ growth, were highly expressed in a clubroot-resistant line of *B. rapa* L. ssp. *Pekinensis* (Yuan et

al., 2021; Li et al., 2022). In addition, the gene expression of *ARF16*, an ARF which represses primary root length and the number of lateral roots, was up-regulated in symptomless roots compared with gall tissue in *B. oleracea* var. *gongylodes* (Ciaghi et al., 2019). These results suggest that these repressor ARFs could play roles in attempts by the host plant to enhance its resistance against clubroot disease. The role of ARFs during clubroot infection can also be associated with other transcriptional factors such as MicroRNAs (miRNAs). MiRNAs are a class of small non-coding RNAs that are highly conserved and regulate gene expression through post-transcriptional repression (Bartel, 2004). The up- or down-regulation of miRNAs during clubroot development could modulate the root architecture and hormone homeostasis by targeting other transcriptional factors such as ARFs and TIR1/AFBs (Xie et al., 2000; Verma et al., 2014; Wei et al., 2023). For instance, in *Brassica rapa* L., ARF8 was found to be targeted by bra-miR167. During *P. brassicae* infection, bra-miR319 and bra-miR167 were inhibited, and their targeted genes, *TCP10* and *ARF8*, were highly expressed. The high expression of these genes contributed to IAA synthesis, leading to cell division, gall initiation, and gall expansion (Wei et al., 2023).

1.4.4 Gretchen Hagen3 (GH3) protein family

Disruption of plant hormone homeostasis is one of the most important changes that lead to clubroot gall formation after infection with *P. brassicae* (Ludwig-Müller and Schuller, 2008). The group II of GH3 protein family capable of conjugation of free IAA to amino acids and thereby inactivating the free auxin were reported to be involved in the regulation of auxin homeostasis during clubroot development (Ludwig-Müller, 2014). In Arabidopsis, several *GH3* genes, including *GH3.2*, *GH3.3*, *GH3.4*, *GH3.5*, *GH3.14*, and *GH3.17* were up-regulated in *P. brassicae*-infected roots at 10 to 28 DAI (Jahn et al., 2013), also *GH3.3* and *GH3.4* expression was up-regulated at 10 and 23 DAI in an Arabidopsis transcriptome analysis (Siemens et al., 2006). Similar results were also found in the roots of Chinese cabbage, where *BrGH3.3* was markedly up-regulated at 3 and 28 DAI, while *BrGH3.4* was up-regulated at 3, 14 and 28 DAI (Robin et al., 2020). The up-regulation of the group II *GH3* genes can be interpreted as means of the plant to control disease symptoms (Ludwig-Müller, 2014). Furthermore, a double mutant of *gh3.5gh3.17* in Arabidopsis demonstrated higher susceptibility to the clubroot pathogen compared to the wild type (Jahn et al., 2013). The susceptibility could be due to elevated levels

of auxin when the conjugation of IAA to the inactive forms is reduced in the double mutant. The GH3 protein family is also the target of ARF transcription factors and it has been reported that *GH3* gene expression is mediated via the nuclear auxin signaling pathway mediated by the TIR receptor family of F-box proteins (Woodward and Bartel, 2005; Lavy and Estelle, 2016). Therefore, the TIR pathway controls auxin balance through the up-regulation of the GH3 auxin conjugate synthetases, which in turn leads to higher expression of *GH3* genes that inhibit auxin signaling by inactivating IAA via conjugation. This feedback loop could be a potential resistance mechanism established by host plants against clubroot.

1.5 ROLES OF SALICYLIC ACID (SA) AND JASMONIC ACID (JA) RESPONSE DURING CLUBROOT DEVELOPMENT

SA and JA are key phytohormones that regulate many physiological processes and defense against various plant diseases. Current thinking is that SA induces resistance against biotrophic and hemi-biotrophic pathogens, and JA induces resistance against necrotrophic pathogens and most insect herbivores (Halim et al., 2006; Robert-Seilaniantz et al., 2011; Gimenez-Ibanez and Solano, 2013). Plant immunity strongly relies on these two hormones, however, the significant overlap and crosstalk between the defense responses mediated by SA, JA, and other plant hormones make it difficult to clearly understand their role in plant resistance (Robert-Seilaniantz et al., 2011). Until now, it has been found that JA and SA defense pathways generally antagonize each other, that is, the accumulation of SA will prevent the accumulation of JA and vice versa (Grant and Lamb, 2006; Thaler et al., 2012). This antagonism has been reported in a total of 17 plant species, including 11 crop plants and six wild species and there is increasing evidence for SA-JA antagonism across plant species (Thaler et al., 2012).

In general, biotrophic pathogen infections that induce SA production in plants tend to inhibit JA-dependent defenses, indicating that the plants prioritize the allocation of resources towards SA-dependent defense rather than JA-dependent responses. Conversely, when pathogens trigger the JA pathway, it can suppress the SA response in plants, for example, the application of JA depresses the expression of SA-dependent genes (Niki et al., 1998; Spoel et al., 2007). Mutation analysis also support this trend. For example, mutations that affect JA signaling that lead to an increase in the expression of the SA-dependent *PR-1* gene, result in improved resistance to *P. syringae* and *P. parasitica* (Kloek et al., 2001; Shah et al., 2001). Conversely,

plants with mutations that hinder SA accumulation exhibit elevated levels of JA-dependent gene expression when exposed to different stimuli compared to their wild-type counterparts (Gupta et al., 2000). In recent years, the identification of receptors of both hormones as well as many transcriptional factors or components involved in their signaling pathways has facilitated the understanding of SA–JA crosstalk. In Arabidopsis, SA signaling pathway requires the *AtNPR1* (*Non expressor of Pathogenesis-Related gene 1*), a redox-sensitive master regulator and a SA receptor (Tada et al., 2021). After being exposed to a pathogen, SA biosynthesis can be triggered (Figure 1.4). In Arabidopsis, approximately 90 % of pathogen-induced SA originates from isochorismate, a compound derived from chorismate through the enzymatic activity of ISOCHORISMATE SYNTHASE1 (ICS1), which is localized in the plastids (Rekhter et al., 2019). The downstream pathway of isochorismate involves only two additional proteins: ENHANCED DISEASE SUSCEPTIBILITY5 (EDS5), responsible for transporting isochorismate from the plastids to the cytosol, and *avrPphB* SUSCEPTIBLE3 (PBS3), a cytosolic amidotransferase. PBS3 plays a crucial role by catalyzing the conjugation of glutamate to isochorismate, resulting in the formation of isochorismate-9-glutamate. This compound then undergoes spontaneous decomposition, giving rise to SA and 2-hydroxy-acryloyl-N-glutamate (Rekhter et al., 2019). The accumulation of SA leads to the expression of *AtNPR1* genes and proteins. Then the *AtNPR1* protein goes through conformational changes, which enable its translocation into the nucleus where it indirectly activates *PATHOGENESIS-RELATED (PR)* gene expression by recruiting TGACG-binding (TGA) transcription factors (Gimenez-Ibanez and Solano, 2013; Withers and Dong, 2016; Backer et al., 2019). The accumulation of PRs increases the host resistance against pathogens by inducing the systemic acquired resistance (SAR), a long lasting systemic broad-spectrum resistance that provides effective protection against a diverse range of pathogenic organisms, including bacteria, fungi, oomycetes, viruses, and nematodes (Klessig et al., 2018). Arabidopsis *npr1* mutants that are deficient in SA signaling showed decreased SAR-triggered *PR* gene expression, specifically *PR1* and *PR5* and increased disease susceptibility, suggesting a central role for *PR* gene-induced SAR in SA induced defence response (Glazebrook et al., 1996). The JA signaling pathway is similar to the auxin signaling pathway which involves SCF-TIR1/AFB receptor and AUX/IAA repressor components. JA responses are regulated through the F-box COI1 (Coronatine-insensitive 1) SCF (Skip-Cullin-F-box) E3 ubiquitin ligase complex and JAZ (jasmonate ZIM-domain) repressors. The recognition

of JA through SCF-COI1 E3 complex leads to proteasome degradation of JAZ proteins activating the downstream transcriptional responses (Thines et al., 2007). When JA concentration is low, JAZ proteins cannot be degraded, they will repress the JA-responsive ethylene-signaling genes *EIN3* (*Ethylene 3*)/*EIL1* (*Ethylene insensitive 3 like 1*), which when expressed leads to suppression of SA synthesis (Chen et al., 2009). On the other hand, SA inhibits JA signaling downstream of the SCF-COI1-JAZ receptor complex by targeting GCC-box motifs in JA-responsive promoters via a negative effect on the accumulation of the transcriptional activator ORA59 (Octadecanoid-Responsive Arabidopsis 59; Van der Does et al., 2013). SA reduces the accumulation of the GCC-box binding transcription factor ORA59, indicating that the antagonistic effect of SA on JA signaling is regulated through transcriptional control by modifying the levels of ORA59. Other regulatory factors that are known to be involved in the SA–JA antagonism including NPR1, WRKY70 (WRKY DNA-binding protein 70), GRX480 (Glutaredoxin 480), ERF1 (Ethylene Response Factor 1), MYC2 (Jasmonate Insensitive 1, Jin1), JAZ1-JAZ3 (Jasmonate Zim-Domain) (Thaler et al., 2012). Although there is growing understanding of the involvement of genes and proteins in SA-JA antagonism, the molecular mechanisms of antagonism remain unclear. In addition, it has been suggested that the antagonism is highly variable both in terms of what is used to induce SA and JA, the timing of induction, and the potential role of genetic variations underlying the antagonism (Thaler et al., 2012). Recently, synergistic SA-JA interactions have also been found in *Populus* and rice, indicating the complexity of crosstalk between SA and JA in plant defense (Ullah et al., 2023).

In the case of clubroot infection, exogenous SA and JA pre-treatment can reduce clubroot disease significantly (Agarwal et al., 2011; Lovelock et al., 2013; Xi et al., 2021; Mencia et al., 2022). It has been suggested that exogenous SA can elevate the levels of gene expression and antioxidant enzyme activities, thereby reducing the contents of reactive oxygen species (ROS) and membrane lipid peroxidation, leading to increased clubroot resistance (Ji et al., 2020). However, the capacity to reduce disease symptoms seems to be dependent on several factors, including application methods (treatment of the soil vs. dipping of the roots), different isolates of *P. brassicae*, the specific timing of treatment, as well as the concentrations of SA or JA employed (Lovelock et al., 2016). SA-JA antagonism also occurred and showed different expression patterns in resistant and susceptible cultivars during clubroot infection. For instance, genes involved in SA-mediate response or SA-signaling pathway were highly up-regulated in the

resistant cultivars of Chinese cabbage and rutabaga (*B. napus*), while JA-mediated responses seemed to be mostly inhibited in these lines (Chen et al., 2016; Galindo-González et al., 2020). In *Arabidopsis*, when monitoring SA and JA responsive genes in infected roots of two accessions: Col-0 (susceptible) and Bur-0 (partially resistant), it was found that SA signaling was activated in Bur-0 but not in Col-0. On the other hand, the JA pathway showed weak activation in Bur-0, whereas it was strongly induced in Col-0 (Lemarié et al., 2015). Also, the activation of WRKY70 (a key regulator of antagonistic responses between SA and JA) was observed in *Arabidopsis* Bur-0 upon *P. brassicae* infection and the induction of SA-mediated defenses and the repression of JA-mediated responses were detected (Jubault et al., 2013). Overall, these results suggest that SA-JA antagonism occurs during clubroot development.

Arabidopsis mutants that affect SA or JA biosynthesis, signaling, or transport pathway were also used as tools to understand the role of SA and JA in clubroot disease defense. The constitutive expressor of *PR genes 5* (*cpr5-2*) and *defense, no death* (*dnd1*) mutants, in which SA responses are constitutively induced, were found to be more resistant to clubroot than the corresponding wild type, while SA-deficient lines [(*NahG*, encoding an SA hydroxylase that degrades SA to catechol), *SA induction-deficient* (*sid2*) and *non-expresser of PR genes* (*npr1*)] that are impaired in SA signaling were highly susceptible to the pathogen (Lemarié et al., 2015; Lovelock et al., 2016). These results suggest that SA signaling is an important defense mechanism against clubroot disease. Additionally, the JA signaling-deficient mutant *jar1* exhibited heightened susceptibility to clubroot, indicating that JA signaling also plays a role in partial inhibition of clubroot development. Moreover, the more pronounced resistance of the *cpr5-2* mutant to clubroot compared to the highly activated JA responses in *eds5-1* implies that the SA pathway is more effective than the JA pathway in conferring clubroot resistance (Lemarié et al., 2015). In general, constitutive SA or JA supply to the plant results in stunted growth. However, a recently characterized protein, Oxidation Resistant 2 (OXR2), was shown to enhance the constitutive SA defense pathway without compromising plant growth in *Arabidopsis*. *Arabidopsis* plants that overexpress *AtOXR2* exhibited a significant reduction in clubroot symptoms and improved growth performance compared to the wild type (Mencia et al., 2022). The findings might help in controlling clubroot disease in the field other than SA or JA pre-treatment.

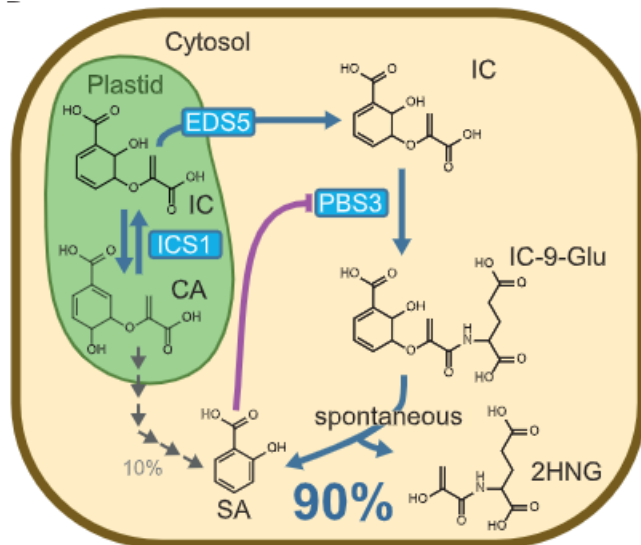


Figure 1.4 Pathogen-induced SA biosynthesis in Arabidopsis. Approximately 10 % of the defense-associated SA is synthesized through the cytosolic PHENYLALANINE AMMONIA LYASE pathway, while the majority, around 90 %, is derived from isochlorismate produced by the plastid-localized enzyme ICS1. The protein EDS5 facilitates the transport of isochlorismate from the plastid to the cytosol. Within the cytosol, PBS3 metabolizes isochlorismate, leading to the formation of isochlorismate-9-glutamate. Through subsequent nonenzymatic decomposition, SA is generated. Figure from Rekhter et al. (2019), with permission.

1.6 HYPOTHESIS TO BE TESTED

The hypothesis to be tested is that the modulation of auxin signaling in the genetic model species *Arabidopsis* that results in altered auxin response will modify *P. brassicae*-induced gall development.

1.7 RESEARCH OBJECTIVES

Objective 1: Test the ability of *P. brassicae* to induce clubroot symptoms in *Arabidopsis* double and quadruple auxin receptor mutant lines.

Objective 2: Characterization of the effects of clubroot infection on *Arabidopsis* auxin receptor mutant lines and these lines expressing the pea *AFB6* (*PsAFB6*) auxin receptor gene.

Objective 3: Determine if auxin and SA-related gene expression is differentially regulated in *Arabidopsis* auxin receptor mutant and/or *PsAFB6*-expressing lines when infected with *P. brassicae* using qRT-PCR. The genes of interest would be marker genes in three different

parts of the auxin response pathway where their gene expression was differentially modulated in *P. brassicae*-resistant and susceptible cultivars of *B. napus*. The first category includes members of the Aux/IAA transcriptional repressors of early auxin-signaling pathway, *IAA9*, *IAA16*, and *IAA19*. The second category includes members of the auxin response factor family, *ARF3*, *ARF5*, and *ARF19*. The third category includes members of the IAA-amino acid conjugate synthetases (GH3 group II protein family) capable of conjugation of free IAA to amino acids, *GH3.3* and *GH3.17*. The link between the SA-mediated defense system and expression of *PsAFB6* in Arabidopsis auxin receptor mutant lines will also be explored by profiling gene expression changes of the key SA biosynthesis (*isochorismate synthase 1*; *ICS1*). As a central component of the SA signaling pathway, and the *PR gene (PR5)* will be monitored to find out if SA signaling pathway was significantly changed after clubroot infection in the *PsAFB6*-expressing auxin receptor mutant lines.

Chapter 2: Effect of pea PsAFB6 auxin receptor on auxin-induced root inhibition in *PsAFB6*-transformed *Arabidopsis* auxin receptor mutant lines

2.1 INTRODUCTION

Recent advancements in auxin biology, specifically in *Arabidopsis thaliana*, have yielded substantial progress in understanding the components and mechanisms responsible for auxin perception and response (Salehin et al., 2015; Lavy and Estelle, 2016). As discussed in Chapter 1, at low levels of auxin, Aux/IAA proteins associate with ARF proteins, repressing transcription of auxin-regulated genes. At high auxin levels, auxin acts as ‘a molecular glue’, binding TIR1/AFB receptor and Aux/IAA proteins together, leading to poly-ubiquitination of the Aux/IAAs and their degradation in the 26S proteasome. The released ARFs allows the transcription of auxin responsive genes (Lavy and Estelle, 2016).

Phylogenetic analysis revealed that the TIR1/AFB auxin-receptor protein family is divided into four clades (TIR1, AFB2, AFB4, and AFB6), with *Arabidopsis* containing three clades (AtTIR1 and AtAFB1 through AtAFB5; Parry et al., 2009), while pea (*Pisum sativum* L.) harbors gene members from all four clades (TIR1a and TIR1b; AFB2; AFB4; AFB6; Jayasinghege et al., 2019). All six members of the TIR1/AFB family of receptors in *Arabidopsis* (Mockaitis and Estelle, 2008; Parry et al., 2009; Prigge et al., 2016; Prigge et al., 2020), and all five members of the TIR1/AFB family of receptors in pea (Ozga et al., 2022), were able to bind Aux/IAA co-receptors in an auxin-dependent manner.

Most studies focused on the functions of auxin receptors are in the model species *Arabidopsis*. Loss or gain-of-function mutation analysis revealed that TIR1 and AFB2 have a prominent role in regulating auxin response in roots (Parry et al., 2009), while AFB1 primarily controls the initial phase of root gravitropic response (Prigge et al., 2020). The *Arabidopsis Atafb4-8* single mutant possessed a larger proportion of small axillary branches (< 5 mm) in comparison to WT, indicating that AtAFB4 controls shoot branching in *Arabidopsis* (Ligerot et al., 2017). For pea auxin receptors, root elongation assays were performed to determine the role of PsTIR1a, PsTIR1b, and PsAFB2 in *Arabidopsis* (Jayasinghege et al., 2019). Transgenic *Arabidopsis* plants expressing PsTIR1a, PsTIR1b, or PsAFB2 exhibited 2,4-D-induced inhibition of root growth in *Arabidopsis* mutants *tir1-10* and/or *tir1-10afb2-3*, reaching levels similar to those observed in mutants expressing the AtTIR1 transgene and resembling the auxin

root-inhibiting activity seen in wild-type seedlings. This restoration of auxin-sensitive root growth in the auxin-resistant mutants demonstrated that these pea auxin receptor genes can complement *AtTIR1* as an auxin receptor in Arabidopsis plants, and indicate that they have a prominent role in regulating auxin response in pea roots (Jayasinghe et al., 2019). In pea, the *RMS2* gene was found to encode the pea auxin receptor AFB4 (Ligerot et al., 2017). The *rms2* mutant exhibited reduced transcript levels of Strigolactones (SLs) biosynthesis genes as well as increased shoot branching, indicating that AFB4 regulates SLs biosynthesis and shoot branching in pea (Ligerot et al., 2017).

Little is known about the function of the AFB6 auxin receptor clade in plants. The presence of the AFB6 clade prior to the divergence of angiosperm and gymnosperm lineages and their continued existence in certain plant families imply that they might have distinct or specialized functions (Parry et al., 2009). In tomato, SlAFB6 is implicated in compound leaf development (Ben-Gera et al., 2012). In pea (*Pisum sativum* L.), pericarp (ovary) *PsAFB6* expression was suppressed by seeds and auxin (4-Cl-IAA), and increased more than 3-fold in response to pericarp deseeding (seed removal; Ozga et al., 2022). Ethylene increased *PsAFB6* transcript abundance during early pericarp development suggesting a unique role for PsAFB6 in ethylene signaling during fruit development (Ozga et al., 2022).

To further explore the function of AFB6 auxin receptors, Arabidopsis auxin receptor double (*tir1 afb2*) and quadruple mutant (*tir1 afb2 afb4 afb5*) lines transformed with the pea auxin receptor *PsAFB6* were used as a tool to test if the pea AFB6 auxin receptor modifies response to auxin in Arabidopsis root growth assays.

2.2 MATERIALS AND METHODS

2.2.1 Plant materials

A description of the Arabidopsis auxin receptor mutant and pea auxin receptor *PsAFB6*-expressing Arabidopsis lines used in this study and the method for transformation of the transgenic lines, are given below. All the Arabidopsis lines used in this study in Chapter 2 were created prior to this project by other members of the Ozga lab. All Arabidopsis lines are in the Columbia ecotype background (Col-0). The wild-type (Col-0 WT designated as WT), auxin receptor double mutant *tir1-10 afb2-3 C* (designated as *tir1afb2C*), and auxin receptor quadruple mutant *tir1-10 afb2-3 afb4-8 afb5-5* (designated as *tir1afb245*) were used. The auxin receptor double and quadruple mutant lines were created using the available single T-DNA insertion mutants from the Arabidopsis Biological Resource Center (Jayasinghe et al., 2019). The T-DNA insertion information of the double and quadruple mutant lines is shown in Appendix Figure A1. The *tir1-10* allele (SALK_090445C) had a T-DNA insertion within the coding region near the 5' end of the gene and was unable to generate full-length transcripts (Parry et al., 2009). In contrast, the *afb2-3* allele (SALK_137151) had T-DNA inserted 37 bp upstream of the transcriptional start site that produced reduced levels of *AFB2* transcript, suggesting the *afb2-3* line likely retained some *AFB2* function (Parry et al., 2009). The *afb4-8* (SALK_201329) and *afb5-5* (SALK_110643) lines with T-DNA insertions in exon 2 and intron 1 regions of the genes, respectively, resulted in the loss of production of full-length mRNA suggesting these alleles are null mutants (Prigge et al., 2016).

The expression of the pea auxin receptor gene *PsAFB6* is driven by the constitutive CaMV-35S promoter in the Arabidopsis transgenic lines. Two independently transformed lines in the auxin receptor double mutant background (*PsAFB6* in *tir1-10 afb2-3 4-8* designated as *PsAFB6/+ 4-8 tir1afb2*; *PsAFB6* in *tir1-10 afb2-3 3-3* designated as *PsAFB6/+ 3-3 tir1afb2*), and three independently transformed lines in the quadruple auxin receptor mutant background (*PsAFB6* in *tir1-10 afb2-3 afb4-8 afb5-5 1-6* designated as *PsAFB6/+ 1-6 tir1afb245*; *PsAFB6* in *tir1-10 afb2-3 afb4-8 afb5-5 3-2* designated as *PsAFB6/+ 3-2 tir1afb245*; *PsAFB6* in *tir1-10 afb2-3 afb4-8 afb5-5 5-9* designated as *PsAFB6/+ 5-9 tir1afb245*) were used. The transgenic *PsAFB6*-expressing Arabidopsis lines were created using a GV3101-pCam1300 plasmid containing *PsAFB6* driven by the CaMV-35S promoter. Agrobacterium-mediated transformation using the floral dip method was used for generating Arabidopsis *PsAFB6*-expressing transgenic

lines (Jayasinghege et al., 2019). PCR was used to confirm *PsAFB6* gene insertion and hygromycin was used to select for homozygous *PsAFB6* lines.

2.2.2 Arabidopsis root growth assays

The auxin receptor double mutant line *tir1afb2C* and quadruple mutant line *tir1afb245*, along with *PsAFB6*-expressing lines in the double (*PsAFB6/+ 4-8 tir1afb2*; *PsAFB6/+ 3-3 tir1afb2*) and quadruple auxin receptor mutant (*PsAFB6/+ 1-6 tir1afb245*; *PsAFB6/+ 3-2 tir1afb245*; *PsAFB6/+ 5-9 tir1afb245*) background, as well as the Columbia wild-type (WT) line were tested for their ability to exhibit auxin-induced (2,4-D) inhibition of root growth with standard root growth assays (Jayasinghege et al., 2019).

For performing root growth assays, Arabidopsis seeds were surface sterilized with 1.5 mL of 70 % ethanol for 2 minutes, followed by second sterilization with 1.5 mL of 2 % NaOCl containing 0.1 % Tween-80 for 10 minutes while vortexing every 2-3 minutes. After sterilization, seeds were washed with sterile water at least three times and re-suspended in 1 mL of sterile water. The seeds were then kept in dark at 4 °C for four days for seed stratification for all lines. Following seed stratification, using a 1 mL sterile pipette tip, individual drops with 1-2 seeds per drop (reduced to 1 seed per drop on plate) were placed in 2 parallel lines (as shown in Appendix Figure A2) onto round plastic 100 x 20 mm Petri plates (TC Dish 100, Sarstedt, Nümbrecht, Germany) containing 1 % aqueous (w/v) bactoagar prepared in half-strength Murashige and Skoog (MS) medium and 1 % (w/v) sucrose (seeds of one mutant or transformed line per plate). Excess water was removed from the plates, the plates were sealed with breathable tape (3M Micropore, St. Paul, Minnesota, USA) and plates were moved to the growth chamber maintained at 22 °C supplemented with continuous (24 h light) cool white-fluorescent light at $155 \pm 20 \mu\text{E m}^2 \text{s}^{-2}$ measured using a LI-188 photometer (Li-Cor Biosciences, Lincoln, Nebraska, USA). The Petri plates were placed in a vertical position and seeds germinated and seedlings were grown vertically for 4 days in a growth chamber for all seed lines except for the auxin receptor quadruple mutant and *PsAFB6* transformed lines in the quadruple mutant background. Seeds of the auxin receptor quadruple mutant grown together with *PsAFB6* transformed lines in the quadruple mutant background were placed onto the petri plates following four days of stratification and then plates were moved to the growth chamber for 5 days to allow an extra day of growth of these quadruple mutants and transformed plants. Four- or

five-day-old uniform-sized seedlings (uniform size across all lines that were grown together) were transferred with a sterilized tweezer to newly prepared bactoagar plates with or without 2,4-D (70 nM) with one exception. On the day of seedling transfer from the bactoagar plates to assay plates with or without 2,4-D, the uniform sized quadruple mutant *tir1afb245* seedlings were shorter in length compared to the uniform-sized seedlings of WT and auxin receptor double mutant *tir1afb2C* in the growth assays where these lines were grown together. To prepare the bactoagar plates supplemented with 2,4-D, filter-sterilized 2,4-D solution was added to autoclaved bactoagar media that was warm and still in liquid state to make the final of 2,4-D concentration to 70 nM. The bactoagar solution (with or without 2,4-D) was mixed thoroughly by swirling and approximately 25 mL of media was poured into each plate. The plates were used within 1-2 days after media preparation. In total six seedlings belonging to three different lines (2 technical replicates per line, 3 lines per Petri plate) were transferred to each bactoagar plate with or without 2,4-D, as shown in Appendix A Figure A2.

Root growth in length was assessed 3 days after transferring seedlings to the root assay plates (media with or without 2,4-D). Lateral root number was counted and root length was measured 5 days after transferring seedlings to the root assay plates to calculate the lateral root density. Sets of root growth assays were conducted with seedlings belonging to different lines categorized in groups as shown in Appendix A Figure A2. Seedlings of different lines within each group were grown together as a set in a growth chamber, two or three sequential sets of seedlings belonging to different lines within each group were grown in the same growth chamber and data from 2 or 3 sequential sets were pooled for obtaining percent root elongation data. The root growth assays for comparing WT, *tir1afb2C* and *tir1afb245* lines categorized in group 1 were conducted in two sequential sets [one set = 38-40 plates per treatment (control or 2,4-D); 76-80 plates total per set] in the same growth chamber (see Appendix A Figure A2 for details). For performing root growth assays with Arabidopsis *PsAFB6*-transgenic lines in the auxin receptor double mutant background categorised in group 2 of Appendix A Figure A2, a total of six seedling per plate composed of two seedlings each of WT, *tir1afb2C* and the independent *PsAFB6*-transgenic lines in the double mutant background represented in two different combinations (combination ii: *PsAFB6/+ 4-8 tir1afb2* or combination iii: *PsAFB6/+ 3-3 tir1afb2*) were performed in two sequential sets in the same growth chamber. The first set consisted of a total of 40 plates [10 plates each of control and 2,4-D media for each transgenic

line (*PsAFB6/+ 4-8 tir1afb2* line and *PsAFB6/+ 3-3 tir1afb2* line)]. The second set consisted of 80 plates total [20 plates each of control and 2,4-D media for each transgenic line (*PsAFB6/+ 4-8 tir1afb2* line and *PsAFB6/+ 3-3 tir1afb2* line)]; see Appendix A Figure 2 for details]. For performing root growth assays with *PsAFB6*-transgenic lines in the auxin receptor quadruple mutant background categorised in group 3 of Appendix A Figure A2, a total of six seedling per plate composed of two seedlings each (technical replicates) of *tir1afb245* along with two seedlings each of *PsAFB6*-transgenic lines in three different combinations (combination iv: *PsAFB6/+ 1-6 tir1afb245* and *PsAFB6/+ 3-2 tir1afb245*; combination v: *PsAFB6/+ 1-6 tir1afb245* and *PsAFB6/+ 5-9 tir1afb245*; combination vi: *PsAFB6/+ 3-2 tir1afb245* and *PsAFB6/+ 5-9 tir1afb245*; Appendix A Figure A2) were performed in three sequential sets in the same growth chamber. The first two sets had a total of 30 plates each (5 plates each of control and 2,4-D media for each line combination within group 3 noted above. The third set was composed of 10 plates each of control and 2,4-D media for each line combination within group 3 noted above; see Appendix A Figure 2 for details).

The plates were initially scanned with an Epson Perfection V850 Pro flatbed scanner (<https://epson.ca>) and images were captured using winRhizo 2020 software on the day the uniform-sized seedlings were transferred to assay plates with or without 2,4-D (day 0 of assay). After scanning, the plates were moved back to the same growth chamber and positioned vertically for further seedling growth. After 3 and 5 days of vertical growth in the growth chamber (days 3 and 5 of assay), the inner surface of the lid of each plate was wiped with a Kimwipe under a laminar flow hood to remove moisture and were rescanned as noted above. The root length of each seedling was measured in the captured images using ImageJ software (<http://rsb.info.nih.gov/ij/>). To accurately measure the root length of each seedling in the software, free hand line was selected to trace the length of the root for measuring the root length at day 3 and day 5 of the root growth assay. Since each image was scanned at original scale, the measured root length was the actual root length. The root length measurements were also validated using a measuring ruler at day 3. The increase in root length for each seedling after 3 days of growth in the assay plates with or without 2,4-D was calculated by subtracting the root length at day 0 from that at day 3 of assay. Root elongation of seedlings was calculated in the auxin-containing medium and expressed as a percentage compared to the same line grown in medium without auxin. Root growth data obtained from two or three subsequent sets of

seedlings belonging to different combinations of lines grown together were pooled to calculate percent root elongation. The number of lateral roots was counted manually and the root length was determined using ImageJ software for each seedling using the images of each line 5 days after the transfer to the assay plates with or without 2,4-D. The lateral root density (cm^{-1}) was determined by dividing the number of lateral roots for each line by the root length at day 5.

2.2.3 RNA extraction and Taqman qRT-PCR assays

To quantify *PsAFB6* gene expression in the Arabidopsis *PsAFB6*-expressing double and quadruple mutant transgenic lines, seedlings were harvested from control media root growth assay plates (no 2,4-D added) after measurement of lateral root numbers (on day 5-6 of growth in these plates) and they were dissected into roots and shoots with a scalpel and collected separately into 15 mL plastic scintillation vials placed onto dry ice and stored at $-80\text{ }^{\circ}\text{C}$. Four biological replicates of shoot tissues per line were used for total RNA extraction where each biological replicate was a pool of shoots obtained from 6 randomly selected seedlings for each line. Root tissue was limited, and problems with contamination occurred in the root samples. One biological replicate was successfully extracted for the Arabidopsis auxin receptor double mutant line and the two lines expressing the pea auxin receptor *PsAFB6* in the double mutant background (composed of a pool of roots obtained from 78 seedlings for *tir1afb2*, 40 seedlings for *PsAFB6/+ 4-8 tir1afb2* and 39 seedlings for *PsAFB6/+ 3-3 tir1afb2*). Two biological replicates of root tissues from the Arabidopsis auxin receptor quadruple mutant line and three lines expressing the pea auxin receptor *PsAFB6* in the quadruple mutant background were extracted for total RNA, where each biological replicate was a pool of roots obtained from 47-48 seedlings for *tir1afb245*, 31-32 seedlings for *PsAFB6/+ 1-6 tir1afb245*, 34-36 seedlings for *PsAFB6/+ 3-2 tir1afb245* and 33-34 seedlings for *PsAFB6/+ 5-9 tir1afb245*.

For RNA extraction, a modified Trizol-based method as described in Ozga et al. (2003) was used. The frozen root or shoot tissues were placed in 2 mL microcentrifuge tubes and ground to a fine powder with 8 3-mm glass beads per tube using a Mini-BeadBeater (Biospec Products) for duration of 30 seconds. Subsequently, 1 mL of Trizol reagent (Ambion, USA) was added to the ground tissue samples, vortexed and incubated at room temperature for 30 minutes and 200 μL of chloroform was added to separate RNA from protein and DNA. After chloroform addition, the tubes were vigorously shaken and incubated at room temperature for 5 minutes,

followed by centrifugation at 4 °C for 15 minutes at 14,800 rpm. The supernatant containing total RNA was carefully transferred to a 1.5 mL microfuge tube. To eliminate polysaccharides and proteoglycans, total RNA was precipitated with 400 µL isopropanol, 250 µL of 1 M sodium citrate (EMD Millipore, USA) and 250 µL of 1 M sodium chloride (Promega, USA). The samples were thoroughly mixed, incubated at room temperature for 15 minutes, and then centrifuged at 4 °C for 15 minutes at 14,800 rpm. Once the supernatant was removed, the RNA pellet was washed with 200 µL of 75 % ethanol to dissolve any organic impurities. Following centrifugation at 4 °C for 5 minutes at 14,800 rpm, the supernatant was discarded. Subsequently, the RNA pellet was resuspended in 600 µL of nuclease-free water (Invitrogen, USA).

For further purification and selective precipitation of RNA, the total RNA extract was subjected to an overnight incubation at 4 °C after adding 200 µL of 8 M lithium chloride (LiCl). The following day the tubes were centrifuged at 4 °C for 30 minutes at 14,800 rpm, and the supernatant was discarded. The RNA pellet was then resuspended in 400 µL of nuclease-free water and subjected to reprecipitation with 40 µL of 3 M sodium acetate (Sigma Aldrich) and 800 µL of 100 % ethanol. After an overnight incubation at -20 °C, the solution was centrifuged at 4 °C for 10 minutes at 14,800 rpm, and the supernatant was discarded. The RNA pellet was washed with 200 µL of 75 % ethanol, followed by centrifugation at 4 °C for 5 minutes at 14,800 rpm, and subsequent removal of the supernatant. The resulting RNA pellet was air-dried for 10 minutes at room temperature to eliminate any remaining ethanol and was then dissolved in 20 µL of nuclease-free water. The concentration of total RNA was determined using a NanoDrop (ND-1000 spectrophotometer, Thermo Fisher Scientific), while the purity was evaluated by measuring absorbance ratios at 260/280 nm and 260/230 nm for each sample. The total RNA samples were stored at -80 °C for DNase treatment.

To eliminate any residual DNA contamination, the high-quality total RNA samples were DNase-treated using the DNA-free kit (Ambion, USA), following the instructions provided by the manufacturer. In a new 1.5 mL microfuge tube, an aliquot of 25 µg of total RNA was diluted with nuclease-free water to a final volume of 88 µL per sample. Subsequently, 10 µL of 10x DNase reaction buffer and 2 µL of DNase I were added to each sample, which was then vortexed, briefly centrifuged, and incubated at 37 °C for 30 minutes for DNase digestion. Then 10 µL of DNase inactivating reagent was added to remove all traces of DNase and divalent cations from the reaction mixture. The mixture was vigorously vortexed for 5 minutes at room

temperature and then quickly centrifuged at 4 °C for 5 minutes at 14,800 rpm. Approximately 85 μ L of supernatant containing DNase-treated total RNA was carefully transferred to a new 1.5 mL microfuge tube and subjected to phase separation with an 85 μ L mixture of phenol:chloroform:isoamyl alcohol (Sigma Aldrich) in a ratio of 25:24:1 at pH 8. The sample was vortexed and then centrifuged at 4 °C at 14,800 rpm for 10 minutes. A 60 μ L aliquot of the upper phase was reprecipitated by adding 10 μ L of 3M sodium acetate at pH 5.2 and 300 μ L of 100 % ethanol. The mixture was vortexed, followed by an overnight incubation at -20 °C. After incubation, the sample was centrifuged at 4 °C for 30 minutes at 14,800 rpm and the supernatant was discarded. The resulting DNA-free total RNA pellet was washed with 200 μ L of 75 % aqueous ethanol by gently rolling the tubes and then centrifuged at 4 °C for 10 minutes at 14,800 rpm. The supernatant was carefully removed and the RNA pellet was air-dried before being resuspended in nuclease-free water. Integrity of total RNA of each sample was assessed using gel electrophoresis. Two clear, sharp and distinct bands of 28S and 18S rRNA were observed on 1.4 % agarose gel for each purified DNase-treated total RNA sample. The concentration and purity of the total RNA were determined using a Nanodrop spectrophotometer as described previously. The DNase-treated total RNA samples were stored at -80 °C until the qRT-PCR assays were performed.

The quantification of relative transcript abundance of candidate genes was conducted using the TaqMan One-Step RT-PCR Master Mix Reagents Kit from Applied Biosystems, in combination with the StepOnePlus Real-Time PCR System Instrument, following the protocol outlined by Kaur et al. (2021). Gene-specific primers and Taqman probes were designed using the PrimerQuest tool from IDT. The probes utilized double-quenched design, with an Iowa Black Fluorescent Quencher (IBFQ) located at the 3' end and a ZEN quencher (N, N-diethyl-4-(4-nitronaphthalen-1-ylazo)-phenylamine) positioned 9 bp from the 5' end containing the 6-FAM (6-carboxyfluorescein) fluorescent dye. Prior to the assays, the DNase-treated total RNA samples were diluted to a concentration of 40 ng/ μ L using nuclease-free water and quantified with a nanodrop spectrophotometer. Each Taqman PCR amplification reaction was composed of 5 μ L of total RNA at a concentration of 40 ng/ μ L, 1.2 μ L each of 5 μ M forward and reverse primers (Table 2.1), 0.5 μ L of 5 μ M Taqman probe, 0.5 μ L of 40x TaqMan arrayScript™ UP Reverse Transcriptase and RNase inhibitor, 10 μ L of 2x TaqMan qRT-PCR mix containing Ultra-Pure AmpliTaq Gold DNA Polymerase, Uracil-DNA glycosylase, dNTPs and dUTP, ROX

passive reference dye, optimized buffer components, and 1.6 μ L of nuclease-free water. The quantification of relative transcript abundance for each sample was performed in 2 technical replicates, in an Optical 96-well reaction plate (Applied Biosystems) covered with MicroAmp Optical Adhesive Film (Applied Biosystems) on a StepOnePlus Real-Time PCR System Instrument. Each plate included a no-template control where nuclease-free water was used instead of total RNA as the template, and a no reverse-transcriptase control. The thermocycler program was reverse transcription at 48 °C for 30 minutes, followed by enzyme activation at 95 °C for 10 minutes, followed by 40 cycles of amplification with denaturation at 95 °C for 15 seconds and annealing/extension at 60 °C for 1 minute.

The efficiency of the qRT-PCR reaction for *PsAFB6* gene was calculated by performing qRT-PCR assay with 10-fold serially diluted series containing six concentrations (1100 to 0.011 ng per well) of a total RNA sample extracted from petal tissue harvested from 100 fully open flowers of *Pisum sativum* “Carneval” cultivar (1 banner petal and two wing petals per flower). The efficiency of the qRT-PCR reaction for *AtPP2AA3* gene was calculated by performing qRT-PCR assays with 10-fold serially diluted series containing six concentrations (1725 to 0.01725 ng per well) obtained by aliquoting equal volumes of total RNA of all the sample tissues. Linear regression curves and the correlation coefficient (r^2) were obtained by plotting the Ct values against logarithmic values of total RNA concentrations for each gene. The reaction efficiency (E) of each gene amplicon was calculated using the slope of the linear regression line with the following formula: $E = (10^{-1/\text{slope}} - 1) * 100$ (Pfaffl, 2001). Primers and probes used in q-RT-PCR assays and their reaction efficiencies and r^2 are given in Table 2.1. The cycle threshold was set to 0.09. Relative transcript abundance for each sample was calculated using a modified Δ Ct method (Livak and Schmittgen, 2001; Nadeau et al., 2011; Jayasinghege, 2017).

Relative *Transcript abundance* = $(1 + \text{Efficiency})^{X - \text{AVE Ct}}$, where X is an arbitrary value equal to or greater than the highest assayed Ct value.

The arbitrary Ct value was set at 33 for *PsAFB6* target gene. The average of Ct values (AVE Ct) was obtained by averaging the Ct values of two technical replicates for each sample. The PROTEIN PHOSPHATASE 2A SUBUNIT A3 (*AtPP2AA3*) gene from *Arabidopsis thaliana* was used as a loading control for each sample when performing qRT-PCR assays. The coefficient of variation of the Ct value of all the samples for the *AtPP2AA3* gene was less than 2

%; therefore, normalizing the transcript abundance values to the reference signal was not performed (Nadeau et al., 2011).

Table 2.1 Taqman primers and probes used for quantification of gene expression in root and shoot tissues of seedlings from the root growth assays by qRT-PCR and their PCR efficiencies and r^2 values.

Gene name	Gene Accession ID	qRT-PCR Primers/Probe Sequences	PCR Efficiency (%), r^2
<i>PsAFB6</i>	KY829119	F: 5'-TCGCTACCGTAGTCCAAAAGT-3' R: 5'-TGCTGGCCAGGGTTCATTA-3' P: 5'-CCCGACTTTACTCATTCCGCCTCTGC-3'	93.81, 0.9960
<i>AtPP2AA3</i>	AT1G13320.1	F: 5'-AGCATGGCCGTATCATGTTCT-3' R: 5'-TGGCCAAAATGATGCAATCTC-3' P: 5'-CACAAACCGCTTGGTTCGACTATCGGAAT-3'	98.77, 0.9985

2.2.4 Statistical analyses

Statistical analysis was performed using IBM SPSS Statistics software version 27.0.1 and RStudio version 2023.06.2+561. For percent root elongation, independent Student's t-test (two-tailed) was used to compare differences between means of the control (no 2,4-D) and 2,4-D treatment within the same line using SPSS. Data were assumed to be distributed normally and homogeneity of variance was assessed with Levene's test. For the number of lateral roots parameter, the experimental design was a two factorial (lines x treatment, control or 2,4-D) with comparison of lines within groups (group 1: WT, *tir1afb2* and *tir1afb245*; group 2: WT, *tir1afb2*, *PsAFB6/+ 4-8 tir1afb2* and *PsAFB6/+ 3-3 tir1afb2*; group 3: *tir1afb245*, *PsAFB6/+ 1-6 tir1afb245*, *PsAFB6/+ 3-2 tir1afb245* and *PsAFB6/+ 5-9 tir1afb245*). A two-way analysis of variance (ANOVA) was performed followed by pairwise comparisons of means with Least Significant Difference (LSD) post-hoc tests using RStudio. Statistical significance was declared at $P \leq 0.05$.

For Taqman qRT-PCR assays, prior to conducting the statistical analysis, the transcript abundance of *PsAFB6* gene was converted to a log₂ scale. Data were assumed to be normally distributed and assessed for homogeneity of variances with Levene's test. A one-way analysis of variance (ANOVA) was performed on the transcript abundance of *PsAFB6* gene in shoots of *Arabidopsis PsAFB6* transformed auxin receptor double and quadruple mutant lines followed by

a LSD post-hoc mean separation test using SPSS. Statistical significance was declared at $P \leq 0.05$.

2.3 RESULTS

2.3.1 *PsAFB6* quantification using qRT-PCR assays in roots and shoots of Arabidopsis transgenic lines used for root growth assays

PsAFB6 transcripts were present in the root and shoot tissues of all Arabidopsis *PsAFB6* transgenic lines in both *tir1afb2* double and *tir1afb245* quadruple mutant backgrounds. No *PsAFB6* transcripts were detected in the non-transgenic auxin receptor double and quadruple mutant lines (Figure 2.1). Although for the root tissue only one biological replicate was assessed for each line of the double mutants expressing *PsAFB6* and two biological replicates for each line of the quadruple mutants expressing *PsAFB6* due to minimal amounts of tissues available, *PsAFB6* transcripts were higher in the roots than the shoot tissues in all transgenic lines (7.2 to 10.7-fold; specifically: 8.6-fold for *PsAFB6/+ 4-8 tir1afb2*, 10.7-fold for *PsAFB6/+ 3-3 tir1afb2*, 8.9-fold for *PsAFB6/+ 1-6 tir1afb245*, 8.6-fold for *PsAFB6/+ 3-2 tir1afb245* and 7.2-fold for *PsAFB6/+ 5-9 tir1afb245*; Figure 2.1). In the shoot tissues (4 biological replicates per line), the *PsAFB6* transgenic lines in the *tir1afb2* double mutant background had an average of at least 0.77×10^5 relative transcript abundance (Ct=22.6; *PsAFB6/+ 3-3 tir1afb2*), with *PsAFB6/+ 4-8 tir1afb2* containing higher levels (Ct=18.2; Appendix Figure A3B). The shoot tissues of the quadruple mutant *PsAFB6* transformed lines had an average of at least 0.53×10^5 relative transcript abundance (Ct=23.0; *PsAFB6/+ 5-9 tir1afb245*), with *PsAFB6/+ 1-6 tir1afb245* and *PsAFB6/+ 3-2 tir1afb245* containing higher levels (Ct=21.5 and 21.2, respectively; Appendix A Figure A3; Appendix Table A1).

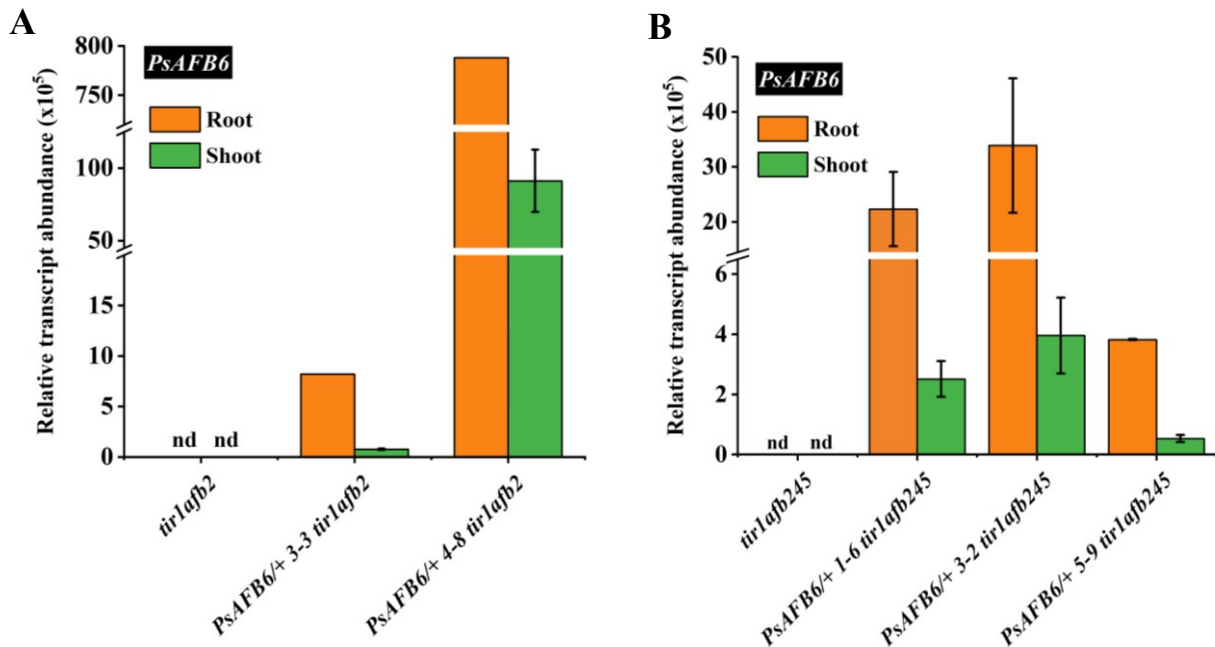


Figure 2.1 Transcript abundance of *PsAFB6* in root and shoot tissues of Arabidopsis *tir1afb2* double and *tir1afb245* quadruple mutants and mutants expressing *PsAFB6*.

PsAFB6 transcript abundance in root and shoot tissues of ten-day-old seedlings of the Arabidopsis non-transgenic *tir1afb2* line and lines transformed with *PsAFB6* in this mutant background (*PsAFB6/+ 3-3 tir1afb2* and *PsAFB6/+ 4-8 tir1afb2*) (A). *PsAFB6* transcript abundance in root and shoot tissues of eleven-day-old seedlings of the Arabidopsis non-transgenic *tir1afb245* line and lines transformed with *PsAFB6* in this mutant background (*PsAFB6/+ 1-6 tir1afb245*, *PsAFB6/+ 3-2 tir1afb245* and *PsAFB6/+ 5-9 tir1afb245*) (B). Seedlings were grown on media for root growth assays for 10-11 days prior to separately harvesting the root and shoot tissues for qRT-PCR. Shoot data are means \pm standard error (SE), n = 4, each biological replicate is a pool of shoots obtained from 6 randomly selected seedlings for each line. Root data for the *tir1afb245* quadruple mutant and its *PsAFB6*-expressing transgenic lines in this background are means \pm standard error (SE), n = 2. For the *tir1afb2* double mutant and *tir1afb2* lines expressing *PsAFB6*, n = 1. Each biological replicate of root tissue is a pool of roots obtained from 78 seedlings for *tir1afb2*, 40 seedlings for *PsAFB6/+ 4-8 tir1afb2*, 39 seedlings for *PsAFB6/+ 3-3 tir1afb2*, 47-48 seedlings for *tir1afb245*, 31-32 seedlings for *PsAFB6/+ 1-6 tir1afb245*, 34-36 seedlings for *PsAFB6/+ 3-2 tir1afb245* and 33-34 seedlings for *PsAFB6/+ 5-9 tir1afb245*. nd: no *PsAFB6* transcripts were detected.

2.3.2 *PsAFB6* expression reduced the auxin response in Arabidopsis root growth assays

In root growth assays, the non-transgenic Arabidopsis *tir1afb2* mutant seedlings showed reduced auxin sensitivity (greater root elongation, 88.7-90.7 % root elongation in 2,4-D treatment relative to control) in the presence of 2,4-D (70 nM) compared to that of the Col-0 WT (7.1-11.97 % root elongation in 2,4-D treatment relative to control) as expected (Figure 2.2A and B). The quadruple-mutant *tir1afb245* exhibited a similar reduction in 2,4-D sensitivity (88.3 % root elongation in 2,4-D treatment relative to control) as that of the *tir1afb2* double mutant (88.7 % root elongation in 2,4-D treatment relative to control). Auxin receptor double and quadruple mutant lines transformed with the pea auxin receptor gene *PsAFB6* exhibited no 2,4-D-induced root growth reduction compared to the control mutant background lines (Figure 2.2B and C).

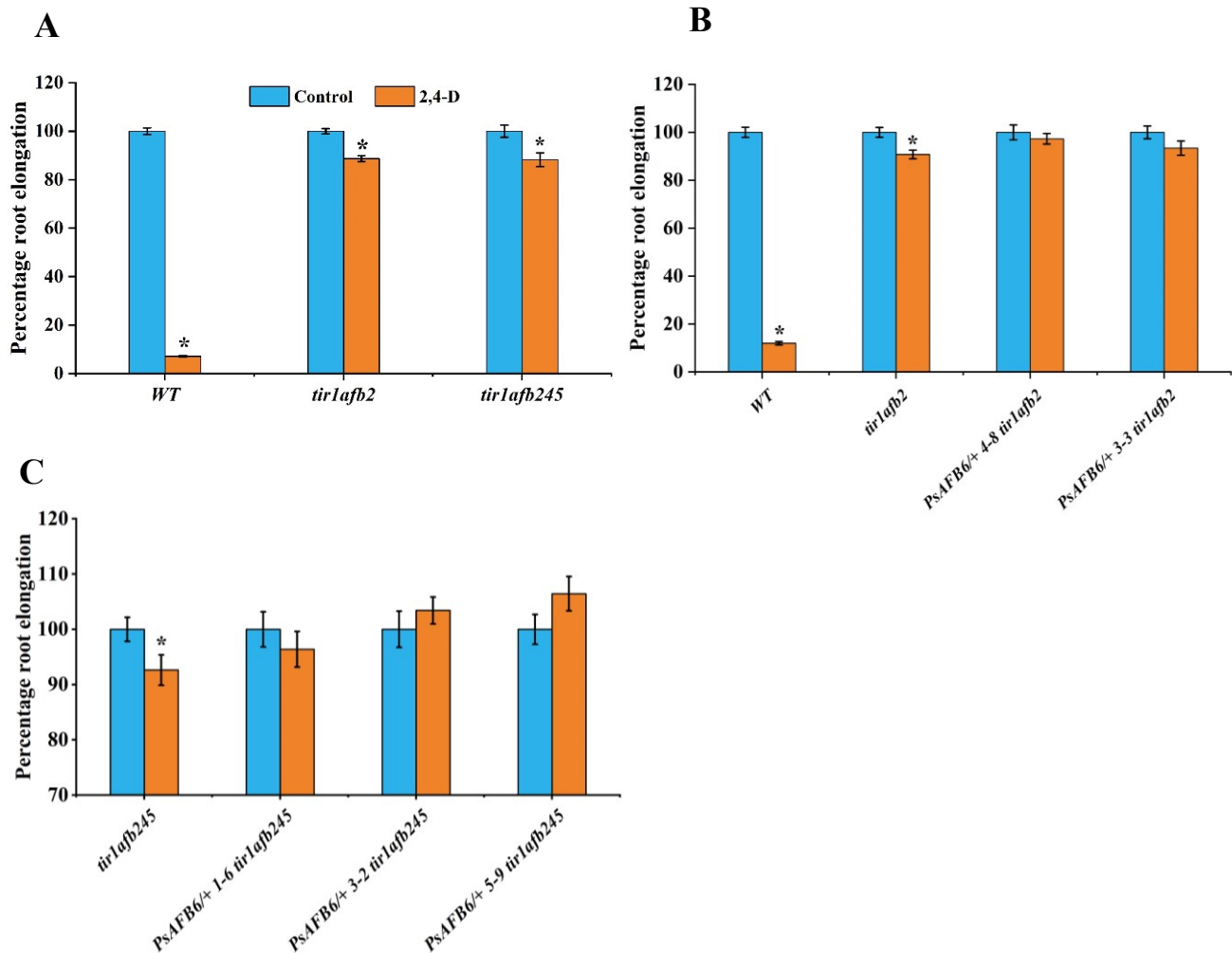


Figure 2.2 The effect of 2,4-D on root elongation of *Arabidopsis tir1afb2* double and quadruple mutants and mutants expressing *PsAFB6*. Four-day-old seedlings of wild type (WT), *tir1afb2* and *PsAFB6*-transformed lines in the double mutant background, and five-day-old seedlings of *tir1afb245* and *PsAFB6*-transformed lines in the quadruple background were transferred to media containing 0 or 70 nM 2,4-D and grown for three days. The seedlings belonging to different lines categorised within a group were grown together in sequential sets in same growth chamber. Data from 2 to 3 sequential sets were pooled for obtaining percent root elongation (see Appendix FigureA2 for details). **(A)** WT, *tir1afb2* and *tir1afb245* lines. **(B)** WT, *tir1afb2* and *PsAFB6*-expressing lines (*PsAFB6/+ 4-8 tir1afb2* and *PsAFB6/+ 3-3 tir1afb2*). **(C)** *tir1afb245* and *PsAFB6*-expressing lines (*PsAFB6/+ 1-6 tir1afb245*, *PsAFB6/+ 3-2 tir1afb245*, *PsAFB6/+ 5-9 tir1afb245*). Root elongation of each genotype in 2,4-D is expressed as a percentage compared to the same line in the bactoagar media without auxin. Data are means \pm SE. The details on the biological replications for each graph is as follows: **(A)** WT: control, n = 77 and 2,4-D, n = 78; *tir1afb2*: control, n = 78 and 2,4-D, n = 78; *tir1afb245*: control, n = 65 and 2,4-D, n = 71; **(B)** WT: control, n = 59 and 2,4-D, n=60; *tir1afb2*: control, n = 60 and 2,4-D, n = 60; *PsAFB6/+ 4-8 tir1afb2*: control, n = 30 and 2,4-D, n = 30; *PsAFB6/+ 3-3 tir1afb2*: control, n = 30 and 2,4-D, n = 30; **(C)** *tir1afb245*: control, n = 59 and 2,4-D, n = 59; *PsAFB6/+ 1-6 tir1afb245*: control, n = 40 and 2,4-D, n = 39; *PsAFB6/+ 3-2 tir1afb245*: control, n = 40 and 2,4-D, n = 40; *PsAFB6/+ 5-9 tir1afb245*: control, n=40 and 2,4-D, n=38. (Black asterisk denotes that the 2,4-D treatment mean is different from that of control within the same line and graph at $P < 0.05$; Two-tailed Student's T-test).

The 9-day-old *Arabidopsis* seedlings of the non-transgenic *tir1afb2* double mutant line had lower lateral root density (89-92 % reduction relative to WT) compared to that of WT seedlings (Figure 2.3A and B, no 2,4-D controls). In the *tir1afb245* quadruple mutant seedlings, 97 % reduction in lateral root density relative to that of WT was observed (Figure 2.3A, no 2,4-D controls). 2,4-D treatment increased the lateral root density in the WT line, but had no effect on the lateral root density in the *tir1afb2* double or *tir1afb245* quadruple mutant lines (Figure 2.3A-C). In general, the presence of the *PsAFB6* gene in the seedlings of *tir1afb2* double and

tir1afb245 quadruple mutant lines had no effect on the lateral root density and this parameter was not influenced by 2,4-D treatment (Figure 2.3B and C).

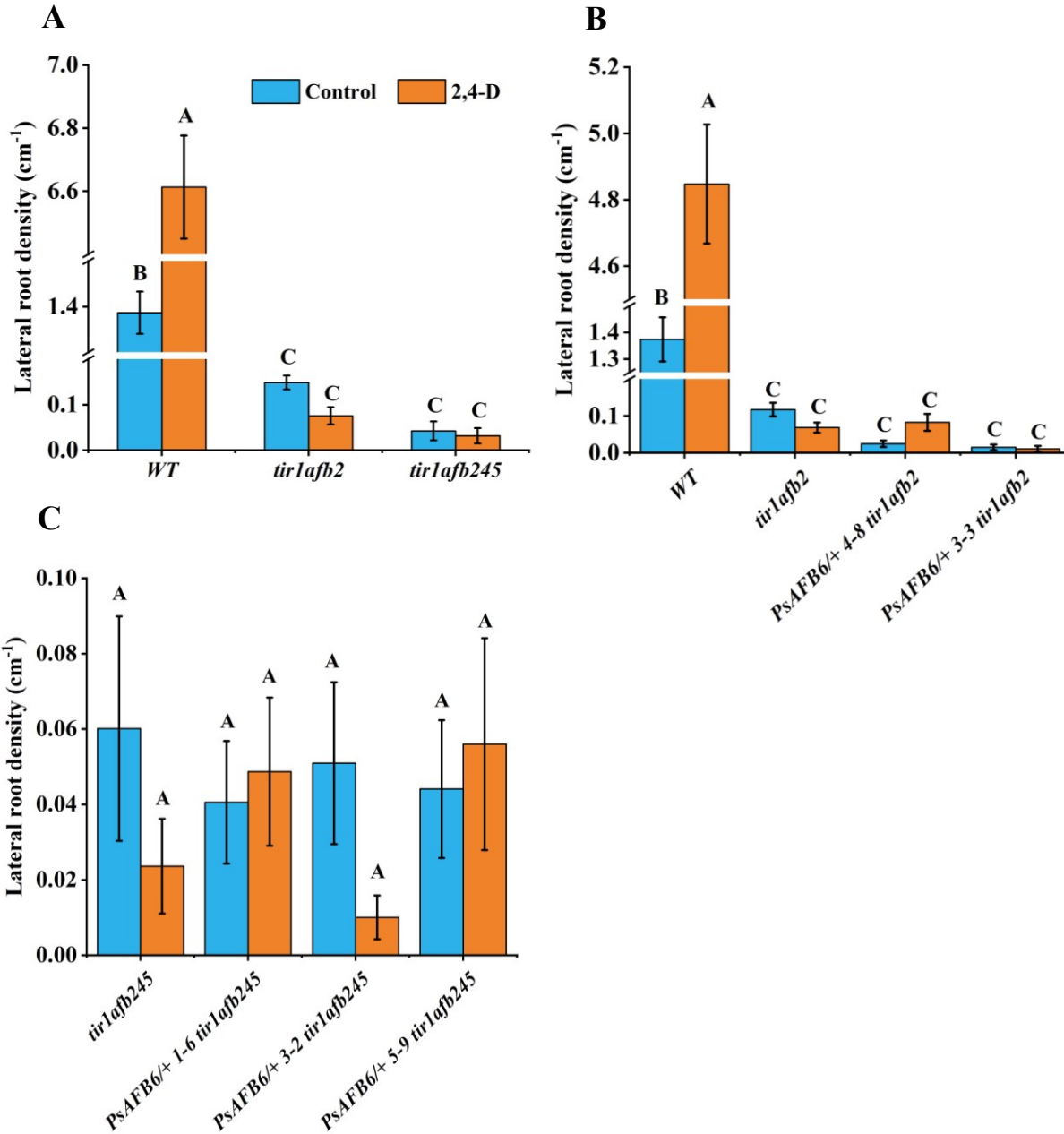


Figure 2.3 The effect of 2,4-D on lateral root density of Arabidopsis *tir1afb2* double and *tir1afb245* quadruple mutants and mutants expressing *PsAFB6*. Four-day-old seedlings of wild type (WT), *tir1afb2* and *PsAFB6*-transformed lines in the double mutant background, and five-day-old seedlings of *tir1afb245* and *PsAFB6*-transformed lines in the quadruple background

were transferred to media containing 0 or 70 nM 2,4-D and grown for five days. The seedlings belonging to different lines categorised within a group were grown together in sequential sets in same growth chamber. Data from 2 to 3 sequential sets were pooled for obtaining lateral root density (see Appendix FigureA2 for details). **(A)** WT, *tir1afb2* and *tir1afb245* lines. **(B)** WT, *tir1afb2* and *PsAFB6*-expressing lines (*PsAFB6/+ 4-8 tir1afb2* and *PsAFB6/+ 3-3 tir1afb2*). **(C)** *tir1afb245* and *PsAFB6*-expressing lines (*PsAFB6/+ 1-6 tir1afb245*, *PsAFB6/+ 3-2 tir1afb245*, *PsAFB6/+ 5-9 tir1afb245*). Data are means \pm SE. The details on the biological replications for each graph are as follows: **(A)** WT: control, n = 77 and 2,4-D, n = 78; *tir1afb2*: control, n = 78 and 2,4-D, n = 78; *tir1afb245*: control, n = 65 and 2,4-D, n = 71; **(B)** WT: control, n = 59 and 2,4-D, n=60; *tir1afb2*: control, n = 60 and 2,4-D, n = 60; *PsAFB6/+ 4-8 tir1afb2*: control, n = 30 and 2,4-D, n = 30; *PsAFB6/+ 3-3 tir1afb2*: control, n = 30 and 2,4-D, n = 30; **(C)** *tir1afb245*: control, n = 59 and 2,4-D, n = 59; *PsAFB6/+ 1-6 tir1afb245*: control, n = 40 and 2,4-D, n = 39; *PsAFB6/+ 3-2 tir1afb245*: control, n = 40 and 2,4-D, n = 40; *PsAFB6/+ 5-9 tir1afb245*: control, n=40 and 2,4-D, n=38). Different letters indicate statistically significant differences between the treatments and lines (Two-way-ANOVA, LSD post-hoc test, $P \leq 0.05$, Appendix Table A2-A4).

2.4 DISCUSSION

2.4.1 *PsAFB6* is expressed in the roots and shoots of Arabidopsis transgenic lines

Due to the absence of the AFB6 clade of auxin receptors in Arabidopsis, there has been a restricted amount of functional characterization reported for these auxin receptors. Phylogenetic analysis groups *PsAFB6* separately from all Arabidopsis TIR1/AFB auxin receptors, and *PsAFB6* has 61-66 % similarity with, and 50-55 % identity with, the Arabidopsis TIR1/AFB auxin receptors (Appendix Figure A4). In Ozga et al. (2022), yeast two-hybrid assays provided evidence that *PsAFB6* can bind pea Aux/IAAs in an auxin-dependent manner, suggesting *PsAFB6* is a functional auxin receptor. The *PsAFB6*-expressing Arabidopsis transgenic lines in auxin receptor double and quadruple mutant backgrounds were generated to determine if *PsAFB6* can function as an auxin receptor in root growth in Arabidopsis similar to that of the receptors TIR1/AFB2. *PsAFB6* transcripts were present in the root and shoot tissues of all Arabidopsis *PsAFB6* transgenic lines in auxin receptor double and quadruple mutant backgrounds (Figure 2.1, Appendix A Figure A3). Auxin (2,4-D) root growth assays were performed to determine if the presence of the *PsAFB6* auxin receptor in Arabidopsis will modify the root growth response.

2.4.2 The *PsAFB6* auxin receptor does not complement AtTIR1 or AtAFB2 in Arabidopsis auxin root growth assays

The non-transgenic Arabidopsis *tir1afb2* mutant displayed reduced auxin sensitivity (88.7-90.7 % root elongation in 2,4-D treatment compared to control) when exposed to 2,4-D (70 nM) in contrast to the WT seedlings (7.1-11.97 % root elongation in 2,4-D treatment relative to control) (Figure 2.2A and B). The quadruple-mutant *tir1afb245* exhibited a similar reduction in 2,4-D sensitivity to that of the *tir1afb2* double mutant, with root elongation measuring at 88.3 % in response to 2,4-D treatment relative to control (Figure 2.2 C). These results are consistent with that reported by other researchers that *TIR1* and *AFB2* are the two major auxin receptor genes that responsible for auxin response in Arabidopsis roots. Dharmasiri et al. 2005b found that the *tir1-1* seedlings exhibited resistance to auxin when compared to the control and the introduction of *afb2-1* into a *tir1-1* background resulted in an additive increase in auxin resistance in root growth assays. Parry et al. (2009) also observed reduced 2,4-D sensitivity in the *Attir1-1 afb2-3* double mutant compared to the *Attir1-1* single mutant. However, the *tir1afb1*,

tir1afb3, and *tir1afb1afb3* mutants displayed similar 2,4-D sensitivity to that of *tir1* seedlings, indicating the major contributions of *TIR1* and *AFB2* to the auxin response in Arabidopsis roots. However, further studies suggest that *AFB4* and *AFB5* may play a minor role in Arabidopsis root growth, and in one study an auxin receptor quadruple mutant *tir1afb2afb4afb5* appeared to have more resistance to auxin (100 nM IAA) than the *tir1afb2* double mutant in root growth assays (Prigge et al., 2020). In this study, auxin receptor *tir1afb2* and *tir1afb245* mutant lines both contain functional AFB1 and AFB3 auxin receptors. Overall, for both IAA-inhibition of root elongation and for the induction of lateral root primordia, the *tir1* allele had the largest effect (higher auxin-resistant root elongation and lowest lateral root production) with the *afb2*, *afb3*, *afb4*, and *afb5* mutations having smaller median effects (Prigge et al., 2020). The *afb1* mutation had little or no effect on root elongation (exhibited auxin inhibition of root elongation similar to the WT), but had a specialized function in rapid auxin-dependent inhibition of root growth and early phase of root gravitropism (Prigge et al., 2020).

The expression of *PsTIR1a* or *PsTIR1b* in transgenic Arabidopsis plants effectively restored the inhibition of root growth by 2,4-D in the Arabidopsis *tir1-10* and *tir1-10afb2-3* mutants, bringing it to levels similar to mutants expressing the *AtTIR1* transgene, thus demonstrating the functionality of both *PsTIR1a* and *PsTIR1b* as auxin receptors (Jayasinghe et al., 2019). Furthermore, in *Attir1-10 afb2-3* seedlings expressing *PsAFB2*, a notable reduction in root length was observed at 70 nM and 90 nM 2,4-D compared to their mutant backgrounds, affirming the functional role of *PsAFB2* as an auxin receptor (Jayasinghe et al., 2019). However, in our study, the introduction of the pea auxin receptor gene *PsAFB6* into both double and quadruple Arabidopsis mutant lines resulted in reduced sensitivity to 2,4-D-induced root growth inhibition, with decreased sensitivity of 2.7-6.5 % and 3.8-13.8 %, respectively, compared to their mutant background lines (Figure 2.2B and C). As *PsAFB6* has been shown to bind pea Aux/IAAs in an auxin-dependent manner (Ozga et al., 2022), two possible hypotheses to explain the current root growth assay data are: 1) *PsAFB6* binds the auxin present in the Arabidopsis root, but initiates an auxin response that differs from that of *TIR1* and *AFB2*, or 2) that *PsAFB6* competes with endogenous auxin receptors for binding of auxin, but does not lead to an auxin response, effectively reducing the overall auxin response. Given that research has indicated that auxin signaling and homeostasis are involved in clubroot pathogenesis in Brassica species (Jahn et al., 2013; Ludwig-Müller, 2014; Robin et al., 2020), in Chapter 3, the *PsAFB6*

transgenic lines with a reduced or altered auxin response are used to test if this change affects clubroot development in these plants.

2.4.3 The PsAFB6 auxin receptor does not complement AtTIR1/AtAFB2 effects on lateral root density in Arabidopsis roots

The 9-day-old Arabidopsis seedlings of the non-transgenic *tir1afb2* double mutant and *tir1afb245* quadruple mutant lines exhibited decreased lateral root density relative to the WT (89-92 % and 97 %, respectively; Figure 2.3A and B). These data suggest that lateral root number was influenced mainly by the auxin receptors TIR1 and AFB2. The loss of *TIR1* in Arabidopsis leading to a significant reduction in lateral root density has been reported in a number of previous studies, suggesting the important role of *TIR1* gene in lateral root formation (Ruegger et al., 1998; Gray et al., 2001; Dharmasiri et al., 2005a; Parry et al., 2009; Prigge et al., 2020). For example, after 10 days of agar medium growth, wild-type Arabidopsis seedlings displayed 6.3 ± 0.4 lateral roots, while *tir1-1* seedlings exhibited only 1.3 ± 0.4 . Examination of *tir1-1* seedlings via confocal microscopy revealed an absence of additional lateral root primordia, indicating a deficiency in the early stages of lateral root formation (Ruegger et al., 1998). Additionally, similar trends in reduction in lateral root number have been observed by Prigge et al. (2020) in *tir1afb2* double mutant and *tir1afb245* quadruple mutant lines as noted in this study. The presence of the PsAFB6 auxin receptor in both the *tir1afb2* double mutants and the *tir1afb245* quadruple mutants did not impact lateral root density (Figure 2.3B and C), suggesting that *PsAFB6* does not affect this parameter in Arabidopsis.

Chapter 3: The effect of auxin receptor modification on clubroot development in *Arabidopsis*

3.1 INTRODUCTION

Plant hormones play a vital role in integrating developmental and environmental cues, forming an intricate signaling network that shapes plant growth and development and responses to abiotic and biotic stresses. Apart from the well-known defense pathways triggered by SA, JAs, and ET, other hormones such as brassinosteroids (BL), auxins, gibberellins (GA), cytokinins (CK), and abscisic acid (ABA) also contribute significantly to how plants respond to pathogen attacks (Robert-Seilaniantz et al., 2007).

Pathogens can undermine plant defense strategies by disrupting the plant's hormonal changes and they can even produce their own plant hormones as part of their invasion strategy (López et al., 2008; Fu and Wang, 2011). For clubroot disease development, the plasmodia have the capability to produce CKs and can enhance the host's CK pool by modifying their biosynthesis and degradation processes (Ludwig-Müller, 2014). There is also evidence that *P. brassicae* can manipulate endogenous auxin levels to facilitate pathogenesis and disease progression, which can be categorized into two main categories: (1) directly promoting disease development by manipulating host auxin biology (e.g., synthesis, homeostasis), and (2) suppression of host defenses through manipulation of hormone signaling networks (Ludwig-Müller and Schuller, 2008; Ludwig-Müller et al., 2009; Jahn et al., 2013; Ludwig-Müller, 2014; Ludwig - Müller, 2022). Multiple genes responsible for enzymes involved in either the IPA or IAox pathway of IAA biosynthesis exhibited up-regulation during clubroot formation, including nitrilase, myrosinase, AO, and FMOs (for more information, refer to introduction 1.2) (Grsic-Rausch et al., 2000; Neuhaus et al., 2000; Ugajin et al., 2003; Devos et al., 2006; Siemens et al., 2006; Ishikawa et al., 2007; Xu et al., 2016; Robin et al., 2020). Elevated auxin levels can lead to the production of disease symptoms including the formation of galls, and/or suppression of salicylic acid (SA)-mediated defenses (Ludwig-Müller et al., 2009; Kunkel and Johnson, 2021). SA-mediated defense signaling and auxin signaling can be mutually antagonistic (Wang et al., 2007). The importance of SA-mediated defense signaling in clubroot disease development is discussed in Chapter 1 section 1.5. Therefore, reducing auxin levels and signaling in the host

plant may be a strategy to reduce disease progression and increase SA-mediated defense against *P. brassicae*.

In this chapter, auxin receptor *tir1afb2* double and *tir1afb245* quadruple mutant lines, along with double and quadruple mutant lines expressing *PsAFB6*, were inoculated with *P. brassicae* to characterize the role of auxin receptors during clubroot development. Gene expression was also examined in the roots of these lines at 21 DAI using qRT-PCR to assess the impact of auxin receptor modifications on specific hormone-related marker genes. Auxin receptors bind with auxin, leading to the degradation of Aux/IAA transcriptional repressors. Gene expression of Aux/IAs (*IAA9*, *IAA16*, and *IAA19*) within the early part of the auxin-signaling pathway was targeted for analysis. The half-life of many Aux/IAs is very short (Abel et al., 1994), and once Aux/IAA proteins are degraded, the expression of their genes is up-regulated as an immediate response to reimpose transcription repression following the initiation of the auxin response (Abel and Theologis, 1996). Plant cells continuously make and degrade Aux/IAs with the flux of Aux/IAs through this cycle modulated by auxin. Therefore, even the stable high and low expression states of Aux/IAs are dependent on flux through the Aux/IAA synthesis-degradation cycle (Leyser, 2018). The expression of Arabidopsis *Aux/IAA* genes are regulated by a diverse number of transcription factors. The CBF1 (CRT binding factor1) and DREB2A (dehydration responsive element binding factor 2A) transcription factors interact with cis-elements in the promoter regions of various stress-related genes to up-regulate the expression of many downstream genes, thereby imparting abiotic stress tolerance. At least one DRE element is present within 500 bp upstream of *IAA9* and *IAA19*, and CBF1 and DREB2A transcription factors were shown to directly regulate *IAA19* (Shani et al., 2017). Also, recessive loss-of-function mutations in *IAA19* decreased tolerance to abiotic stress (Shani et al., 2017). Plants from gain of function mutations in *IAA16* (*iaa16-1*; Rinaldi et al., 2012) and *IAA19* (Tatematsu et al., 2004) produce fewer lateral roots. According to the transcriptomic data analysis of the Zhou et al. (2020) study completed in the Ozga lab (unpublished data), gene expression was up-regulated for *IAA9* at 14 and 21 DAI, and *IAA16* down regulated at 7 and 14 DAI with *P. brassicae* in the pathogen-resistant rutabaga cultivar (*Brassica napus subsp. rapifera*), while being minimally affected in the susceptible rutabaga cultivar. *IAA19* gene expression was either up-regulated or less downregulated at 14 and 21 DAI with *P. brassicae* in the pathogen-resistant rutabaga cultivar compared to the susceptible rutabaga cultivar.

The degradation of Aux/IAs release auxin response factors (ARFs) that activate or repress expression of auxin response genes. Low expression of *Aux/IAs* and *ARFs* would indicate a low auxin response state potentially reducing clubroot disease progression. Members of the auxin response factor family, namely *ARF3*, *ARF5*, and *ARF19* were chosen for gene expression analysis. ARFs regulate the expression of early auxin-responsive genes by specifically binding to auxin response elements (AuxREs) in target gene promoters to direct the expression of downstream target genes (Roosjen et al., 2018). About half of all Arabidopsis genes exhibit the occurrence of a canonical AuxREs within the proximal 1000 base pairs of their gene promoter sequences (Mironova et al., 2014). This ARF binding site specificity allows auxin regulation in many cellular processes and events. Some studies also provide evidence that the function of ARFs is integrated into higher-order transcription factor complexes, which play a role in regulating or fine-tune auxin responses (Scacchi et al., 2010; Kelley et al., 2012; Mironova et al., 2014; Chandler, 2016). Coupling elements such as a pyrimidine-rich Y-patch or AuxRE-like motif within 50 bp of the AuxRE, as well as the G-box abscisic acid (ABA) response element (ABRE) in the vicinity of AuxREs, cooperativity with other trans-acting factors, affect auxin response in Arabidopsis (Mironova et al., 2014). Five ARFs, *ARF5*, *ARF6*, *ARF7*, *ARF8*, and *ARF19* function as transcriptional activators, while the others were characterised as transcriptional repressors (Ulmasov et al., 1999; Tiwari et al., 2003). The expression levels of both activator and repressor ARFs can be changed in host plants after infection with *P. brassicae*. Expression trends in the rutabaga transcriptome (Zhou et al., 2020) showed that *ARF3* and *ARF19* at 14 and 21 DAI with *P. brassicae* was up-regulated or up-regulated to a greater extent in the roots of the susceptible cultivar compared to the resistant cultivar (Ozga lab, unpublished). *ARF7* and *ARF19* regulate lateral root formation via direct activation of auxin-mediated transcription of LATERAL ORGAN BOUNDARIES-DOMAIN16/ASYMMETRIC LEAVES2-LIKE18 (LBD16/ASL18) and/or LBD29/ASL16 in Arabidopsis roots (Okushima et al., 2005; Okushima et al., 2007).

ARF5 gene expression showed downregulation in the clubroot-infected roots of Arabidopsis at 14, 17, and 21 DAI, and *ARF7* a slight down-regulation at 14 and 17 DAI, while *ARF8* showed a slight transcriptional upregulation at 17 DAI (Jahn et al., 2013). *ARF5* and *ARF7* partially overlap in their function as positive regulators of lateral root formation (Hardtke et al., 2004). As an auxin-responsive target of the prototypical *ARF5*/MP, BREVIXRADIX (*BRX*) can

physically interact with ARF5/MP. This interaction serves as a positive cofactor, enhancing auxin-related gene transcription in the root meristem in Arabidopsis (Scacchi et al., 2010).

GH3 group II genes can conjugate free IAA to amino acids (Westfall et al., 2012), reducing the levels of free IAA that the pathogen could use for gall formation. Thus, genes from members of the *GH3* group II protein family, denoted as *GH3.3*, and *GH3.17* were assessed for gene expression. As one of the early/primary auxin-responsive gene families, *GH3* transcripts were detected within five minutes following the application of 10^{-8} M of 2,4-D (Hagen and Guilfoyle, 1985). In Arabidopsis, 8 out of the 19 *GH3* proteins are associated with the modification of IAA, which includes AtGH3.1, AtGH3.2, AtGH3.3, AtGH3.4, AtGH3.5/WES1, AtGH3.6/DFL1, AtGH3.9, and AtGH3.17/VAS2 (Westfall et al., 2012). A variety of transcription factors can regulate the expression of *GH3* genes. For example, WRINKLED1 (WRI1) transcriptional regulator attenuates *GH3.3* expression through interaction with TEOSINTE BRANCHED1/CYCLOIDEA/ PROLIFERATING CELL FACTOR 20 (TCP20) to maintain auxin homeostasis in roots of Arabidopsis (Kong et al., 2022). A knockout mutation of *GH3.17* demonstrated that *GH3.17* plays a predominant role in controlling root elongation in Arabidopsis (Guo et al., 2022). In Arabidopsis, several *GH3* genes, including *GH3.2*, *GH3.3*, *GH3.4*, *GH3.5*, *GH3.14*, and *GH3.17* were up-regulated in *P. brassicae*-infected roots at 10 to 28 DAI (Jahn et al., 2013), also *GH3.3* and *GH3.4* expression was up-regulated at 10 and 23 DAI in an Arabidopsis transcriptome analysis (Siemens et al., 2006).

This study also explores the connection between the SA-mediated defense system and auxin by examining gene expression changes in key SA biosynthesis components (such as *isochorismate synthase 1*; *ICS1*) and monitoring the *PR* gene (*PR5*) to assess potential alterations in the SA signaling pathway following clubroot infection in the lines. Arabidopsis possesses two *ICS* genes: *ICS1* (also recognized as *SID2*) and *ICS2*. In Arabidopsis *ics1* mutants, the total accumulation of SA was reduced to approximately 5-10 % of the levels seen in wild-type plants following infection by either the virulent fungal biotroph *Erysiphe orontii* or avirulent strains of the bacterial necrotroph *Pseudomonas syringae* pv. *Maculicola*, demonstrating the key role of *ICS1* in SA biosynthesis associated with pathogen infection (Wildermuth et al., 2001). Activation of the SA-mediated defense system aligns with the activation of *PR* genes, which encode proteins with antimicrobial properties, are believed to be the effectors of plant systemic acquired resistance (SAR), conferring broad-spectrum resistance

to pathogens (Backer et al., 2019). The expression of PR genes can be activated or suppressed by different transcription factors. For instance, the Arabidopsis Di19 (Drought-induced) transcriptional regulator has been linked to the plant's response to drought stress by boosting the expression of pathogenesis-related genes PR1, PR2, and PR5 (Liu et al., 2013). The constitutive expressor of *PR genes 5 (cpr5-2)* and *defense, no death (dnd1)* mutants, in which SA responses are constitutively induced, were found to be more resistant to clubroot than the corresponding wild type, while SA-deficient lines (*NahG*, encoding an SA hydroxylase that degrades SA to catechol), *SA induction-deficient (sid2 or ICS1)* and *non-expressor of PR genes (npr1)* that are impaired in SA signaling were highly susceptible to the pathogen (Lemarié et al., 2015; Lovelock et al., 2016). These results suggest that SA signaling is an important defense mechanism against clubroot disease.

We propose to determine the gene expression patterns of specific *Aux/IAA*, *ARF* and *GH3* genes that are marker genes for auxin response and auxin homeostasis, and defense response (*ICS1* and *PR5*) in Arabidopsis lines of interest that could potentially be modified leading to an increase in clubroot tolerance (Figure 3.1).

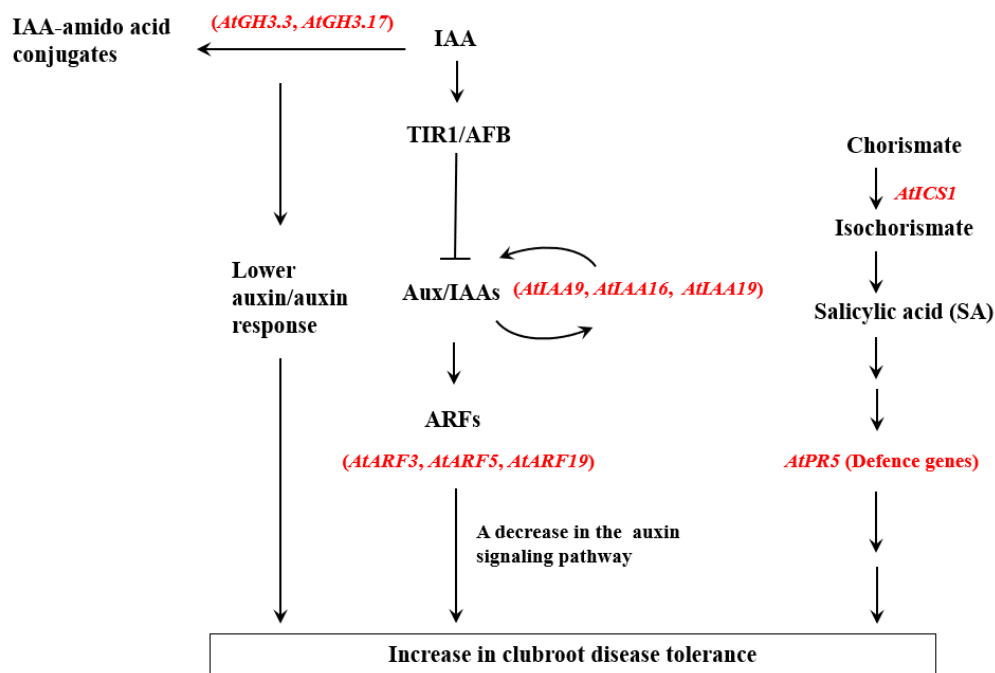


Figure 3.1 A diagram of auxin response and defense response marker genes used for gene expression analysis in Arabidopsis roots in response to clubroot pathogen inoculation. Upon

perception of auxin by the TIR1/AFB receptors, degradation of the auxin-signaling repressor Aux/IAAs occurs, allowing the expression of *ARFs* leading to auxin response. *GH3* genes regulate auxin homeostasis by conjugating free IAA to IAA-amido conjugates. Pathogen-induced SA, derived from chorismate by *ICS1*, activates *PR* gene expression (including *PR5*) facilitating SA-mediated defense response against the pathogen.

3.2 MATERIALS AND METHODS

3.2.1 Plant material

All Arabidopsis lines are in the Columbia ecotype background (Col-0). The lines used in this study were the auxin receptor *tir1afb2C*, *tir1afb2A2* and *tir1afb2D1* double mutant and *tir1afb245* quadruple mutant lines, along with *PsAFB6*-expressing lines in the double mutant background of *tir1afb2C* (*PsAFB6/+ 4-8 tir1afb2*; *PsAFB6/+ 3-3 tir1afb2*) and quadruple auxin receptor mutant (*PsAFB6/+ 1-6 tir1afb245*; *PsAFB6/+ 3-2 tir1afb245*; *PsAFB6/+ 5-9 tir1afb245*), and the Columbia wild-type (WT) line. All Arabidopsis auxin receptor double and quadruple mutant lines, and transgenic lines expressing *PsAFB6* in these mutant backgrounds were created prior to this project by other members of the Ozga lab (as described in Chapter 2 section 2.2.1), except for the *tir1afb2A2* and *tir1afb2D1* double mutant lines that were created for this study as described below.

3.2.2 Creation of additional non-transgenic Arabidopsis *tir1-10 afb2-3* double mutant lines

In order to compare three independently created Arabidopsis *tir1afb2* double mutant lines for susceptibility to clubroot disease progression, an additional two independent auxin receptor double mutant lines were generated (*tir1afb2A2* and *tir1afb2D1*). The *Attir1-10* and *Atafb2-3* auxin receptor single mutant lines were homozygous and background cleaned by backcrossing these mutant lines with Col-0 WT plants in the Ozga lab prior to this study. The auxin receptor single mutant *Attir1-10C1* and *Atafb2-3A2* lines were used as the female parents. The auxin receptor *Attir1-10C1* single mutant female parent plants were selectively hand-pollinated with pollen from three independently generated *Atafb2-3* auxin receptor single mutant plant lines that served as male parents (*Atafb2-3A2*, *Atafb2-3B1*, and *Atafb2-3D1*). The auxin receptor *Atafb2-3A2* single mutant female parent plants were selectively hand-pollinated with pollen from four independently generated auxin receptor *Attir1-10* single mutant plant lines that served as male parents (*Attir1-10A5*, *Attir1-10A7*, *Attir1-10B13* and *Attir1-10C1*). Altogether, there were 7 different cross types: (♀ x ♂: *Attir1-10C1* X *Atafb2-3A2*, *Attir1-10C1* X *Atafb2-3B1*, *Attir1-10C1* X *Atafb2-3D1*, *Atafb2-3A2* X *Attir1-10A5*, *Atafb2-3A2* X *Attir1-10A7*, *Atafb2-3A2* X *Attir1-10B13* and *Atafb2-3A2* X *Attir1-10C1* (see Appendix B Figure B1 for details). Seeds of auxin receptor *Attir1-10* and *Atafb2-3* single mutant homozygous lines were suspended separately in 1 mL of Milli-Q water, placed onto water-saturated Sunshine #4 mix (SunGro Horticulture, Vancouver, BC, Canada) in pots (10.5 x 10.5 cm) using 5 mL disposable plastic

dropper pipettes. There were altogether 28 pots; 6 pots of *Attir1-10C1* plants and 8 pots of *Atafb2-3A2* plants that served as female parent plant (or maternal plants) and the remaining 14 pots of male parent plants (or paternal plants) with 2 pots per independently generated lines of *Attir1-10* (*Atafb2-3A2*, *Atafb2-3B1*, and *Atafb2-3D1*) and *Atafb2-3* (*Attir1-10A5*, *Attir1-10A7*, *Attir1-10B13* and *Attir1-10C1*) single mutant auxin receptor lines. The pots were stratified in darkness at 4 °C for four days, followed by transfer to a growth cabinet maintained at 22 °C with a 16 h photoperiod under cool white-fluorescent light at $206 \pm 13 \mu\text{E m}^2 \text{s}^{-2}$. The pots of *Attir1-10* and *Atafb2-3* paternal and maternal plants were kept apart at a distance of 35 cm within a growth cabinet. After a week of plant growth in the growth cabinet, seedlings were thinned to 5-8 healthy plants per pot and each pot was covered with a pollination bag (20.5 x 61 cm) with the support of skewer sticks to prevent cross-pollination. Plants were fertilized weekly (one time per week) with a solution of 10-10-10 NPK. After approximately 24 days of plant growth in the growth cabinet after the transfer, plants started to produce floral buds. The floral buds of auxin receptor *Attir1-10C1* and *Atafb2-3A2* single mutant maternal plants that were still green and closed were emasculated (anthers removed) using forceps, with the carpels remaining intact and attached to the plant. For each cross type, the carpels of the emasculated auxin receptor *Attir1-10C1* and *Atafb2-3A2* single mutant maternal plants were hand-pollinated with pollen from respective auxin receptor single mutant paternal plants. The pollinated carpels were covered with a piece of plastic wrap to retain moisture and prevent further cross-pollination and were tagged on the day of pollination with parental cross details. Three to four days after pollination, approximately 3 to 8 pollinated carpels per cross type showing signs of ovary growth (swelling or successful fertilization) had their plastic wraps removed and were allowed to grow until maturity (when the silique outer wall color changed to yellow or brown). Intact mature siliques were harvested approximately 14 to 17 days post-pollination. Each individual silique containing the F1 seed generation generated from a cross of *Attir1-10* and *Atafb2-3* single mutant parent lines was collected separately in a microcentrifuge tube, and dried with Drierite desiccant for a week and stored in the cold room maintained at 4 °C until further use.

For determining the presence of mutant genes within the F1 seed lines, 10-15 seeds per cross type were grown in 36 cell inserts trays (insert size 2 1/8 in. x 2 3/8 in. x 2 1/4 in. deep; 1-2 seed(s) per cross type per insert) filled with water saturated Sunshine #4 mix. Trays were covered with plastic domes to maintain moisture and placed in dark at 4 °C for four days for

seed stratification and subsequently moved to the growth cabinet maintained at the same parameters mentioned above. After one week of growth in the growth cabinets, the plastic domes were removed and seedlings were thinned to one per insert. After 2-3 weeks of growth in the growth cabinet, when seedlings developed 4-8 rosette leaves, fresh rosette leaf tissue was used for each seedling to perform the direct PCR assays. The PCR assays were performed on 5-10 seedlings per cross type with the SALK T-DNA specific primer LBb1.3 (LB), and the LP and RP primer sets for each gene (Appendix B Table 1; two PCR reactions for each auxin receptor gene for one seedling). PCR reactions were prepared using Phire Plant Direct PCR kit (Thermo Scientific) as per the manufacturer recommendations. For each seedling, a piece of rosette leaf tissue that is approximately 2 mm in diameter was removed manually using forceps and placed in a 200 μ L PCR tube (Thermo Fisher) with 15 μ L of dilution buffer. Then the leaf sample was crushed with a pipette tip by pressing it briefly against the tube wall until the solution become greenish. This dilution buffer was briefly centrifuged and 0.5 μ L of the supernatant was used as a template for a PCR reaction. The PCR reaction (total volume 20 μ L) consisted of 3.5 μ L nuclease-free water, 10 μ L of 2X Phire Plant Direct PCR Master Mix, 2 μ L each of 5 μ M of LP, RP and LB primers (Appendix B Table 1) and 0.5 μ L of template. The PCR amplification was performed with initial denaturation at 98 $^{\circ}$ C for 5 minutes followed by 40 cycles of denaturation at 98 $^{\circ}$ C for 5 seconds, annealing at 63.7 $^{\circ}$ C for 5 seconds, and extension at 72 $^{\circ}$ C for 25 seconds. The final extension step was carried out at 72 $^{\circ}$ C for 1 minute. Subsequently, PCR product(s) were subjected to separation by gel electrophoresis on 1.2% w/v agarose gel (prepared using 40 mM Trizma base, 1 mM EDTA and 20 mM glacial acetate in 1x TAE buffer pH = 8) with 8 μ L SYBR Safe DNA gel stain (Invitrogen). The gel was subjected to electrophoresis in a 1x TAE buffer at 150 V for approximately 15-20 min with 12 μ L of 100 bp DNA ladder with fragment size ranging from 100 to 5000 bp (O'GeneRuler Express). Six seedlings from from *Attir1-10C1* X *Atafb2-3A2*, 6 seedlings from *Attir1-10C1* X *Atafb2-3B1*, 6 seedlings from *Attir1-10C1* X *Atafb2-3D1*, 7 seedlings from *Atafb2-3A2* X *Attir1-10A5*, 5 seedlings from *Atafb2-3A2* X *Attir1-10A7*, 5 seedlings from *Atafb2-3A2* X *Attir1-10B13* and 5 seedlings from *Atafb2-3A2* X *Attir1-10C1* showing heterozygosity for both auxin receptor *Attir1-10* and *Atafb2-3* genes were allowed to grow until maturity (two bands per PCR reaction amplify in heterozygous plants, one from the WT gene (amplified from LP and RP primers), and one from the gene with the T-DNA insert (amplified from LB and RP primers). Flowers from the heterozygous plants were self-fertilized,

siliques per plant were harvested, the resulting seeds were dried with Drierite desiccant for a week and stored in the cold room maintained at 4 °C until further use.

The last step was to identify the homozygous auxin receptor *Attir1-10 afb2-3* double mutant lines from the seeds obtained from self-fertilized heterozygous auxin receptor *Attir1-10 afb2-3* mutant lines. Self-fertilized seeds (27) of heterozygous auxin receptor *Attir1-10 afb2-3* mutant lines obtained from each cross type were grown to the 4-8 rosette leaf stage in 36 well-insert trays in a growth cabinet. The details of the plant growth procedure and growth cabinet conditions followed were described previously. All the seedlings were first screened for auxin receptor *Attir1-10* T-DNA insertion using direct PCR method described previously. Seedlings that showed homozygosity for auxin receptor *Attir1-10* T-DNA insertion were further screened for auxin receptor *Atafb2* T-DNA insertion using direct PCR method described previously. Only one band per PCR reaction amplifies from the gene containing the T-DNA insert (amplified from LB and RP primers) is expected for each gene in a line homozygous for a *Attir1-10 afb2-3* double mutant. The two independently generated auxin receptor *tir1afb2A2* and *tir1afb2D1* double mutant plants obtained from *Attir1-10C1* X *Atafb2-3A2* and *Attir1-10C1* X *Atafb2-3D1* crosses, respectively, were covered with plastic tubes, allowed to self-fertilize and to grow until maturity, and mature siliques with seeds were harvested and dried with Drierite desiccant for a week and stored in the cold room maintained at 4 °C until further use. For seed increase of two independently generated auxin receptor *tir1afb2A2* and *tir1afb2D1* double mutant lines, 12 plants each line were grown as described previously in 36 cell inserts trays to ensure enough seeds were harvested for performing clubroot-inoculation assays. Each plant was re-assessed for homozygosity of the T-DNA insertion in both auxin receptor genes *Attir1-10* and *Atafb2-3* using direct PCR and gel electrophoresis as described previously. These plants were covered with plastic tubes, allowed to self-fertilize and grow until maturity, and mature siliques with seeds were harvested and dried with Drierite desiccant for a week and then stored in the cold room maintained at 4 °C until further use.

3.2.3 Peat-based medium growth system for performing clubroot-inoculation assays with *Arabidopsis* auxin receptor mutants and mutants-expressing *PsAFB6*

3.2.3.1 Seed germination

For performing clubroot inoculation assays a peat-based medium plant growth system was developed. *Arabidopsis* seeds belonging to different lines as shown in Appendix B Figure B2 were grown together as a set in a growth chamber. *Arabidopsis* WT, auxin receptor *tir1afb2C* double mutant and *tir1afb245* quadruple mutant lines, along with quadruple mutants expressing *PsAFB6* (*PsAFB6/+ 1-6 tir1afb245*, *PsAFB6/+ 3-2 tir1afb245* and *PsAFB6/+ 5-9 tir1afb245*) were grown together as a set designated as set 1. *Arabidopsis* WT and *tir1afb2* double mutant lines (*tir1afb2C*, *tir1afb2A2* and *tir1afb2D1*) were grown together as set 2. *Arabidopsis* WT, *tir1afb2C* double mutant and double mutants expressing *PsAFB6* (*PsAFB6/+ 3-3 tir1afb2* and *PsAFB6/+ 4-8 tir1afb2*) were grown together as a set 3. The clubroot inoculation assays were conducted in 72 cell inserts trays filled with water-saturated peat-based medium (Sunshine #4 mix). Each tray consisted of 12 packs; each pack consisted of 6 cells with each cell 3.8 x 3.8 x 5.7 cm in size. Approximately 400 seeds of each line within a set were suspended separately in 1 mL of Milli-Q water and approximately 4-6 seeds of a line were placed within a cell using a 5 mL disposable plastic dropper pipette in at least 12 cells (2 packs), and each pack was randomly placed within a tray. For set 1, 4 biological replications for each line consisting of 12 seedlings per replicate (2 packs) were clubroot-inoculated. Two packs per line were randomly placed within a tray, and a total of 4 trays were used. For non-inoculated control seedlings, 3 biological replications consisting of 6 plants per replicate (1 pack) were planted. For set 2, 6 biological replications for each line consisting of 12 plants (2 packs) per replication were inoculated with the clubroot pathogen. Three packs per line were randomly placed within a tray, 4 trays were used. For non-inoculated control seedlings, 3 biological replications consisting of 6 plants per replicate (1 pack) were planted. For set 3, 3 biological replications for each line consisting of 12 seedlings per replicate (2 packs) were clubroot-inoculated. Three packs per line were randomly placed within a tray, and a total of 2 trays were used. For non-inoculated control seedlings, 3 biological replications consisting of 6 plants per replicate (1 pack) were planted. All the clubroot-inoculated trays were double contained in a large black plastic tray and were separated from the non-inoculated control trays. Both non-inoculated control trays and clubroot-inoculated trays were grown together in the same growth chamber. After the seed placement onto the

sunshine mix in the trays, trays were covered with plastic lid and kept in dark at 4 °C for four days for seed stratification and then transferred to the growth cabinet maintained at 22 °C with a 16 h photoperiod under cool white-fluorescent light at $206 \pm 13 \mu\text{E m}^2 \text{s}^{-2}$ for the remaining duration of the experiment until harvested. One week after plants were transferred to the growth chamber, tray lids were removed, extra water in trays was drained, seedlings were thinned to one healthy seedling per cell insert with tweezers and plants were fertilized weekly with 10-10-10 N-P-K (100 ppm) until harvested. In the third week of plant growth in the growth cabinets, plants were clubroot-inoculated and did not receive NPK fertilizer this week. Each experimental set was repeated at least twice over time to gauge consistency of response.

3.2.3.2 *Pathogen material and inoculum preparation*

A *P. brassicae* single spore isolate of pathotype 3H (P3-SACAN-SS1) obtained from the lab of Dr. Stephen Strelkov (University of Alberta) was used as the clubroot inoculum. The clubroot resting spore inoculum suspension was prepared by using frozen (-20 °C) pre-washed clubroot infected root galls of Chinese cabbage, following the method adapted from Strelkov et al. (2006). Briefly, 60 mg of frozen gall material was cut from the middle of a well-developed gall and was ground using a mortar and pestle in 100 mL of distilled water. The resulting homogenate was filtered through eight layers of cheesecloth to remove plant debris. The clubroot spore concentration in the filtrate was estimated using a modified Neubauer counting chamber of the hemocytometer (refer to Appendix B Figure B3 for details). The spore suspension was adjusted with distilled water to obtain a final spore concentration of approximately 1×10^5 spores/mL. The prepared clubroot resting spore suspension was immediately used for inoculations.

3.2.3.3 *Clubroot Inoculations*

Sixteen-day-old *Arabidopsis* seedlings at the 4 to 6-leaf stage (4 rosette and 2 cotyledonary leaves) were inoculated by pipetting 2 mL of the clubroot spore suspension (1×10^5 spores/mL) using pipette tips with filters onto the peat-based medium around each seedling to ensure sufficient disease pressure and symptom development. Non-inoculated control seedlings received 2 mL of Milli-Q water. Two days after inoculation, plants were watered to maintain consistent moisture content but were not fertilized this week. Approximately one week after the

plants were clubroot-inoculated, a weekly application of 10-10-10 NPK (100 ppm) fertilization was given until harvested. To prevent cross-contamination during watering or fertilizing, gloves were changed and separate glass cylinders were used for watering non-inoculated controls and clubroot-inoculated plants. For each set of Arabidopsis clubroot-inoculation assays, 6 Chinese cabbage seedlings were clubroot-inoculated and served as a positive control for confirming the virulence of the clubroot spores. In detail, 12-15 seeds of Chinese cabbage (Granaat EC05) were pre-germinated on moistened Whatman filter paper #1 (Whatman International Ltd., Maidstone, UK) in a round plastic 100 x 20 mm Petri plate (TC Dish 100, Sarstedt, Nümbrecht, Germany). On the day of clubroot-inoculations, seven-day-old Chinese cabbage seedlings were transplanted to a 6-cell pack (one seedling per cell) filled with water-saturated peat-based medium and the seedling was immediately inoculated with 2 mL of the clubroot spore suspension (1×10^5 spores/mL). At 32 DAI (days after clubroot-inoculation), clubroot-inoculated Chinese cabbage plants were harvested together with Arabidopsis plants and clubroot symptoms were noted.

3.2.3.4 Digitized clubroot disease rating

At 32 DAI, plant roots were washed carefully three times in tap water using fine tip brush to remove the rooting medium. Subsequently, the plants were transferred to pre-labeled glass tubes filled with tap water. Seedlings were gently dried using paper towels and images of the root-shoot transition zone were captured using a Zeiss Axiocam ERc 5s Rev. 2.0 digital camera (Carl Zeiss Microscopy GmbH, Göttingen, Germany) mounted on a Zeiss Discovery V8 dissecting stereoscope. The imaging setup included a Zeiss 0.5x Achromat S lens as the objective lens and a widefield 10x/23 mm plane eyepiece. For clubroot disease rating, the captured microscopic images of the root-shoot transition region of Arabidopsis plants were used to score clubroot severity.

The severity of clubroot infection in Arabidopsis roots was assessed using a seven point 0-to-3 scale scoring (Strelkov et al. 2016, modified for Arabidopsis): 0 = no tissue swelling or galling; 0.5 = minimal swelling on the primary or lateral roots observed, most roots were symptom-free; 1 = minor swelling on the primary and lateral roots, most roots were symptom-free; 1.5 = obvious swelling on the primary or lateral roots, most roots were symptom-free; 2 = obvious swelling on primary and lateral roots with a moderately reduced fine root system; 2.5 = moderate swelling on primary and lateral roots with a moderately reduced fine root system; 3 =

severe galling of the primary and lateral roots with a significantly reduced fine root system or decayed roots (Figure 3.2). The resulting severity scores were then converted to clubroot disease severity index (DI): $DI (\%) = \{[\sum (n \times 0) + (n \times 0.5) + (n \times 1) + (n \times 1.5) + + (n \times 2) + + (n \times 2.5) + (n \times 3)]/N \times 7\} \times 100 \%$, where n is the number of plants in a class, N is the total number of plants, and 0, 0.5, 1, 1.5, 2, 2.5 and 3 are the symptom severity classes.

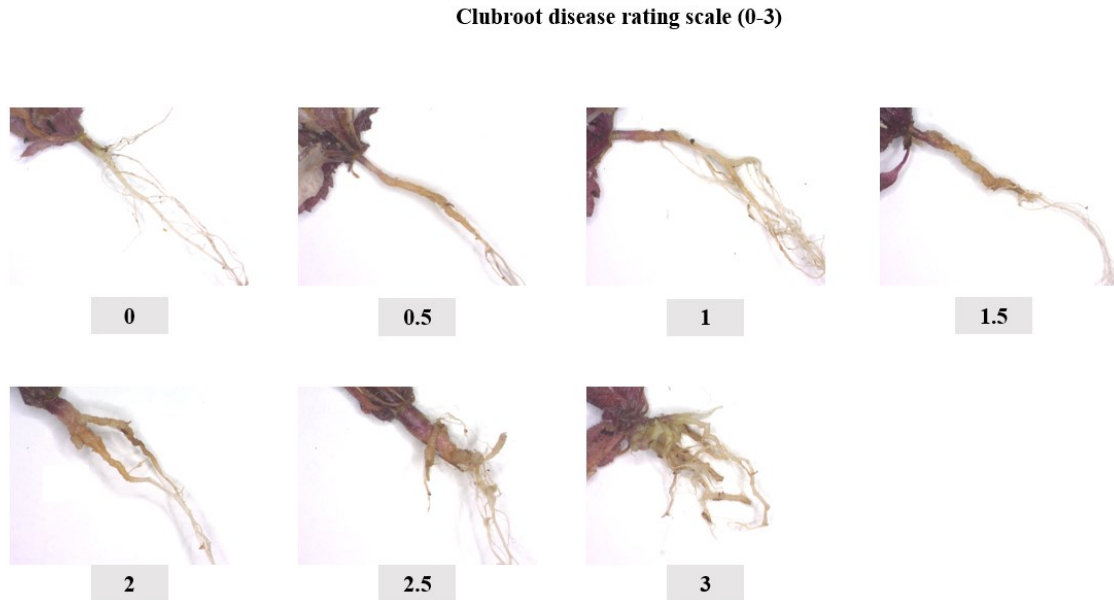


Figure 3.2 Representative microscopic images of the disease rating scale for clubroot symptoms on root-shoot transition zone of Arabidopsis. Clubroot disease severity was assessed based on a 7-point scale scoring at 0.5 intervals from 0-3; where 0 = no visible galls or symptoms, and 3 being severely infected or decayed roots.

3.2.3.5 Root-shoot transition region fresh weight analysis in Arabidopsis plants

At 32 DAI, after the microscopic images of the root-shoot transition region of Arabidopsis non-inoculated and clubroot-inoculated plants were captured for each line within a set, 1.5 cm of the root-shoot transition region of each seedling was dissected using scalpel. For each line, within a treatment type (non-inoculated or clubroot-inoculated) six root samples were pooled as one biological replication for measuring the fresh weight of the root-shoot transition region. Later, the average fresh weight of the root-shoot transition region per seedling was calculated by

divided the fresh weight of the sample by 6. The plants that had decayed roots due to clubroot-inoculation at 32 DAI, were not included in this analysis.

3.2.4 RNA extraction and Taqman qRT-PCR assays

For total RNA extraction and qRT-PCR assays, WT, auxin receptor *tir1afb2C* double and *tir1afb245* quadruple mutant lines and mutants expressing *PsAFB6* in double (*PsAFB6/+ 4-8 tir1afb2*) and quadruple (*PsAFB6/+ 3-2 tir1afb245*) backgrounds were selected based on the *PsAFB6* transcript abundance reported in chapter 2 (Figure 2.1 and Appendix Figure A3). This experiment was sequenced over two days to allow for sufficient time for tissue harvest.

On experiment day one, for the non-inoculated treatment approximately 6 seeds per cell were placed onto water-saturated peat-based medium (6 cells per pack) and 12 packs per line were randomly placed in trays. On experiment day two, for the clubroot-inoculated treatment approximately 6 seeds per cell were placed onto water-saturated peat-based medium (6 cells per pack) and 12 packs per line were randomly placed in trays. After the seed placement onto the peat-based medium, trays were covered with plastic lids and kept in dark at 4 °C for four days for seed stratification and then transferred to growth cabinets maintained at 22 °C with a 16 h photoperiod under cool white-fluorescent light at $206 \pm 13 \mu\text{E m}^2 \text{s}^{-2}$ for the remaining duration of the experiment until harvested. Both non-inoculated control trays and clubroot-inoculated trays were grown together in the same growth chamber. Watering and fertilization of plants were performed as described above.

Sixteen-day-old *Arabidopsis* seedlings were inoculated with the clubroot spore inoculum suspension at 1×10^5 spores/mL. This clubroot inoculum suspension was used within 4 hours of its preparation and was prepared following the procedure described previously. At 21 DAI, a total of 4 biological replications for each treatment (non-inoculated and clubroot-inoculated) per line were harvested and each biological replication consisted of 16-18 seedlings per line. Whole roots were washed three times in tap water, three times in Milli-Q water, pat-dried with paper towels, and the root-shoot transition zone and roots (referred to as root tissue) were dissected from the plants using a scalpel and collected into 15 mL plastic scintillation vials placed onto dry ice and stored at -80 °C until further processed for total RNA extraction.

The frozen root tissues were ground to a fine powder with a combination of manual grinding with a pre-cooled mortar and pestle in liquid N₂ and bead-beating using a Mini-

BeadBeater (Biospec Products). Total RNA was extracted from this finely ground frozen root tissue using a modified Trizol-based method as described in Ozga et al. (2003) and detailed previously in Materials and Methods section of Chapter 2. The TaqMan One-Step RT-PCR Master Mix Reagents Kit (Applied Biosystems) was used to quantify the relative transcript abundance of candidate genes on a StepOnePlus Real-Time PCR System Instrument (Applied Biosystems) as described previously in Materials and Methods section of Chapter 2. Gene-specific qRT-PCR primers and Taqman probes were designed with the PrimerQuest tool from IDT using double-quenched probes with an Iowa Black Fluorescent Quencher (IBFQ) at the 3' end, and a ZEN (N, N-diethyl-4-(4-nitronaphthalen-1-ylazo)-phenylamine) quencher positioned 9 bp from the 6-FAM (6-carboxyfluorescein) fluorescent dye-containing 5' end (see Table 3.1).

Table 3.1 Taqman primers and probes used for quantification of gene expression by qRT-PCR assays in root tissues of non-inoculated control and 21d-*P. brassicae*-inoculated *Arabidopsis Columbia* wild-type (WT), auxin receptor *tir1afb2C* double and *tir1afb245* quadruple mutant lines, and mutant lines expressing *PsAFB6* (*PsAFB6/+ 4-8 tir1afb2* and *PsAFB6/+ 3-2 tir1afb245*), and their PCR efficiencies and r^2 values.

Gene name	Arabidopsis Gene Accession ID	qRT-PCR Primers/Probe Sequences	PCR Efficiency (%), r^2
<i>Aux/IAA</i> genes			
<i>AtAux/IAA9</i>	At5g65670	F: 5'-TCCTACAGGAAGAACACATTGG-3' R: 5'-CATACTGACCTTCACGAAGAGAG-3' P: 5'-ACAGTGACGAAGTTGATGGGAGGC-3'	101.11, 0.9997
<i>AtAux/IAA16</i>	At3g04730	F: 5'-AGATAAAGATGGCGACTGGATG-3' R: 5'-CGATTGCTTCTGATCCCTTCA-3' P: 5'-AGGAGACGTACCGTGGGAGATGTT-3'	97.01, 0.9996
<i>AtAux/IAA19</i>	At3g15540	F: 5'-ACAACCTGCGAATACGTTACCA-3' R: 5'-ACCTCTTGCATGACTCTAGAAAC-3' P: 5'-AAAGATGGGAGACTGGATGCTCGCC-3'	88.64, 0.9916
<i>ARF</i> genes			
<i>AtARF3</i>	At2g33860.1	F: 5'-AGAGAAGCAGGATTGGCTTT-3' R: 5'-CAAGACCCTCTGGAATCTCAAT-3' P: 5'-ATTCGCGCCACAGACTTTGAGGAATC-3'	89.31, 0.9971
<i>AtARF5</i>	At1g19850	F: 5'-GATTGGAAGGACTACTAACTCACC-3' R: 5'-TCCCATGGATCATCTCCTACA-3' P: 5'-CACAAAGCTCGGGTTGGAAGCTTG-3'	96.61, 0.9959
<i>AtARF19</i>	At1g19220	F: 5'-GAAGATCCGCTAACCTCTGATT-3' R: 5'-CACGCAGTTCACAACTCTTC-3'	94.72, 0.9995

		P: 5'-TTCGTGATCGGTGTAGACGAGTTTCC-3'	
<i>GH3</i> genes			
<i>AtGH3.3</i>	At2g23170	F: 5'-GAAAGAAGCTCGCCGACGATA-3' R: 5'-GGTCCGGTTTGGTCAAGAT-3' P: 5'-ACCCGGCCATTAAAGAGAGCATGT-3'	94.72, 0.9995
<i>AtGH3.17</i>	At1g28130	F: 5'-CCGTTGGTTTCAACGATGTATG-3' R: 5'-ATGTTAGGAAGAAGCGTGTAGG-3' P: 5'-AATCCGTTGTGTGATCCTGCCGAT-3'	93.13, 0.9981
<i>ICS</i> genes			
<i>AtICS1</i>	At1g74710	F: 5'-GCTGCTCTGCATCCAAC-3' R: 5'-GTCCCGCATACATTCCTCTATC-3' P: 5'-TGTTTGTGGGCTTCCAGCAGAAGA-3'	95.80, 0.9994
<i>PR</i> genes			
<i>AtPR5</i>	At1g75040	F: 5'-TCTAAGGAACAATTGCCCTACC-3' R: 5'-GCACCTGGAGTCAATTCAAATC-3' P: 5'-AAGGACCCAAGCTCGGCGAT-3'	96.92, 0.9994

3.2.5 Statistical analyses

Statistical analyses were performed using IBM SPSS Statistics software version 27.0.1 and RStudio version 2023.06.2+561. For clubroot-inoculation assays, the comparison of lines within a set was performed for clubroot disease index (Set 1: WT, *tir1afb2C*, *tir1afb245*, *PsAFB6/+ 1-6 tir1afb245*, *PsAFB6/+ 3-2 tir1afb245* and *PsAFB6/+ 5-9 tir1afb245*; Set 2: WT, *tir1afb2C*, *tir1afb2A2*, and *tir1afb2D1*; Set 3: WT, *tir1afb2C*, *PsAFB6/+ 4-8 tir1afb2* and *PsAFB6/+ 3-3 tir1afb2*). A one-way analysis of variance (ANOVA) was performed followed by pairwise comparisons of means with Least Significant Difference (LSD) post-hoc tests using SPSS (Appendix Tables B3-B5). Statistical significance was declared at $P \leq 0.05$.

The experimental design for the fresh weights of the root-shoot transition region of the plants was a two-factor factorial, treatment (non-inoculated and clubroot-inoculated) and lines within sets (Set 1: WT, *tir1afb2C*, *tir1afb245*, *PsAFB6/+ 1-6 tir1afb245*, *PsAFB6/+ 3-2 tir1afb245*, and *PsAFB6/+ 5-9 tir1afb245*; Set 2: WT, *tir1afb2C*, *tir1afb2A2*, and *tir1afb2D1*; Set 3: WT, *tir1afb2C*, *PsAFB6/+ 4-8 tir1afb2*, and *PsAFB6/+ 3-3 tir1afb2*). A two-way analysis of variance (ANOVA) was performed followed by pairwise comparisons of means with LSD post-hoc tests using RStudio (Appendix Tables B6-B8). Statistical significance was declared at $P \leq 0.05$.

For Taqman qRT-PCR assays, prior to conducting the statistical analysis, the transcript abundance of each gene was converted to a \log_2 scale. Data were assumed to have normal distribution with homogeneity of variance. The experimental design for Taqman qRT-PCR assays was a two-factor factorial, (treatments (non-inoculated and clubroot-inoculated) and lines (WT, *tir1afb2C*, *PsAFB6/+ 4-8 tir1afb2*, *tir1afb245*, and *PsAFB6/+ 3-2 tir1afb245*) within genes. A two-way ANOVA was performed followed by pairwise comparisons of means with LSD post-hoc tests using RStudio (Appendix Table B2, B9-B18). Statistical significance was declared at $P \leq 0.05$.

3.3 RESULTS

3.3.1 Two new lines of auxin receptor double mutants were generated when *tir1-10* was the female parent

In preliminary experiments performed by Anu Jayasinghege in the Ozga/Strelkov lab, data from one double mutant auxin receptor line of *tir1-10* and *afb2-3* suggested that the double mutant exhibited reduced clubroot symptoms compared to the WT line. Therefore, additional lines of auxin receptor double mutants were generated to characterize clubroot disease progression in this mutant background. Two independently generated auxin receptor *tir1afb2A2* and *tir1afb2D1* double mutant lines were obtained when *tir1-10* was the female parent (*Attir1-10C1 X Atafb2-3A2* and *Attir1-10C1 X Atafb2-3D1*, respectively; Figure 3.3; see Appendix B Table B1 and Figure B1 for details). The crosses involving *Atafb2-3A2* single mutant female parent and the four independently generated auxin receptor *Attir1-10* single mutant plant lines that served as male parents (*Attir1-10A5*, *Attir1-10A7*, *Attir1-10B13* and *Attir1-10C1*) did not produce homozygous auxin receptor *tir1afb2* double mutant lines.

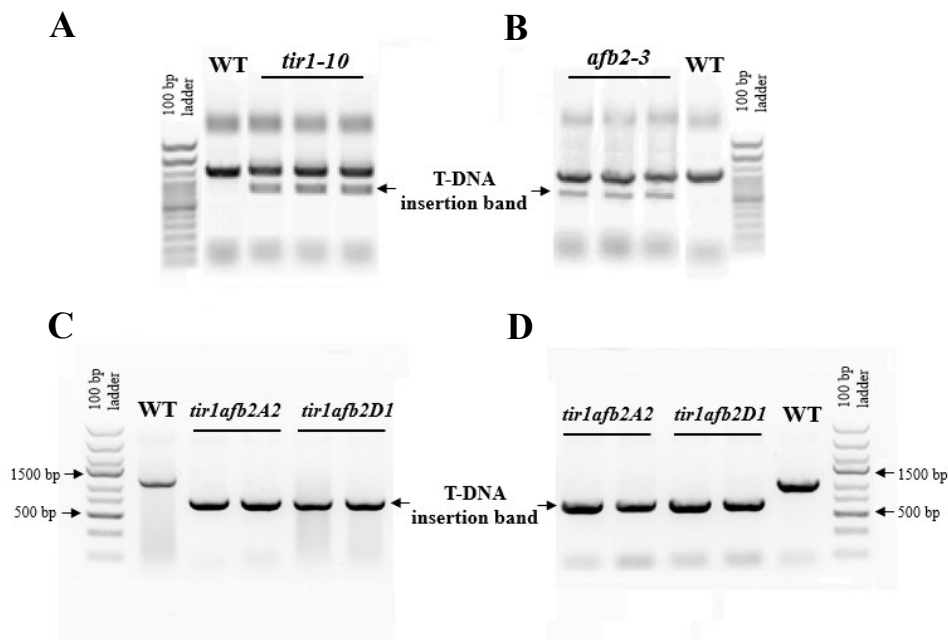


Figure 3.3 Molecular characterization of auxin receptor *tir1-10 afb2-3* T-DNA insertion in double mutant lines in Columbia-wild type (WT) background. Agarose gels showing PCR genotyping for analysis of T-DNA insertion of auxin receptors *tir1-10* and *afb2-3* in *tir1afb2* double mutant heterozygous [A, B] and homozygous [C, D] plants at DNA level using fresh leaf material. Genes with observed expected amplicons sizes: [A, C]: *tir1-10* and [B, D]: *afb2-3* were

amplified using direct PCR with primer sets reported in Appendix B Table 1. For a WT plant, one band per PCR reaction was amplified with the Left (LP) and right (RP) primers. The PCR product size for *tir1-10* and *afb2-3* amplified from the T-DNA-specific LB primer and the RP primer was smaller than the WT PCR product. For a heterozygous plant, two bands per PCR reaction amplified, one from the WT gene (amplified from the LP and RP primers), and one from the gene with the T-DNA insert (amplified from the LB and RP primers). Only one band per PCR reaction amplified from the gene containing the T-DNA insert (amplified from the LB and RP primers) for homozygous plants. See Appendix B Table B1 for primer details.

3.3.2 *PsAFB6* quantification using qRT-PCR assays in roots of clubroot-inoculated and non-inoculated *Arabidopsis* transgenic lines

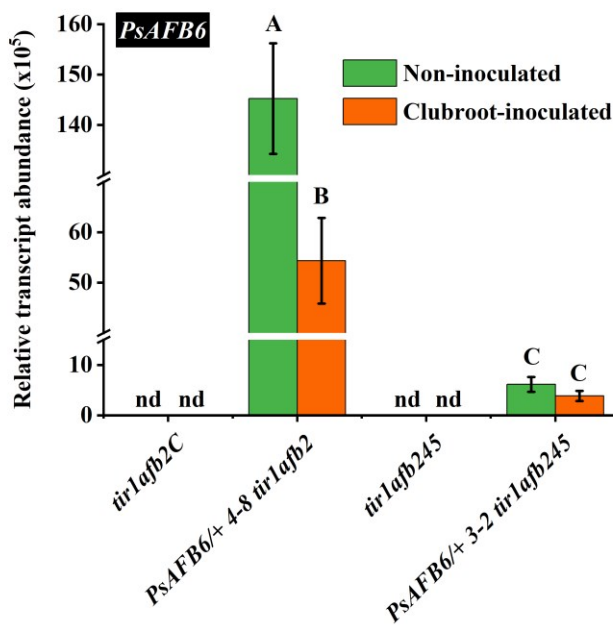


Figure 3.4 Transcript abundance of *PsAFB6* in clubroot-inoculated and non-inoculated root tissue of *Arabidopsis tir1afb2C* double mutant, *tir1afb245* quadruple mutant, and mutants expressing *PsAFB6* at 21 DAI. Seedlings were grown on peat-based medium for 16 days prior to inoculation and roots were harvested at 21 DAI for qRT-PCR. Data are means \pm standard error (SE). Biological replicates for the non-inoculated *tir1afb2C* line, n = 3; for the clubroot-inoculated *tir1afb2C* line, n = 4; for clubroot-inoculated and non-inoculated *tir1afb2* double mutant expressing *PsAFB6* (*PsAFB6*^{+/+} 4-8 *tir1afb2*) and *tir1afb245* quadruple mutant

and mutant expressing *PsAFB6* (*PsAFB6/+ 3-2 tir1afb245*), n = 4. The number of seedlings pooled for each biological replicate of non-inoculated root tissue was 18 seedlings for each line. The number of seedlings pooled for each biological replicate of clubroot-inoculated root tissue was 18 for *tir1afb2C*, 18 seedlings for *PsAFB6/+ 4-8 tir1afb2*, 16 seedlings for *tir1afb245*, and 18 seedlings for *PsAFB6/+ 3-2 tir1afb245*. Different letters indicate significantly different means among treatments and lines (Two-way-ANOVA, LSD post-hoc test, $P \leq 0.05$, Appendix Table B2). nd: no *PsAFB6* transcripts were detected.

PsAFB6 transcripts were present in both clubroot-inoculated and non-inoculated Arabidopsis *PsAFB6* transgenic *tir1afb2* (*PsAFB6/+ 4-8 tir1afb2*) and *tir1afb245* (*PsAFB6/+ 3-2 tir1afb245*) lines at 21 DAI. No *PsAFB6* transcripts were detected in the non-transgenic auxin receptor double and quadruple mutant lines (Figure 3.4). *PsAFB6* transcripts were higher in the non-inoculated *PsAFB6* expressing line *PsAFB6/+ 4-8 tir1afb2* than after clubroot-inoculation (2.7-fold; Figure 3.4; Appendix Table B2). The roots of the lowest *PsAFB6*-expressing treatment (clubroot-inoculated *PsAFB6/+ 3-2 tir1afb245* line), still contained substantial *PsAFB6* transcripts (1×10^5 relative transcript abundance) at 21 DAI.

3.3.3 Clubroot disease index calculation indicates reducing auxin response reduces disease progression

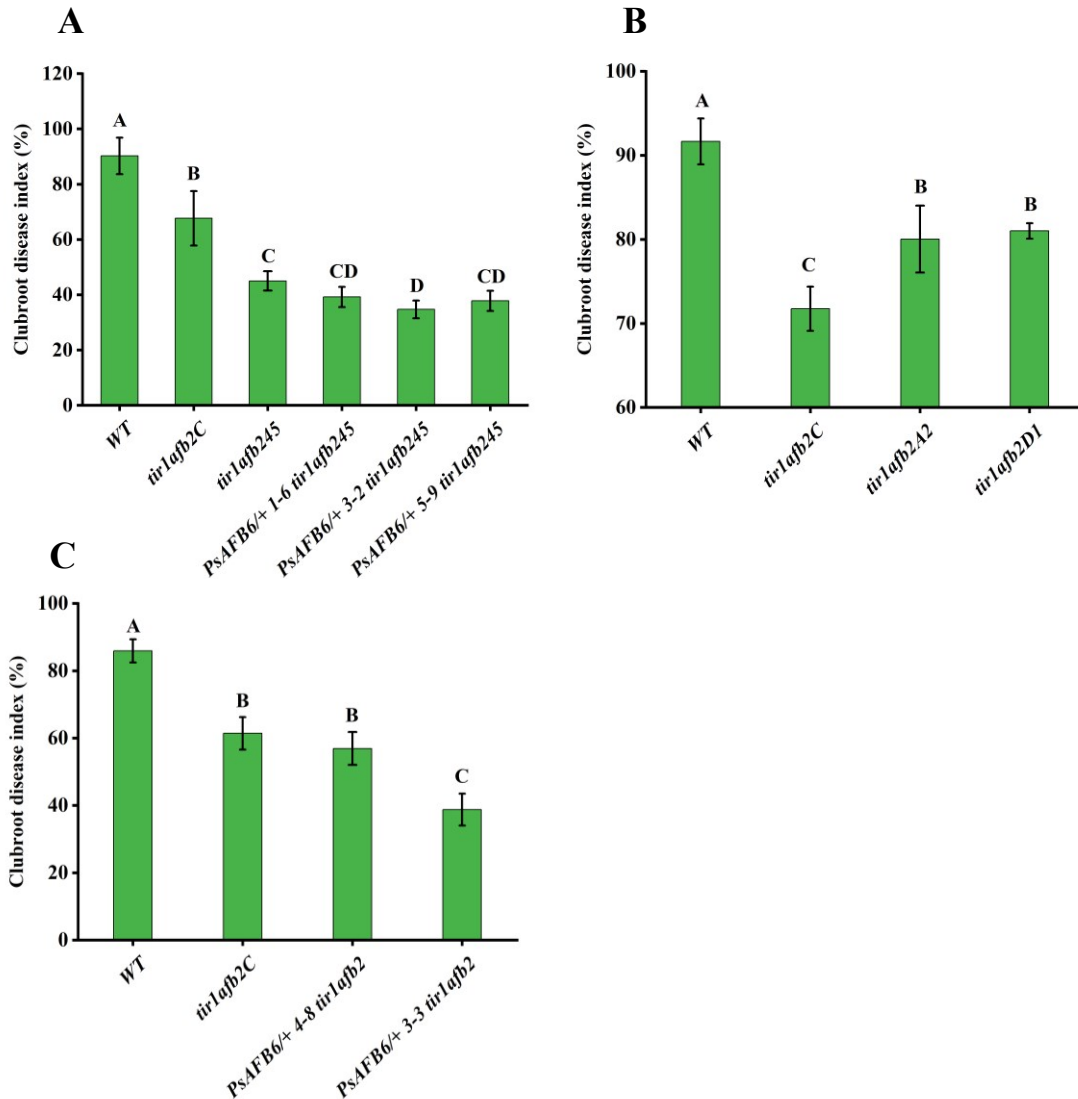


Figure 3.5 Clubroot disease severity index (DI) of Arabidopsis auxin receptor *tir1afb2* double and *tir1afb245* quadruple mutants and mutants expressing *PsAFB6* caused by *P. brassicae* at 32 DAI. The DI was calculated using digitized images of the root-shoot transition zone of plants at 32 DAI (48-day-old plants with 16 days of seedling growth prior to clubroot-inoculation followed by 32 days of growth after clubroot-inoculation in the peat-based medium). Clubroot disease severity was assessed based on a 7-point scale scoring at 0.5 intervals from 0-3; where 0 = no visible galls or symptoms, and 3 being severely infected or decayed roots (see Figure 3.2 for representative pictures). Plant lines were grown together in the same growth chamber within sets, (A) Set 1: Wild type (WT), *tir1afb2C*, *tir1afb245* and lines transformed with

PsAFB6 in *tir1afb245* mutant background (*PsAFB6/+ 1-6 tir1afb245*, *PsAFB6/+ 3-2 tir1afb245* and *PsAFB6/+ 5-9 tir1afb245*); **(B)** Set 2: WT and three independently generated auxin receptor double mutant lines (*tir1afb2C*, *tir1afb2A2* and *tir1afb2D1*); and Set 3: **(C)** WT, *tir1afb2C* and *PsAFB6*-expressing lines (*PsAFB6/+ 4-8 tir1afb2* and *PsAFB6/+ 3-3 tir1afb2*). Data are means \pm standard error (SE). The details on the biological replications for each graph are as follows: **(A)** n=4 per line, **(B)** n=6 per line, and **(C)** n=3 per line. Each biological replication is a pool of 10-12 plants for each line. Different letters indicate significantly different means among lines within sets (One-way-ANOVA, LSD post-hoc test, $P \leq 0.05$, Appendix Tables B3-5). A high disease index value suggests plants developed strong clubroot symptoms, whereas those plants with a low disease index value indicates plants developed minor symptoms.

The WT line exhibited the highest disease index (DI) when inoculated with *P. brassicae* (DI = 90.3 %), followed by the *tir1afb2C* double mutant (DI = 67.7 %), then the *tir1afb245* quadruple mutant (DI = 45.0 %) lines at 32 DAI (Figure 3.5A; see Figure 3.6 for representative images of lines at 32 DAI). One of the three lines expressing *PsAFB6* in the quadruple mutant background (*PsAFB6/+ 3-2 tir1afb245* line) had a lower DI (34.7 %) than the *tir1afb245* line (45.0 %; Figure 3.5A). The *PsAFB6/+ 1-6 tir1afb245* and *PsAFB6/+ 5-9 tir1afb245* lines had lower average DIs, but they were not significantly different from the quadruple mutant control line.

Three independently created *tir1afb2* double mutant lines all showed milder clubroot disease symptoms with ~ 10-20 % lower values for clubroot disease index (71.8-81 %) compared to the WT (DI=91.7 %) at 32 DAI (Figure 3.5B; see Figure 3.7 for representative images of lines at 32 DAI). Expression of *PsAFB6* in the *tir1afb2* mutant background (*PsAFB6/+ 3-3 tir1afb2* line) resulted in a low DI (38.8 %) than that for the *tir1afb2C* line (61.4 %; Figure 3.5C; see Figure 3.8 for representative images of lines at 32 DAI). The *PsAFB6/+ 4-8 tir1afb2* line had a slightly lower average DI, but it was not significantly different from the *tir1afb2C* line.

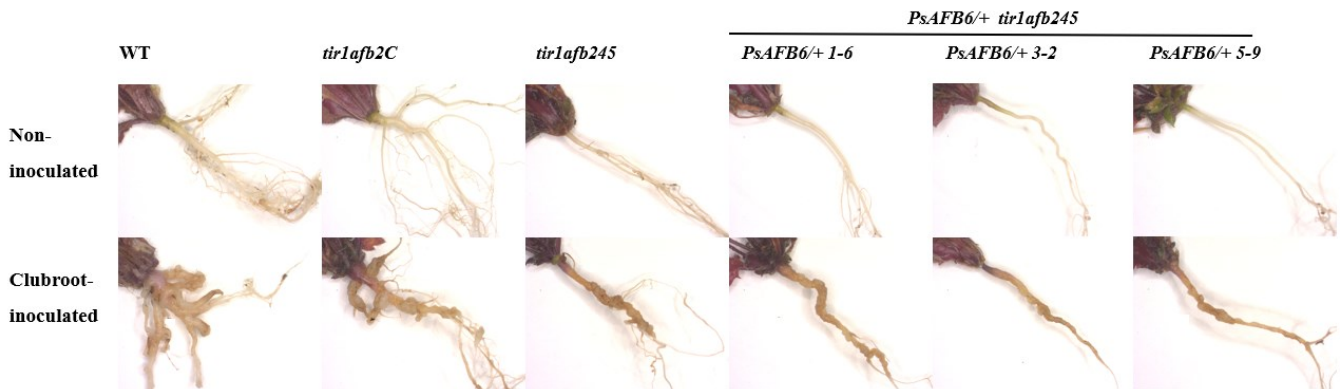


Figure 3.6 Representative microscopic images of the root-shoot transition region of clubroot-inoculated and non-inoculated *Arabidopsis* Columbia wild-type (WT), auxin receptor *tir1afb2* double and *tir1afb245* quadruple mutant lines, and *PsAFB6*-expressing quadruple mutant lines at 32 DAI.

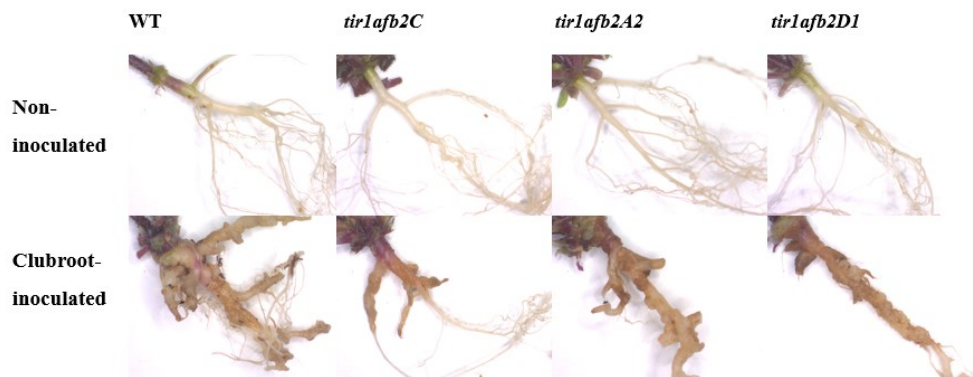


Figure 3.7 Representative microscopic images of the root-shoot transition region of clubroot-inoculated and non-inoculated *Arabidopsis* Columbia wild-type (WT), auxin receptor *tir1afb2* double mutant lines at 32 DAI.

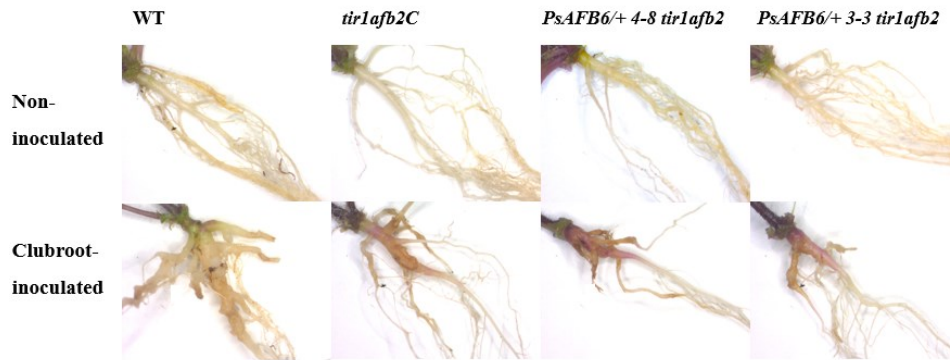


Figure 3.8 Representative microscopic images of the root-shoot transition region of clubroot-inoculated and non-inoculated *Arabidopsis* Columbia wild-type (WT), auxin receptor *tir1afb2* double mutant and double mutant lines expressing *PsAFB6* at 32 DAI.

3.3.4 Frequency distribution of disease severity in clubroot-inoculated *Arabidopsis* lines

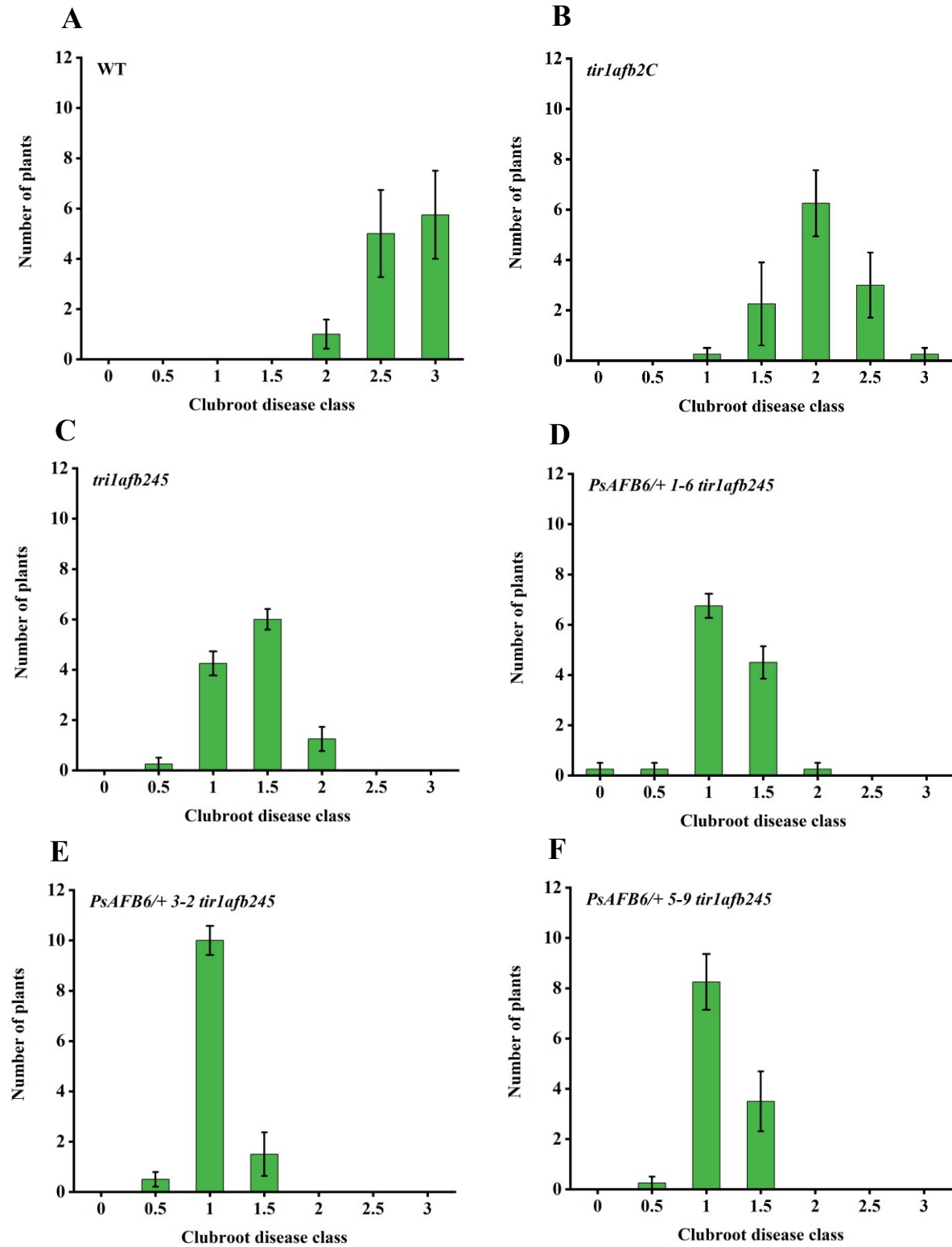


Figure 3.9 The frequency distribution of disease severity in *P. brassicae*-inoculated Arabidopsis WT, *tir1afb2* and *tir1afb245* mutant lines, and mutant lines expressing *PsAFB6* at 32 DAI. Frequency distribution of disease severity in clubroot-inoculated Arabidopsis WT (A), *tir1afb2C* (B), *tir1afb245* (C), *PsAFB6/+ 1-6 tir1afb245* (D), *PsAFB6/+ 3-2 tir1afb245* (E) and *PsAFB6/+ 5-9 tir1afb245* (F) lines that were grown together in same growth chamber. Clubroot disease severity was assessed from digitized images of the root-shoot transition zone of plants at 32 DAI based on a 7-point scale scoring at an interval of 0.5 from 0-3 where 0 = no visible galls (no infection or symptoms) and 3 being the severely infected or roots decayed. Data are means \pm standard error (SE), n=4 biological replicates. Each biological replicate is a pool of 11-12 roots for each line. This is the frequency distribution of data presented in Figure 3.5A.

At 32 DAI, the *P. brassicae*-inoculated WT plants developed severe clubroot disease symptoms, with a median disease severity class of 2.5 (Figure 3.9A). Plants from the auxin receptor *tir1afb2C* double mutant line developed milder disease symptoms, shifting the frequency distribution to a lower disease severity class median of 2; (Figure 3.9B). Clubroot symptoms for the *tir1afb245* quadruple mutant line were less severe than the *tir1afb2C* double mutant line, with a median disease severity class of 1.5 (Figure 3.9C). Expression of *PsAFB6* in the *tir1afb245* mutant background shifted the frequency distribution lower in all three independent transgenic lines with a median disease severity class of 1 (Figure 3.9D-F).

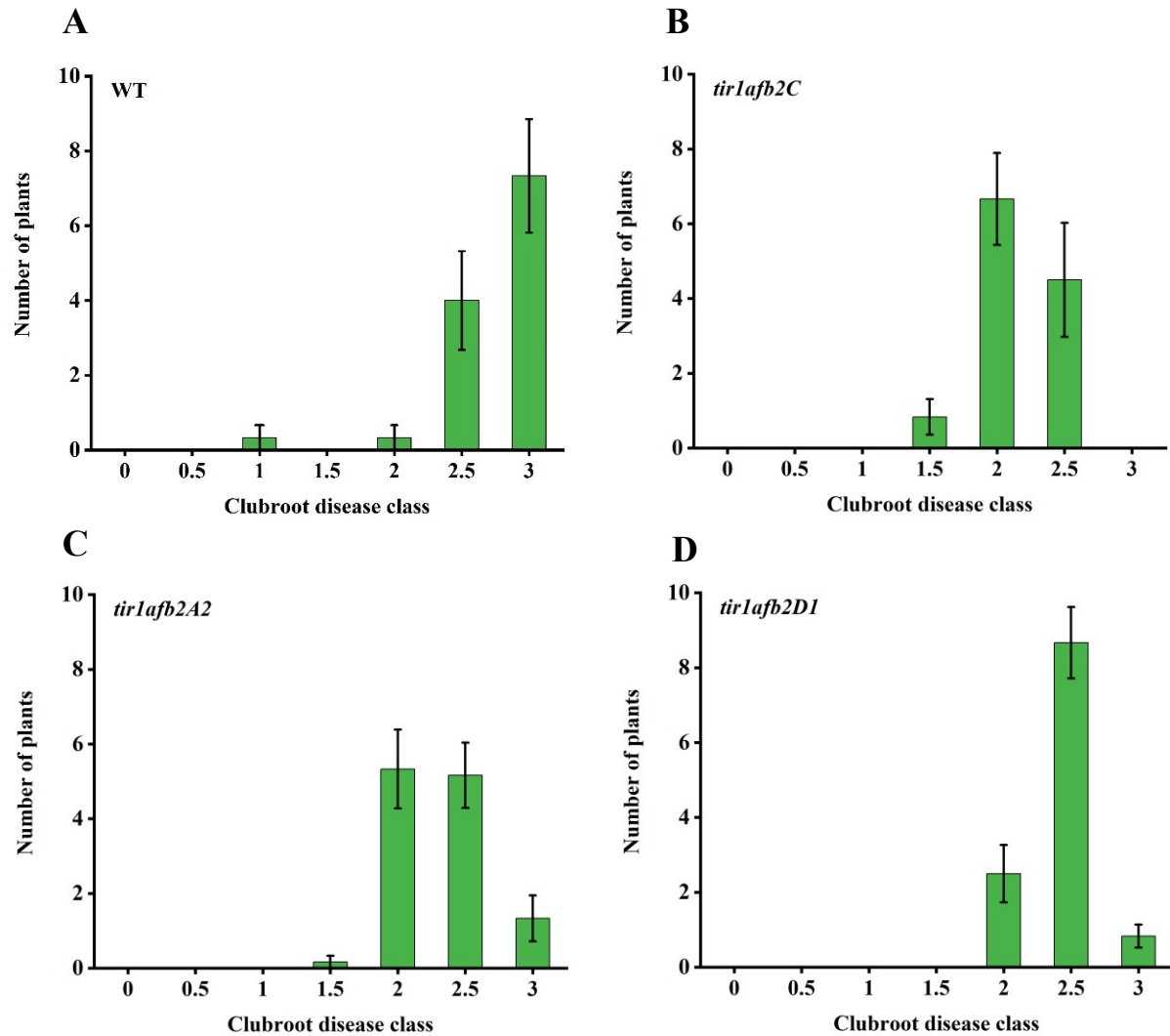


Figure 3.10 Frequency distribution of disease severity in *P. brassicae*-inoculated *Arabidopsis tir1afb2* mutant lines at 32 DAI. Frequency distribution of disease severity in clubroot-inoculated *Arabidopsis* WT (**A**), *tir1afb2C* (**B**), *tir1afb2A2* (**C**) and *tir1afb2D1* (**D**) lines that were grown together in same growth chamber. Clubroot disease severity was assessed from digitized images of the root-shoot transition zone of plants at 32 DAI based on a 7-point scale scoring at an interval of 0.5 from 0-3 where 0 = no visible galls (no infection or symptoms) and 3 being the severely infected or roots decayed. Data are means \pm standard error (SE), n=6 biological replicates. Each biological replicate is a pool of 10-12 roots for each line. This is the frequency distribution of data presented in Figure 3.5B.

Similar to the separate experimental set presented in Figure 3.9A, at 32 DAI the *P. brassicae*-inoculated WT plants in this set developed severe clubroot disease symptoms, with a median disease severity class of 3 (Figure 3.10A). Plants from all three independently generated *tir1afb2* auxin receptor mutant lines developed milder disease symptoms than the WT line, shifting the frequency distribution to a lower median disease severity rating of 2 for the *tir1afb2C* line, and 2.5 for lines *tir1afb2A2* and *tir1afb2D1* (Figure 3.10B-D).

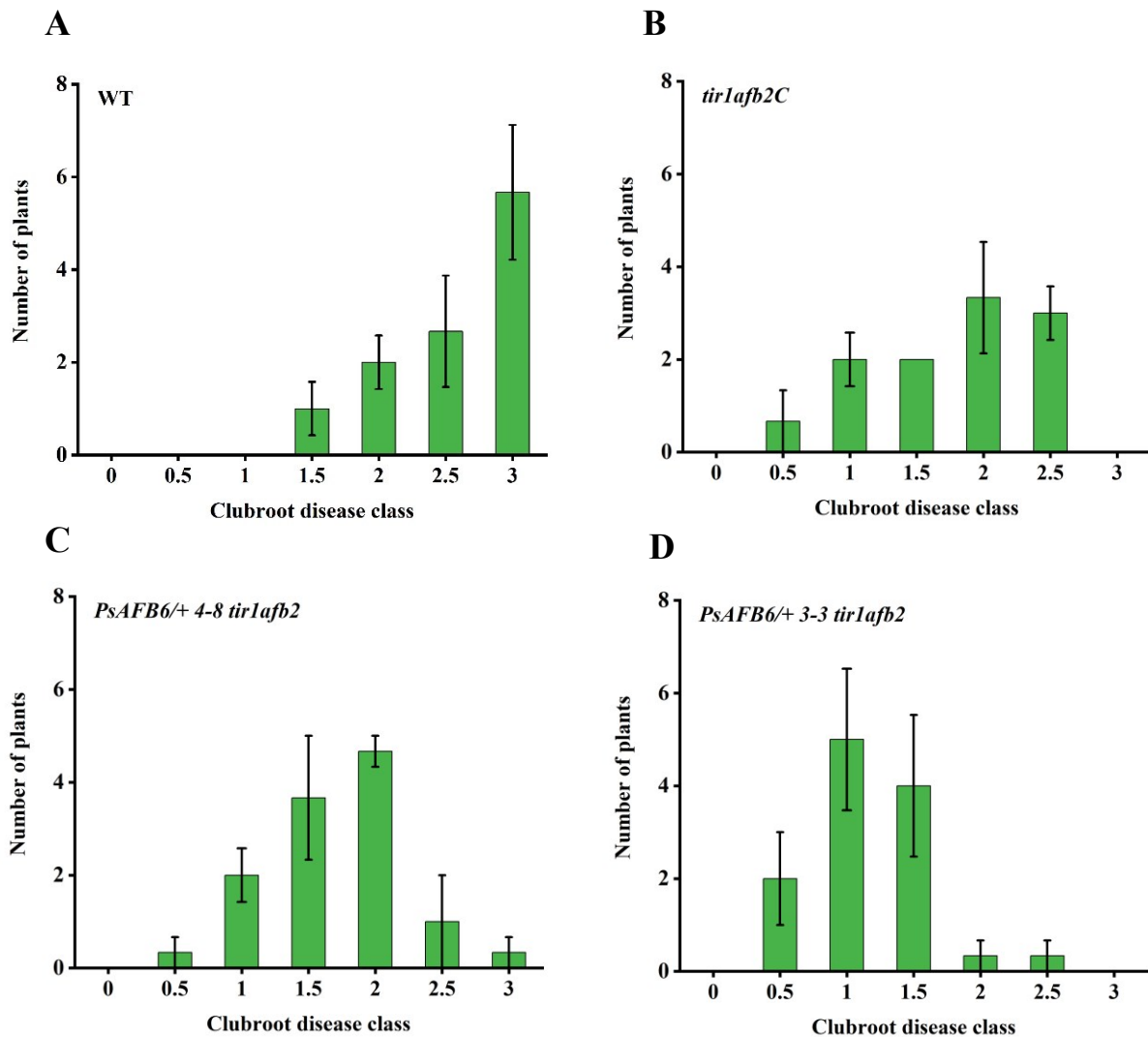


Figure 3.11 Frequency distribution of disease severity in *P. brassicae*-inoculated Arabidopsis *tir1afb2* mutant line and mutant lines expressing *PsAFB6* at 32 DAI. Frequency distribution of disease severity in clubroot-inoculated Arabidopsis WT (A), *tir1afb2C* (B), *PsAFB6/+ 4-8*

tir1afb2 (C), *PsAFB6/+ 3-3 tir1afb2* (D) lines that were grown together in same growth chamber. Clubroot disease severity was assessed from digitized images of the root-shoot transition zone of plants at 32 DAI based on a 7-point scale scoring at an interval of 0.5 from 0-3 where 0 = no visible galls (no infection or symptoms) and 3 being the severely infected or roots decayed. Data are means \pm standard error (SE), n=3 biological replicates. Each biological replicate is a pool of 10-12 roots for each line. This is the frequency distribution of data presented in Figure 3.5C.

The *P. brassicae*-inoculated WT plants in this set also developed severe clubroot disease symptoms, with a median disease severity class of 2.5, and the auxin receptor *tir1afb2C* double mutant line developed milder disease symptoms than the WT line with a median disease severity class of 2, at 32 DAI (Figure 3.11A and B), similar to the results in separate experimental sets presented in Figures 3.9A and B and 3.10A and B. Expression of *PsAFB6* in the *tir1afb2* double mutant background shifted the frequency distribution lower in both independent transgenic lines with a median disease severity class of 1.5 in *PsAFB6/+ 4-8 tir1afb2* and 1 in *PsAFB6/+ 3-3 tir1afb2* (Figure 3.11C and D).

3.3.5 Average fresh weights of the root-shoot transition region are consistent with the DI ratings in response to *P. brassicae* inoculation

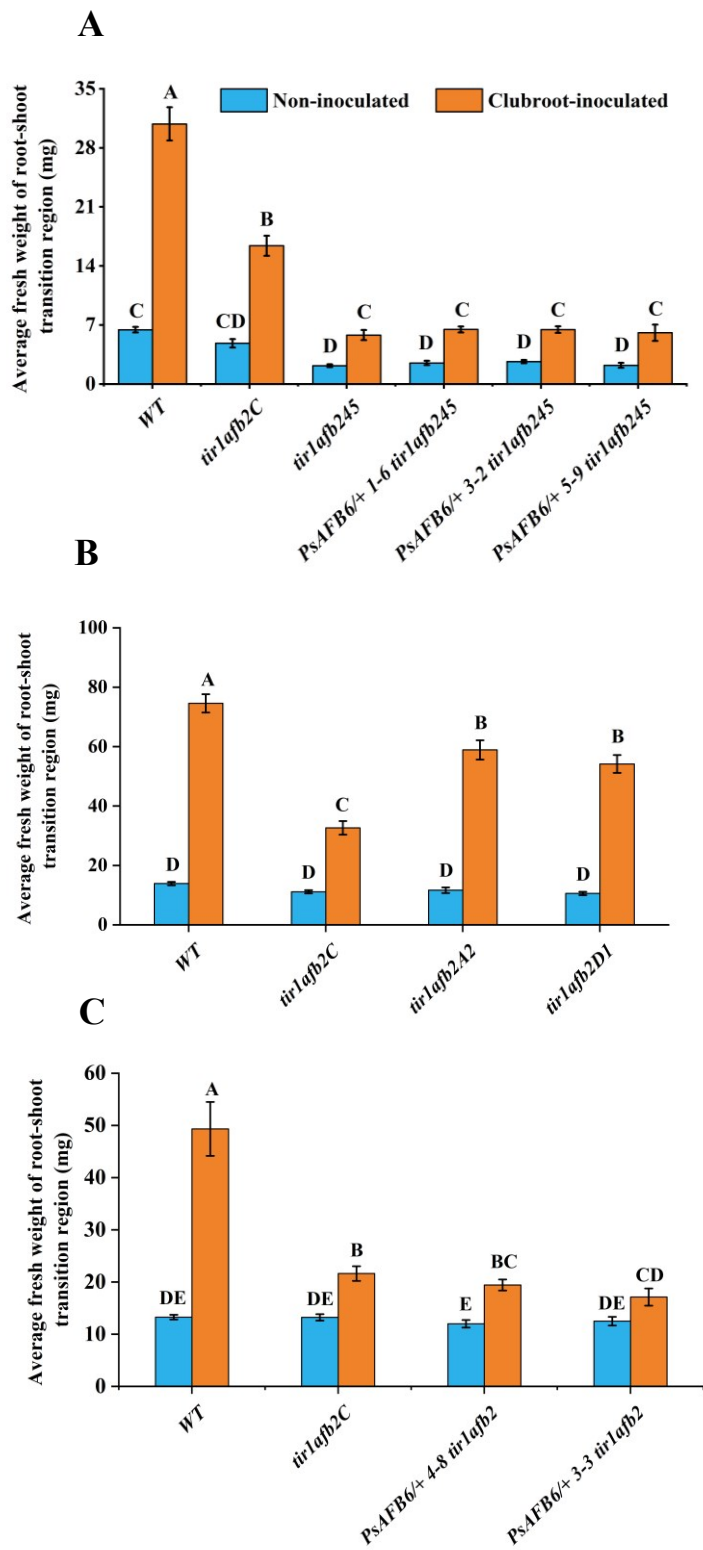


Figure 3.12 Root-shoot transition region fresh weights of clubroot-inoculated and non-inoculated Arabidopsis WT, *tir1afb2* and *tir1afb245* mutant lines, and mutants expressing *PsAFB6* at 32 DAI. Plants (48-day-old) with 16 days of seedling growth prior to clubroot-inoculation followed by 32 days of growth after clubroot-inoculation in the peat-based medium were assessed. Plant lines were grown together in same growth chamber within sets: **(A)** Set 1: Wild type (WT), *tir1afb2C*, *tir1afb245* and lines transformed with *PsAFB6* in *tir1afb245* mutant background (*PsAFB6/+ 1-6 tir1afb245*, *PsAFB6/+ 3-2 tir1afb245* and *PsAFB6/+ 5-9 tir1afb245*); **(B)** Set 2: WT and three independently generated auxin receptor double mutant lines (*tir1afb2C*, *tir1afb2A2* and *tir1afb2D1*); **(C)** Set 3: WT, *tir1afb2C* and *PsAFB6*-expressing lines (*PsAFB6/+ 4-8 tir1afb2* and *PsAFB6/+ 3-3 tir1afb2*). Data are means \pm standard error (SE). The root-shoot transition region (1.5 cm in length) with attached roots from 6 plants per line per treatment were pooled and weighed. Data are means \pm standard error (SE). The details on the biological replications for each graph are as follows: **(A)** WT: non-inoculated, n = 3 and clubroot-inoculated, n = 4; *tir1afb2C*: non-inoculated, n = 3 and clubroot-inoculated, n = 7; *tir1afb245*: non-inoculated, n = 3 and clubroot-inoculated, n = 6; *PsAFB6/+ 1-6 tir1afb245*: non-inoculated, n = 3 and clubroot-inoculated, n = 6; *PsAFB6/+ 3-2 tir1afb245*: non-inoculated, n = 3 and clubroot-inoculated, n = 7; *PsAFB6/+ 5-9 tir1afb245*: non-inoculated, n=3 and clubroot-inoculated, n=4. **(B)** WT: non-inoculated, n = 3 and clubroot-inoculated, n=8; *tir1afb2C*: non-inoculated, n = 3 and clubroot-inoculated, n = 12; *tir1afb2A2*: non-inoculated, n = 3 and clubroot-inoculated, n=9; *tir1afb2D1*: non-inoculated, n = 3 and clubroot-inoculated, n = 8. **(C)** WT: non-inoculated, n = 3 and clubroot-inoculated, n=2; *tir1afb2C*: non-inoculated, n = 3 and clubroot-inoculated, n = 7; *PsAFB6/+ 4-8 tir1afb2*: non-inoculated, n = 3 and clubroot-inoculated, n = 8; *PsAFB6/+ 3-3 tir1afb2*: non-inoculated, n = 3 and clubroot-inoculated, n = 8. Different letters indicate significantly different means among treatments and lines within sets (Two-way-ANOVA, LSD post-hoc test, $P \leq 0.05$, Appendix Table B6-8).

The average root-shoot transition region fresh weight was greater in all of the clubroot-inoculated Arabidopsis lines compared to their respective non-inoculated lines at 32 DAI due to clubroot-induced hypertrophy in this tissue (Figure 3.12). The *P. brassicae*-inoculated WT plants exhibited the highest tissue fresh weight (~4.8 times higher than the non-inoculated controls),

followed by the auxin receptor *tir1afb2C* double mutant line (~3.4 times higher than the non-inoculated control) and the least affected was the quadruple mutant (~2.6 times higher than the non-inoculated control) (Figure 3.12A). The trend in average fresh root weight among the *P. brassicae*-inoculated *WT*, *tir1afb2C*, and *tir1afb245* lines was similar to the trend observed for clubroot disease index (compare Figures 3.5A and 3.12A). The trend of lower average fresh root weight in all *tir1afb2* lines compared to the *WT* line inoculated with *P. brassicae* was also similar to the trend observed for clubroot disease index (compare Figures 3.5B and 3.12B). The *PsAFB6*-expressing double mutant *PsAFB6/+ 3-3 tir1afb2* line exhibited lower fresh weight (20.8 % reduction) than the *tir1afb2C* double mutant (Figure 3.12C, clubroot-inoculated), similar to the lower DI rating for this line compared to the double mutant control (Figure 3.5C).

3.3.6 qRT-PCR quantification of hormone-related genes in the clubroot-inoculated and non-inoculated roots of transgenic lines at 21 DAI

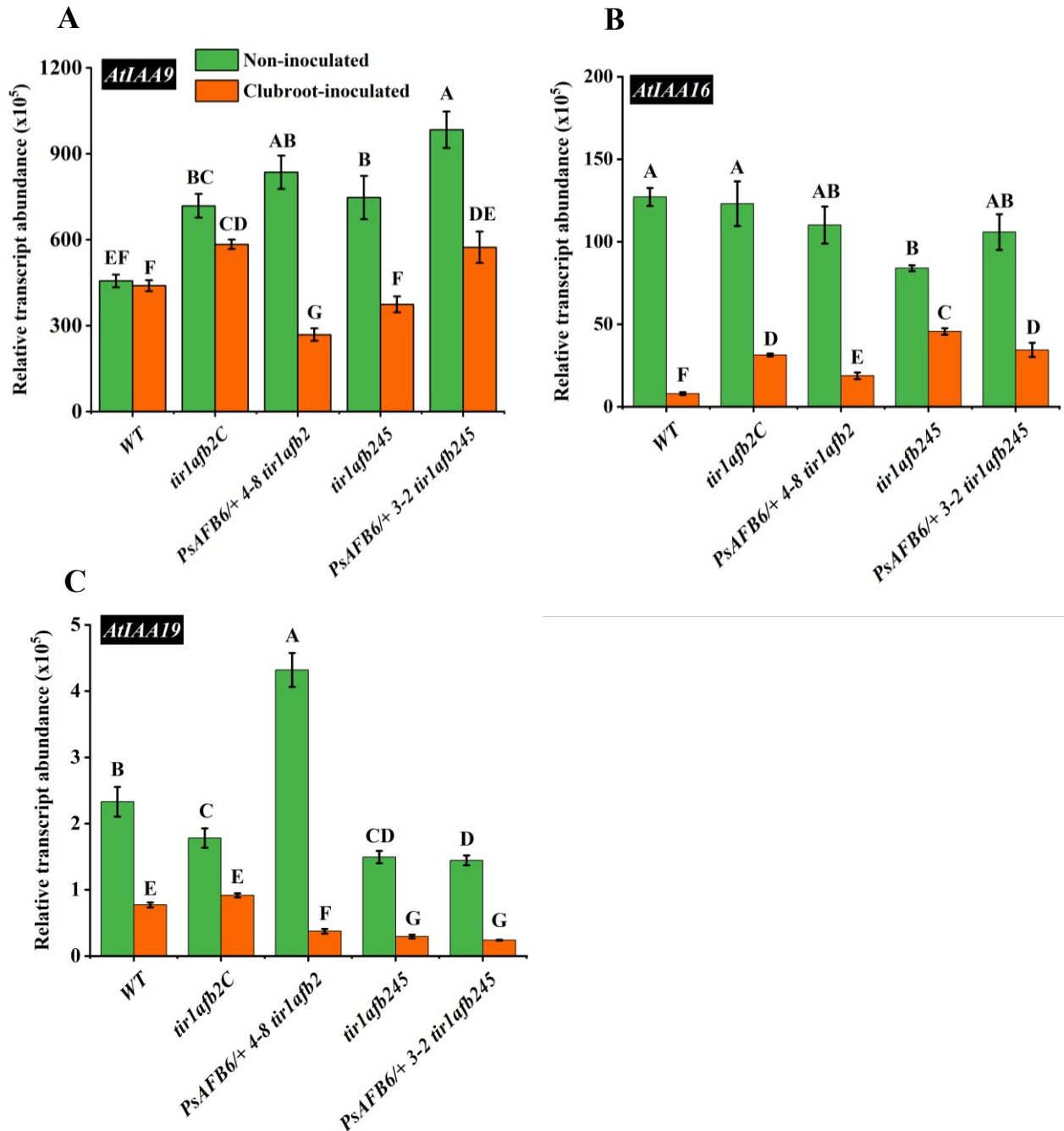


Figure 3.13 Transcript abundance of *AtIAA9*, *AtIAA16*, and *AtIAA19* in clubroot-inoculated and non-inoculated root tissue of Arabidopsis WT, *tir1afb2* double mutant, *tir1afb245* quadruple mutant, and mutants expressing *PsAFB6* at 21 DAI. *AtIAA9* (A), *AtIAA16* (B), and *AtIAA19* (C) transcript abundance in clubroot-inoculated and non-inoculated

Arabidopsis WT, *tir1afb2C* double mutant and mutants expressing *PsAFB6* (*PsAFB6/+ 4-8 tir1afb2*), *tir1afb245* quadruple mutant and mutants expressing *PsAFB6* (*PsAFB6/+ 3-2 tir1afb245*) at 21 DAI. Seedlings were grown on peat-based medium for 16 days prior to inoculation and roots were harvested at 21 DAI for qRT-PCR. Data are means \pm standard error (SE). For all lines and treatments, n=4 biological replicates, except the non-inoculated WT line, where, n = 3, Each biological replicate of non-inoculated root tissue is a pool of 18 seedlings for each line. The number of seedlings pooled for each biological replicate of clubroot-inoculated root tissue was 17-18 for WT, 18 for *tir1afb2C*, 18 for *PsAFB6/+ 4-8 tir1afb2*, 16 for *tir1afb245*, and 18 for *PsAFB6/+ 3-2 tir1afb245*. Different letters indicate significantly different means among treatments and lines within genes (Two-way-ANOVA, LSD post-hoc test, $P \leq 0.05$, Appendix Tables B9-B11).

In non-inoculated plants, a decrease in auxin response in the *tir1afb2C* and *tir1afb245* lines, increased *AtIAA9* transcript abundance compared to the WT line (Fig. 3.13A). Expression of *PsAFB6* in the *tir1afb2* auxin mutant background did not change *AtIAA9* transcript abundance; however, an increase in *AtIAA9* transcript abundance was observed in the *tir1afb245* mutant background line expressing *PsAFB6*. Inoculation with *P. brassicae* did not affect the transcript abundance of *AtIAA9* in the WT or *tir1afb2C* mutant line, but transcript abundance was reduced in the *tir1afb245* line (2-fold) compared to the non-inoculated controls at 21 DAI. Expression of *PsAFB6* reduced *AtIAA9* transcript abundance in the inoculated *tir1afb2* mutant line by 3.1-fold relative to the non-inoculated control at 21 DAI (Figure 3.13A; Appendix Table B9).

AtIAA16 transcript abundance was similar across the lines of non-inoculated plants with one exception, lower transcript abundance was observed in the *tir1afb245* line (Figure 3.13B). Inoculation with *P. brassicae* reduced the transcript abundance of *AtIAA16* in all lines compared to their non-inoculated controls, with the greatest reduction observed in the WT line (~16.0-fold), followed by *tir1afb2C* (~3.9-fold), then the *tir1afb245* (~1.8-fold) mutant lines at 21 DAI. Expression of *PsAFB6* in both double and quadruple auxin receptor mutant backgrounds reduced *AtIAA16* transcript abundance when inoculated with *P. brassicae* (Figure 3.13B; Appendix Table B10).

In non-inoculated plants, a decrease in auxin response in the *tir1afb2C* and *tir1afb245* lines decreased *AtIAA19* transcript abundance compared to the WT. Expression of *PsAFB6* in the *tir1afb2* auxin mutant background increased *AtIAA19* transcript abundance by 2.4-fold compared to the *tir1afb2C* mutant line, but it did not affect transcript levels in the *tir1afb245* mutant background. Inoculation with *P. brassicae* reduced the transcript abundance of *AtIAA19* in all lines compared to their non-inoculated controls, with the greatest reduction observed in the *tir1afb245* mutant line (~5.1-fold), followed by WT line (~3.0-fold), then the *tir1afb2C* mutant line (~1.9-fold) at 21 DAI. In *P. brassicae*-inoculated plants at 21 DAI, expression of *PsAFB6* in the *tir1afb2* mutant background decreased *AtIAA19* transcript abundance by 2.4-fold compared to the *tir1afb2C* line, but *PsAFB6* expression had no effect on that in the *tir1afb245* mutant background (Figure 3.13C; Appendix Table B11).

Overall, the transcript abundance of *AtIAA16* and *AtIAA19* decreased in the roots of all lines after *P. brassicae* inoculation at 21 DAI. Furthermore, expression of *PsAFB6* in the *tir1afb2* mutant background decreased the transcript abundance of *AtIAA9*, *AtIAA16* and *AtIAA19* in the roots of *P. brassicae*-inoculated plants at 21 DAI.

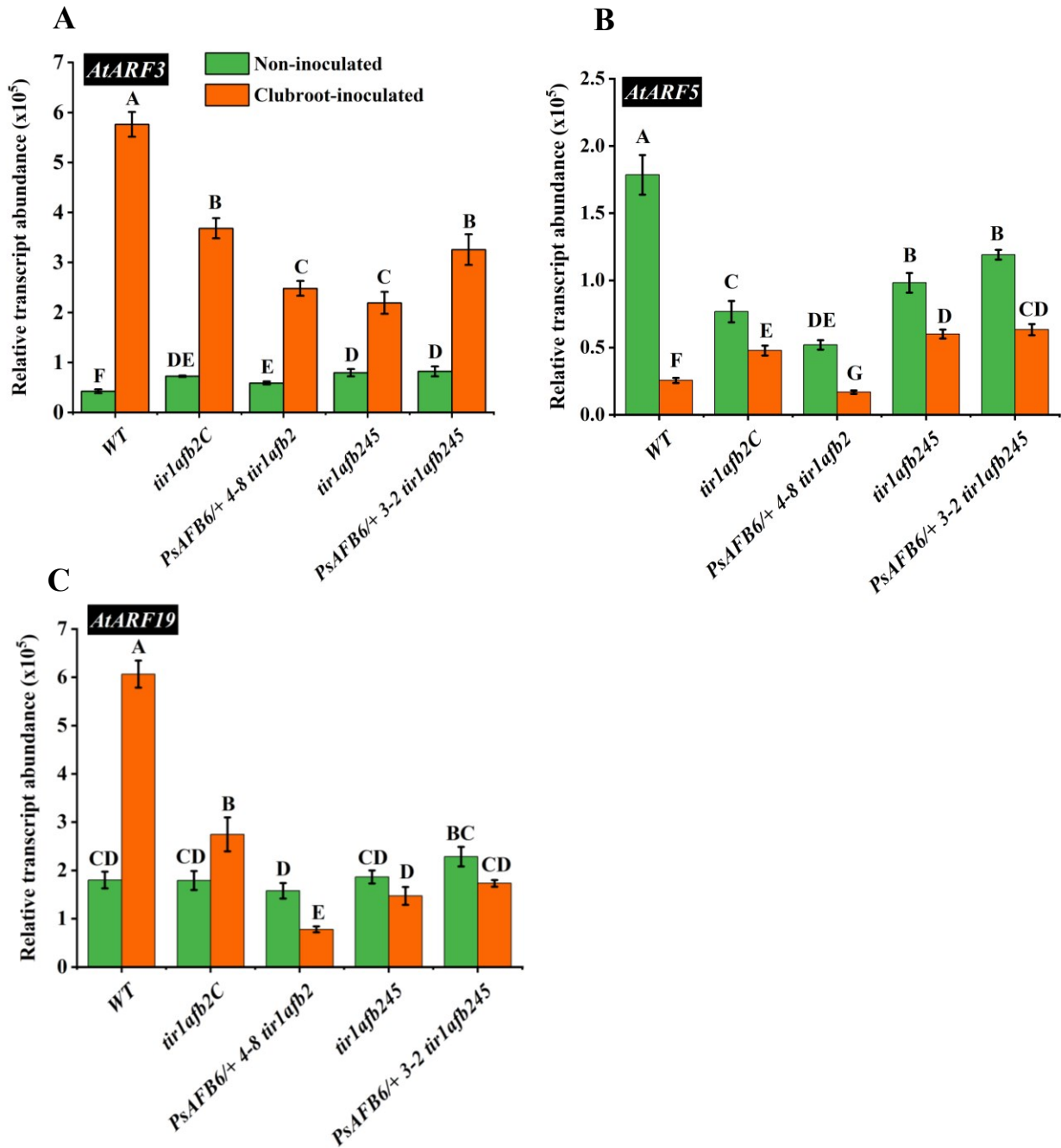


Figure 3.14 Transcript abundance of *AtARF3*, *AtARF5*, and *AtARF19* in clubroot-inoculated and non-inoculated root tissue of Arabidopsis WT, *tir1afb2* double mutant, *tir1afb245* quadruple mutant, and mutants expressing *PsaAFB6* at 21 DAI. *AtARF3* (A), *AtARF5* (B), and *AtARF19* (C) transcript abundance in clubroot-inoculated and non-inoculated Arabidopsis WT, *tir1afb2C* double mutant and mutants expressing *PsaAFB6* (*PsaAFB6/+ 4-8*

tir1afb2), *tir1afb245* quadruple mutant and mutants expressing *PsAFB6* (*PsAFB6/+ 3-2 tir1afb245*) at 21 DAI. Seedlings were grown on peat-based medium for 16 days prior to inoculation and roots were harvested at 21 DAI for qRT-PCR. Data are means \pm standard error (SE). For all lines and treatments, n=4 biological replicates, except the non-inoculated WT line, where, n = 3, Each biological replicate of non-inoculated root tissue is a pool of 18 seedlings for each line. The number of seedlings pooled for each biological replicate of clubroot-inoculated root tissue was 17-18 for WT, 18 for *tir1afb2C*, 18 for *PsAFB6/+ 4-8 tir1afb2*, 16 for *tir1afb245*, and 18 for *PsAFB6/+ 3-2 tir1afb245*. Different letters indicate significantly different means among treatments and lines within genes (Two-way-ANOVA, LSD post-hoc test, $P \leq 0.05$, Appendix Tables B12-B14).

Minimal to no differences in *AtARF3* transcript abundance was observed among the lines of non-inoculated plants (Figure 3.14A). Inoculation with *P. brassicae* increased the transcript abundance of *AtARF3* in all lines compared to their non-inoculated controls, with the greatest induction observed in the WT line (~13.5-fold), followed by *tir1afb2C* mutant (~5.1-fold), then the *tir1afb245* mutant line (~2.8-fold) at 21 DAI. In the *P. brassicae*-inoculated plants, expression of *PsAFB6* in the *tir1afb2* mutant background decreased *AtARF3* transcript abundance by 1.5-fold compared to the *tir1afb2* line; however, *PsAFB6* expression in the *tir1afb245* mutant background increased transcript abundance by 1.5-fold compared to the *tir1afb245* line at 21 DAI (Figure 3.14A; Appendix Table B12).

In non-inoculated plants, a reduction in auxin response in the *tir1afb2C* and *tir1afb245* lines decreased the abundance of *AtARF5* transcripts (Figure 3.14B). Expression of *PsAFB6* in the *tir1afb2* auxin mutant background decreased *AtARF5* transcript abundance by 1.5-fold compared to the *tir1afb2C* line, but it had no impact on *AtARF5* transcript levels in the *tir1afb245* mutant background. When inoculated with *P. brassicae*, the transcript abundance of *AtARF5* decreased in all plant lines compared to their non-inoculated controls 21 DAI, with the largest reduction of *AtARF5* transcripts observed in the WT line (~7.0-fold), followed by the *tir1afb2C* and *tir1afb245* lines with a 1.6-fold reduction each. In *P. brassicae*-inoculated plants, expression of *PsAFB6* in the *tir1afb2* auxin mutant background decreased *AtARF5* transcript

abundance by 2.8-fold compared to the *tir1afb2C* line, but it had no effect on *AtARF5* transcript levels in the *tir1afb245* quadruple mutant background (Figure 3.14B; Appendix Table B13).

Minimal to no differences were observed in *AtARF19* transcript abundance among the lines of non-inoculated plants (Figure 3.14C). Inoculation with *P. brassicae* increased *AtARF19* transcript abundance in the WT (~3.4-fold) and *tir1afb2C* (~1.5-fold) lines compared to their non-inoculated controls at 21 DAI. *AtARF19* transcript abundance decreased with decreasing auxin response (WT > *tir1afb2* > *tir1afb245*) in the *P. brassicae*-inoculated lines at 21 DAI. Expression of *PsAFB6* in the *tir1afb2* mutant background decreased *ARF19* transcript abundance by 2.4-fold compared to the *tir1afb2C* line in *P. brassicae*-inoculated plants at 21 DAI (Figure 3.14C; Appendix Table B14).

In summary, the transcript abundance of *AtARF3* increased while the *AtARF5* transcript abundance decreased in all lines after *P. brassicae* inoculation at 21 DAI. Both *AtARF3* and *AtARF19* transcript abundance decreased with decreasing auxin response (WT > *tir1afb2* > *tir1afb245*) in *P. brassicae*-inoculated plants at 21 DAI. In addition, the introduction of *PsAFB6* into the *tir1afb2* double mutant background resulted in a reduction in the transcript abundance of *AtARF3*, *AtARF5*, and *AtARF19* in the roots of *P. brassicae*-inoculated plants at 21 DAI.

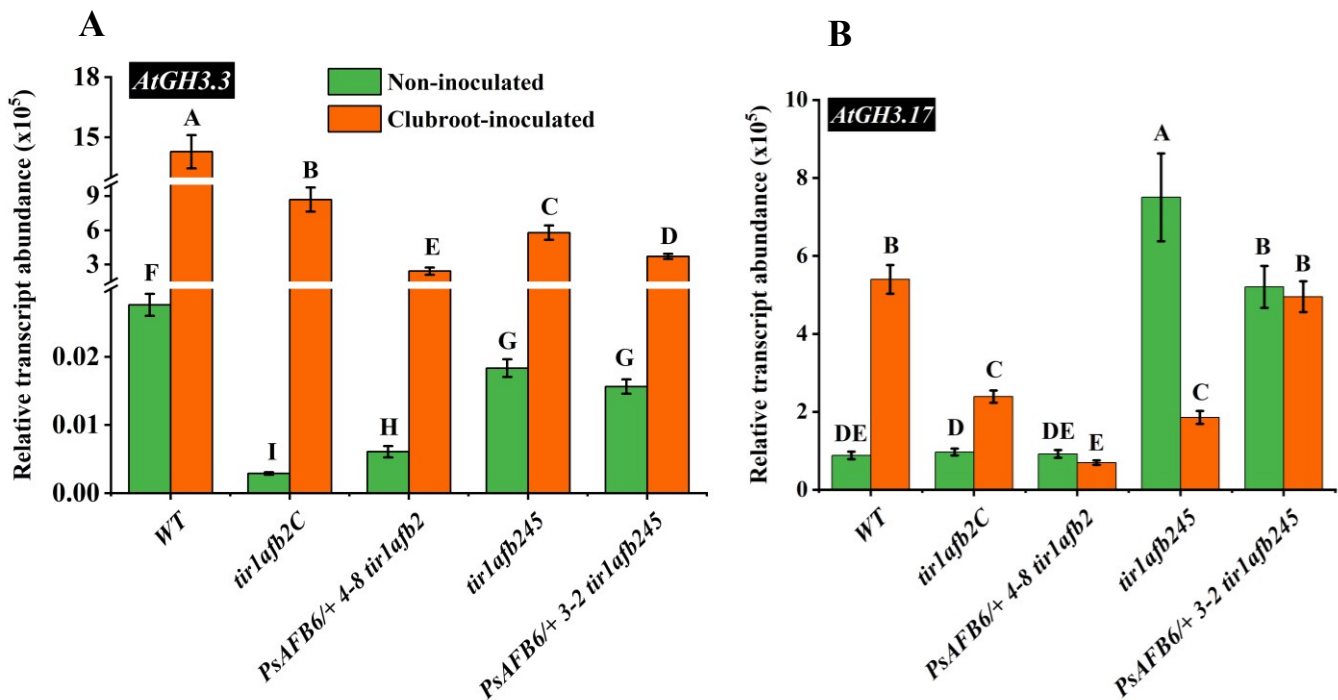


Figure 3.15 Transcript abundance of *AtGH3.3* and *AtGH3.17* in clubroot-inoculated and non-inoculated root tissue of Arabidopsis WT, *tir1afb2* double mutant, *tir1afb245* quadruple mutant, and mutants expressing *PsAFB6* at 21 DAI. *AtGH3.3* (A) and *AtGH3.17* (B) transcript abundance in clubroot-inoculated and non-inoculated root tissue of Arabidopsis WT, *tir1afb2C* double mutant, *tir1afb245* quadruple mutant, and mutants expressing *PsAFB6* at 21 DAI. Seedlings were grown on peat-based medium for 16 days prior to inoculation and roots were harvested at 21 DAI for qRT-PCR. Data are means \pm standard error (SE). For all lines and treatments, n=4 biological replicates, except the non-inoculated WT line, where n = 3. Each biological replicate of non-inoculated root tissue is a pool of 18 seedlings for each line. The number of seedlings pooled for each biological replicate of clubroot-inoculated root tissue was 17-18 for WT, 18 for *tir1afb2*, 18 for *PsAFB6/+ 4-8 tir1afb2*, 16 for *tir1afb245*, and 18 for *PsAFB6/+ 3-2 tir1afb245*. Different letters indicate significantly different means among treatments and lines within genes (Two-way-ANOVA, LSD post-hoc test, $P \leq 0.05$, Appendix Table B15-16).

In non-inoculated plants, the reduction in auxin response in the *tir1afb2C* and *tir1afb245* lines led to a decrease in *AtGH3.3* transcript levels when compared to the WT line, with a greater decrease in transcript abundance exhibited in the *tir1afb2C* line relative to the WT line (Figure 3.15A). In the *tir1afb2* auxin mutant background, the expression of *PsAFB6* led to a 2.1-fold increase in *AtGH3.3* transcript abundance, while it had no effect on transcript levels in the *tir1afb245* quadruple mutant background. When inoculated with *P. brassicae*, the transcript abundance of *AtGH3.3* markedly increased in all plant lines compared to their non-inoculated controls, with the highest transcript levels occurring in the WT line, followed by the *tir1afb2C* line, then the *tir1afb245* line. In *P. brassicae*-inoculated plants, expression of *PsAFB6* in the *tir1afb2* and *tir1afb245* auxin mutant backgrounds decreased *AtGH3.3* transcript abundance by 3.6-fold and 1.6-fold, respectively, compared to their respective background lines (Figure 3.15A; Appendix Table B15).

In non-inoculated plants, a decrease in auxin response in the *tir1afb2C* did not affect the transcript abundance of *AtGH3.17*; however, the *tir1afb245* line had higher transcript levels (8.5-fold) compared to the WT and *tir1afb2C* lines (Figure 3.15B). Expression of *PsAFB6* in the *tir1afb2* auxin mutant background did not change *AtGH3.17* transcript abundance; however, a

decrease in *AtGH3.17* transcript abundance was observed in the *tir1afb245* mutant background line expressing *PsAFB6*. Inoculation with *P. brassicae* increased *AtGH3.17* transcript abundance in the WT (~6.1-fold) and *tir1afb2C* (~2.5-fold) lines while it decreased *AtGH3.17* transcript abundance in the *tir1afb245* (~4.0-fold) line compared to their non-inoculated controls at 21 DAI. In the *P. brassicae*-inoculated plants, expression of *PsAFB6* in the *tir1afb2* mutant background decreased *AtGH3.17* transcript abundance by 3.4-fold compared to the *tir1afb2* line; however, *PsAFB6* expression in the *tir1afb245* mutant background increased transcript abundance by 2.7-fold compared to the *tir1afb245* line at 21 DAI (Figure 3.15B; Appendix Table B16).

In summary, the transcript abundance of *AtGH3.3* increased in the roots of all lines after *P. brassicae* inoculation at 21 DAI. Furthermore, expression of *PsAFB6* in the *tir1afb2* mutant background decreased the transcript abundance of *AtGH3.3* and *AtGH3.17* in the roots of *P. brassicae*-inoculated plants at 21 DAI.

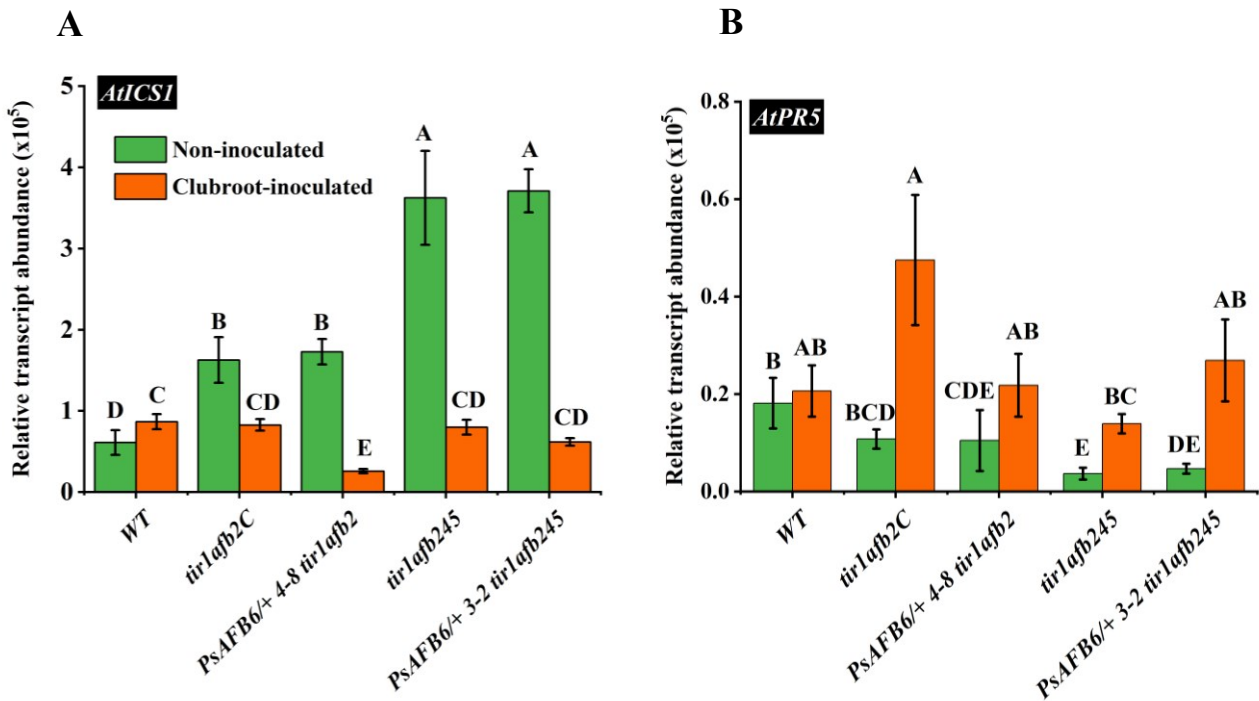


Figure 3.16 Transcript abundance of *AtICS1* and *AtPR5* in clubroot-inoculated and non-inoculated root tissue of Arabidopsis WT, *tir1afb2* double mutant, *tir1afb245* quadruple mutant, and mutants expressing *PsAFB6* at 21 DAI. *AtICS1* (A) and *AtPR5* (B) transcript abundance in clubroot-inoculated and non-inoculated root tissue of Arabidopsis WT, *tir1afb2C* double mutant, *tir1afb245* quadruple mutant, and mutants expressing *PsAFB6* at 21 DAI. Seedlings were grown on peat-based medium for 16 days prior to inoculation and roots were harvested at 21 DAI for qRT-PCR. Data are means \pm standard error (SE). For all lines and treatments, n=4 biological replicates, except the non-inoculated WT line, where, n = 3. Each biological replicate of non-inoculated root tissue is a pool of 18 seedlings for each line. The number of seedlings pooled for each biological replicate of clubroot-inoculated root tissue was 17-18 for WT, 18 for *tir1afb2*, 18 for *PsAFB6/+ 4-8 tir1afb2*, 16 for *tir1afb245*, and 18 for *PsAFB6/+ 3-2 tir1afb245*. Different letters indicate significantly different means among treatments and lines within genes (Two-way-ANOVA, LSD post-hoc test, $P \leq 0.05$, Appendix Table B17-18).

In non-inoculated plants, a decrease in auxin response in the *tir1afb2C* and *tir1afb245* lines, increased *AtICS1* transcript abundance compared to the WT line at 21 DAI (Figure 3.16A). Expression of *PsAFB6* in the *tir1afb2* and *tir1afb245* auxin mutant background had no effect on *AtICS1* transcript levels. Inoculation with *P. brassicae* slightly increased *AtICS1* transcript abundance in the WT line (~1.4-fold), while it decreased *AtICS1* transcript abundance in the *tir1afb2C* (~2.0-fold) and *tir1afb245* (~4.5-fold) lines compared to their non-inoculated controls at 21 DAI. In *P. brassicae*-inoculated plants at 21 DAI, expression of *PsAFB6* in the *tir1afb2* mutant background decreased *AtICS1* transcript abundance by 3.2-fold compared to the *tir1afb2C* line, but *PsAFB6* expression had no effect on that in the *tir1afb245* mutant background (Figure 3.16A; Appendix Table B17).

In non-inoculated plants, *AtPR5* transcript abundance was not affected by lower auxin response in the *tir1afb2C* line, but a decrease in transcript abundance was observed in the *tir1afb245* line compared to the WT line (Figure 3.16B). Expression of *PsAFB6* did not affect *AtPR5* transcript abundance in the non-inoculated lines in either mutant background. Inoculation with *P. brassicae* did not affect the transcript abundance of *AtPR5* in the WT, but transcript abundance was higher in the *tir1afb2C* (~4.4-fold) and *tir1afb245* (~3.8-fold) lines compared to their non-inoculated controls at 21 DAI. Expression of *PsAFB6* in both double and quadruple auxin receptor mutant backgrounds did not affect *AtPR5* transcript abundance when plants were inoculated with *P. brassicae* (Figure 3.16B; Appendix Table B18).

Overall, in non-inoculated plants, a decrease in auxin response (*tir1afb2C* and *tir1afb245* lines) increased *AtICS1* transcript abundance, and *P. brassicae* inoculation reduced the *AtICS1* transcript abundance in these lines at 21 DAI (Figure 3.16A). The transcript abundance of *AtPR5* increased in the roots of plants with lower auxin response (*tir1afb2C* and *tir1afb245* lines) after *P. brassicae* inoculation compared to their non-inoculated controls at 21 DAI.

3.4 DISCUSSION

3.4.1 Reduction in auxin signaling reduced *P. brassicae*-induced disease development in *Arabidopsis*

The WT line displayed the most significant disease symptoms when inoculated with *P. brassicae*, (DI = 90.3 %), with the auxin receptor mutants exhibiting less severe disease symptoms (*tir1afb2*, DI = 67.7 %; *tir1afb245*, DI = 45.0 % at 32 DAI; Figure 3.5A). Less severe clubroot disease symptoms were also observed in all three separately generated *tir1afb2* double mutant lines compared to the WT line (Figure 3.5B), further confirming a reduction in clubroot progression in the *tir1afb2* lines.

Additional confirmation that reduced auxin response was associated with reduced clubroot disease progression was obtained by measuring the fresh weights of the root-shoot transition region among the lines tested. At 32 DAI, the *P. brassicae*-inoculated WT plants had the most severe disease symptoms and the highest root-shoot transition region fresh weights due to greater hypertrophy of this tissue (4.8 times higher fresh weight than the non-inoculated control; Figure 3.12). The lines with reduced auxin response had lower root-shoot transition region fresh weights at 32 DAI with *P. brassicae* than the WT line (*tir1afb2*, 3.4-fold and *tir1afb245*, 2.6-fold higher fresh weight than the respective non-inoculated controls; Figure 3.12).

These findings demonstrate that reduced auxin response in plant tissues can decrease progression of clubroot disease. A previous report indicated that the single auxin receptor mutants *tir1* and *afb1-3*, and the double mutant *afb1-3afb2-3* had increased clubroot susceptibility (Jahn et al., 2013). However, the auxin receptor double mutant *tir1afb2* and quadruple mutant *tir1afb245* lines have stronger auxin-resistant phenotypes (lower auxin response) than those assessed in Jahn et al. (2013) study. Therefore, a minimal threshold of auxin response reduction appears to be required to reduce clubroot disease progression in *Arabidopsis*.

Disruption of the auxin response can also be accomplished through mutations in the *Aux/IAAs* genes. For example, the *AXR3* gene encodes the IAA17 protein, which is a part of the Aux/IAA family. The *axr3-1* mutation leads to enhanced stability of IAA17, resulting in its accumulation at elevated levels, making it highly auxin-resistant and lacking root hairs (Leyser et al., 1996). *Arabidopsis axr3-1* and wild type lines were inoculated with *P. brassicae* spore concentrations of 10^5 , 10^6 , and 10^7 spores/mL (Alix et al., 2007). The DI values for *axr3-1* were 43, 56, and 69, which were significantly lower than those observed in the wild type (DI: 93, 100,

and 100) at 21 DAI (Alix et al., 2007). These data are consistent with our results that reduced auxin response in plant tissues can decrease progression of clubroot disease. The single auxin receptor mutant *tir1-1*, which has a less auxin-resistant phenotype than *axr3-1*, was also assessed and reported to be similar in susceptibility to *P. brassicae* as the WT (Alix et al., 2007). These results are consistent with a requirement for a threshold reduction in auxin response to be reached in the plant to reduce clubroot disease progression in Arabidopsis.

Modification of auxin signaling has been reported to control or inhibit the progression of plant disease caused by other biotrophic pathogens plant diseases in Arabidopsis. Arabidopsis *afb1* and *afb3* single mutant showed fewer disease symptoms in comparison to the wild type Arabidopsis upon infection by the soilborne root pathogen *Verticillium dahlia* (Fousia et al., 2018). Repressing auxin signaling through miRNA-mediated suppression of the F-box auxin receptors TIR1, AFB2, and AFB3 increased resistance to *Pseudomonas syringae* (Navarro et al., 2006). In addition, the absence of the plant signaling component *SGT1b* leads to a weakened auxin response, which, in turn, boosts the plant's resistance to *Fusarium culmorum* in Arabidopsis buds and flowers (Cuzick et al., 2009).

3.4.2 *PsAFB6* expression in auxin receptor *tir1afb2* and *tir1afb245* mutant backgrounds lead to a trend to reduce *P. brassicae*-induced disease development

Expression of *PsAFB6* in the auxin receptor *tir1afb2* double mutant background line *PsAFB6/+ 3-3 tir1afb2* reduced the DI to 38.8 %, which was nearly 20 % lower than the DI of the *tir1afb2* double mutant (61.4 %; Figure 3.5C). Consistently, the *P. brassicae*-inoculated *PsAFB6*-expressing *tir1afb2* line (*PsAFB6/+ 3-3 tir1afb2*) also showed a 20.8 % reduction in the root-shoot transition region fresh weight compared to the inoculated *tir1afb2* line (Figure 3.12C). A second independently *PsAFB6*-transformed line exhibited a slightly lower average DI than *tir1afb2*, but its DI mean was not significantly different than that of *tir1afb2*. However, the expression of *PsAFB6* in the *tir1afb2* double mutant background shifted the frequency distribution from a median disease severity class of 2 in the *tir1afb2* line to lower median disease severity classes in both *PsAFB6*-expressing lines (1.5 in *PsAFB6/+ 4-8 tir1afb2* and 1 in *PsAFB6/+ 3-3 tir1afb2*; Figure 3.11B, C and D). As expression of *PsAFB6* in the *tir1afb2* double mutant background reduced auxin response in auxin root growth inhibition assays (see

chapter 2), at least one mechanism for reduction of clubroot disease progress observed in the *PsAFB6-tir1afb2* transgenic lines is likely reduction in auxin response.

Expression of *PsAFB6* in the auxin receptor *tir1afb245* quadruple mutant background line *PsAFB6/+ 3-2 tir1afb245* reduced the DI by 10.3 % compared to the *tir1afb245* line (Figure 3.5A). Two other independently *PsAFB6*-transformed lines in the quadruple mutant background (*PsAFB6/+ 1-6 tir1afb245* and *PsAFB6/+ 5-9 tir1afb245* lines) had lower DI means but the means were not significantly different from that of the *tir1afb245* line (Figure 3.5A). However, expression of *PsAFB6* in the *tir1afb245* mutant background shifted the frequency distribution lower in all three independent transgenic lines with a median disease severity class of 1 compared to the *tir1afb245* line (median disease severity class of 1.5; Figure 3.9D-F). As expression of *PsAFB6* in the *tir1afb245* quadruple mutant background reduced auxin response in auxin root growth inhibition assays (see chapter 2), similar to the *PsAFB6-tir1afb2* transgenic lines, at least one mechanism for reduction of clubroot disease progress observed in the *PsAFB6-tir1afb245* transgenic lines is likely reduction in auxin response.

Similar to that in Arabidopsis, Canola (cv. Westar) lines expressing *PsAFB6* also exhibited a reduction (9-15 %) in their DI and a reduction (19-20 %) in their surface area at the root-shoot transition area compared to their respective transgenic null controls at 30 DAI with *P. brassicae* (Liu, 2023). In legumes, it has been found that the expression of *LjAFB6* was triggered in reaction to nitrate supply and was primarily concentrated in the meristematic regions of both primary and lateral roots. Moreover, phenotypic assessments conducted on two separate null mutants demonstrated its specific involvement in regulating the elongation of both primary and lateral roots in response to auxin, suggesting the role of AFB6 in both primary and lateral roots growth and development (Rogato et al., 2021).

Overall, the disease rating results suggest that reduction in auxin response reduces *P. brassicae*-induced disease development in Arabidopsis, and that a threshold level of auxin response reduction is required to reduce *P. brassicae*-induced disease development.

3.4.3 Plant hormone-related gene expression in Arabidopsis roots of *tir1afb2* and *tir1afb245* lines in response to clubroot pathogen inoculation at 21 DAI

In 10-day-old Arabidopsis seedlings, Takato et al. 2017 reported that endogenous IAA levels were increased in auxin-signaling mutants (including *tir1afb123*) and that the elevated

IAA levels were associated with up-regulation of *YUC* auxin biosynthesis genes in these mutants, compared to WT controls. Consistently, endogenous IAA levels were repressed in *TIR1*-overexpression lines compared to their respective controls, and that the lower IAA levels were associated with down-regulation of *YUC* genes. These observations suggest that endogenous IAA levels are regulated by auxin biosynthesis in a feedback manner, and the Aux/IAA and TIR1/AFB-mediated auxin-signaling pathway regulates *YUC* gene expression. In this study, in non-inoculated plants, a reduction in auxin response in the *tir1afb2C* and *tir1afb245* lines increased *AtIAA9* transcript abundance compared to the WT line (1.6-fold; Figure 3.17). One possibility is that one or a combination of auxin receptors (AFB1, AFB3) that are functional in both *tir1afb2C* and *tir1afb245* lines are involved in specifically binding and degrading IAA9 resulting in increased *IAA9* expression at this developmental stage in the roots under the elevated IAA levels that occur in auxin signaling mutants.

Reduction in auxin response had no effect on the transcript abundance of *AtIAA16* in the *tir1afb2C* mutant line. However, in the *tir1afb245* line, there was a 1.5-fold reduction in *AtIAA16* transcript abundance compared to non-inoculated WT line (Figure 3.17), suggesting that the auxin receptors that are functional in *tir1afb2C*, but not in *tir1afb245* (AFB4 and AFB5) are involved in degrading IAA16 at this developmental stage in the roots. The reduced auxin response in the *tir1afb2C* and *tir1afb245* lines led to a 1.3-fold and 1.6-fold decrease in *AtIAA19* transcript abundance compared to the WT line, respectively (Figure 3.17). In Arabidopsis 35S-*TIR1* over-expressing lines, *AtIAA19* showed a 3 to 5-fold increase in root tissue relative to wild type while the *tir1-1afb1-1afb2-1afb3-1* (*tir1afb123*) quadruple mutant line exhibited a 2-fold decrease in *AtIAA19* transcript abundance compared to the wild type (Takato et al., 2017), which is consistent with the gene expression trend in the current study for *AtIAA19* (Takato et al., 2017). The reduction in *AtIAA19* expression in the auxin receptor mutant lines may indicate that functional TIR1 and AFB2 auxin receptor are involved in specifically binding and degrading IAA19, and in their absence in these mutants *IAA19* transcript levels are lower due to a lower turnover of IAA19 protein.

In non-inoculated plants, a decline in auxin response in the *tir1afb2C* and *tir1afb245* lines resulted in a 1.7 to 1.9-fold increase in *AtARF3* transcript abundance compared to the WT (Figure 3.17). AtARF3 is an atypical auxin response factor that lacks the PB1 domain and can bind to IAA directly, thus mediating the noncanonical AUX/IAA-independent auxin signaling

pathway (Simonini et al., 2018). Higher *AtARF3* expression in the *tir1afb2C* and *tir1afb245* lines may be the result of elevated IAA levels (that occur in auxin signaling mutants) stimulating *AtARF3* expression leading to an alternate auxin signaling pathway when the SCF^{TIR/AFB} auxin signaling was lower in double and quadruple auxin receptor mutant lines. On the contrary, AtARF5 and AtARF19 function as transcription activators by specifically binding to auxin response elements (AuxREs) in target gene promoters to direct the expression of downstream target genes (Roosjen et al., 2018). The transcript abundance of *AtARF5* was reduced (1.8 to 2.3-fold) in the *tir1afb2C* and *tir1afb245* lines relative to the non-inoculated WT due to reduced auxin signaling in these lines at this stage of root development. *AtARF19* transcript abundance didn't change in either auxin receptor mutant line, suggesting that it minimally involved in auxin signaling under non-biotic stress conditions at this stage of root development (Figure 3.17).

GH3 group II genes (include *GH3.3*, and *GH3.17*) code for proteins that can conjugate free IAA to amino acids (Westfall et al., 2012), reducing the levels of free IAA. Reduced auxin signaling in the *tir1afb2C* and *tir1afb245* lines, reduced *AtGH3.3* transcript levels in non-inoculated plants (9.6 and 1.5-fold, respectively) compared to the WT line (Figure 3.17). These data indicate that the SCF^{TIR1/AFB} auxin signaling pathway regulates *AtGH3.3* expression. The auxin response factor ARF17 is known to control GH3 transcriptional response, including GH3.2 and GH3.3 (Mallory et al., 2005). A reduction of *AtGH3.3* transcript abundance was also observed in the hypocotyls of *tir1-1* and *afb2-3* single and *tir1-1afb2-3* double mutant lines relative to the WT control line (Lakehal et al., 2019). The *tir1afb245* line displayed higher *AtGH3.17* transcript levels (8.5-fold) compared to the WT (Figure 3.17). As characterization of *gh3* septuple mutants revealed that GH3.17 plays a prominent role in root elongation in Arabidopsis (Guo et al., 2022), and a variety of transcription factors may regulate the expression of *GH3* genes to bring about auxin-regulated processes during root development.

In non-inoculated plants, a reduction in auxin response in both the *tir1afb2C* and *tir1afb245* lines resulted in an increased *AtICS1* transcript abundance (2.7 to 5.9-fold) compared to the WT line, indicating that reduced auxin response tends to enhance SA biosynthesis. It has been reported that SA and auxin signaling pathways are mutually antagonistic (Wang et al., 2007; Iglesias et al., 2011). SA triggers a widespread suppression of genes linked to auxin, such as the *TIR1* receptor gene. This leads to the stabilization of Aux/IAA repressor proteins, ultimately blocking auxin responses (Wang et al., 2007). When auxin response is reduced in the *tir1afb2C*

and *tir1afb245* line, its inhibitory effect on SA is also reduced, leading to the increased gene expression of SA biosynthesis gene *AtICS1*.

Under non-biotic stress conditions (non-inoculated treatment), expression of the marker defense gene *AtPR5* was either not affected (*tir1afb2* line) or reduced *tir1afb245* line compared to the WT line (Iglesias et al., 2011).

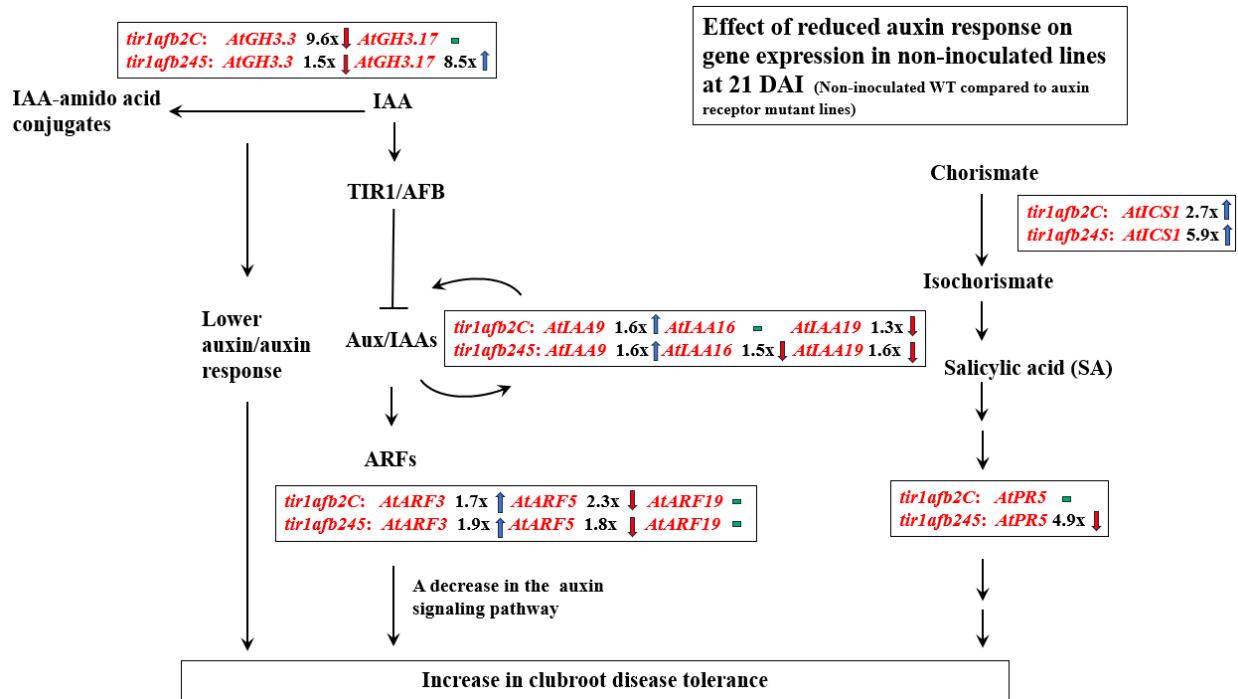


Figure 3.17 Expression profiles of auxin metabolism and signaling genes and genes associated with SA biosynthesis and defense signaling in Arabidopsis roots of non-inoculated control *tir1afb2C* and *tir1afb245* lines harvested at the 21 DAI time point. Upon perception of auxin by the TIR1/AFB receptors, degradation of the auxin-signaling repressor Aux/IAAs occurs, allowing the expression of ARFs leading to auxin response. Upon Aux/IAA degradation, expression of Aux/IAA genes is stimulated to attenuate auxin response. GH3 genes regulate auxin homeostasis by conjugating free IAA to IAA-amido conjugates. Pathogen-induced SA, derived from chorismate by *ICS1*, activates *PR* gene expression (including *PR5*) facilitating SA-mediated defense response against the pathogen. Fold changes in transcript abundance of the auxin receptor mutant line *tir1afb2C* or *tir1afb245* compared to the WT line are indicated and arrows denote direction of change (higher, blue arrow; lower, red arrow; green dash line, no change).

3.4.4 Plant hormone-related gene expression in Arabidopsis roots of WT, *tir1afb2* and *tir1afb245* lines in response to clubroot pathogen inoculation at 21 DAI

Inoculation with *P. brassicae* had no effect on the transcript abundance of *AtIAA9* in the WT or *tir1afb2C* mutant lines. However, in the *tir1afb245* line, there was a 2-fold reduction in transcript abundance compared to non-inoculated control at 21 DAI (Figure 3.18). Inoculation with *P. brassicae* decreased the transcript abundance of both *AtIAA16* and *AtIAA19* in all lines compared to their non-inoculated controls at 21 DAI. These expression data suggest that *P. brassicae* inoculation affected the auxin signaling pathway at 21 DAI and the reduction in *AtIAA16* and *AtIAA19* transcript abundance in WT and auxin receptor mutant lines may reflect less turnover of these Aux/IAAs these lines (Figure 3.18).

Consistently, transcriptomic analysis of WT Arabidopsis found that *AtIAA16* and *AtIAA19* transcript abundance was down-regulated at both 10 and 23 DAI with *P. brassicae* (Siemens et al., 2006). Based on the transcriptomic data analysis conducted by Zhou et al. (2020) in the Ozga lab (unpublished data), the gene expression of *IAA16* was found to be down-regulated at 7, 14 and 21 DAI with *P. brassicae* when compared to the non-inoculated control, and there was a greater down regulation of *IAA16* expression in the pathogen-resistant rutabaga cultivar (*Brassica napus subsp. rapifera*) than the susceptible cv. at 7 and 14 DAI. In general, a trend in down-regulation of *IAA19* expression at 7, 14 and 21 DAI with *P. brassicae* was observed when compared to the non-inoculated control in both *P. brassicae* resistant and susceptible rutabaga cultivars.

The transcript abundance of *AtARF3* increased in all lines compared to their non-inoculated controls after *P. brassicae* inoculation. The *P. brassicae*-induction of *AtARF3* expression was reduced with increasing loss of auxin response at 21 DAI (induction of WT line, ~13-fold; *tir1afb2C*, ~5.1-fold; *tir1afb245*, ~2.8-fold). Similar to this study, in WT Arabidopsis, transcriptomic analysis revealed that transcript abundance of *AtARF3* increased at 10 DAI and 23 DAI with *P. brassicae* compared to the non-inoculated controls (Siemens et al., 2006).

The transcript abundance of *AtARF5* decreased in all plant lines compared to their non-inoculated controls at 21 DAI with *P. brassicae*. The most substantial reduction in *AtARF5* transcripts was observed in the WT line (~7.0-fold), followed by the *tir1afb2C* and *tir1afb245* lines, each exhibiting a 1.6-fold reduction. Similarly, down-regulation of *ARF5* gene expression

was observed in clubroot-infected roots of *Arabidopsis* at 14, 17, and 21 DAI (Jahn et al., 2013). As noted by Jahn et al. (2013), ARF5 plays a role in governing embryonic roots, reducing its activity might disrupt the structured layers within roots and diminish the growth of lateral roots while promoting the development of undifferentiated galls.

An increase in *AtARF19* transcript abundance in the WT line (~3.4-fold) and the *tir1afb2C* line (~1.5-fold) was observed compared to their non-inoculated controls at 21 DAI with *P. brassicae*. *AtARF19* transcript abundance decreased with increasing loss of auxin response (WT > *tir1afb2* > *tir1afb245*) in the *P. brassicae*-inoculated lines at 21 DAI (Figure 3.18). Lower levels of *AtARF3* and *AtARF19* transcript abundance in the auxin receptor mutants inoculated with *P. brassicae* compared to the WT line reflects lower auxin signaling/response, and this decreasing auxin response may contribute to the reduction in clubroot symptoms associated with these auxin receptor mutant lines.

AtGH3.3 transcript levels markedly increased in all plant lines compared to their non-inoculated controls at 21 DAI with *P. brassicae*, with the highest expression in the WT line, followed by the *tir1afb2C* line, and then the *tir1afb245* line. This suggests that infection with clubroot pathogen markedly increased auxin conjugation activity to reduce free IAA levels through upregulation of *AtGH3.3* gene. Following inoculation with *P. brassicae*, *AtGH3.17* transcript abundance also increased in the WT (~6.1-fold) and *tir1afb2C* (~2.5-fold) lines, while it decreased in the *tir1afb245* (~4.0-fold) line compared to their non-inoculated controls at 21 DAI (Figure 3.18).

In Chinese cabbage (*Brassica rapa*), similarly, a marked increase in the expression of the *BrGH3.3* gene at 14 and 28 DAI, and also the *BrGH3.5* gene at 14 DAI within the root tissues of clubroot-infected plants compared to non-inoculated control was observed (Robin et al., 2020). In addition, in *A. thaliana*, multiple members of the *AtGH3* family, including *GH3.2*, *GH3.3*, *GH3.4*, *GH3.5*, *GH3.14*, and *GH3.17*, exhibited increased expression at 24 and 28 DAI in *P. brassicae*-infected plants compared to the non-inoculated control (Jahn et al., 2013). Jahn et al. (2013) suggested that conjugation of IAA to amino acids mediated by *GH3.2*, *GH3.3*, *GH3.4*, and *GH3.17* is likely a detoxification response by the host plant to counteract the elevated levels of auxin produced in the root galls. Lower levels of *AtGH3.3* and *AtGH3.17* transcript abundance in the auxin receptor mutants inoculated with *P. brassicae* compared to the WT line

reflects lower auxin signaling/response, and this decreasing auxin response may contribute to the reduction in clubroot symptoms associated with these auxin receptor mutant lines.

The *AtICS1* transcript abundance increased in WT (1.4-fold) while it decreased in the *tir1afb2C* (~2.0-fold) and *tir1afb245* (~4.5-fold) lines compared to their non-inoculated controls at 21 DAI with *P. brassicae*. The decrease *AtICS1* transcript abundance in this comparison is a result of high levels of *AtICS1* transcript occurring in the auxin receptor mutant lines.

Inoculation with *P. brassicae* had no effect on the transcript abundance of *AtPR5* in the WT line. However, in the *tir1afb2C* (~4.4-fold) and *tir1afb245* (~3.8-fold) lines, the transcript abundance of *AtPR5* was higher compared to their non-inoculated controls at 21 DAI (Figure 3.18). These data suggest that plant defense genes are stimulated in the auxin receptor mutant lines when challenged with *P. brassicae* infection.

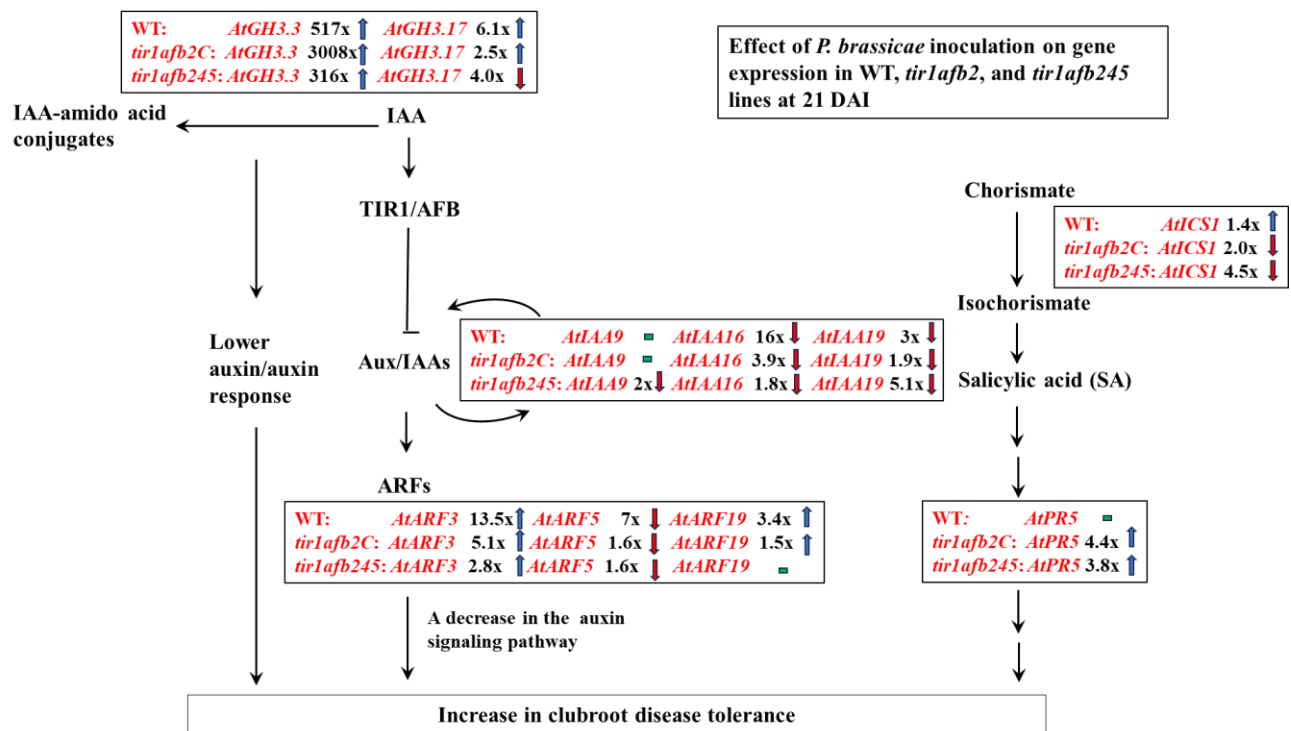


Figure 3.18 Expression profiles of auxin metabolism and signaling genes and genes associated with SA biosynthesis and defense signaling in Arabidopsis roots of clubroot-inoculated WT, *tir1afb2C* and *tir1afb245* lines harvested at the 21 DAI.

Upon perception of auxin by the TIR1/AFB receptors, degradation of the auxin-signaling repressor Aux/IAAs occurs, allowing the expression of *ARFs* leading to auxin response. Upon

Aux/IAA degradation, expression of Aux/IAA genes is stimulated to attenuate auxin response. *GH3* genes regulate auxin homeostasis by conjugating free IAA to IAA-amido conjugates. Pathogen-induced SA, derived from chorismate by *ICS1*, activates *PR* gene expression (including *PR5*) facilitating SA-mediated defense response against the pathogen. Fold changes in transcript abundance of the WT, auxin receptor mutant line *tir1afb2C* or *tir1afb245* compared to their respective non-inoculated controls are indicated and arrows denote direction of change (higher, blue arrow; lower, red arrow; green dash line, no change).

3.4.5 Effect of reduced auxin response on plant hormone-related gene expression in Arabidopsis roots in clubroot-inoculated lines at 21 DAI

When compared to the WT line, reduction in auxin response in the *tir1afb2C* and *tir1afb245* lines had more minimal or no effect on the transcript abundance of *AtIAA9* and *AtIAA19* when inoculated with *P. brassicae* at 21 DAI (Figure 3.19). However, after clubroot inoculation the transcript abundance of *AtIAA16* in the *tir1afb2C* and *tir1afb245* lines increased 3.9- and 5.7-fold (respectively) relative to the WT line at 21 DAI, likely indicating that reducing auxin response modified IAA16 turnover leading to higher transcript abundance, and potentially greater inhibition of IAA16-responsive gene expression.

In plants inoculated with *P. brassicae*, the transcript abundance of *AtARF3* and *AtARF19* decreased with increasing loss of auxin response (WT > *tir1afb2C* > *tir1afb245*) at 21 DAI, an expected response as these are auxin-induced transcription factors (Figure 3.19). However, in the *P. brassicae*-inoculated treatment, *AtARF5* transcript abundance was higher in the *tir1afb2C* (1.9-fold) and *tir1afb245* mutant (2.3-fold) lines compared to the clubroot-inoculated WT line. In the non-inoculated controls, *AtARF5* transcript abundance was reduced (1.8 to 2.3-fold) in the *tir1afb2C* and *tir1afb245* lines relative to the WT (Figure 3.17). As ARF5 plays a role in governing embryonic roots, higher transcript abundance of *AtARF5* in the auxin receptor mutant lines may indicate more normal growth of lateral roots than in the WT line when inoculated with *P. brassicae*.

In *P. brassicae*-inoculated plants, the transcript abundance of *AtGH3.3* and *AtGH3.17* decreased with loss of auxin response (WT > *tir1afb245* ≥ *tir1afb2C*) at 21 DAI, an expected response as these are auxin-induced transcription factors (Figure 3.19).

Reduction in auxin response in *tir1afb2C* and *tir1afb245* mutant lines did not affect the transcript abundance of *AtICS1* and *AtPR5* compared to the WT line when inoculated with *P. brassicae* at 21 DAI (Figure 3.19).

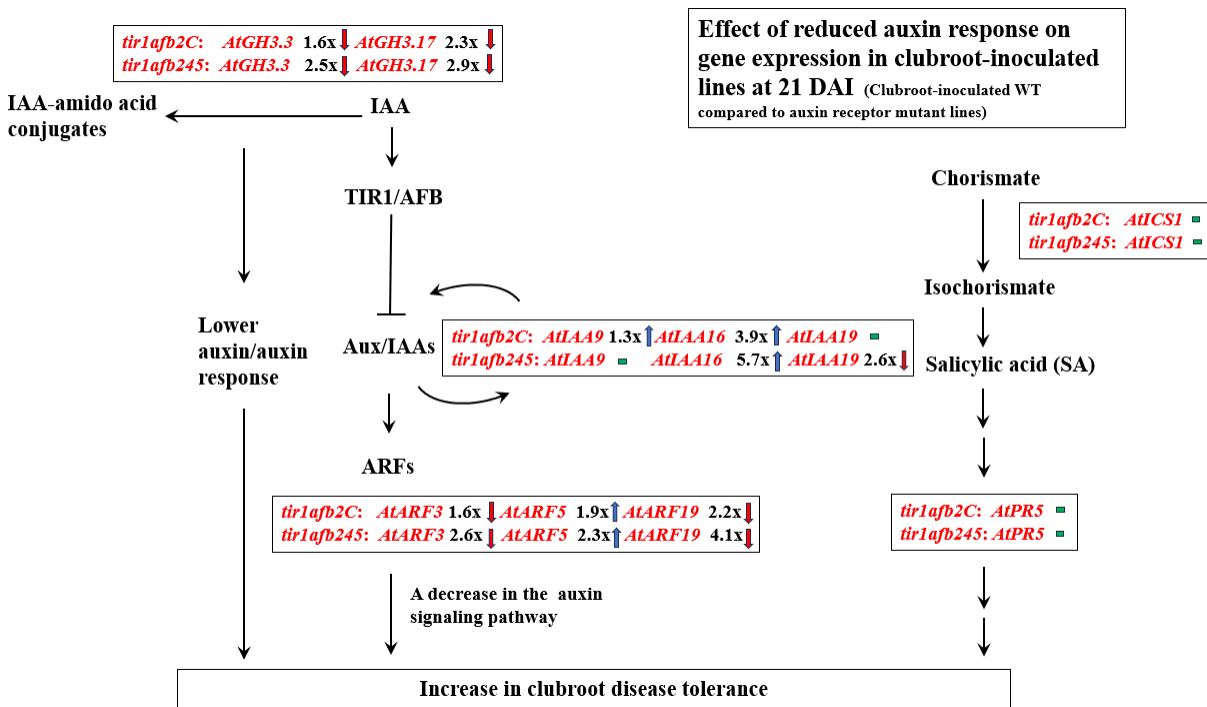


Figure 3.19 Expression profiles of auxin metabolism and signaling genes and genes associated with SA biosynthesis and defense signaling in Arabidopsis roots of clubroot-inoculated *tir1afb2C* and *tir1afb245* lines compared to the WT line harvested at the 21 DAI. Upon perception of auxin by the TIR1/AFB receptors, degradation of the auxin-signaling repressor Aux/IAAs occurs, allowing the expression of ARFs leading to auxin response. Upon Aux/IAA degradation, expression of Aux/IAA genes is stimulated to attenuate auxin response. GH3 genes regulate auxin homeostasis by conjugating free IAA to IAA-amido conjugates. Pathogen-induced SA, derived from chorismate by *ICS1*, activates *PR* gene expression (including *PR5*) facilitating SA-mediated defense response against the pathogen. Fold changes in transcript abundance of the auxin receptor mutant line *tir1afb2C* or *tir1afb245* compared to the

clubroot-inoculated WT line are indicated and arrows denote direction of change (higher, blue arrow; lower, red arrow; green dash line, no change).

3.4.6 Plant hormone-related gene expression in Arabidopsis roots of non-inoculated and clubroot-inoculated *PsAFB6*-expressing *tir1afb2* and *tir1afb245* lines harvested at the 21 DAI time point.

In the non-inoculated treatment, only a few differences in transcript abundance with variable changes were observed in the genes assessed as the result of *PsAFB6* expression in the auxin receptor mutant backgrounds (Figure 3.20). In clubroot inoculated plants, expression of *PsAFB6* in the *tir1afb2* auxin receptor mutant background decreased the transcript abundance of the *Aux/IAA* genes (*AtIAA9*, *AtIAA16*, and *AtIAA19*), *ARF* genes (*AtARF3*, *AtARF5*, and *AtARF19*), and *GH3* genes (*AtGH3.3* and *AtGH3.17*) (Figure 3.21), suggesting that expression of *PsAFB6* reduced auxin response in this line, consistent with results of the auxin root growth assays described in Chapter 2. Expression of *PsAFB6* in the *tir1afb245* auxin receptor mutant background resulted in fewer differences and more variable changes in the transcript abundance of the gene assessed when plants were inoculated with *P. brassicae*.

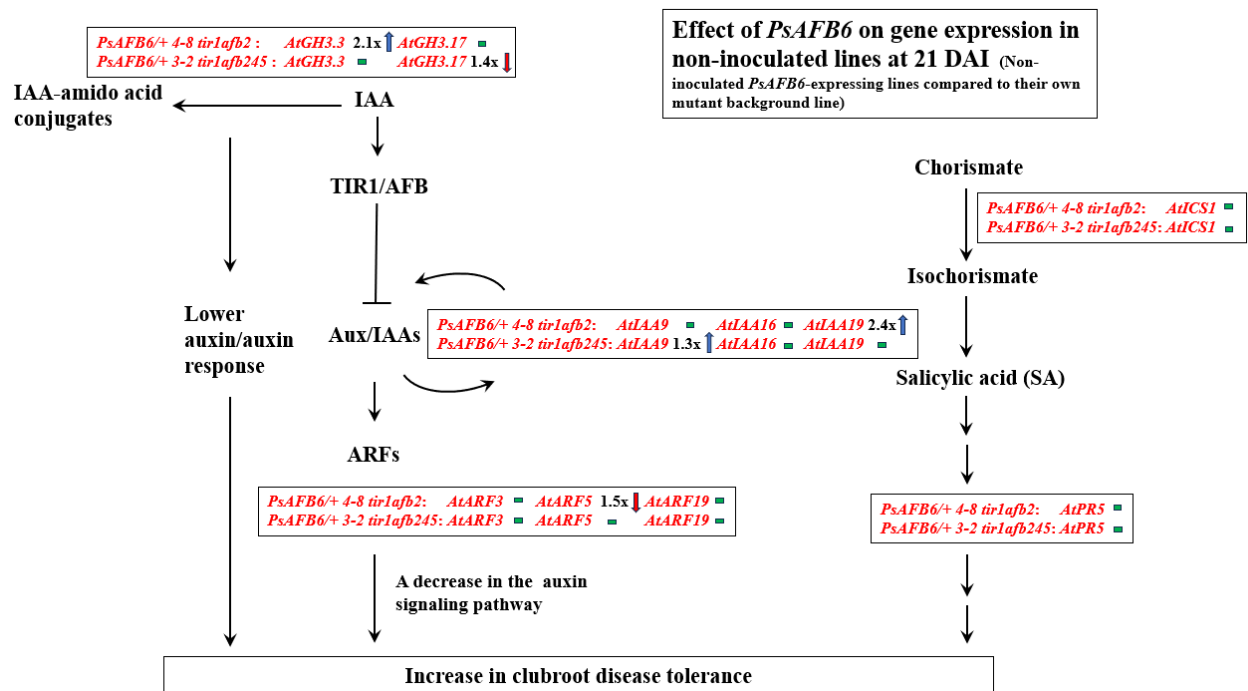


Figure 3.20 Expression profiles of auxin metabolism and signaling genes and genes associated with SA biosynthesis and defense signaling in Arabidopsis roots of non-inoculated *PsAFB6/+ 4-8 tir1afb2* and *PsAFB6/+ 3-2 tir1afb245* lines compared to their respective auxin receptor mutant backgrounds at the 21 DAI experimental time point.

Upon perception of auxin by the TIR1/AFB receptors, degradation of the auxin-signaling repressor Aux/IAAs occurs, allowing the expression of *ARFs* leading to auxin response. Upon Aux/IAA degradation, expression of Aux/IAA genes is stimulated to attenuate auxin response. *GH3* genes regulate auxin homeostasis by conjugating free IAA to IAA-amido conjugates. Pathogen-induced SA, derived from chorismate by *ICS1*, activates *PR* gene expression (including *PR5*) facilitating SA-mediated defense response against the pathogen. Fold changes in transcript abundance of the *PsAFB6/+ 4-8 tir1afb2* and *PsAFB6/+ 3-2 tir1afb245* lines compared to their respective mutant background lines are indicated and arrows denote direction of change (higher, blue arrow; lower, red arrow; green dash line, no change).

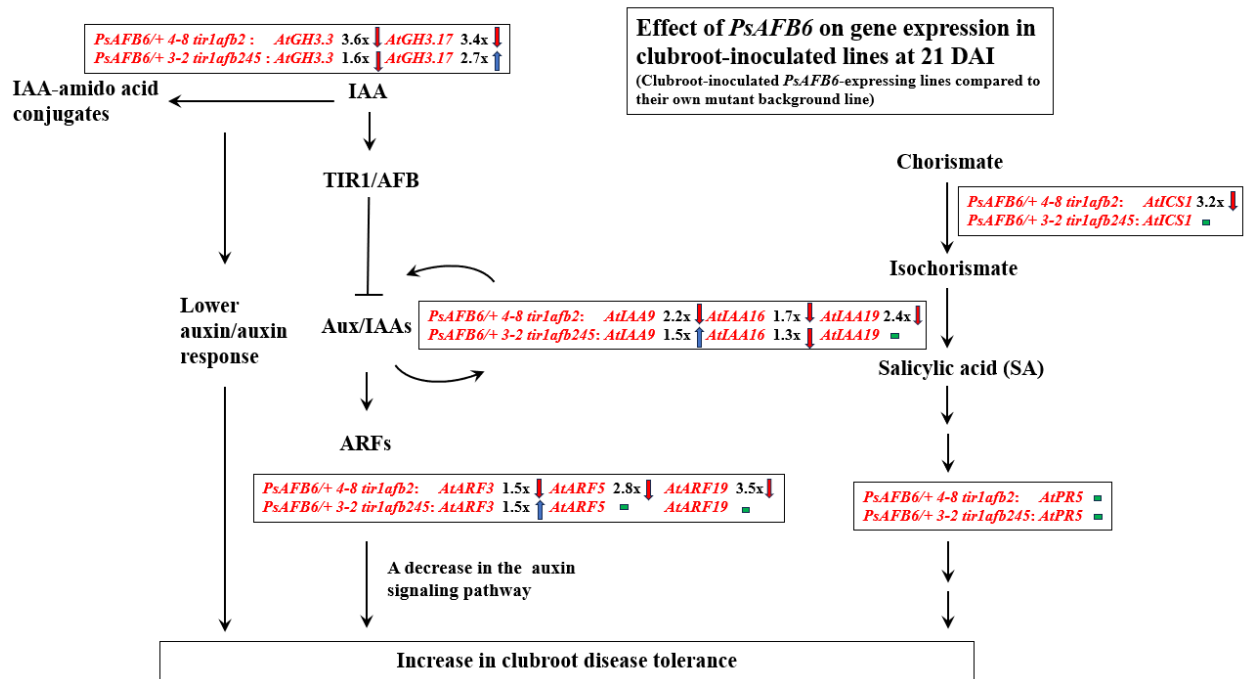


Figure 3.21 Expression profiles of auxin metabolism and signaling genes and genes associated with SA biosynthesis and defense signaling in Arabidopsis roots of clubroot-inoculated *PsAFB6/+ 4-8 tir1afb2* and *PsAFB6/+ 3-2 tir1afb245* lines compared to their respective mutant backgrounds at the 21 DAI time point. Upon perception of auxin by the TIR1/AFB receptors, degradation of the auxin-signaling repressor Aux/IAAs occurs, allowing the expression of *ARFs* leading to auxin response. Upon Aux/IAA degradation, expression of Aux/IAA genes is stimulated to attenuate auxin response. *GH3* genes regulate auxin homeostasis by conjugating free IAA to IAA-amido conjugates. Pathogen-induced SA, derived from chorismate by *ICS1*, activates *PR* gene expression (including *PR5*) facilitating SA-mediated defense response against the pathogen. Fold changes in transcript abundance of the *PsAFB6/+ 4-8 tir1afb2* and *PsAFB6/+ 3-2 tir1afb245* lines compared to their respective mutant background lines are indicated and arrows denote direction of change (higher, blue arrow; lower, red arrow; green dash line, no change).

3.5 CONCLUSION

In summary, reduced auxin response in the auxin receptor mutants was associated with reduced clubroot disease progression in Arabidopsis, and it is likely that a threshold level of auxin response reduction is required to reduce *P. brassicae*-induced disease development. The transcript abundance of auxin-response gene expression markers, *AtARF3*, *AtARF19*, *AtGH3.3* and *AtGH3.17*, decreased with loss of auxin response (WT > *tir1afb2C* ≥ *tir1afb245*) at 21 DAI, confirming reduced auxin signaling in the auxin receptor mutant lines when inoculated with *P. brassicae* (Figure 3.19). Inoculation with *P. brassicae* had no effect on the transcript abundance of *AtPR5* in the WT line. However, in the *tir1afb2C* and *tir1afb245* lines, the transcript abundance of *AtPR5* was higher compared to their non-inoculated controls at 21 DAI (Figure 3.18), suggesting that plant defense genes are stimulated in the auxin receptor mutant lines when challenged with *P. brassicae* infection.

When *PsAFB6* was expressed in auxin receptor *tir1afb2* and *tir1afb245* mutant backgrounds, there was a trend to reduce *P. brassicae*-induced disease development. In clubroot inoculated plants, expression of *PsAFB6* in the *tir1afb2* auxin receptor mutant background decreased the transcript abundance of the *Aux/IAA* genes (*AtIAA9*, *AtIAA16*, and *AtIAA19*), *ARF* genes (*AtARF3*, *AtARF5*, and *AtARF19*), and *GH3* genes (*AtGH3.3* and *AtGH3.17*) (Figure 3.21), suggesting that expression of *PsAFB6* reduced auxin response in this line, consistent with results of the auxin root growth assays described in Chapter 2.

Chapter 4: General conclusions and future perspectives

4.1 GENERAL CONCLUSIONS

The plant hormone auxin plays a central role as a signaling molecule, influencing various aspects of the plant lifecycle. Precise control of the auxin response is essential to ensure optimal plant growth in dynamic environmental conditions (Han and Hwang, 2018; Ma et al., 2018). However, clubroot disease pathogen that manipulating host auxin signaling that lead to hyperplasia and hypertrophy of the infected roots, resulting in the formation of root galls and above-ground symptoms (Ludwig-Müller and Schuller, 2008; Ludwig-Müller, 2014). Hence, manipulating the plant host's auxin signaling might offer a potential method to inhibit clubroot gall formation caused by *P. brassicae*. In this study, Arabidopsis auxin receptor double mutant (*tir1afb2*) and quadruple mutant (*tir1afb245*), and mutants expressing *PsAFB6* lines were assessed for their ability in suppressing clubroot disease progression. Auxin (2,4-D) root growth assays was performed first to test if auxin response was reduced or modified in these lines. The result found that the non-transgenic Arabidopsis *tir1afb2* mutant displayed reduced auxin sensitivity (88.7-90.7 % root elongation in 2,4-D relative to control) and the quadruple-mutant *tir1afb245* exhibited a similar reduction in 2,4-D sensitivity (88.3 % root elongation in 2,4-D relative to control). These results suggest that *TIR1* and *AFB2* are the two major auxin receptor genes that responsible for auxin response in Arabidopsis roots. In addition, the introduction of the pea auxin receptor gene *PsAFB6* into both double and quadruple Arabidopsis mutant lines resulted in reduced sensitivity to 2,4-D-induced root growth inhibition compared to their mutant background lines, suggesting that *PsAFB6* was effective in reducing the overall auxin response. The lateral roots number was also measured in these lines and the results showed that the auxin receptors *TIR1* and *AFB2* predominantly influenced lateral root formation, with some additional impact from *AFB4/AFB5* auxin receptors.

Clubroot inoculation assays found that WT line displayed the most significant disease symptoms when inoculated with *P. brassicae*, with the *tir1afb2* double mutants exhibiting less severe disease symptoms, followed by the *tir1afb245* quadruple mutant. Expressing *PsAFB6* in the backgrounds of auxin receptor mutants *tir1afb2* and *tir1afb245* showed a tendency to decrease the development of *P. brassicae*-induced disease. These findings indicate that the diminished auxin response in the auxin receptor mutants is linked to a decrease in clubroot

disease progression in Arabidopsis. It is probable that achieving a certain threshold level of auxin response reduction is necessary to mitigate the development of *P. brassicae*-induced disease. Plant hormone-related gene expression in Arabidopsis roots of non-inoculated and clubroot-inoculated *tir1afb2* double and *tir1afb245* quadruple mutant, and mutants expressing *PsAFB6* was quantified at the 21 DAI. The results found that at 21 DAI, the transcript levels of key auxin-response genes—*AtARF3*, *AtARF19*, *AtGH3.3*, and *AtGH3.17*—showed a decrease correlating with diminished auxin response ($WT > tir1afb2C \geq tir1afb245$) when inoculated with *P. brassicae*, affirming reduced auxin signaling in the auxin receptor mutant lines. Remarkably, in the WT line, clubroot inoculation had no impact on *AtPR5* transcript abundance. Conversely, in the *tir1afb2C* and *tir1afb245* lines, *AtPR5* transcript levels were notably higher compared to their non-inoculated counterparts at 21 DAI, suggesting an activation of plant defense genes in these mutant lines after clubroot infection. Furthermore, in clubroot-inoculated plants, the presence of *PsAFB6* in the *tir1afb2* auxin receptor mutant background led to reduced transcript levels of *Aux/IAA* genes (*AtIAA9*, *AtIAA16*, and *AtIAA19*), *ARF* genes (*AtARF3*, *AtARF5*, and *AtARF19*), and *GH3* genes (*AtGH3.3* and *AtGH3.17*). This indicates that the expression of *PsAFB6* reduced the auxin response in this line, consistent with the outcomes observed in the auxin root growth assays in Chapter 2. In conclusion, the decrease in auxin response contributed to a reduction in the progression of clubroot symptoms in Arabidopsis. This supports the hypothesis that the clubroot pathogen disturb auxin signaling and utilize auxin for root galls development.

4.2 FUTURE PERSPECTIVES

In Chapter 2, auxin response in the transgenic lines was tested with auxin (70 nM of 2,4-D) inhibition root growth assays. Naturally occurring plant auxins consist of the widely found indole-3-acetic acid (IAA), indole-3-butyric acid, phenylacetic acid (PAA, a mild auxin), and the chlorinated auxin 4-chloroindole-3-acetic acid (4-Cl-IAA) (Reinecke et al., 1999). It has been reported that both 4-Cl-IAA and IAA effectively restricted Arabidopsis root elongation. However, 4-Cl-IAA exhibited a higher inhibition compared to IAA at same auxin concentrations in wild-type seedlings. Conversely, in the *Attir1-10 afb2-3* double mutant line, IAA showed a similar inhibition level as 4-Cl-IAA. In addition, expression of *PsTIR1a*, *PsTIR1b*, or *AtTIR1* in *Attir1-10 afb2-3* double mutant line restored the superior root inhibitory effect of 4-Cl-IAA

compared to that of IAA (Jayasinghege et al., 2019). Therefore, in future studies, it will be interesting to determine if auxin response can be reduced or modified in auxin receptor double mutant (*tir1afb2*) and quadruple mutant (*tir1afb245*), and mutants expressing *PsAFB6* lines with different concentration of IAA or 4-Cl-IAA. In the root growth assays, each plate was initially scanned with an Epson Perfection V850 Pro flatbed scanner (<https://epson.ca>) and images were captured using winRhizo 2020 software, then the root length of each seedling was measured in the captured images using ImageJ software. However, it will be interesting to measure the root length with other software such as MyROOT for the semi-automatic quantification of root growth of seedlings growing directly in agar plates.

In Chapter 3, in the quadruple mutant background, one of the three *PsAFB6*-expressing lines (*PsAFB6/+ 3-2 tir1afb245* line) exhibited a lower DI at 34.7% compared to the *tir1afb245* line (45.0%). The other lines showed lower average DIs, but the differences were not statistically significant compared to the quadruple mutant control line. In the *tir1afb2* mutant background, expression of *PsAFB6* in the *PsAFB6/+ 3-3 tir1afb2* line resulted in a lower DI at 38.8% compared to the *tir1afb2C* line (61.4%). The DI of *PsAFB6/+ 4-8 tir1afb2* line didn't show significant difference from the *tir1afb2C* line. These results indicate that there is likely a threshold level of auxin response reduction to reduce *P. brassicae*-induced disease development. Therefore, it is important to determine the specific threshold of auxin response reduction that results in a decrease in the development of clubroot galls. To do this, the reduction of auxin response should be tested first in each line with different methods such as root growth assays and qRT-PCR quantification of gene expression in auxin signaling pathways, including *TIR1/AFB* auxin receptors, *Aux/IAAs* repressors and *ARFs* genes, etc. Additionally, in clubroot inoculation assays, maintaining a consistent inoculum density within a narrow range is essential for ensuring experiment uniformity. To achieve this, a second method for quantifying the clubroot spore concentration is required. In Zhou et al. 2020 transcriptomic data analysis, rutabaga (*B. napus* subsp. *rapifera* Metzg) resistant and susceptible cultivars were inoculated with *P. brassicae* and their transcriptomes were analyzed at 7, 14, and 21 DAI. In future studies, to find out how plant hormone-related genes response in early phrase of clubroot infection, qRT-PCR assays can be performed at both 7 and 14 DAI for the transgenic lines.

References

- Abel S, Oeller PW, Theologis A** (1994) Early Auxin-Induced Genes Encode Short-Lived Nuclear Proteins. *Proc Natl Acad Sci U S A* **91**: 326–330. doi: 10.1073/pnas.91.1.326
- Abel S, Theologis A** (1996) Early Genes and Auxin Action. *Plant Physiol* **11**: 9–10. doi: 10.1104/pp.111.1.9
- Agarwal A, Kaul V, Faggian R, Rookes JE, Ludwig-Müller J, Cahill DM** (2011) Analysis of global host gene expression during the primary phase of the *Arabidopsis thaliana* *Plasmodiophora brassicae* interaction. *Funct Plant Biol* **38**: 462–478. doi: 10.1071/FP11026
- Alix K, Lariagon C, Delourme R, Manzanares-Dauleux M** (2007) Exploiting natural genetic diversity and mutant resources of *Arabidopsis thaliana* to study the *A. thaliana*-*Plasmodiophora brassicae* interaction. *Plant Breed* **126**: 218–221. doi:10.1111/j.1439-0523.2007.01314.x
- Arase F, Nishitani H, Egusa M, Nishimoto N, Sakurai S, Sakamoto N, Kaminaka H** (2012) IAA8 involved in lateral root formation interacts with the TIR1 auxin receptor and ARF transcription factors in Arabidopsis. *PLoS One* **7**: e43414. doi: 10.1371/journal.pone.0043414
- Backer R, Naidoo S, van den Berg N** (2019) The NONEXPRESSOR OF PATHOGENESIS-RELATED GENES 1 (NPR1) and related family: Mechanistic insights in plant disease resistance. *Front Plant Sci* **10**: 102. doi: 10.3389/fpls.2019.00102
- Bajguz A, Piotrowska A** (2009) Conjugates of auxin and cytokinin. *Phytochem* **70**: 957–969. doi:10.1016/j.phytochem.2009.05.006
- Bartel DP** (2004) MicroRNAs: Genomics, Biogenesis, Mechanism, and Function. *Cell* **116**: 281–297. doi: 10.1016/S0092-8674(04)00045-5
- Ben-Gera H, Shwartz I, Shao MR, Shani E, Estelle M, Ori N** (2012) ENTIRE and GOBLET promote leaflet development in tomato by modulating auxin response. *Plant J* **70**: 903–915. doi: 10.1111/j.1365-313X.2012.04939.x
- Bhattacharya I, Dixon GR** (2010) Management of clubroot disease (*Plasmodiophora brassicae*) of brassicas using trap cropping techniques. *Acta Hort* **867**: 157–163. doi: 10.17660/actahortic.2010.867.20
- Cai Z, Zeng DE, Liao J, Cheng C, Sahito ZA, Xiang M, Fu M, Chen Y, Wang D** (2019) Genome-wide analysis of auxin receptor family genes in *Brassica juncea* var. *Tumida*. *Genes* **10**: 1–15. doi:10.3390/genes10020165

- Cancé C, Martin-Arevalillo R, Boubekeur K, Dumas R** (2022) Auxin response factors are keys to the many auxin doors. *New Phytol* **235**: 402–419. doi: 10.1111/nph.18159
- Cao M, Chen R, Li P, Yu Y, Zheng R, Ge D, Zheng W, Wang X, Gu Y, Gelová Z, et al** (2019) TMK1-mediated auxin signalling regulates differential growth of the apical hook. *Nature* **568**: 240–243. doi: 10.1038/s41586-019-1069-7
- Chandler JW** (2016) Auxin response factors. *Plant Cell Environ* **39**: 1014–1028. doi: 10.1111/pce.12662
- Chapman EJ, Estelle M** (2009) Mechanism of auxin-regulated gene expression in plants. *Annu Rev Genet* **43**: 265–285. doi: 10.1146/annurev-genet-102108-134148
- Chen H, Xue L, Chintamanani S, Germain H, Lin H, Cui H, Cai R, Zuo J, Tang X, Li X, et al** (2009) ETHYLENE INSENSITIVE3 and ETHYLENE INSENSITIVE3-LIKE1 repress SALICYLIC ACID INDUCTION DEFICIENT2 expression to negatively regulate plant innate immunity in Arabidopsis. *Plant Cell* **21**: 2527–2540. doi: 10.1105/tpc.108.065193
- Chen J, Pang W, Chen B, Zhang C, Piao Z** (2016) Transcriptome Analysis of *Brassica rapa* Near-Isogenic Lines Carrying Clubroot-Resistant and – Susceptible Alleles in Response to *Plasmodiophora brassicae* during Early Infection. *Front Plant Sci* **6**: 1–14. doi: 10.3389/fpls.2015.01183
- Ciaghi S, Schwelm A, Neuhauser S** (2019) Transcriptomic response in symptomless roots of clubroot infected kohlrabi mirrors resistant plants. *BMC Plant Biol* **391516**: 1–19. doi: 10.1186/s12870-019-1902-z
- Cuzick A, Maguire K, Hammond-Kosack KE** (2009) Lack of the plant signalling component SGT1b enhances disease resistance to *Fusarium culmorum* in Arabidopsis buds and flowers. *New Phytol* **181**: 901–912. doi: 10.1111/j.1469-8137.2008.02712.x
- Daval S, Belcour A, Gazengel K, Legrand L, Gouzy J, Cottret L, Lebreton L, Aigu Y, Mougel C, Manzanares-Dauleux MJ** (2019) Computational analysis of the *Plasmodiophora brassicae* genome: mitochondrial sequence description and metabolic pathway database design. *Genomics* **111**: 1629–1640. doi: 10.1016/j.ygeno.2018.11.013
- Devos S, Laukens K, Deckers P, Van Der Straeten D, Beeckman T, Inzé D, Van Onckelen H, Witters E, Prinsen E** (2006) A hormone and proteome approach to picturing the initial metabolic events during *Plasmodiophora brassicae* infection on Arabidopsis. *Mol Plant Microbe Interact* **19**: 1431–1443. doi: 10.1094/MPMI-19-1431
- Devos S, Prinsen E** (2006) Plant hormones: A key in clubroot development. *Commun Agric Appl Biol Sci* **71**: 869–872
- Dharmasiri N, Dharmasiri S, Estelle M** (2005a) The F-box protein TIR1 is an auxin receptor. *Nature* **435**: 441–445. doi: 10.1038/nature03543

- Dharmasiri N, Dharmasiri S, Weijers D, Lechner E, Yamada M, Hobbie L, Ehrismann JS, Jürgens G, Estelle M** (2005b) Plant development is regulated by a family of auxin receptor F box proteins. *Dev Cell* **9**: 109–119. doi: 10.1016/j.devcel.2005.05.014
- Diederichsen E, Frauen M, Linders EGA, Hatakeyama K, Hirai M** (2009) Status and perspectives of clubroot resistance breeding in crucifer crops. *J Plant Growth Regul* **28**: 265–281. doi: 10.1007/s00344-009-9100-0
- Diederichsen E, Sacristan MD** (1996) Disease response of resynthesized *Brassica napus* L. lines carrying different combinations of resistance to *Plasmodiophora brassicae* Wor. *Plant Breed* **115**: 5–10. doi: 10.1111/j.1439-0523.1996.tb00862.x
- Dixon GR** (2006) The biology of *Plasmodiophora brassicae* Wor. - A review of recent advances. *Acta Hort* **706**: 271–282. doi: 10.17660/ActaHortic.2006.706.32
- Dixon GR** (2009a) *Plasmodiophora brassicae* in its environment. *J Plant Growth Regul* **28**: 212–228. doi: 10.1007/s00344-009-9098-3
- Dixon GR** (2009b) The Occurrence and Economic Impact of *Plasmodiophora brassicae* and Clubroot Disease. *J Plant Growth Regul* 194–202. doi: 10.1007/s00344-009-9090-y
- Van der Does D, Leon-Reyes A, Koornneef A, Van Verk MC, Rodenburg N, Pauwels L, Goossens A, Körbes AP, Memelink J, Ritsema T, et al** (2013) Salicylic acid suppresses jasmonic acid signaling downstream of SCF^{COI1}-JAZ by targeting GCC promoter motifs via transcription factor ORA59. *Plant Cell* **25**: 744–761. doi: 10.1105/tpc.112.108548
- Donald C, Porter I** (2009) Integrated control of clubroot. *J Plant Growth Regul* **28**: 289–303. doi: 10.1007/s00344-009-9094-7
- Donald EC, Porter IJ, Faggian R, Lancaster RA** (2006) An Integrated Approach to the Control of Clubroot in Vegetable Brassica Crops. *Acta Hort* 283–300. doi:10.17660/ActaHortic.2006.706.33
- Doyle OPE, Clancy KJ** (1987) Effects of eight fungicides on clubroot of brassicas, disease severity and plant yield. *Ann Appl Biol* **110**: 50–51
- Dreher KA, Brown J, Saw RE, Callis J** (2006) The Arabidopsis Aux/IAA protein family has diversified in degradation and auxin responsiveness. *Plant Cell* **18**: 699–714. doi: 10.1105/tpc.105.039172
- Ellis CM, Nagpal P, Young JC, Hagen G, Guilfoyle TJ, Reed JW** (2005) AUXIN RESPONSE FACTOR1 and AUXIN RESPONSE FACTOR2 regulate senescence and floral organ abscission in *Arabidopsis thaliana*. *Development* **132**: 4563–4574. doi: 10.1242/dev.02012

- Fousia S, Tsafouros A, Roussos PA, Tjamos SE** (2018) Increased resistance to *Verticillium dahliae* in Arabidopsis plants defective in auxin signalling. *Plant Pathol* **67**: 1749–1757. doi: 10.1111/ppa.12881
- Friberg H, Lagerlöf J, Rämert B, L L** (2005) Germination of *Plasmodiophora brassicae* resting spores stimulated by a non-host plant. *Eur J Plant Pathol* **113**: 275–281. doi: 10.1007/s1065 8-005-2797-0
- Fu J, Wang S** (2011) Insights into auxin signaling in plant-pathogen interactions. *Front Plant Sci* **2**: 1–7. doi: 10.3389/fpls.2011.00074
- Gahatraj S, Shrestha SM, Devkota TR, Rai HH** (2019) A review on clubroot of crucifers: symptoms, life-cycle of pathogen, factors affecting severity, and management strategies. *Arch agric environ sci* **4**: 342–349. doi: 10.26832/24566632.2019.0403012
- Galindo-González L, Manolii V, Hwang SF, Strelkov SE** (2020) Response of *Brassica napus* to *Plasmodiophora brassicae* Involves Salicylic Acid-Mediated Immunity: An RNA-Seq-Based Study. *Front Plant Sci* **11**: 1–20. doi: 10.3389/fpls.2020.01025
- Gimenez-Ibanez S, Solano R** (2013) Nuclear jasmonate and salicylate signaling and crosstalk in defense against pathogens. *Front Plant Sci* **4**: 1–11. doi: 10.3389/fpls.2013.00072
- Glazebrook J, Rogers EE, Ausubel FM** (1996) Isolation of Arabidopsis Mutants With Enhanced Disease Susceptibility by Direct Screening. *Genetics* **143**: 973–982. doi: 10.1093/genetics/ 143.2.973
- Goh T, Kasahara H, Mimura T, Kamiya Y, Fukaki H** (2012) Multiple AUX/IAA-ARF modules regulate lateral root formation: The role of Arabidopsis SHY2/IAA3-mediated auxin signalling. *Phil Trans R Soc B* **367**: 1461–1468. doi: 10.1098/rstb.2011.0232
- Göhre V, Robatzek S** (2008) Breaking the barriers: Microbial effector molecules subvert plant immunity. *Annu Rev Phytopathol* **46**: 189–215. doi: 10.1146/annurev.phyto.46.120407.110050
- Grant M, Lamb C** (2006) Systemic immunity. *Curr Opin Plant Biol* **9**: 414–420. doi: 10.1016/j.pbi.2006.05.013
- Gray WM, Kepinski S, Rouse D, Leyser O, Estelle M** (2001) Auxin regulates SCF^{TIR1}-dependent degradation of AUX/IAA proteins. *Nature* **414**: 271–276. doi: 10.1038/35104500
- Greenham K, Santner A, Castillejo C, Mooney S, Sairanen I, Ljung K, Estelle M** (2011) The AFB4 auxin receptor is a negative regulator of auxin signaling in seedlings. *Curr Biol* **21**: 520–525. doi: 10.1016/j.cub.2011.02.029

- Grsic-Rausch S, Kobelt P, Siemens JM, Bischoff M, Ludwig-Muller J** (2000) Expression and Localization of Nitrilase during Symptom Development of the Clubroot Disease in Arabidopsis. *Plant Physiol* **122**: 369–378. doi: 10.1104/pp.122.2.369
- Guilfoyle TJ, Hagen G** (2012) Getting a grasp on domain III/IV responsible for Auxin Response Factor-IAA protein interactions. *Plant Sci* **190**: 82–88. doi: 10.1016/j.plantsci.2012.04.003
- Guilfoyle TJ, Hagen G** (2007) Auxin response factors. *Curr Opin Plant Biol* **10**: 453–460. doi: 10.1016/j.pbi.2007.08.014
- Guo R, Hu Y, Aoi Y, Hira H, Ge C, Dai X, Kasahara H, Zhao Y** (2022) Local conjugation of auxin by the GH3 amido synthetases is required for normal development of roots and flowers in Arabidopsis. *Biochem Biophys Res Commun* **589**: 16–22. doi: 10.1016/j.bbrc.2021.11.109
- Gupta V, Willits MG, Glazebrook J** (2000) *Arabidopsis thaliana* EDS4 contributes to salicylic acid (SA)-dependent expression of defense responses: Evidence for inhibition of jasmonic acid signaling by SA. *Mol Plant Microbe Interact* **13**: 503–511. doi: 10.1094/MPMI.2000.13.5.503
- Guseman JM, Hellmuth A, Lanctot A, Feldman TP, Moss BL, Klavins E, Calderón Villalobos LIA, Nemhauser JL** (2015) Auxin-induced degradation dynamics set the pace for lateral root development. *Development* **142**: 905–909. doi: 10.1242/dev.117234
- Gutierrez L, Bussell JD, Păcurar DI, Schwambach J, Păcurar M, Bellini C** (2009) Phenotypic plasticity of adventitious rooting in Arabidopsis is controlled by complex regulation of AUXIN RESPONSE FACTOR transcripts and microRNA abundance. *Plant Cell* **21**: 3119–3132. doi: 10.1105/tpc.108.064758
- Hagen G** (2015) Auxin signal transduction. *Essays Biochem* **58**: 1–12. doi: 10.1042/BSE0580001
- Hagen G, Guilfoyle T** (2002) Auxin-responsive gene expression: Genes, promoters and regulatory factors. *Plant Mol Biol* **49**: 373–385. doi: 10.1023/A:1015207114117
- Hagen G, Guilfoyle TJ** (1985) Rapid Induction of Selective Transcription by Auxins. *Mol Cell Biol* **5**: 1197–1203. doi: 10.1128/mcb.5.6.1197-1203.1985
- Halim VA, Vess A, Scheel D, Rosahl S** (2006) The role of salicylic acid and jasmonic acid in pathogen defence. *Plant Biol* **8**: 307–313. doi: 10.1055/s-2006-924025
- Hamann T, Benkova E, Bäurle I, Kientz M, Jürgens G** (2002) The Arabidopsis *BODENLOS* gene encodes an auxin response protein inhibiting MONOPTEROS-mediated embryo patterning. *Genes Dev* **16**: 1610–1615. doi: 10.1101/gad.229402

- Hamann T, Mayer U, Jürgens G** (1999) The auxin-insensitive *bodenlos* mutation affects primary root formation and apical-basal patterning in the Arabidopsis embryo. *Development* **126**: 1387–1395. doi: 10.1242/dev.126.7.1387
- Hamilton HA, Crete R** (2010) Influence of soil moisture, soil pH, and liming sources on the incidence of clubroot, the germination and growth of cabbage produced in mineral and organic soils under controlled conditions. *Can J Plant Sci* **58**: 45–53. doi: 10.4141/cjps78-010
- Hammond-Kosack KE, Parker JE** (2003) Deciphering plant-pathogen communication: Fresh perspectives for molecular resistance breeding. *Curr Opin Biotechnol* **14**: 177–193. doi: 10.1016/S0958-1669(03)00035-1
- Han S, Hwang I** (2018) Integration of multiple signaling pathways shapes the auxin response. *J Exp Bot* **69**: 189–200. doi: 10.1093/jxb/erx232
- Hardtke CS, Ckurshumova W, Vidaurre DP, Singh SA, Stamatiou G, Tiwari SB, Hagen G, Guilfoyle TJ, Berleth T** (2004) Overlapping and non-redundant functions of the Arabidopsis auxin response factors MONOPTEROS and NONPHOTOTROPIC HYPOCOTYL 4. *Development* **131**: 1089–1100. doi: 10.1242/dev.00925
- Howard RJ, Strelkov SE, Harding MW, L L** (2010) Clubroot of cruciferous crops-New perspectives on an old disease. *Can J Plant Pathol* **32**: 43–57. doi: 10.1080/07060661003621761
- Hwang SF, Ahmed HU, Zhou Q, Fu H, Turnbull GD, Fredua-Agyeman R, Strelkov SE, Gossen BD, Peng G** (2019) Influence of resistant cultivars and crop intervals on clubroot of canola. *Can J Plant Sci* **99**: 862–872. doi: 10.1139/cjps-2019-0018
- Hwang SF, Ahmed HU, Zhou Q, Turnbull GD, Strelkov SE, Gossen BD, Peng G** (2015) Effect of host and non-host crops on *Plasmodiophora brassicae* resting spore concentrations and clubroot of canola. *Plant Pathol* **64**: 1198–1206. doi: 10.1111/ppa.12347
- Hwang SF, Howard RJ, Strelkov SE, Gossen BD, Peng G** (2014) Management of clubroot (*Plasmodiophora brassicae*) on canola (*Brassica napus*) in western Canada. *Can J Plant Pathol* **36**: 49–65. doi: 10.1080/07060661.2013.863806
- Hwang SF, Strelkov SE, Feng J, Gossen BD, Howard RJ** (2012) *Plasmodiophora brassicae*: a review of an emerging pathogen of the Canadian canola (*Brassica napus*) crop. *Mol Plant Pathol* **13**: 105–113. doi: 10.1111/j.1364-3703.2011.00729.x
- Iglesias MJ, Terrile MC, Casalongué CA** (2011) Auxin and salicylic acid signalings counteract during the adaptive response to stress. *Plant Signal Behav* **6**: 452–454. doi: 10.4161/psb.6.3.14676

- Ishikawa T, Okazaki K, Kuroda H, Itoh K, Mitsui T, Hori H** (2007) Molecular cloning of *Brassica rapa* nitrilases and their expression during clubroot development. *Mol Plant Pathol* **8**: 623–637. doi: 10.1111/j.1364-3703.2007.00414.x
- Jahn L, Mucha S, Bergmann S, Horn C, Staswick P, Steffens B, Siemens J, Ludwig-Müller J** (2013) The clubroot pathogen (*Plasmodiophora brassicae*) influences auxin signaling to regulate auxin homeostasis in Arabidopsis. *Plants* **2**: 726–749. doi: 10.3390/plants2040726
- Javed MA, Schwelm A, Zamani-Noor N, Salih R, Silvestre Vañó M, Wu J, González García M, Heick TM, Luo C, Prakash P, et al** (2023) The clubroot pathogen *Plasmodiophora brassicae*: A profile update. *Mol Plant Pathol* **89**–106. doi: 10.1111/mpp.13283
- Jayasinghege C** (2017) Characterization of Auxin Receptors and Auxin-Ethylene Interaction During Pea Fruit Development. University of Alberta.
- Jayasinghege CPA, Ozga JA, Nadeau CD, Kaur H, Reinecke DM** (2019) TIR1 auxin receptors are implicated in the differential response to 4-Cl-IAA and IAA in developing pea fruit. *J Exp Bot* **70**: 1239–1253. doi: 10.1093/jxb/ery456
- Jez JM** (2022) Connecting primary and specialized metabolism: Amino acid conjugation of phytohormones by GRETCHEN HAGEN 3 (GH3) acyl acid amido synthetases. *Curr Opin Plant Biol*. doi: 10.1016/j.pbi.2022.102194. doi: 10.1016/j.pbi.2022.102194
- Ji R, Gao S, Bi Q, Wang Y, Lv M, Ge W, Feng H** (2020) The Salicylic Acid Signaling Pathway Plays an Important Role in the Resistant Process of *Brassica rapa* L. ssp. *pekinensis* to *Plasmodiophora brassicae* Woronin. *J Plant Growth Regul*. doi: 10.1007/s00344-020-10105-4
- Jones JDG, Dang JL** (2006) The plant immune system. *Nature* **444**: 323–329. doi: 10.1038/nature0528
- Jubault M, Lariagon C, Tacconnat L, Renou JP, Gravot A, Delourme R, Manzanares-Dauleux MJ** (2013) Partial resistance to clubroot in Arabidopsis is based on changes in the host primary metabolism and targeted cell division and expansion capacity. *Funct Integr Genomics* **13**: 191–205. doi: 10.1007/s10142-013-0312-9
- Kageyama K, Asano T** (2009) Life cycle of *plasmodiophora brassicae*. *J Plant Growth Regul* **28**: 203–211. doi: 10.1007/s00344-009-9101-z
- Kaur H, Ozga JA, Reinecke DM** (2021) Balancing of hormonal biosynthesis and catabolism pathways, a strategy to ameliorate the negative effects of heat stress on reproductive growth. *Plant Cell Environ* **44**: 1486–1503. doi: 10.1111/pce.13820
- Ke J, Ma H, Gu X, Thelen A, Brunzelle JS, Li J, Xu HE, Melcher K** (2015) Structural basis for recognition of diverse transcriptional repressors by the TOPLESS family of corepressors. *Sci Adv* **1**: 1–12. doi: 10.1126/sciadv.1500107

- Kelley DR, Arreola A, Gallagher TL, Gasser CS** (2012) ETTIN (ARF3) physically interacts with KANADI proteins to form a functional complex essential for integument development and polarity determination in Arabidopsis. *Development* **139**: 1105–1109. doi: 10.1242/dev.067918
- Kim BC, Soh MS, Kang BJ, Furuya M, Nam HG** (1996) Two dominant photomorphogenic mutations of *Arabidopsis thaliana* identified as suppressor mutations of *hy2*. *Plant J* **9**: 441–456. doi: 10.1046/j.1365-313x.1996.09040441.x
- Kim SH, Bahk S, An J, Hussain S, Nguyen NT, Do HL, Kim JY, Hong JC, Chung WS** (2020) A Gain-of-Function Mutant of IAA15 Inhibits Lateral Root Development by Transcriptional Repression of *LBD* Genes in Arabidopsis. *Front Plant Sci* **11**: 1–11. doi: 10.3389/fpls.2020.01239
- Klessig DF, Choi HW, Dempsey DA** (2018) Systemic acquired resistance and salicylic acid: Past, present, and future. *Mol Plant Microbe Interact* **31**: 871–888. doi: 10.1094/MPMI-03-18-0067-CR
- Kloek AP, Verbsky ML, Sharma SB, Schoelz JE, Vogel J, Klessig DF, Kunkel BN** (2001) Resistance to *Pseudomonas syringae* conferred by an *Arabidopsis thaliana* coronatine-insensitive (*coi1*) mutation occurs through two distinct mechanisms. *Plant J* **26**: 509–522. doi: 10.1046/j.1365-313X.2001.01050.x
- Kong Q, Low PM, Lim ARQ, Yang Y, Yuan L, Ma W** (2022) Functional Antagonism of WRI1 and TCP20 Modulates GH3.3 Expression to Maintain Auxin Homeostasis in Roots. *Plants* **11**: 454. doi: 10.3390/plants11030454
- Kowata-Dresch LS, May-De Mio LL** (2012) Clubroot management of highly infested soils. *Crop Prot* **35**: 47–52. doi: 10.1016/j.cropro.2011.12.012
- Kunkel BN, Harper CP** (2018) The roles of auxin during interactions between bacterial plant pathogens and their hosts. *J Exp Bot* **69**: 245–254. doi: 10.1093/jxb/erx447
- Kunkel BN, Johnson JMB** (2021) Auxin Plays Multiple Roles during Plant-Pathogen Interactions. *Cold Spring Harb Perspect Biol* **13**. doi: 10.1101/cshperspect.a040022
- Lakehal A, Chaabouni S, Cavel E, Le Hir R, Ranjan A, Raneshan Z, Novák O, Păcurar DI, Perrone I, Jobert F, et al** (2019) A Molecular Framework for the Control of Adventitious Rooting by TIR1/AFB2-Aux/IAA-Dependent Auxin Signaling in Arabidopsis. *Mol Plant* **12**: 1499–1514. doi: 10.1016/j.molp.2019.09.001
- Lavy M, Estelle M** (2016) Mechanisms of auxin signaling. *Development* **143**: 3226–3229. doi: 10.1242/dev.131870

- Leboldus JM, Manolii VP, Turkington TK, Strelkov SE** (2012) Adaptation to *Brassica* host genotypes by a single-spore isolate and population of *Plasmodiophora brassicae* (clubroot). *Plant Dis* **96**: 833–838. doi: 10.1094/PDIS-09-11-0807
- Lemarié S, Robert-Seilaniantz A, Lariagon C, Lemoine J, Marnet N, Jubault M, Manzanares-Dauleux MJ, Gravot A** (2015) Both the Jasmonic Acid and the Salicylic Acid Pathways Contribute to Resistance to the Biotrophic Clubroot Agent *Plasmodiophora brassicae* in Arabidopsis. *Plant Cell Physiol* **56**: 2158–2168. doi: 10.1093/pcp/pcv127
- Leyser HMO, Pickett FB, Dharmasiri S, Estelle M** (1996) Mutations in the *AXR3* gene of Arabidopsis result in altered auxin response including ectopic expression from the SAUR-AC1 promoter. *Plant J* **10**: 403–413. doi: 10.1046/j.1365-313x.1996.10030403.x
- Li SB, Xie ZZ, Hu CG, Zhang JZ** (2016) A review of auxin response factors (ARFs) in plants. *Front Plant Sci* **7**: 1–7. doi: 10.3389/fpls.2016.00047
- Li Y, Han S, Qi Y** (2022) Advances in structure and function of auxin response factor in plants. *J Integr Plant Biol* **1**. doi: 10.1111/jipb.13392
- Ligerot Y, Germain AD Saint, Waldie T, Troadec C, Citerne S, Kadakia N, Pillot J, Prigge M, Bendahmane A, Leyser O, et al** (2017) The pea branching *RMS2* gene encodes the PsAFB4/5 auxin receptor and is involved in an auxin-strigolactone regulation loop. *PLoS Genet* **13**: 1–29. doi: 10.1371/journal.pgen.1007089
- Liscum E, Reed JW** (2002) Genetics of Aux/IAA and ARF action in plant growth and development. *Plant Mol Biol* **49**: 387–400. doi: 10.1023/A:1015255030047
- Liu H** (2023) The role of auxin and indole glucosinolates in defense against clubroot infection in *Brassica napus*. University of Alberta, Edmonton
- Liu L, Qin L, Zhou Z, Hendriks WGHM, Liu S, Wei Y** (2020) Refining the life cycle of *Plasmodiophora brassicae*. *Phytopathology* **110**: 1704–1712. doi: 10.1094/PHYTO-02-20-0029-R
- Liu WX, Zhang FC, Zhang WZ, Song LF, Wu WH, Chen YF** (2013) Arabidopsis Di19 functions as a transcription factor and modulates *PRI*, *PR2*, and *PR5* expression in response to drought stress. *Mol Plant* **6**: 1487–1502. doi: 10.1093/mp/sst031
- Livak KJ, Schmittgen TD** (2001) Analysis of relative gene expression data using real-time quantitative PCR and the $2^{-\Delta\Delta CT}$ method. *Methods* **25**: 402–408. doi: 10.1006/meth.2001.1262
- López MA, Bannenberg G, Castresana C** (2008) Controlling hormone signaling is a plant and pathogen challenge for growth and survival. *Curr Opin Plant Biol* **11**: 420–427. doi: 10.1016/j.pbi.2008.05.002

- Lovelock DA, Donald CE, Conlan XA, Cahill DM** (2013) Salicylic acid suppression of clubroot in broccoli (*Brassica oleracea* var. *italica*) caused by the obligate biotroph *Plasmodiophora brassicae*. *Australas Plant Pathol* **42**: 141–153. doi: 10.1007/s13313-012-0167-x
- Lovelock DA, Sola I, Marschollek S, Donald CE, Rusak G, Van Pee K-H, Ludwig-muller, Cahill DM** (2016) Analysis of salicylic acid-dependent pathways in *Arabidopsis thaliana* following infection with *Plasmodiophora brassicae* and the influence of salicylic acid on disease. *Mol Plant Pathol* 1–15. doi: 10.1111/mpp.12361
- Ludwig - Müller J** (2022) What Can We Learn from -Omics Approaches to Understand Clubroot Disease? *Int J Mol Sci* **23**: 6293. doi: 10.3390/ijms23116293
- Ludwig-Müller J** (2011) Auxin conjugates: their role for plant development and in the evolution of land plants. *J Exp Bot* **62**: 1757–1773. doi: 10.1093/jxb/erq412
- Ludwig-Müller J** (2014) Auxin homeostasis, signaling, and interaction with other growth hormones during the clubroot disease of Brassicaceae. *Plant Signal Behav* **9**: 37–41. doi: 10.4161/psb.28593
- Ludwig-Müller J, Prinsen E, Rolfe SA, Scholes JD** (2009) Metabolism and plant hormone action during clubroot disease. *J Plant Growth Regul* **28**: 229–244. doi: 10.1007/s00344-009-9089-4
- Ludwig-Müller J, Schuller A** (2008) What can we learn from clubroots: Alterations in host roots and hormone homeostasis caused by *Plasmodiophora brassicae*. *Eur J Plant Pathol* **121**: 291–302. doi: 10.1007/s10658-007-9237-2
- Luo J, Zhou JJ, Zhang JZ** (2018) Aux/IAA gene family in plants: Molecular structure, regulation, and function. *Int J Mol Sci* **19**: 1–17. doi: 10.3390/ijms19010259
- Lv B, Yu Q, Liu J, Wen X, Yan Z, Hu K, Li H, Kong X, Li C, Tian H, et al** (2020) Non-canonical AUX/IAA protein IAA 33 competes with canonical AUX/IAA repressor IAA5 to negatively regulate auxin signaling. *EMBO J* **39**: 1–14. doi: 10.15252/embj.2019101515
- Ma Q, Grones P, Robert S** (2018) Auxin signaling: A big question to be addressed by small molecules. *J Exp Bot* **69**: 313–328. doi: 10.1093/jxb/erx375
- Malka SK, Cheng Y** (2017) Possible interactions between the biosynthetic pathways of indole glucosinolate and Auxin. *Front Plant Sci* **8**: 2131. doi: 10.3389/fpls.2017.02131
- Mallory AC, Bartel DP, Bartel B** (2005) MicroRNA-directed regulation of Arabidopsis Auxin Response Factor17 is essential for proper development and modulates expression of early auxin response genes. *Plant Cell* **17**: 1360–1375. doi: 10.1105/tpc.105.031716

- Mencia R, Welchen E, Auer S, Ludwig-Müller J** (2022) A Novel Target (Oxidation Resistant 2) in *Arabidopsis thaliana* to Reduce Clubroot Disease Symptoms via the Salicylic Acid Pathway without Growth Penalties. *Horticulturae* **8**: 9. doi: 10.3390/horticulturae8010009
- Mironova V V., Omelyanchuk NA, Wiebe DS, Levitsky VG** (2014) Computational analysis of auxin responsive elements in the *Arabidopsis thaliana* L. genome. *BMC Genom* **15**: S4. doi: 10.1186/1471-2164-15-S12-S4
- Mockaitis K, Estelle M** (2008) Auxin receptors and plant development: A new signaling paradigm. *Annu Rev Cell Dev Biol* **24**: 55–80. doi: 10.1146/annurev.cellbio.23.090506.123214
- Morgan KE, Zarembinski TI, Theologis A, Abel S** (1999) Biochemical characterization of recombinant polypeptides corresponding to the predicted $\beta\alpha\alpha$ fold in Aux/IAA proteins. *FEBS Lett* **454**: 283–287. doi: 10.1016/S0014-5793(99)00819-4
- Müller CJ, Valdés AE, Wang G, Ramachandran P, Beste L, Uddenberg D, Carlsbecker A** (2016) PHABULOSA mediates an auxin signaling loop to regulate vascular patterning in *Arabidopsis*. *Plant Physiol* **170**: 956–970. doi: 10.1104/pp.15.01204
- Nadeau CD, Ozga JA, Kurepin L V., Jin A, Pharis RP, Reinecke DM** (2011) Tissue-specific regulation of gibberellin biosynthesis in developing pea seeds. *Plant Physiol* **156**: 897–912. doi: 10.1104/pp.111.172577
- Nagpal P, Walker LM, Young JC, Sonawala A, Timpte C, Estelle M, Reed JW** (2000) AXR2 encodes a member of the Aux/IAA protein family. *Plant Physiol* **123**: 563–573. doi: 10.1104/pp.123.2.563
- Naseem M, Srivastava M, Tehseen M, Ahmed N** (2015) Auxin Crosstalk to Plant Immune Networks: A Plant-Pathogen Interaction Perspective. *Curr Protein Pept Sci* **16**: 389–394. doi: 10.2174/1389203716666150330124911
- Navarro L, Dunoyer P, Jay F, Arnold B, Dharmasiri N, Estelle M, Voinnet O, Jones JDG** (2006) A Plant miRNA Contributes to Antibacterial Resistance by Repressing Auxin Signaling. *Science* **312**: 434–436. doi: 10.1126/science.1125317
- Neuhaus K, Grsic-Rausch S, Sauerteig S, Ludwig-Müller J** (2000) *Arabidopsis* plants transformed with nitrilase 1 or 2 in antisense direction are delayed in clubroot development. *J Plant Physiol* **156**: 756–761. doi: 10.1016/S0176-1617(00)80243-6
- Niki T, Mitsuhashi I, Seo S, Ohtsubo N, Ohashi Y** (1998) Antagonistic effect of salicylic acid and jasmonic acid on the expression of pathogenesis-related (PR) protein genes in wounded mature tobacco leaves. *Plant Cell Physiol* **39**: 500–507. doi: 10.1093/oxfordjournals.pcp.a029397

- Okrent RA, Wildermuth MC** (2011) Evolutionary history of the GH3 family of acyl adenylases in rosids. *Plant Mol Biol* **76**: 489–505. doi: 10.1007/s11103-011-9776-y
- Okushima Y, Fukaki H, Onoda M, Theologis A, Tasaka M** (2007) ARF7 and ARF19 regulate lateral root formation via direct activation of *LBD/ASL* genes in *Arabidopsis*. *Plant Cell* **19**: 118–130. doi: 10.1105/tpc.106.047761
- Okushima Y, Overvoorde PJ, Arima K, Alonso JM, Chan A, Chang C, Ecker JR, Hughes B, Liu A, Nguyen D, et al** (2005) Functional Genomic Analysis of the AUXIN RESPONSE FACTOR Gene Family Members in *Arabidopsis thaliana*: Unique and Overlapping Functions of ARF7 and ARF19. *Plant Cell* **17**: 444–463. doi: 10.1105/tpc.105.036723
- Overvoorde PJ, Okushima Y, Alonso JM, Chan A, Chang C, Ecker JR, Hughes B, Liu A, Onodera C, Quach H, et al** (2005) Functional genomic analysis of the *AUXIN/INDOLE-3-ACETIC ACID* gene family members in *Arabidopsis thaliana*. *Plant Cell* **17**: 3282–3300. doi: 10.1105/tpc.105.036723
- Ozga JA, Jayasinghe CPA, Kaur H, Gao L, Nadeau CD, Reinecke DM** (2022) Auxin receptors as integrators of developmental and hormonal signals during reproductive development in pea. *J Exp Bot* **73**: 4094–4112. doi: 10.1093/jxb/erac152
- Ozga JA, Yu J, Reinecke DM** (2003) Pollination-, development-, and auxin-specific regulation of gibberellin 3 β -hydroxylase gene expression in pea fruit and seeds. *Plant Physiol* **131**: 1137–1146. doi: 10.1104/pp.102.015974
- Parry G, Calderon-Villalobos LI, Prigge M, Peret B, Dharmasiri S, Itoh H, Lechner E, Gray WM, Bennett M, Estelle M** (2009) Complex regulation of the TIR1/AFB family of auxin receptors. *Proc Natl Acad Sci U S A* **106**: 22540–22545. doi: 10.1073/pnas.0911967106
- Peng G, Lahlali R, Hwang SF, Pageau D, Hynes RK, McDonald MR, Gossen BD, Strelkov SE** (2014) Crop rotation, cultivar resistance, and fungicides/biofungicides for managing clubroot (*Plasmodiophora brassicae*) on canola. *Can J Plant Pathol* **36**: 99–112. doi: 10.1080/07060661.2013.860398
- Pfaffl MW** (2001) A new mathematical model for relative quantification in real-time RT-PCR. *Nucleic Acids Res* **29**: 0. doi: 10.1093/nar/29.9.e45
- Piotrowska A, Bajguz A** (2011) Conjugates of abscisic acid, brassinosteroids, ethylene, gibberellins, and jasmonates. *Phytochemistry* **72**: 2097–2112. doi: 10.1016/j.phytochem.2011.08.012
- Piya S, Shrestha SK, Binder B, Neal Stewart C, Hewezi T** (2014) Protein-protein interaction and gene co-expression maps of ARFs and Aux/IAAs in *Arabidopsis*. *Front Plant Sci* **5**: 1–9. doi: 10.3389/fpls.2014.00744

- Plant AR, Larrieu A, Causier B** (2021) Repressor for hire! The vital roles of TOPLESS-mediated transcriptional repression in plants. *New Phytol* **231**: 963–973. doi: 10.1111/nph.17428
- Ploense SE, Wu MF, Nagpal P, Reed JW** (2009) A gain-of-function mutation in IAA18 alters Arabidopsis embryonic apical patterning. *Development* **136**: 1509–1517. doi: 10.1242/dev.025932
- Powers SK, Strader LC** (2020) Regulation of auxin transcriptional responses. *Developmental Dynamics* **249**: 483–495. doi: 10.1002/dvdy.139
- Prigge MJ, Greenham K, Zhang Y, Santner A, Castillejo C, Mutka AM, O'Malley RC, Ecker JR, Kunkel BN, Estelle M** (2016) The Arabidopsis auxin receptor F-box proteins AFB4 and AFB5 are required for response to the synthetic auxin picloram. *G3-GENES GENOM GENET* **6**: 1383–1390. doi: 10.1534/g3.115.025585
- Prigge MJ, Platre M, Kadakia N, Zhang Y, Greenham K, Szutu W, Pandey BK, Bhosale RA, Bennett MJ, Busch W, et al** (2020) Genetic analysis of the Arabidopsis TIR1/AFB auxin receptors reveals both overlapping and specialized functions. *Elife* **9**: 1–28. doi: 10.7554/eLife.54740
- Ramos JA, Zenser N, Leyser O, Callis J, Ramos JA, Zenser N, Leyser O, Callisa J** (2022) Rapid Degradation of Auxin/Indoleacetic Acid Proteins Requires Conserved Amino Acids of Domain II and Is Proteasome Dependent. *Plant Cell* **13**: 2349–2360. doi: 10.1105/tpc.010244
- Reinecke DM, Ozga JA, Ilićilić N, Magnus V, Kojić B, Prodić K-P** (1999) Molecular properties of 4-substituted indole-3-acetic acids affecting pea pericarp elongation. *Plant Growth Regul* **27**: 39–48. doi: 10.1023/A:1006013216818
- Rekhter D, Lüdke D, Ding Y, Feussner K, Zienkiewicz K, Lipka V, Wiermer M, Zhang Y, Feussner I** (2019) Isochorismate-derived biosynthesis of the plant stress hormone salicylic acid. *Science* **365**: 498–502. doi: 10.1126/science.aaw1720
- Rinaldi MA, Liu J, Enders TA, Bartel B, Strader LC** (2012) A gain-of-function mutation in IAA16 confers reduced responses to auxin and abscisic acid and impedes plant growth and fertility. *Plant Mol Biol* **79**: 359–373. doi: 10.1007/s11103-012-9917-y
- Robert-Seilaniantz A, Grant M, Jones JDG** (2011) Hormone crosstalk in plant disease and defense: More than just JASMONATE-SALICYLATE antagonism. *Annu Rev Phytopathol* **49**: 317–343. doi: 10.1146/annurev-phyto-073009-114447
- Robert-Seilaniantz A, Navarro L, Bari R, Jones JD** (2007) Pathological hormone imbalances. *Curr Opin Plant Biol* **10**: 372–379. doi: 10.1016/j.pbi.2007.06.003

- Robin AHK, Saha G, Laila R, Park JI, Kim HT, Nou IS** (2020) Expression and role of biosynthetic, transporter, receptor, and responsive genes for auxin signaling during clubroot disease development. *Int J Mol Sci* **21**: 1–23. doi: 10.3390/ijms21155554
- Rogato A, Valkov VT, Nadzieja M, Stougaard J, Chiurazzi M** (2021) The lotus japonicus *AFB6* gene is involved in the auxin dependent root developmental program. *Int J Mol Sci* **22**: 8495. doi: 10.3390/ijms22168495
- Rolfe SA, Strelkov SE, Links MG, Clarke WE, Robinson SJ, Djavaheri M, Malinowski R, Haddadi P, Kagale S, Parkin IAP, et al** (2016) The compact genome of the plant pathogen *Plasmodiophora brassicae* is adapted to intracellular interactions with host *Brassica spp.* *BMC Geno* **17**: 1–15. doi: 10.1186/s12864-016-2597-2
- Roosjen M, Paque S, Weijers D** (2018) Auxin Response Factors: Output control in auxin biology. *J Exp Bot* **69**: 179–188. doi: 10.1093/jxb/erx237
- Rouse D, Mackay P, Stirnberg P, Estelle M, Leyser O** (1998) Changes in Auxin Response from Mutations in an *AUX/IAA* Gene. *Science* (1979) **279**: 1371–1373. doi: 10.1126/science.279.5355.1371
- Ruegger M, Dewey E, Gray WM, Hobbie L, Turner J, Estelle M** (1998) The TIR1 protein of Arabidopsis functions in auxin response and is related to human SKP2 and yeast Grr1p. *Genes Dev* **12**: 198–207. doi: 10.1101/gad.12.2.198
- Sabatini S, Beis D, Wolkenfelt H, Murfett J, Guilfoyle T, Malamy J, Benfey P, Leyser O, Bechtold N, Weisbeek P, et al** (1999) An auxin-dependent distal organizer of pattern and polarity in the Arabidopsis root. *Cell* **99**: 463–472. doi: 10.1016/S0092-8674(00)81535-4
- Salehin M, Bagchi R, Estelle M** (2015) SCF^{TIR1/AFB}-based auxin perception: Mechanism and role in plant growth and development. *Plant Cell* **27**: 9–19. doi: 10.1105/tpc.114.133744
- Sato A, Yamamoto KT** (2008) Overexpression of the non-canonical Aux/IAA genes causes auxin-related aberrant phenotypes in Arabidopsis. *Physiol Plant* **133**: 397–405. doi: 10.1111/j.1399-3054.2008.01055.x
- Scacchi E, Salinas P, Gujas B, Santuari L, Krogan N, Ragni L, Berleth T, Hardtke CS** (2010) Spatio-temporal sequence of cross-regulatory events in root meristem growth. *Proc Natl Acad Sci U S A* **107**: 22734–22739. doi: 10.1073/pnas.1014716108
- Schlereth A, Möller B, Liu W, Kientz M, Flipse J, Rademacher EH, Schmid M, Jürgens G, Weijers D** (2010) MONOPTEROS controls embryonic root initiation by regulating a mobile transcription factor. *Nature* **464**: 913–916. doi: 10.1038/nature08836
- Schwelm A, Dixelius C, Ludwig-Müller J** (2016) New kid on the block—the clubroot pathogen genome moves the plasmodiophorids into the genomic era. *Eur J Plant Pathol* 531–542. doi: 10.1007/s10658-015-0839-9

- Shah J, Kachroo P, Nandi A, Klessig DF** (2001) A recessive mutation in the Arabidopsis *SSI2* gene confers SA- and NPR1-independent expression of *PR* genes and resistance against bacterial and oomycete pathogens. *Plant J* **25**: 563–574. doi: 10.1046/j.1365-313x.2001.00992.x
- Shani E, Salehin M, Zhang Y, Sanchez SE, Doherty C, Wang R, Mangado CC, Song L, Tal I, Pisanty O, et al** (2017) Plant Stress Tolerance Requires Auxin-Sensitive Aux/IAA Transcriptional Repressors. *Curr Biol* **27**: 437–444. doi: 10.1016/j.cub.2016.12.016
- Sharma K, Gossen BD, McDonald MR, L L** (2011) Effect of temperature on cortical infection by *Plasmodiophora brassicae* and clubroot severity. *Phytopathology* **101**: 1424–1432. doi: 10.1094/PHYTO-04-11-0124
- Shi Q, Zhang Y, To VT, Shi J, Zhang D, Cai W** (2020) Genome-wide characterization and expression analyses of the auxin/indole-3-acetic acid (Aux/IAA) gene family in barley (*Hordeum vulgare* L.). *Sci Rep* **10**: 1–14. doi: 10.1038/s41598-020-66860-7
- Siemens J, Keller I, Sarx J, Kunz S, Schuller A, Nagel W, Schmülling T, Parniske M, Ludwig-Müller J** (2006) Transcriptome analysis of Arabidopsis clubroots indicate a key role for cytokinins in disease development. *Mol Plant-Microbe Interact* **19**: 480–494. doi: 10.1094/MPMI-19-0480
- Siemens J, Nagel M, Ludwig-Müller J, Sacristán MD** (2002) The interaction of *Plasmodiophora brassicae* and *Arabidopsis thaliana*: Parameters for disease quantification and screening of mutant lines. *J Phytopathol* **150**: 592–605. doi: 10.1046/j.1439-0434.2002.00818.x
- Simonini S, Deb J, Moubayidin L, Stephenson P, Valluru M, Freire-Rios A, Sorefan K, Weijers D, Friml J, Østergaard L** (2016) A noncanonical auxin-sensing mechanism is required for organ morphogenesis in Arabidopsis. *Genes Dev* **30**: 2286–2296. doi: 10.1101/gad.285361.116
- Simonini S, Mas PJ, Mas CMVS, Østergaard L, Hart DJ** (2018) Auxin sensing is a property of an unstructured domain in the Auxin Response Factor ETTIN of Arabidopsis thaliana. *Sci Rep* **8**: 13563. doi: 10.1038/s41598-018-31634-9
- Spaepen S, Vanderleyden J** (2011) Auxin and Plant-Microbe Interactions. *Cold Spring Harb Perspect Biol* **3**: a001438. doi: 10.1101/cshperspect.a001438
- Spoel SH, Johnson JS, Dong X** (2007) Regulation of tradeoffs between plant defenses against pathogens with different lifestyles. *Proc Natl Acad Sci U S A* **104**: 18842–18847. doi: 10.1073/pnas.0708139104
- Strelkov SE, Hwang S-F, Howard RJ, Hartman M, Turkington TK** (2011) Progress towards the Sustainable Management of Clubroot [*Plasmodiophora brassicae*] of Canola on the Canadian Prairies. *Prairie Soils & Crops Journal* **4**: 114–121. doi: 10.7939/r3-vxq6-js48

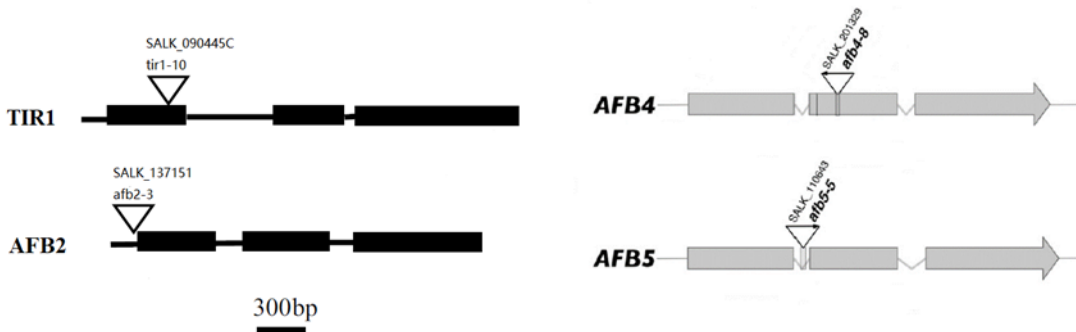
- Tada Y, Spoel SH, Pajerowska-mukhtar K, Mou Z, Song J, Wang C, Zuo J, Dong X** (2021) Plant Immunity Requires Conformational Charges of NPR1 via S-Nitrosylation and Thioredoxins. *Science* (1979) **321**: 952–956. doi: 10.1126/science.1156970
- Takato S, Kakei Y, Mitsui M, Ishida Y, Suzuki M, Yamazaki C, Hayashi KI, Ishii T, Nakamura A, Soeno K, et al** (2017) Auxin signaling through SCF^{TIR1/AFBs} mediates feedback regulation of IAA biosynthesis. *Biosci Biotechnol Biochem* **81**: 1320–1326. doi: 10.1080/09168451.2017.1313694
- Tamura K, Stecher G, Kumar S** (2021) MEGA11: Molecular Evolutionary Genetics Analysis Version 11. *Mol Biol Evol* **38**: 3022–3027. doi: 10.1093/molbev/msab120
- Tan X, Calderon-Villalobos LIA, Sharon M, Zheng C, Robinson C V., Estelle M, Zheng N** (2007) Mechanism of auxin perception by the TIR1 ubiquitin ligase. *Nature* **446**: 640–645. doi: 10.1038/nature05731
- Tanaka S, Ito S ichi** (2013) Pathogenic and genetic diversity in *Plasmodiophora brassicae* (clubroot) from Japan. *J Gen Plant Pathol* **79**: 297–306. doi: 10.1007/s10327-013-0456-4
- Tatematsu K, Kumagai S, Muto H, Sato A, Watahiki MK, Harper RM, Liscum E, Yamamoto KT** (2004) *Massugu2* Encodes Aux/IAA19, an Auxin-Regulated Protein That Functions Together with the Transcriptional Activator NPH4/ARF7 to Regulate Differential Growth Responses of Hypocotyl and Formation of Lateral Roots in *Arabidopsis thaliana*. *Plant Cell* **16**: 379–393. doi: 10.1105/tpc.018630
- Thaler JS, Humphrey PT, Whiteman NK** (2012) Evolution of jasmonate and salicylate signal crosstalk. *Trends Plant Sci* **17**: 260–270. doi: 10.1016/j.tplants.2012.02.010
- Thines B, Katsir L, Melotto M, Niu Y, Mandaokar A, Liu G, Nomura K, He SY, Howe GA, Browse J** (2007) JAZ repressor proteins are targets of the SCF^{COI1} complex during jasmonate signalling. *Nature* **448**: 661–665. doi: 10.1038/nature05960
- Tian Q, Reed JW** (1999) Control of auxin-regulated root development by the *Arabidopsis thaliana* *SHY2/AA3* gene. *Development* **126**: 711–721. doi: 10.1242/dev.126.4.711
- Tiwari SB, Hagen G, Guilfoyle T** (2003) The roles of auxin response factor domains in auxin-responsive transcription. *Plant Cell* **15**: 533–543. doi: 10.1105/tpc.008417
- Tiwari SB, Wang X, Hagen G, Guilfoyle TJ, Tiwari SB, Wang X, Hagen G, Guilfoyle TJ** (2001) AUX/IAA Proteins Are Active Repressors, and Their Stability and Activity Are Modulated by Auxin. *Plant Cell* **13**: 2809–2822. doi: 10.1105/tpc.010289
- Uehara T, Okushima Y, Mimura T, Tasaka M, Fukaki H** (2008) Domain II mutations in CRANE/IAA18 suppress lateral root formation and affect shoot development in *Arabidopsis thaliana*. *Plant Cell Physiol* **49**: 1025–1038. doi: 10.1093/pcp/pcn079

- Ugajin T, Takita K, Takahashi H, Mitsui T, Hayakawa T, Hori H, Muraoka S, Tada T, Ohyama T** (2003) Increase in Indole 3-acetic Acid (IAA) level and Nitrilase Activity in Turnips Induced by *Plasmodiophora brassicae* Infection. *Plant Biotechnol* **20**: 215–220. doi: 10.5511/plantbiotechnology.20.215
- Ullah C, Chen YH, Ortega MA, Tsai CJ** (2023) The diversity of salicylic acid biosynthesis and defense signaling in plants: Knowledge gaps and future opportunities. *Curr Opin Plant Biol* **72**: 102349. doi: 10.1016/j.pbi.2023.102349
- Ulmasov T, Hagen G, Guilfoyle TJ** (1999) Activation and repression of transcription by auxin-response factors (transcriptional activators dimerization domain AuxRE). *Proc Natl Acad. Sci U S A* **96**: 5844–5849. doi: 10.1073/pnas.96.10.584
- Verma SS, Rahman MH, Deyholos MK, Basu U, Kav NNV** (2014) Differential expression of miRNAs in *Brassica napus* root following infection with *Plasmodiophora brassicae*. *PLoS One* **9**: e86648 doi: 10.1371/journal.pone.0086648
- Vernoux T, Brunoud G, Farcot E, Morin V, Van Den Daele H, Legrand J, Oliva M, Das P, Larrieu A, Wells D, et al** (2011) The auxin signalling network translates dynamic input into robust patterning at the shoot apex. *Mol Syst Biol* **7**: 508. doi: 10.1038/msb.2011.39
- Wang D, Pajeroska-Mukhtar K, Culler AH, Dong X** (2007) Salicylic Acid Inhibits Pathogen Growth in Plants through Repression of the Auxin Signaling Pathway. *Curr Biol* **17**: 1784–1790. doi: 10.1016/j.cub.2007.09.025
- Wang H, Tian CE, Duan J, Wu K** (2008) Research progresses on GH3s, one family of primary auxin-responsive genes. *Plant Growth Regul* **56**: 225–232. doi: 10.1007/s10725-008-9313-4
- Wang J, Wang L, Mao Y, Cai W, Xue H, Chenal X** (2005) Control of Root Cap Formation by MicroRNA-Targeted Auxin Response Factors in Arabidopsis. *Plant Cell* **17**: 2204–2216. doi: 10.1105/tpc.105.033076
- Wang R, Estelle M** (2014) Diversity and specificity: auxin perception and signaling through the TIR1/AFB pathway. *Curr Opin Plant Biol* **21**: 51–58. doi: 10.1016/j.pbi.2014.06.006
- Wang Y, Zheng X, Sarenqimuge S, von Tiedemann A** (2023) The soil bacterial community regulates germination of *Plasmodiophora brassicae* resting spores rather than root exudates. *PLoS Pathogens*, **19**: 1-24. doi:10.1371/journal.ppat.1011175
- Waseem M, Ahmad F, Habib S, Li Z** (2018) Genome-wide identification of the auxin/indole-3-acetic acid (Aux/IAA) gene family in pepper, its characterisation, and comprehensive expression profiling under environmental and phytohormones stress. *Sci Rep* **8**: 1–12. doi: 10.1038/s41598-018-30468-9

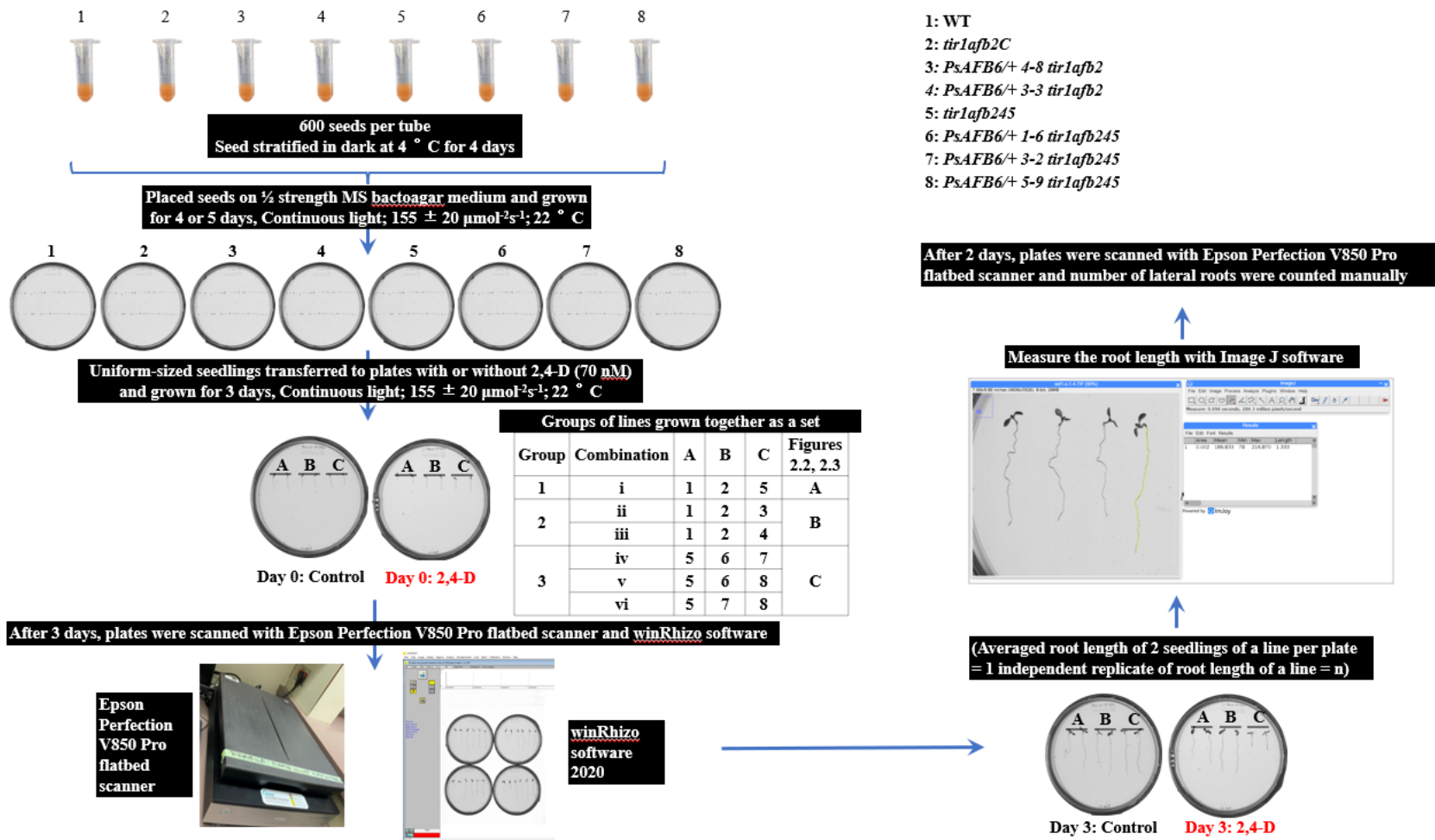
- Wei X, Liao R, Zhang X, Zhao Y, Xie Z, Yang S, Su H, Wang Z, Zhang L, Tian B, et al** (2023) Integrative Transcriptome, miRNAs, Degradome, and Phytohormone Analysis of *Brassica rapa* L. in Response to *Plasmodiophora brassicae*. *Int J Mol Sci* **24**: 2414. doi: 10.3390/ijms24032414
- Wei X, Zhang Y, Zhao Y, Xie Z, Hossain MR, Yang S, Shi G, Lv Y, Wang Z, Tian B, et al** (2021) Root Transcriptome and Metabolome Profiling Reveal Key Phytohormone-Related Genes and Pathways Involved Clubroot Resistance in *Brassica rapa* L. *Front Plant Sci* **12**: 1–17. doi: 10.3389/fpls.2021.759623
- Westfall CS, Zubieta C, Herrmann J, Kapp U, Nanao MH, Jez JM** (2012) Structural Basis for Prereceptor Modulation of Plant Hormones by GH3 Proteins. *Science* **336**: 1704–1708. doi: 10.1126/science.1220757
- Wildermuth MC, Dewdney J, Wu G, Ausubel FM** (2001) Isochorismate synthase is required to synthesize salicylic acid for plant defence. *Nature* **414**: 562–5. doi: 10.1038/35107108
- Wilmoth JC, Wang S, Tiwari SB, Joshi AD, Hagen G, Guilfoyle TJ, Alonso JM, Ecker JR, Reed JW** (2005) NPH4/ARF7 and ARF19 promote leaf expansion and auxin-induced lateral root formation. *Plant J* **43**: 118–130. doi: 10.1111/j.1365-313X.2005.02432.x
- Withers J, Dong X** (2016) Posttranslational Modifications of NPR1: A Single Protein Playing Multiple Roles in Plant Immunity and Physiology. *PLoS Pathog* **12**: 1–9. doi: 10.1371/journal.ppat.1005707
- Wojtaczka P, Ciarkowska A, Starzynska E, Ostrowski M** (2022) The GH3 amidosynthetases family and their role in metabolic crosstalk modulation of plant signaling compounds. *Phytochemistry* **194**. doi: 10.1016/j.phytochem.2021.113039
- Woodward AW, Bartel B** (2005) Auxin: Regulation, Action, and Interaction. *Ann Bot* **95**: 707–735. doi: 10.1093/aob/mci083
- Xi D, Li X, Gao L, Zhang Z, Zhu Y, Zhu H** (2021) Application of exogenous salicylic acid reduces disease severity of *Plasmodiophora brassicae* in pakchoi (*Brassica campestris* ssp. *chinensis* Makino). *PLoS One* **16**: 1–11. doi: 10.1371/journal.pone.0248648
- Xie Q, Frugis G, Colgan D, Chua NH** (2000) Arabidopsis NAC1 transduces auxin signal downstream of TIR1 to promote lateral root development. *Genes Dev* **14**: 3024–3036. doi: 10.1101/gad.852200
- Xu L, Ren L, Chen K, Liu F, Fang X** (2016) Putative role of IAA during the early response of *Brassica napus* L. to *Plasmodiophora brassicae*. *Eur J Plant Pathol* **145**: 601–613. doi: 10.1007/s10658-016-0877-y

- Yano S, Tanaka S, Kameya-Iwaki M, Katumoto K** (1991) Relation of Ca²⁺ efflux to germination of resting spores of clubroot fungus. Faculty of Agriculture, Yamaguchi University **39**: 105–112
- Yuan Y, Qin L, Su H, Yang S, Wei X, Wang Z, Zhao Y, Li L, Liu H, Tian B, et al** (2021) Transcriptome and Coexpression Network Analyses Reveal Hub Genes in Chinese Cabbage (*Brassica rapa* L. ssp. *pekinensis*) During Different Stages of *Plasmodiophora brassicae* Infection. Front Plant Sci **12**: 1–14. doi: 10.3389/fpls.2021.650252
- Zahr K, Sarkes A, Yang Y, Ahmed H, Zhou Q, Feindel D, Harding MW, Feng J** (2021) *Plasmodiophora brassicae* in Its Environment: Effects of Temperature and Light on Resting Spore Survival in Soil. Phytopathology **111**: 1743–1750. doi: 10.1094/PHYTO-09-20-0415-R
- Zhao Y** (2012) Auxin biosynthesis: A simple two-step pathway converts tryptophan to indole-3-Acetic acid in plants. Mol Plant **5**: 334–338. doi: 10.1093/mp/ssr104
- Zhao Y** (2014) Auxin Biosynthesis. Arabidopsis Book **12**: e0173. doi: 10.1199/tab.0173
- Zheng Z, Guo Y, Novák O, Chen W, Ljung K, Noel JP, Chory J** (2016) Local auxin metabolism regulates environment induced hypocotyl elongation. Nat Plants **2**:16025. doi: 10.1038/NPLANTS.2016.25
- Zhou Q, Galindo-Gonzalez L, Manolii V, Hwang SF, Strelkov SE** (2020) Comparative transcriptome analysis of rutabaga (*Brassica napus*) cultivars indicates activation of salicylic acid and ethylene-mediated defenses in response to *Plasmodiophora brassicae*. Int J Mol Sci **21**: 1–26. doi: 10.3390/ijms21218381

APPENDIX A



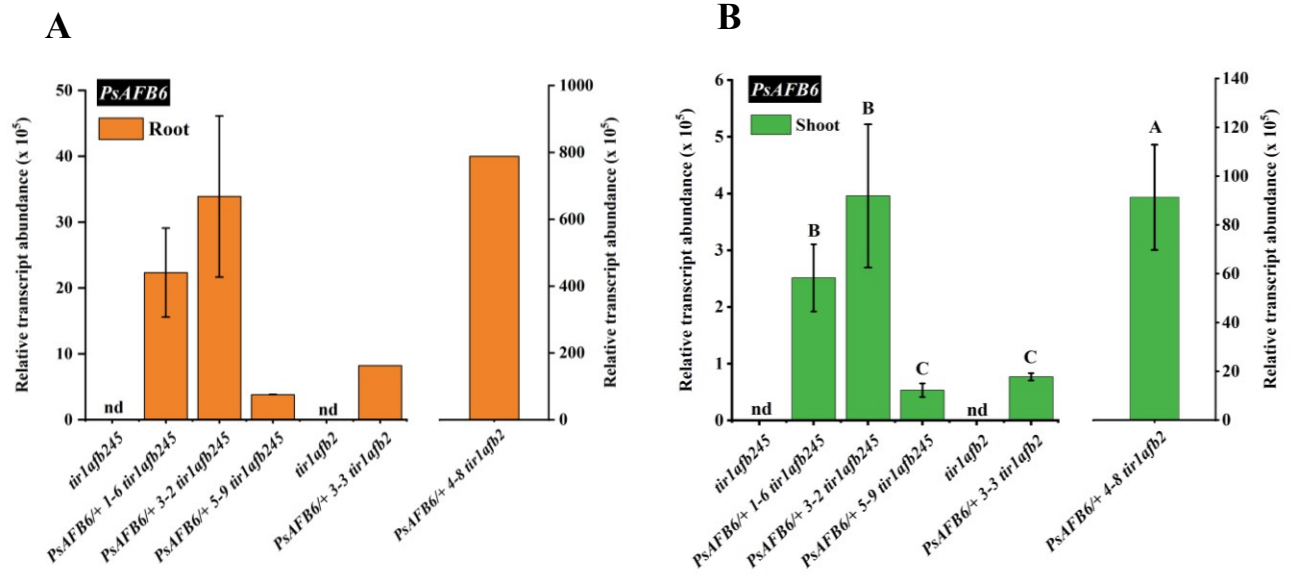
Appendix Figure A1. Diagrams of the *AtTIR1*, *AtAFB2*, *AtAFB4* and *AtAFB5* auxin receptor T-DNA insertion sites. The positions of mutant lesions are shown above the genes with white triangles denoting the position of T-DNA insertion (Parry et al., 2009; Prigge et al., 2016). The *tir1-10* allele (SALK_090445C), *afb4-8* allele (SALK_201329), and *afb5-5* allele (SALK_110643) are null mutants since the insertion is either in the intron or exon that results in the loss of full-length mRNA. The *afb2-3* allele (SALK_137151) has a T-DNA insertion 37 bp upstream of the transcriptional start site that results in some AFB2 function retention.



Appendix Figure A2. Overview of the root growth assays. Arabidopsis seeds of *tir1afb2* double and *tir1afb245* quadruple auxin receptor mutant lines and the lines expressing *PsAFB6* in the mutant backgrounds were surface sterilized and stratified in dark at 4 °C for 4 days. Using a 1 mL sterilized pipette tip, two parallel lines of seeds (15-20 total per plate) were placed onto 1 % bactoagar (w/v)

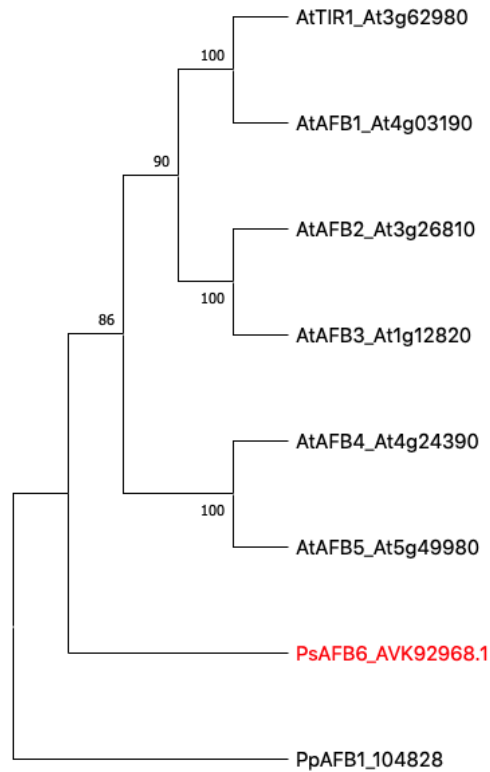
plates prepared in half-strength MS medium and 1 % (w/v) sucrose (seeds of one mutant or transformed line per plate). After 4 (double mutant and *PsAFB6*-transformed lines in this mutant background) or 5 (quadruple mutant and *PsAFB6*-transformed lines in this mutant background) days, seedlings were transferred to new half-strength bactoagar medium with (70 nM 2,4-D) or without 2,4-D (control) and grown for 3 and 5 days prior to measuring root length, and 5 days prior to counting lateral root number.

- Each plate contained six seedlings of three different lines (2 technical replicate per line per plate) and were grown in sets as outlined below: The seedlings of Arabidopsis Col-0 WT (1), *tir1afb2* double mutant (2), and *tir1afb245* quadruple mutant (5) were organized in the plates as group 1 (see table above), grown together as a set, and data from this set is presented in Figs. 2.2A and 2.3A.
- The seedlings of Arabidopsis Col-0 WT (1), *tir1afb2* double mutant (2), *PsAFB6*-expressing *tir1afb2* lines *PsAFB6/+ 4-8 tir1afb2* (3) and *PsAFB6/+ 3-3 tir1afb2* (4) were organized in the plates as group 2 (see table above), grown together as a set, and data from this set is presented in Figs. 2.2B and 2.3B.
- The seedlings of Arabidopsis *tir1afb245* quadruple mutant (5) and *PsAFB6*-expressing *tir1afb245* lines *PsAFB6/+ 1-6 tir1afb245* (6), *PsAFB6/+ 3-2 tir1afb245* (7) and *PsAFB6/+ 5-9 tir1afb245* (8) were organized in the plates as group 3 (see table above), grown together as a set, and data from this set is presented in Figs. 2.2C and 2.3C.
- Data from two to three sequential sets were pooled for obtaining percent root elongation and number of lateral roots. Plates were scanned with an Epson Perfection V850 Pro flatbed scanner at Day 0, Day 3 and Day 5 of the root growth assay, root length was measured with ImageJ software and quantified as percent root elongation in the auxin-containing medium expressed as percentage compared to the same line grown in medium without auxin. The number of lateral roots for each line was counted on Day 5 of the root growth assay using scanned images of the plates. The lateral root density (cm^{-1}) was calculated by dividing the number of lateral roots for each line by the root length at Day 5.



Appendix Figure A3. *PsAFB6* transcript abundance in root and shoot tissues of *Arabidopsis tir1afb2* double and *tir1afb245* quadruple mutants expressing *PsAFB6*. *PsAFB6* transcript abundance in shoot (A) or root (B) tissues of ten-day-old seedlings of *Arabidopsis* non-transgenic *tir1afb2* and *tir1afb2* transformed with *PsAFB6* (*PsAFB6*^{+/+} 3-3 *tir1afb2* and *PsAFB6*^{+/+} 4-8 *tir1afb2*), and eleven-day-old seedlings of *Arabidopsis* non-transgenic *tir1afb245* mutant and *tir1afb245* transformed with *PsAFB6* in this mutant background (*PsAFB6*^{+/+} 1-6 *tir1afb245*, *PsAFB6*^{+/+} 3-2 *tir1afb245* and *PsAFB6*^{+/+} 5-9 *tir1afb245*). Seedling were grown on media for root growth assays for 10-11 days prior to separately harvesting the root and shoot tissues for qRT-PCR. Shoot data are means \pm standard error (SE), n = 4, each biological replicate is a pool of shoots obtained from 6 randomly selected seedlings for each line. Root data for the *tir1afb245* quadruple mutant and *PsAFB6*-expressing transgenic lines in this mutant background are means \pm standard error (SE), n = 2. For the *tir1afb2* double mutant line and *tir1afb2* lines expressing *PsAFB6*, n = 1. Each biological replicate of root tissue is a pool of roots obtained from 78 seedlings for *tir1afb2*, 40 seedlings for *PsAFB6*^{+/+} 4-8 *tir1afb2*, 39 seedlings for *PsAFB6*^{+/+} 3-3 *tir1afb2*, 47-48 seedlings for *tir1afb245*, 31-32 seedlings for *PsAFB6*^{+/+} 1-6 *tir1afb245*, 34-36 seedlings for *PsAFB6*^{+/+} 3-2 *tir1afb245* and 33-34 seedlings for *PsAFB6*^{+/+} 5-9 *tir1afb245*. Different letters for shoot data indicate statistically significant differences between the lines (One-way-ANOVA, LSD post-hoc test, P \leq 0.05, Appendix Table A1). nd: no *PsAFB6* transcripts were detected.

A



B

Amino Acid similarity	AtTIR1	AtAFB1	AtAFB2	AtAFB3	AtAFB4	AtAFB5
% Similarity with PsAFB6	64.98	61.84	66.02	66.2	61.32	60.62
% Identity with PsAFB6	54.87	52.26	53.65	54.18	50.17	50.17

Appendix Figure A4. A phylogenetic tree and amino acid percent global similarities and identities showing the association of *Pisum sativum* auxin receptor PsAFB6 with Transport Inhibitor Response 1 and Auxin-Signaling F-box (TIR1/AFB) proteins from *Arabidopsis thaliana* (At). (A) For phylogenetic tree construction, amino acid sequences were first aligned with the MUSCLE (MUltiple Sequence Comparison by Log Expectation) multiple sequence alignment tool using default settings, then the tree was constructed using a neighbor-joining method with a bootstrap analysis of 1000 replications, Poisson correction model, and complete deletion treatment in the MEGA 11 package (Tamura et al., 2021). The tree was rooted with the AFB1 transcription factor from *Physcomitrium patens* (Pp). Numbers in the branches represent

the percentage bootstrap support and branches with values less than 50 % are condensed. Full-length protein sequences of *Arabidopsis thaliana* Transport Inhibitor Response 1 and Auxin-Signaling F-box (TIR1/AFB) proteins were obtained from *Arabidopsis thaliana* genome annotation version TAIR10 (<https://www.arabidopsis.org/>). Full-length protein sequence of *P. sativum* auxin receptor PsAFB6 was retrieved from NCBI GenBank. Protein sequences were aligned with Clustal Omega (<https://www.ebi.ac.uk/Tools/msa/clustalo/>; Sievers et al., 2011) using default settings and the output was generated in Pearson or FASTA sequence format.

(B) Global similarity and identity percentages were calculated based on BLOSUM62 matrix on amino acid sequences of *Pisum sativum* auxin receptor PsAFB6 with those of Transport Inhibitor Response 1 and Auxin-Signaling F-box (TIR1/AFB) proteins from *Arabidopsis thaliana* using Sequence Identity and Similarity (SISA) program (<http://imed.med.ucm.es/Tools/sias.html>).

Appendix Table A1. The probability, degrees of freedom and F values for the relative transcript abundance of *PsAFB6* in the shoot tissues of ten-day-old seedlings of the Arabidopsis *PsAFB6*-expressing lines (*PsAFB6/+ 4-8 tir1afb2* vs. *PsAFB6/+ 3-3 tir1afb2* vs. *PsAFB6/+ 1-6 tir1afb245* vs. *PsAFB6/+ 3-2 tir1afb245* vs. *PsAFB6/+ 5-9 tir1afb245*) in one-way ANOVA analysis followed by mean separation using LSD post-hoc test performed on data presented in Figure 2.1 and Appendix Figure A3.

Gene name	Lines	
	F value	Pr(>F)
<i>PsAFB6</i>	70.1106	<0.0001
Degrees of freedom	4	

LSD post-hoc test (p-values)	<i>PsAFB6/+ 1-6 tir1afb245</i>	<i>PsAFB6/+ 3-2 tir1afb245</i>	<i>PsAFB6/+ 5-9 tir1afb245</i>	<i>PsAFB6/+ 4-8 tir1afb2</i>	<i>PsAFB6/+ 3-3 tir1afb2</i>
<i>PsAFB6/+ 1-6 tir1afb245</i>	1				
<i>PsAFB6/+ 3-2 tir1afb245</i>	0.3433	1			
<i>PsAFB6/+ 5-9 tir1afb245</i>	0.0004	<0.0001	1		
<i>PsAFB6/+ 4-8 tir1afb2</i>	<0.0001	<0.0001	<0.0001	1	
<i>PsAFB6/+ 3-3 tir1afb2</i>	0.0050	0.0007	0.2337	<0.0001	1

Appendix Table A2. The probability, degrees of freedom and F values on the lateral root density for treatments (Control vs. 2,4-D), lines (WT vs. *tir1afb2* vs. *tir1afb245*) and treatments x lines interaction in two-way ANOVA analysis followed by mean separation using LSD post-hoc test performed on data presented in Figure 2.3A.

	Treatments		Lines		Treatments x Lines	
	F value	Pr(>F)	F value	Pr(>F)	F value	Pr(>F)
Lateral root density	847.9000	<0.0001	1943.8000	<0.0001	863.4000	<0.0001
Degrees of freedom	1		2		2	

LSD post-hoc test (p-values)	WT-Control	WT-2,4-D	<i>tir1afb2</i> -Control	<i>tir1afb2</i> -2,4-D	<i>tir1afb245</i> -Control	<i>tir1afb245</i> -2,4-D
WT-Control	1					
WT-2,4-D	<0.0001	1				
<i>tir1afb2</i> -Control	<0.0001	<0.0001	1			
<i>tir1afb2</i> -2,4-D	<0.0001	<0.0001	0.4756	1		
<i>tir1afb245</i> -Control	<0.0001	<0.0001	0.3228	0.7573	1	
<i>tir1afb245</i> -2,4-D	<0.0001	<0.0001	0.2654	0.6760	0.9226	1

Appendix Table A3. The probability, degrees of freedom and F values on the lateral root density for treatments (Control vs. 2,4-D), lines (WT vs. *tir1afb2* vs. *PsAFB6/+ 4-8 tir1afb2* vs. *PsAFB6/+ 3-3 tir1afb2*) and treatments x lines interaction in two-way ANOVA analysis followed by mean separation using LSD post-hoc test performed on data presented in Figure 2.3B.

	Treatments		Lines		Treatments x Lines	
	F value	Pr(>F)	F value	Pr(>F)	F value	Pr(>F)
Lateral root density	299.5000	<0.0001	620.0000	<0.0001	201.3000	<0.0001
Degrees of freedom	1		3		3	

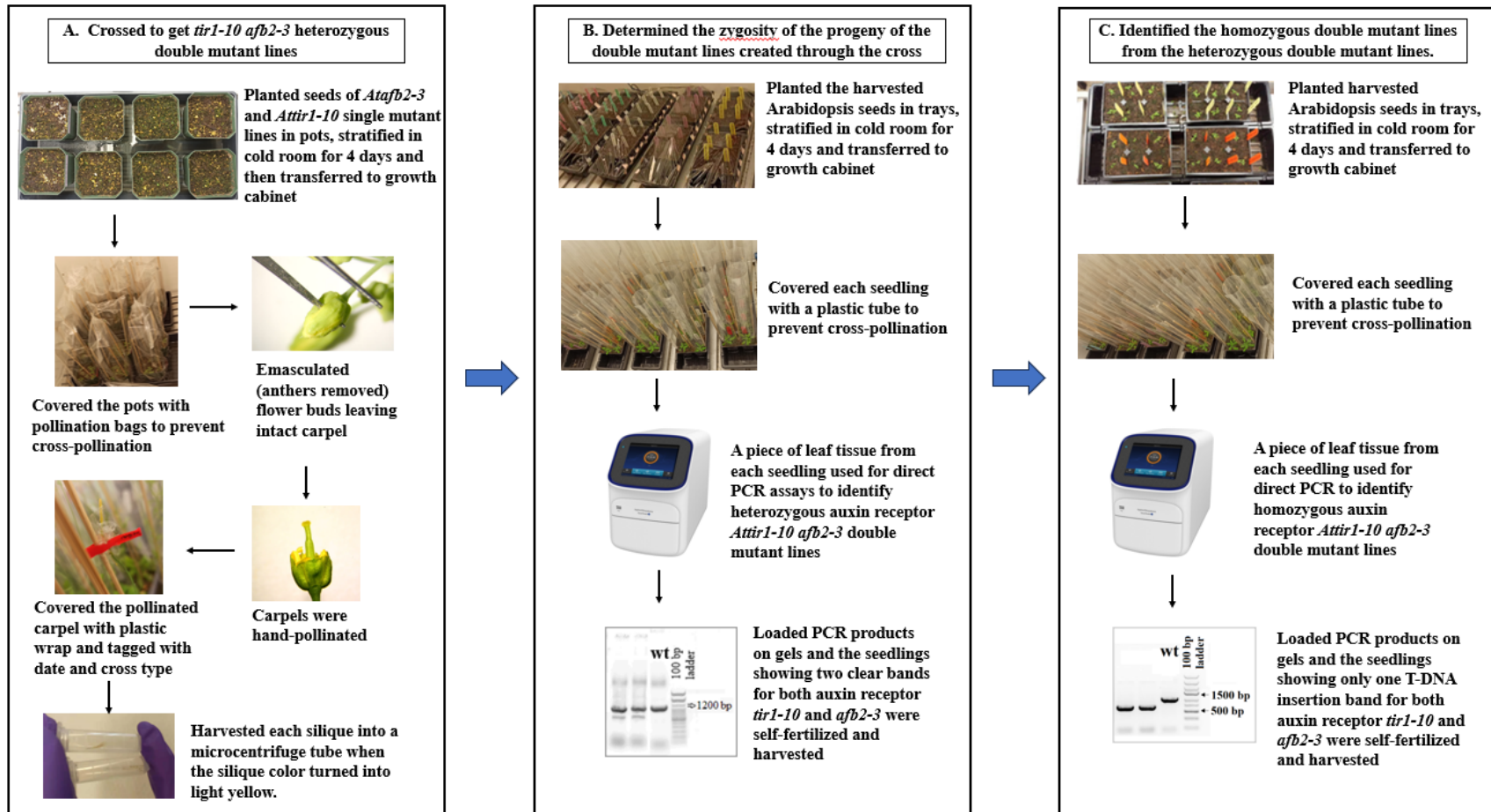
LSD post-hoc test (p-values)	WT-Control	WT-2,4-D	<i>tir1afb2</i> -Control	<i>tir1afb2</i> -2,4-D	<i>PsAFB6/+ 4-8 tir1afb2</i> -Control	<i>PsAFB6/+ 4-8 tir1afb2</i> -2,4-D	<i>PsAFB6/+ 3-3 tir1afb2</i> -Control	<i>PsAFB6/+ 3-3 tir1afb2</i> -2,4-D
WT-Control	1							
WT-2,4-D	<0.0001	1						
<i>tir1afb2</i> -Control	<0.0001	<0.0001	1					
<i>tir1afb2</i> -2,4-D	<0.0001	<0.0001	0.6710	1				
<i>PsAFB6/+ 4-8 tir1afb2</i> -Control	<0.0001	<0.0001	0.5127	0.7581	1			
<i>PsAFB6/+ 4-8 tir1afb2</i> -2,4-D	<0.0001	<0.0001	0.8070	0.9184	0.7223	1		
<i>PsAFB6/+ 3-3 tir1afb2</i> -Control	<0.0001	<0.0001	0.4685	0.7052	0.9514	0.6772	1	
<i>PsAFB6/+ 3-3 tir1afb2</i> -2,4-D	<0.0001	<0.0001	0.4517	0.6848	0.9323	0.6597	0.9808	1

Appendix Table A4. The probability, degrees of freedom and F values on the lateral root density for treatments (Control vs. 2,4-D), lines (*tir1afb245* vs. *PsAFB6/+ 1-6 tir1afb245* vs. *PsAFB6/+ 3-2 tir1afb245* vs. *PsAFB6/+ 5-9 tir1afb245*) and treatments x lines interaction in two-way ANOVA analysis followed by mean separation using LSD post-hoc test performed on data presented in Figure 2.3C.

	Treatments		Lines		Treatments x Lines	
	F value	Pr(>F)	F value	Pr(>F)	F value	Pr(>F)
Lateral root density	1.2960	0.2560	0.2600	0.8540	0.8560	0.4640
Degrees of freedom	1		3		3	

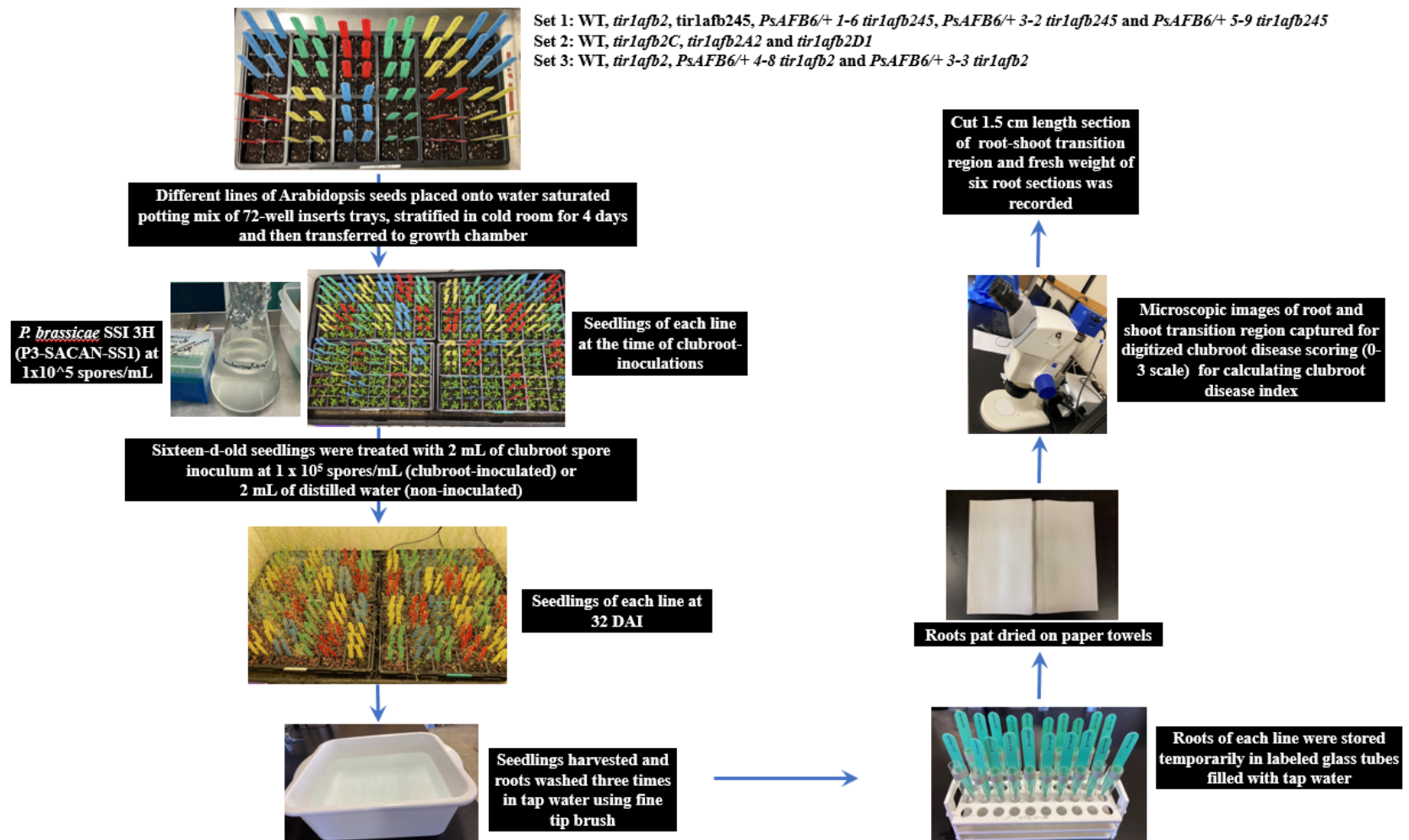
LSD post-hoc test (p-values)	<i>tir1afb245</i> -Control	<i>tir1afb245</i> -2,4-D	<i>PsAFB6/+ 1-6 tir1afb245</i> -Control	<i>PsAFB6/+ 1-6 tir1afb245</i> -2,4-D	<i>PsAFB6/+ 3-2 tir1afb245</i> -Control	<i>PsAFB6/+ 3-2 tir1afb245</i> -2,4-D	<i>PsAFB6/+ 5-9 tir1afb245</i> -Control	<i>PsAFB6/+ 5-9 tir1afb245</i> -2,4-D
<i>tir1afb245</i> -Control	1							
<i>tir1afb245</i> -2,4-D	0.1609	1						
<i>PsAFB6/+ 1-6 tir1afb245</i> -Control	0.5012	0.5579	1					
<i>PsAFB6/+ 1-6 tir1afb245</i> -2,4-D	0.6971	0.3896	0.7985	1				
<i>PsAFB6/+ 3-2 tir1afb245</i> -Control	0.7527	0.3450	0.7433	0.9440	1			
<i>PsAFB6/+ 3-2 tir1afb245</i> -2,4-D	0.0853	0.6389	0.3356	0.2258	0.1972	1		
<i>PsAFB6/+ 5-9 tir1afb245</i> -Control	0.5818	0.4789	0.9111	0.8852	0.8290	0.2827	1	
<i>PsAFB6/+ 5-9 tir1afb245</i> -2,4-D	0.8895	0.2708	0.6308	0.8215	0.8750	0.1528	0.7111	1

APPENDIX B



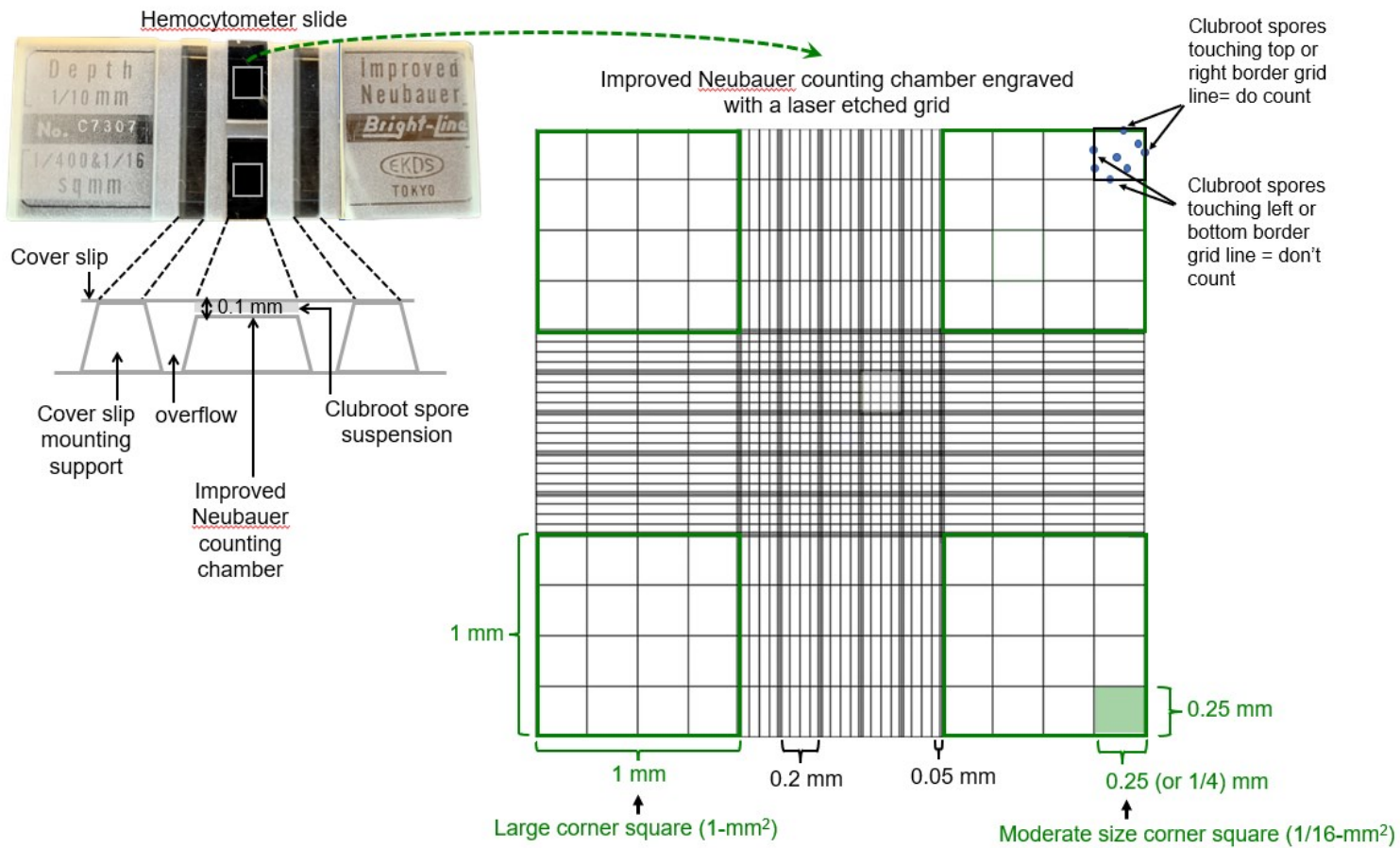
Appendix Figure B1. The procedure of creation of auxin receptor *tir1afb2A2* and *tir1afb2D1* double mutant lines. First, the *Atafb2-3* and *Attir1-10* single mutants were crossed to obtain *tir1afb2* heterozygous double mutant lines (A). Seeds of background

cleaned homozygous lines each of auxin receptor *Atafb2-3* and *Attir1-10* single mutants were planted in pots (10.5 x 10.5 cm) filled with Sunshine #4 mix. The pots were stratified in darkness at 4 °C for four days, followed by transfer to a growth cabinet maintained at 22 °C with a 16-h photoperiod under cool white-fluorescent light at $206 \pm 13 \mu\text{E m}^2 \text{s}^{-2}$. The pots of paternal and maternal plants were kept at a distance of 35 cm within a growth cabinet. After one week, seedlings were thinned to 5-8 plants per pot and each pot was covered with a pollination bag (20.5 x 61cm) with the support of skewer sticks to prevent cross-pollination. At around 24 days, the floral buds of the maternal plants were emasculated (anthers removed) using forceps, the stigmas of the carpels were hand-pollinated with pollen from paternal plants and pollinated carpels were covered with a piece of plastic wrap to retain moisture and prevent cross-pollination. The plastic wrap was removed at 3-4 days post-pollination and the siliques were harvested at maturity when they changed color to yellow/brown. Each silique was collected in a separate microcentrifuge tube, and placed in a sealed container with Drierite desiccant to dry for one week at room temperature and then stored at 4 °C. Secondly, the zygoty of the double mutant *Attir1-10 afb2-3* line was determined (**B**). Seeds were placed onto water saturated Sunshine #4 mix filled in 36 cell inserts trays (insert size 2 1/8 in. x 2 3/8 in. x 2 1/4 in. deep). After stratification in dark at 4 °C for four days, the trays were transferred to the growth cabinet maintained under the same conditions mentioned above. After 2 weeks of plant growth, a piece of rosette leaf tissue from each seedling was used for perform direct PCR assays with *Atafb2-3* and *Attir1-10* SALK T-DNA specific primers (LBb1.3, LP and RP) followed by agarose gel electrophoresis. Identified heterozygous double mutant lines were self-fertilized, harvested and stored in the cold room maintained at 4 °C. Thirdly, the homozygous double mutant lines were identified (**C**). Seeds of the verified heterozygous double mutant lines were planted in 36 well-insert trays, stratified and transferred to the growth cabinet maintained under the same conditions mentioned above. After 2 weeks of plant growth, a piece of rosette leaf tissue from each seedling was used for performing direct PCR assays and agarose gel electrophoresis. Seedlings showing homozygosity for both mutations (*tir1-10 afb2-3*) produced a clear single band for the T-DNA insertion using direct PCR assays. A cross involving *tir1-10C1* as the female parent and *afb2A2* and *afb2D1* as the male parents successfully produced two homozygous auxin receptor double mutant lines *tir1afb2A2* and *tir1afb2D1*.



Appendix Figure B2. The procedure of clubroot inoculation assays. Arabidopsis seeds of different lines within each set were randomly planted in 72-well insert trays, stratified in the cold room for 4 days and transferred to a growth chamber maintained at 22 °C with a 16 h photoperiod under cool white-fluorescent light at $206 \pm 13 \mu\text{E m}^2 \text{s}^{-2}$. After 16 days of growth in the growth chamber,

plants were inoculated by pipetting (using filtered tips) 2 mL of the clubroot spore suspension (1×10^5 spores/mL) into the peat-based medium around the seedling of each cell. Non-inoculated control seedlings received 2 mL of Milli-Q water. At 32 DAI, plants were harvested and roots were washed three times in tap water and three times in Milli-Q water using a fine-tip brush. Then the roots were stored temporarily in labeled glass tubes filled with tap water. Roots were pat-dried using paper towels and microscope images of the root-shoot transition region were captured. Clubroot disease severity index (DI) was calculated using the scoring of the clubroot disease symptom development assigned to the digitized images of root-shoot transition region of plants. Subsequently, 1.5 cm-long section of the root-shoot transition region was cut and fresh weight of six root sections was recorded. The average fresh weight of root-shoot transition region of *Arabidopsis* for clubroot-inoculated and non-inoculated control seedlings for each line was calculated.



Appendix Figure B3. The schematic representation of the improved Neubauer counting chamber within the hemocytometer for estimating the clubroot resting spore concentration. A hemocytometer is a rectangular glass slide measuring 30 mm in width, 70 mm in length, and 4 mm in thickness. It features a central H-shaped indentation that separates the slide into two counting chambers. Each chamber contains a laser-etched square grid measuring 3 mm x 3 mm, divided into 9 large squares, each with a 1 mm² area. The large corner squares, outlined in a thick green border, are further divided into 16 moderate-size squares, shaded in green,

with a 0.0625 mm² or 1/16 mm² area. The four corner squares from both chambers are used for estimating the clubroot resting spore concentration. Within each moderate-size square, spores are counted, and the counts within one large corner square were summed. When viewed under a microscope at 40x magnification, clubroot resting spores appear as spherical moderate-sized structures with a distinct hyaline thick cell wall. Spores touching the top and right grid borders were included in the count, while those touching the bottom and left grid borders were excluded. The average of clubroot spore counts across the 8 large corner squares was calculated. Finally, the average number of spores per large corner square was multiplied by a factor of 10⁴ to obtain the average number of clubroot spores per mL of suspension.

```

1 ATGGAACCAC AAACCATGAA TCCCAGTTCA GTCTTTCCAG ATGAAGTGCT
51 GGAGAGAATT CTCAGCATGG TGAAGTCACG CAAAGACAAG AGTTCGGTTT
101 CATTGGTTTG CAAAGACTGG TTCGACGCTG AAAGATGGTC GAGAAAAGAAT
151 GTGTTCATAG GTAACGTGTA TTCCGTTACA CCAGAGATCT TGACTIONAAG
201 ATTTCCGAAT GTTCGAAGTG TTACATTGAA AGGGAAGCCA CGTTTCTCTG
251 ATTTCAACTT GGTTCTGCT AATTGGGGTG CTGATATTCA TCCATGGCTT
301 GTTGTTTTTCG CTGAAAAGTA CCCTTTTCTT GAAGAGTTAA GGCTTAAGAG
351 AATGGTTGTT ACTGATGAGA GTTTAGAGTT TCTGGCTTTT TCGTTTCCGA
401 ATTTTAAAGC TCTTTCTCTT TTGAGCTGTG ATGGATTTAG CACTGATGGT
451 TTAGCTGCTG TTGCTACTAA TTGCAAGAAC TTAACAGAGC TTGACATACA
501 AGAGAATGGT ATCGAAGACA AAAGCGGTAA CTGGTTGAGT TGCTTCCCAG
551 AAAGCTTTAC ATCATTGGAA GTGTTGAAC T TGCCAACCT AACCAATGAA
601 GTAAACATCG ACGCGCTAGA GAAACTTGTT GGTAGGTGCA AATCATTGAA
651 GACTTTGAAG GTTAACAAAA GCGTAACGCT GGAACAGTTG AAAAAACTTC
701 TTGTTGCGCG CCCTCAGTTA TGTGAGCTTG GCAGTGGCTC ATTTTTCGAA
751 GAGCTGACAT CTCAGCAGTA TGCAGAGCTC GAAACCGCGT TCAAAAATTG
801 TAAAAGCCTT CACACCCTGT CTGGTTTATG GGTGGCTTCA GCGCGATATC
851 TTCAAGTTCT ATACCCTGCG TGCGCGAATC TGACTIONTTTT GAATTTTAGC
901 TATGCTCCTC TTGACAGTGA AGATCTTACC AAGATTCTTG TTCACTGTCC
951 TAATCTTCGA CGTCTTTGGG TTGTTGACAC CGTTGAAGAC AAGGGACTTG
1001 AAGCGGTTGG ATCGAACTGT CCATTGCTTG AGGAACTGCG TGTTTTTCCCT
1051 GCAGATCCGT TTGACGAGGA AGCTGAAGGC GGGGTGACTG AATCGGGGTT
1101 TGTTGCTGTC TCTGAAGGAT GCCGGAAGCT TCACTATGTT CTCTACTTTT
1151 GTCGTCAAAT GACCAATGCT GCTGTCGCTA CCGTAGTCCA AAACTGCC
1201 GACTTTACTC ATTTCCGCCT CTGCATAATG AACCCTGGCC AGCAAGATTA
1251 CCTGACGGAC GAACCTATGG ACGAGGCCTT CGGAGAAGTT GTTAAGAACT
1301 GCACTAAACT TCAGAGGCTC GCTGTATCAG GTTATCTAAC GGACCTCACA
1351 TTCGAGTATA TAGGAAAGTA TGCCAAAAAC TTGAAAACGC TTTTCGGTGGC
1401 TTTTGCAGGA AGCAGTGATT GGGGAATGGA GTGTGTACTG GTCGGATGTC
1451 CGAAACTGAG AAAACTCGAG ATAAGAGACA GTCCATTCGG AAATGCAGCG
1501 CTTTTGGCAG GTTTGGAGAA GTACGAGTCG ATGAGGTCAC TTTGGATGTC
1551 GTCCTGCAGA CTGACGATGA ATGGATGTAG ATTTTTGGCA GGAGAAAAGC
1601 CGAGGTTGAA TGTCGAAGTA ATGCAGGAAG AAGGAGCGA TGATAGTCGG
1651 GCCGAAAAAC TTTATGTTTA TCGATCTGTT GCCGGGCCAA GAAGGGATGC
1701 ACCTCCTTTT GTTCTCACTC TCTGA

```

Appendix Figure B4. The complete coding sequence of the auxin receptor *PsAFB6* (KY829119) from *P. sativum* L. cv. I3 (Alaska-type). Forward and reverse qPCR primers and probe binding sites are colored and underlined in green, red, and orange respectively.

```

1 ATGTCCCCGG AAGAGGAGCT ACAGAGCAAT GTATCGGTGG CTAGTTCTTC
51 ACCTACTAGC AATTGCATCT CCAGGAACAC TCTAGGAGGA CTTAAAGAGC
101 ATAACACTTT GGGTCTCTCT GATTGTTCTT CTGTTGGAAG CTCTACTCTC
151 TCTCCCCTTG CTGAAGATGA CAAAGCTACT ATCAGCCTCA AGGCTACGGA
201 GCTGACACTT GGTCTTCCTG GATCACAATC TCCTGCGAGA GACACAGAGC
251 TTAACCTTTT GAGCCCAGCA AAGCTAGATG AGAAGCCATT CTTTCCTTTG
301 CTTCCCTTCTA AAGATGAGAT ATGCTCCTCC TCGCAAAAAGA ACAATGCATC
351 GGGAAACAAA AGAGGCTTTT CTGACACAAT GGATCAGTTT GCTGAAGCTA
401 AAAGTTCAGT GTATACTGAG AAAAAGTGGT TGTTCCCTGA AGCAGCAGCC
451 ACCCAGTCTG TAACAAAGAA AGATGTGCCA CAAAACATAC CCAAAGGACA
501 GTCTAGCACT ACAAACAATA GCTCTAGTCC ACCTGCAGCC AAGGCACAAA
551 TTGTCGGTTG GCCTCCAGTG AGATCCTACA GGAAGAACAC ATTGGCCACT
601 ACTTGTAAGA ACAGTGACGA AGTTGATGGG AGGCCAGGTT CTGGGGCTCT
651 CTTCGTGAAG GTCAGTATG ATGGTGCTCC TTATCTGAGG AAAGTTGACC
701 TGAGGAGCTA CACTAACTAC GGGGAGCTTT CTTCAGCCTT GGAGAAAATG
751 TTCACCACTT TCACTCTTGG TCAATGTGGA TCTAATGGAG CTGCTGGGAA
801 GGATATGCTT AGTGAGACCA AGCTCAAGGA TCTTTTGAAT GGAAAAGACT
851 ATGTGCTCAC TTATGAGGAT AAGGATGGTG ACTGGATGCT TGTTGGAGAT
901 GTTCCGTGGG AGATGTTTAT TGATGTCTGC AAGAAGCTGA AGATAATGAA
951 AGGGTGTGAT GCTATTGGGT TAGCTGCAGC TCCGAGAGCA ATGGAGAAAT
1001 CGAAGATGAG AGCTTAA

```

Appendix Figure B5. The complete coding sequence of gene encoding auxin/indole-3-acetic acid 9 protein (*AtAux/IAA9*; At5g65670) retrieved from *Arabidopsis thaliana* genome annotation version TAIR10 (<https://www.arabidopsis.org>). Forward and reverse qPCR primers and probe binding sites are colored and underlined in green, red, and orange respectively.

```

1 ATGATTAATT TTGAGGCCAC GGAGCTGAGA TTAGGGCTAC CGGGTGGGAA
51 TCACGGAGGA GAAATGGCTG GAAAAAATAA TGGTAAAAGA GGATTTTCTG
101 AGACTGTTGA TCTCAAACCTG AATCTTTTCAT CGACGGCTAT GGATTCAGTT
151 TCCAAAGTCG ATTTAGAGAA TATGAAGGAG AAGGTCGTAA AACCACCAGC
201 CAAGGCACAA GTTGTGGGAT GGCCACCGGT ACGATCTTTC CGCAAGAACG
251 TCATGTCCGG CCAAAAACCG ACCACCGGAG ATGCCACCGA AGGAAACGAT
301 AAGACTTCTG GCAGCAGTGG AGCCACCTCA TCCGCCTCCG CATGTGCCAC
351 CGTGGCTTAT GTGAAGGTTA GCATGGACGG TGCACCGTAC CTACGGAAAA
401 TTGACTTGAA ACTCTACAAA ACTTACCAAG ATCTCTCCAA CGCCTTAAGC
451 AAAATGTTTA GCTCTTTTAC CATAGGCAAC TATGGACCAC AAGGAATGAA
501 AGATTTTCATG AATGAGAGTA AATTGATCGA TCTTCTAAAC GGATCAGATT
551 ATGTTCCAAC ATATGAAGAT AAAGATGGCG ACTGGATGCT TGTAGGAGAC
601 GTACCGTGGG AGATGTTTGT TGATTCATGC AAACGTATAC GAATAATGAA
651 GGGATCAGAA GCAATCGGAC TTGCTCCAAG GGCATTAGAA AAGTGCAAGA
701 ACAGAAGTTG A

```

Appendix Figure B6. The complete coding sequence of gene encoding auxin/indole-3-acetic acid 16 protein (*AtAuxIAA16*; At3g04730) retrieved from *Arabidopsis thaliana* genome annotation version TAIR10 (<https://www.arabidopsis.org/>). Forward and reverse qPCR primers and probe binding sites are colored and underlined in green, red, and orange respectively.

```

1 ATGGAGAAGG AAGGACTCGG GCTTGAGATA ACGGAGCTGA GATTGGGGCT
51 TCCGGGGAGA GATGTGGCAG AGAAGATGAT GAAGAAGAGA GCTTTCACGG
101 AGATGAATAT GACGTCGTCG GGTAGTAATA GTGATCAATG TGAAAGCGGC
151 GTCGTTTTCAT CTGGTGGTGA CGCTGAGAAG GTTAATGATT CGCCGGCGGC
201 GAAAAGCCAG GTGGTGGGGT GGCCACCGGT TTGTTCTTAC CGGAAGAAAA
251 ACAGCTGTAA GGAAGCTTCG ACCACGAAAAG TGGGGTTAGG GTATGTGAAA
301 GTGAGCATGG ATGGTGTGCC TTATTTGAGG AAGATGGATC TTGGTTCGAG
351 CCAAGGCTAT GATGATCTAG CTTTGCTCT TGATAAGCTC TTCGGTTTCC
401 GTGGCATCGG TGTGGCCTTG AAAGATGGTG ACAACTGCGA ATACGTTACC
451 ATATACGAAG ACAAAGATGG AGACTGGATG CTCGCCGGTG ATGTACCTTG
501 GGGGATGTTT CTAGAGTCAT GCAAGAGGTT GAGAATAATG AAAAGATCGG
551 ATGCTACCGG GTTTGGGCTG CAGCCTAGAG GAGTAGACGA GTGA

```

Appendix Figure B7. The complete coding sequence of gene encoding auxin/indole-3-acetic acid 19 protein (*AtAux/IAA19*; At3g15540) retrieved from *Arabidopsis thaliana* genome annotation version TAIR10 (<https://www.arabidopsis.org/>). Forward and reverse qPCR primers and probe binding sites are colored and underlined in green, red, and orange respectively.

1 TAATGTCTCT CTCTCCACGC ACAAAGGTC TAAAAGCCAC ACCACACACA
51 TCAGTCACCA GACGTAGCAG AGAGCCTCAC TGTTGCAGAG AGCACTCAGT
101 ACTGTTCTGT TTCTCTGATA CCTCTCTCTC TCCTCTCTCT TTTAACATTG
151 TCCAAATTAA AAATCTAAAC TTTTTTCTA GTTTTTTTTT TTTCTTTAAT
201 AGAAAAGTTT TTTTTCTCCA CGGCTTAAAG ACTCACTCAT CACTGTGCTA
251 CTA CTACTCTCTC TTCTTTTGGC TGAGAGGGTA AAAGTCATGA AGAAACTCCT
301 CTGAGTTTTT TTTCTTTCTT TCTTATAATA AAGCTCTTAT CTTTATCTCT
351 GTTTCTCTCT CTTTAATGGG TGGTTTAATC GATCTGAACG TGATGGAGAC
401 GGAGGAAGAC GAAACGCAAA CGCAAACACC GTCTTCAGCT TCTGGGTCTG
451 TCTCTCCTAC TTCGTCTTCT TCAGCTTCTG TGTCTGTGGT GTCTTCGAAT
501 TCTGCTGGTG GAGGGGTTTG TTTGGAGCTG TGGCATGCTT GTGCTGGACC
551 CCTTATCTCT CTACCAAAAA GAGGAAGCCT TGTGTTGTAT TTCCCTCAGG
601 GACATTTGGA ACAAGCCCCC GATTTCTCCG CCGCGATTTA CGGGCTCCCT
651 CCTCACGTGT TCTGTCGTAT TCTCGATGTT AAGCTTCACG CAGAGACGAC
701 TACAGATGAA GTTTATGCTC AAGTCTCTCT TCTTCCTGAG TCAGAGGACA
751 TTGAGAGGAA GGTGCGTGAA GGAATTATAG ATGTTGATGG TGGAGAGGAA
801 GATTATGAAG TGCTTAAGAG GTCTAATACT CCTCACATGT TTTGCAAAAC
851 CCTTACTGCT TCTGATACAA GCACCCATGG TGGTTTCTCT GTTCCTCGCC
901 GAGCTGCTGA GGATTGCTTC CCTCCTCTGG ACTATAGCCA GCCCCGGCCT
951 TCTCAGGAGC TTCTTGCTAG GGATCTTCAT GGCCTGGAGT GGCGATTTCTG
1001 CCACATTTAT CGAGGGCAAC CTAGGAGGCA TTTGCTCACT ACCGGGTGGA
1051 GTGCGTTTGT GAACAAGAAG AAGCTTGTCT CTGGTGATGC TGTGCTTTTC
1101 CTTAGAGGAG ATGATGGCAA ACTGCGACTG GGAGTTAGAA GAGCTTCTCA
1151 AATCGAAGGC ACCGCTGCTC TCTCGGCTCA ATATAATCAG AATATGAACC
1201 ACAACAATTT CTCTGAAGTA GCTCATGCCA TATCGACCCA TAGCGTTTTTC
1251 AGCATTTCCCT ACAACCCCAA GGCAAGCTGG TCAAACCTCA TAATCCCTGC
1301 ACCAAAGTTC TTGAAGGTTG TTGACTATCC CTTTTGCATT GGGATGAGAT
1351 TTAAAGCGAG GGTGAATCT GAAGATGCAT CTGAGAGAAG ATCCCTGGG
1401 ATTATAAGTG GTATCAGCGA CTTGGATCCA ATCAGGTGGC CTGGTTCAAA
1451 ATGGAGATGC CTTTTGGTAA GGTGGGACGA CATTGTGGCA AATGGGCATC
1501 AACAGCGTGT CTCGCCATGG GAGATCGAAC CATCTGGTTC CATCTCCAAT
1551 TCAGGCAGCT TCGTAACAAC TGGTCCCAAG **AGAAGCAGGA** **TTGGCTTTTC**
1601 **CTCAGGAAAG** **CCTGATATCC** **CTGTCTCTGA** **GGGGATTTCG** **GCCACAGACT**
1651 **TTGAGGAATC** **ATTGAGATTC** **CAGAGGGTCT** **TGCAAGGTCA** AGAAATTTTT
1701 CCGGGTTTTA TCAACACTTG TTCGGATGGT GGAGCCGGTG CCAGGAGAGG
1751 CCGCTTCAAA GGAACAGAAT TTGGTGACTC TTATGGTTTC CATAAGGTCT
1801 TGCAAGGTCA AGAAACAGTT CCCGCTACT CAATAACCGA TCATCGGCAG
1851 CAGCACGGGT TGAGCCAGAG GAACATTTGG TGTGGGCCGT TCCAGAACTT
1901 TAGTACACGT ATCCTCCCC CATCTGTATC ATCATCACCC TCTTCCGTCT
1951 TGCTTACCAA CTCGAACAGT CCTAACGGAC GTCTGGAAGA CCATCACGGA
2001 GGTTCAGGCA GATGCAGGCT GTTTGGTTTC CCATTAACCG ACGAAACCAC
2051 AGCAGTTGCA TCTGCGACGG CTGTCCCTG CGTTGAAGGG AATTCCATGA
2101 AAGGTGCGTC AGCTGTTCAA AGCAATCATC ATCATTCGCA AGGAAGGGAC
2151 ATCTATGCAA TGAGAGACAT GTTGCTAGAC ATTGCTCTCT AGAAGGGTTC
2201 TTTGGTTTCT GTGTTTTATT TGCTTGTTGG TTAAGTAAAG TTCTTATTTT
2251 AGTTGATGAT GACTTGCTGC TAACTTTTGG AATGTCACAA GTTGTGACTT

2301 ATGAGAGACT TGTAACCTG GTTCAAGAAT GTTCTGTGTT AGGTTCAATT
2351 TAAAAAGTGT TTGCATCAAT TCCGGTTATT TGTGTTTGTA CCAACCGGTT
2401 CAATTCGTAA TTCTAATTTA ACCGGAAGGA

Appendix Figure B8. The complete coding sequence of gene encoding auxin response factor 3 (*AtARF3*; At2g33860.1) retrieved from *Arabidopsis thaliana* genome annotation version TAIR10 (<https://www.arabidopsis.org>). Forward and reverse qPCR primers and probe binding sites are colored and underlined in green, red, and orange respectively.

1 ATGATGGCTT CATTGTCTTG TGTGGAAGAC AAGATGAAAA CAAGTTGTTT
51 GGTAAATGGT GGAGGAACTA TAACAACAAC AACATCTCAA TCTACCTTGC
101 TTGAAGAGAT GAAGCTGTTG AAAGACCAGT CAGGTACAAG AAAGCCGGTA
151 ATAAACTCGG AGCTATGGCA CGCTTGTGCA GGCCCTTTGG TGTGTCTCCC
201 TCAAGTTGGG AGCTTAGTGT ATTACTTCTC ACAAGGTCAT AGCGAGCAGG
251 TTGCTGTTTC AACCAGAAGA TCAGCAACAA CACAAGTTCC TAATTATCCG
301 AACCTTCCAT CTCAGTTGAT GTGTCAAGTC CATAATGTTA CTCTTCATGC
351 TGACAAAGAC AGTGACGAAA TCTATGCTCA GATGAGTCTT CAACCTGTTC
401 ACTCTGAGAG AGATGTGTTC CCTGTACCAG ACTTTGGAAT GCTGAGAGGA
451 AGTAAGCACC CGACTGAGTT TTTCTGCAAA ACACTTACTG CAAGTGACAC
501 AAGCACACAT GGAGGTTTCT CAGTGCCACG TAGAGCTGCA GAGAAGCTAT
551 TTCCACCATT GGACTACTCA GCACAGCCGC CAACGCAAGA GCTTGTAGTT
601 CGAGATCTTC ATGAGAATAC TTGGACATTT CGCCATATCT ACCGAGGGCA
651 ACCAAAGAGA CATCTCCTAA CTACAGGATG GAGTTTGTTC GTTGATCGA
701 AGAGATTGAG AGCTGGGGAT TCTGTTTTGT TCATCAGGGA TGAGAAGTCA
751 CAACTTATGG TCGGTGTTAG GCGTGCCAAT CGCCAACAAA CAGCACTTCC
801 TTCATCAGTT CTCTCAGCGG ATAGTATGCA CATCGGTGTT CTTGCTGCTG
851 CTGCTCACGC AACCGCCAAC CGTACTCCTT TTTTGATATT CTATAATCCA
901 AGAGCTTGTC CAGCAGAGTT CGTGATCCCT CTAGCTAAGT ACCGTAAGGC
951 GATATGCGGG TCTCAGCTCT CAGTTGGTAT GAGATTTGGA ATGATGTTTG
1001 AAACTGAAGA TTCCGGGAAA CGAAGGTACA TGGGAACTAT TGTTGGAATC
1051 AGCGATTTGG ATCCGTTGAG ATGGCCTGGT TCTAAGTGGC GTAACCTTCA
1101 GGTAGAATGG GATGAGCCTG GATGTAATGA TAAACCTACT CGGGTCAGTC
1151 CATGGGATAT CGAAACACCT GAAAGTCTCT TCATTTTTCC TTCTCTGACC
1201 TCAGGACTCA AACGTCAGCT CCATCCATCT TACTTTGCTG GTGAAACTGA
1251 ATGGGGTAGC TTGATAAAAC GGCCACTTAT ACGTGTTCCT GATTCCGCGA
1301 ATGGGATTAT GCCATATGCA TCTTTCCCTA GTATGGCTTC GGAGCAGCTT
1351 ATGAAAATGA TGATGAGGCC TCACAACAAC CAAAATGTAC CATCTTTCAT
1401 GTCTGAGATG CAGCAGAATA TTGTAATGGG GAATGGAGGT TTGCTAGGAG
1451 ATATGAAGAT GCAGCAACCC CTGATGATGA ACCAGAAATC TGAGATGGTG
1501 CAGCCACAAA ACAAGCTAAC AGTGAACCCA TCTGCTTCTA ATACGAGTGG
1551 CCAAGAACAG AATCTTTCAC AGAGTATGAG TGCTCCTGCT AAACCTGAGA
1601 ACTCTACACT CTCTGGTTGC AGCTCTGGTA GAGTCCAACA TGGACTTGAG
1651 CAGTCAATGG AACAGGCAAG CCAGGTTACT ACATCCACAG TGTGTAATGA
1701 GGAAAAGGTT AATCAGCTAC TTCAGAAAAC GGGTGCTTCG TCGCCTGTAC
1751 AAGCTGATCA ATGTCTTGAC ATTACTCATC AGATTTACCA ACCACAGTCT
1801 GATCCAATAA ATGGATTCTC TTTCTTGAA ACTGATGAGC TGACATCACA
1851 AGTCTCTTCC TTCCAGTCTC TTGCCGGATC ATACAAGCAA CCATTCATTC
1901 TATCCTCCCA GGATTCTTCA GCTGTTGTGT TACCGGATTC CACAAACTCA
1951 CCGCTGTTTC ATGATGTGTG GGACACTCAG TTGAACGGTC TCAAGTTTGA
2001 CCAGTTCAGT CCCTTGATGC AGCAGGACCT TTATGCTAGT CAGAATATCT
2051 GTATGAGTAA TAGCACAACC AGTAACATTC TAGATCCTCC ACTCTCAAAC
2101 ACAGTCCTTG ATGACTTCTG TGCCATCAAA GACACTGATT TCCAGAACCA
2151 CCCTTCTGGT TGTTTGGTTG GAAACAACAA CACTAGCTTT GCTCAAGATG
2201 TCCAGTCGCA GATCACATCA GCTAGCTTTG CAGACTCACA GGCTTCTCT
2251 CGCCAAGATT TTCCAGATAA TTCTGGAGGC ACTGGTACAT CTTCAAGCAA
2301 TGTTGATTTT GATGATTGTA GTCTGCGGCA AAATAGTAAA GGCTCATCAT
2351 GGCAGAAAAT TGCGACACCC CGCGTCCGAA CCTACACTAA GGTTCAAAAA

2401 ACCGGGTCAG TCGGGAGATC AATTGATGTC ACAAGCTTTA AAGACTACGA
 2451 GGAGCTAAAA TCTGCTATCG AATGCATGTT TGGATTGGAA GGACTACTAA
 2501 CTCACCCACA AAGCTCGGGT TGGAAGCTTG TATATGTTGA TTATGAGAGT
 2551 GATGTTCTGC TTGTAGGAGA TGATCCATGG GAAGAGTTTG TGGGATGCGT
 2601 AAGGTGCATA AGGATATTGT CGCCAACCTGA GGTCCAGCAG ATGAGTGAAG
 2651 AAGGGATGAA GCTTTTGAAC AGCGCAGGCA TTAACGATCT TAAGACTTCT
 2701 GTTTCATAA

Appendix Figure B9. The complete coding sequence of gene encoding auxin response factor 5 (*AtARF5*; At1g19850) retrieved from *Arabidopsis thaliana* genome annotation version TAIR10 (<https://www.arabidopsis.org/>). Forward and reverse qPCR primers and probe binding sites are colored and underlined in green, red, and orange respectively.

1 ATGAAAGCTC CATCAAATGG ATTTCTTCCA AGTTCCAACG AAGGAGAGAA
51 GAAGCCAATC AATTCTCAAC TATGGCACGC TTGTGCAGGG CCTTTAGTTT
101 CATTACCTCC TGTGGGAAGT CTTGTGGTTT ACTTCCCTCA AGGACACAGC
151 GAGCAAGTTG CAGCATCGAT GCAGAAGCAA ACAGATTTTA TACCAAATTA
201 CCCAAATCTT CTTTCTAAGC TGATTTGCTT GCTTCACAGT GTTACATTAC
251 ATGCTGATAC CGAAACAGAT GAAGTCTATG CACAAATGAC TCTTCAACCT
301 GTGAATAAGT ATGATAGAGA AGCATTGCTA GCTTCTGATA TGGGCTTGAA
351 GCTAAACAGA CAACCTACTG AGTTTTTTTGTG CAAGACTCTT ACTGCAAGTG
401 ACACAAGCAC TCATGGTGGG TTCTCTGTAC CGCGTCGTGC AGCTGAGAAA
451 ATATTCCCTC CTCTTGATTT CTCGATGCAA CCGCCTGCGC AAGAGATTGT
501 AGCTAAAGAT TTACATGATA CTACATGGAC TTTCAGACAT ATCTATCGAG
551 GCCAACCCAAA AAGACACTTG CTTACCACAG GTTGGAGCGT TTTTGTTAGC
601 ACAAAGAGAC TATTTGCGGG TGATTCAGTT TTGTTTGTAAGAGATGAGAA
651 ATCACAGCTG ATGTTGGGTA TAAGACGTGC AAATAGACAA ACTCCGACTC
701 TTTCCCTCATC GGTTCATATCC AGCGACAGTA TGCACATTGG GATACTTGCA
751 GCTGCAGCTC ATGCTAATGC CAATAGTAGC CCTTTTACCA TCTTCTTCAA
801 TCCAAGGGCA AGTCCTTCAG AGTTTGTAGT TCCTTTAGCC AAATACAACA
851 AAGCCTTATA CGCTCAAGTA TCTCTAGGAA TGAGATTCCG GATGATGTTT
901 GAGACTGAGG ATTGTGGGGT TCGTAGATAT ATGGGTACAG TCACAGGTAT
951 TAGTGATCTT GACCCTGTAA GATGAAAAGG CTCACAATGG CGTAATCTTC
1001 AGGTAGGATG GGATGAATCA ACAGCTGGAG ATAGGCCAAG CCGAGTATCC
1051 ATATGGGAAA TCGAACCCGT CATAACTCCT TTTTACATAT GTCCTCCTCC
1101 ATTTTTTCAGA CCTAAGTACC CGAGGCAACC CGGGATGCCA GATGATGAGT
1151 TAGACATGGA AAATGCTTTC AAAAGAGCAA TGCCTTGGAT GGGAGAAGAC
1201 TTTGGGATGA AGGACGCACA GAGTTCGATG TTCCCTGGTT TAAGTCTAGT
1251 TCAATGGATG AGTATGCAGC AAAACAATCC ATTGTCAGGT TCTGCTACTC
1301 CTCAGCTCCC GTCCGCGCTC TCATCTTTTA ACCTACCAA CAATTTTGCT
1351 TCCAACGACC CTTCCAAGCT GTTGAACTTC CAATCCCCAA ACCTCTCTTC
1401 CGCAAATTCC CAATTCAACA AACCGAACAC GGTTAACCAT ATCAGCCAAC
1451 AGATGCAAGC ACAACCAGCC ATGGTGAAAT CTCACAACA ACAACAACA
1501 CAACAACAAC AACACCAACA CCAACAACA CAACTGCAAC AACAACAACA
1551 ACTACAGATG TCACAGCAAC AGGTGCAGCA ACAAGGGATT TATAACAATG
1601 GTACGATTGC TGTGCTAAC CAAGTCTCTT GTCAAAGTCC AAACCAACCT
1651 ACTGGATTCT CTCAGTCTCA GCTTCAGCAG CAGTCAATGC TCCCTACTGG
1701 TGCTAAAATG ACACACCAGA ACATAAATTC TATGGGGAAT AAAGGCTTGT
1751 CTCAAATGAC ATCGTTTGCG CAAGAAATGC AGTTTCAGCA GCAACTGGAA
1801 ATGCATAACA GTAGCCAGTT ATTAAGAAAC CAGCAAGAAC AGTCCTCTCT
1851 CCATTCATTA CAACAAAATC TGTCCCAAAA TCCTCAGCAA CTCCAAATGC
1901 AACACAATC ATCAAAACCA AGTCCTTCAC AACAGCTTCA GTTGCAGCTA
1951 CTGCAGAAGC TACAGCAGCA GCAACAGCAG CAGTCGATTC CTCCAGTAAG
2001 CTCATCCTTA CAGCCACAAT TATCAGCGTT GCAGCAGACA CAAAGCCATC
2051 AATTGCAACA ACTTCTGTGC TCTCAAAATC AACAGCCCTT GGCACATGGT
2101 AATAACAGCT TCCCAGCTTC AACTTTTCATG CAGCCTCCAC AGATTTCAGGT
2151 GAGTCCTCAG CAGCAAGGAC AGATGAGTAA CAAAAATCTT GTAGCCGCTG
2201 GAAGATCACA TTCTGGCCAC ACAGATGGAG AAGCTCCTTC TTGTTCAACC
2251 TCACCTTCCG CCAATAACAC GGGACATGAT AATGTTTCAC CGACAAATTT
2301 CCTGAGCAGA AATCAACAGC AAGGACAAGC TGCATCTGTA TCTGCATCTG
2351 ATTCAGTCTT TGAGCGCGCA AGCAATCCGG TCCAAGAGCT TTATACAAA

2401 ACTGAGAGCC GGATCAGTCA AGGCATGATG AATATGAAGA GTGCTGGTGA
 2451 ACATTTTCAGA TTTAAAAGCG CGGTAACAGA TCAAATCGAT GTATCCACAG
 2501 CGGGAACGAC GTACTGTCCCT GATGTTGTTG GCCCTGTACA GCAGCAACAA
 2551 ACTTTCCAC TACCATCATT TGGTTTTGAT GGAGACTGCC AATCTCATCA
 2601 TCCAAGAAAC AACTTAGCTT TCCCTGGTAA TCTCGAAGCC GTAACCTCTG
 2651 ATCCACTCTA TTCTCAAAAG GACTTTCAA ACTTGGTTC CAACTATGGC
 2701 AACACACCAA GAGACATTGA GACGGAGCTG TCCAGTGCTG CAATCAGTTC
 2751 TCAGTCATTT GGTATTCCCA GCATTCCCTT TAAGCCCGGA TGTTCAAATG
 2801 AGGTTGGCGG CATCAATGAT TCAGGAATCA TGAATGGTGG AGGACTGTGG
 2851 CCCAATCAGA CTCAACGAAT GCGAACATAT ACAAAGGTT AAAAAACGAGG
 2901 GTCAGTAGGT AGATCAATAG ATGTTACCCG TTATAGCGGC TATGATGAAC
 2951 TTAGGCATGA CTTAGCGAGA ATGTTTGCA TCGAAGGACA GCTCGAAGAT
 3001 CCGCTAACCT CTGATTGGAA ACTCGTCTAC ACCGATCACG AAAACGATAT
 3051 TTTACTAGTT GGTGATGATC CTTGGGAAGA GTTTGTGAAC TGCGTGCAGA
 3101 ACATAAAGAT ACTATCATCA GTAGAAGTTC AGCAAATGAG CTTAGACGGA
 3151 GATCTTGCAG CTATCCCAAC CACAAACCAA GCCTGCAGCG AAACAGACAG
 3201 CGGAAATGCT TGGAAAGTAC ACTATGAAGA CACTTCTGCT GCAGCTTCTT
 3251 TCAACAGATA G

Appendix Figure B10. The complete coding sequence of gene encoding auxin response factor 19 (*AtARF19*; At1g19220) retrieved from *Arabidopsis thaliana* genome annotation version TAIR10 (<https://www.arabidopsis.org/>). Forward and reverse qPCR primers and probe binding sites are colored and underlined in green, red, and orange respectively.

```

1 ATGACCGTTG ATTCAGCTCT GCGATCTCCG ATGATGCACT CACCGTCCAC
51 TAAGGACGTG AAGGCTCTAA GGTTCAATTGA GGAGATGACA CGTAACGTCCG
101 ATTTTCGTTCA GAAGAAAGTG ATTAGAGAGA TACTTAGTCG TAACTCGGAC
151 ACTGAGTACC TGAAACGGTT TGGTCTCAAG GGATTCACTG ACCGTAAAAC
201 ATTTAAGACC AAAGTTCCGG TGGTTATCTA CGATGATCTT AAACCGGAGA
251 TTCAACGTAT TGCCAATGGT GACCGGTCAA TGATCTTGTC TTCTTACCCC
301 ATCACAGAGT TCCTCACAAG CTCTGGGACA TCAGCTGGTG AAAGGAAGTT
351 GATGCCAACC ATTGATGAAG ACATGGACCG ACGTCAGCTT TTATACAGTC
401 TTCTCATGCC TGTGATGAAT CTCTACGTGC CCGGATTAGA CAAAGGCAAG
451 GCTCTATATT TTTTGTTCGT GAAGACGGAA TCGAAGACTC CCGGTGGATT
501 ACCAGCACGT CCGGTGCTCA CGAGTTATTA CAAAAGCGAA CAATTCAAGA
551 GACGTCCTAA CGATCCGTAC AACGTGTACA CGAGCCCTAA CGAAGCCATC
601 CTTTGTCCAG ACTCATCCCA AAGCATGTAC ACGCAGATGC TTTGTGGTCT
651 CCTTATGCGT CACGAAGTCC TCCGTCTCGG CGCCGTCTTC GCTTCTGGTC
701 TCCTCCGTGC CATTGGATTC CTTCAAACCA ATTGGAAAGA ACTCGCCGAC
751 GATATCTCCA CCGGTACCTT AAGTTCAAGA ATCTCTGACC CGGCCATTAA
801 AGAGAGCATG TCCAAGATCT TGACCAAACC GGACCAAGAA CTGGCTGATT
851 TCATAACTTC GGTATGTGGT CAAGACAATA GTTGGGAAGG TATTATTACT
901 AAGATTTGGC CTAACACTAA GTACCTTGAC GTCATCGTTA CTGGAGCCAT
951 GGCTCAGTAT ATCCCGATGC TTGAGTACTA TAGCGGCGGG TTACCGATGG
1001 CTTGCACGAT GTATGCATCG TCCGAGAGTT ACTTTGGGAT CAACTTGAAA
1051 CCAATGTGTA AACCTTCTGA GGTTCCTTAT ACCATTATGC CAAACATGGC
1101 ATACTTCGAG TTTCTCCCTC ATCATGAAGT CCCAACCGAA AAATCCGAAC
1151 TTGTGGAGCT AGCTGATGTC GAGGTCGGGA AAGAGTACGA GCTTGTGATC
1201 ACAACCTATG CTGGGCTTAA CCGTTATAGA GTTGGTGATA TTCTTCAGGT
1251 GACTGGATTC TACAATTCCG CTCCACAGTT CAAGTTTGTG CGGAGGAAGA
1301 ACGTTTTGCT TAGCATTGAG TCGGATAAAA CCGATGAAGC TGAGCTCCAA
1351 AGCGCGGTTG AGAACGCATC GCTCTTACTT GGAGAGCAAG GAACTCGTGT
1401 TATCGAGTAC ACGAGCTATG CAGAGACGAA GACTATACCT GGCCATTATG
1451 TCATTTACTG GGAGCTTCTA GTGAAGGATC AAACCAATCC TCCAAATGAC
1501 GAAGTCATGG CTCGGTGCTG CTTGGAAAATG GAGGAGTCGT TGAACTCTGT
1551 GTATAGACAA AGTCGGGTTG CGGATAAGTC GATAGGACCA CTCGAGATAC
1601 GTGTTGTGAA GAATGGAACG TTCGAGGAGC TCATGGACTA TGCCATCTCC
1651 AGAGGCGCAT CGATCAATCA GTACAAGGTG CCGAGGTGTG TGAGTTTCAC
1701 GCCAATAATG GAGCTTCTTG ACTCAAGGGT TGTATCTACA CACTTCAGCC
1751 CAGCTTTGCC ACATTGGTCA CCAGAACGTC GTCGTTGA

```

Appendix Figure B11. The complete coding sequence of gene encoding Gretchen Hagen 3.3 acyl acid amido synthetase (*AtGH3.3*; *At2g23170*) retrieved from *Arabidopsis thaliana* genome annotation version TAIR10 (<https://www.arabidopsis.org/>). Forward and reverse qPCR primers and probe binding sites are colored and underlined in green, red, and orange respectively.

1 TTTCTAACTA GACAAGGCCA TGTGTGTTGT AGGACCTCCC AAATATATAT
51 TTTCTAATAA TTATTTTCATC ATTTGCCAAT TTATTATATA ACCATTTCTC
101 ATCCTTCTCC TCATAACCACC AAAAACCAAC CTTCAAGAAC AGAGAAGAAG
151 TGATTCTCTA AACAAACAAA ATAAAATAAA ACTCTTCTTT CTCTATTTCT
201 GTTGAAGGTA CCTCATCATT GCAACACAAA CTTAAAGCTT TGTTTGTGTC
251 TGCTTTTCAGA CAATGATACC AAGTTACGAC CCAAATGATA CAGAGGCTGG
301 TCTCAAGCTT CTCGAGGATC TGACAACAAA TGCAGAGGCT ATCCAACAAC
351 AAGTTCTTCA CCAAATACTC TCTCAAAACT CTGGAACTCA ATATCTCCGA
401 GCATTTCTGG ACGGAGAAGC CGACAAGAAT CAACAAAGCT TCAAAAACAA
451 AGTCCCTGTG GTGAATTATG ACGACGTAAA GCCTTTCATT CAACGAATCG
501 CTGATGGAGA ATCATCTGAT ATCGTCTCTG CTCAGCCCAT CACAGAACTC
551 CTCACTAGTT CGGGGACTTC TGCAGGAAAG CCGAAGTTGA TGCCTTCTAC
601 AGCTGAAGAA TTGGAAAGGA AGACATTTTT CTACAGCATG CTTGTGCCTA
651 TCATGAACAA ATATGTGGAT GGGCTAGATG AGGGAAAAGG GATGTATCTT
701 CTATTCATAA AACCAGAGAT CAAGACTCCG TCAGGTCTAA TGGCCCGTCC
751 TGTTTTGACC AGCTACTACA AAAGTCAACA TTTCAGAAAC AGACCATTCA
801 ACAAGTACAA CGTCTACACT AGCCCTGACC AGACCATTCT TTGTCAAGAC
851 AGCAAGCAGA GCATGTACTG TCAGCTTCTC TGCGGTCTAG TACAGCGATC
901 TCATGTCCTA AGAGTCGGAG CTGTCTTTGC CTCTGCCTTT CTTTCGAGCAG
951 TCAAGTTCTT GGAGGATCAT TACAAAGAGC TTTGCGCTGA CATTAGAACC
1001 GGTACTGTCA CTAGCTGGAT CACTGACTCA TCCTGCAGAG ACTCGGTCTT
1051 GTCGATCCTT AATGGCCCAA ATCAAGAATT GGCTGATGAA ATTGAGAGTG
1101 AGTGCGCTGA AAAGTCGTGG GAAGGAATCT TGAGGAGGAT ATGGCCTAAG
1151 GCTAAATATG TTGAGGTGAT TGTGACTGGT TCGATGGCTC AATACATTCC
1201 GACACTAGAG TTTTATAGCG GAGGTTTACC GTTGGTTTCA ACGATGTATG
1251 CTTCTCTGA GTGTTACTTT GGTATCAACC TTAATCCGTT GTGTGATCCT
1301 GCCGATGTTT CCTACACGCT TCTTCTAAC ATGGCTTACT TCGAGTTCTT
1351 GCCCGTCGAC GACAAATCCC ACGAAGAGAT TCACTTTGCA ACTCACTCCA
1401 ACACCGATGA TGATGATGAT GCTCTCAAGG AAGATCTCAT CGTCAATCTT
1451 GTTAATGTCTG AAGTCGGTCA ATACTACGAA ATCGTCATCA CTACATTCAC
1501 AGGTTTGTAC AGATACAGAG TAGGCGATAT TCTAAAAGTG ACGGGTTTCC
1551 ACAACAAAGC GCCTCAATTC CGTTTTCGTGC AGCGAAGAAA CGTTGTACTA
1601 AGCATCGACA CTGACAAAAC GAGCGAAGAA GATCTACTAA ACGCAGTGAC
1651 ACAAGCTAAA CTAAACCATC TTCAACATCC TTCAAGCCTC TTGCTCACGG
1701 AGTACACAAG CTACGCAGAC ACGTCATCAA TCCCAGGGCA TTACGTGCTC
1751 TTCTGGGAGC TAAAGCCACG TCACAGCAAT GACCCACCAA AGCTTGACGA
1801 CAAGACAATG GAGGATTGTT GCTCTGAGGT TGAGGATTGT TTGGATTACG
1851 TCTACAGGAG ATGCAGGAAC AGGGACAAGT CGATTGGGCC ATTGGAGATA
1901 AGAGTGGTGA GTTTGGGCAC GTTTGATTCG TTAATGGATT TTTGTGTCTC
1951 ACAAGGATCA TCTTTGAATC AGTATAAGAC TCCAAGATGT GTTAAATCTG
2001 GAGGAGCTCT TGAGATTCTT GATTCCAGAG TTATTGGGAG GTTCTTCAGT
2051 AAGAGAGTTC CTCAATGGGA ACCACTTGGT TTAGATTCTT ARACTTACT
2101 TCTTTTTCTT TAATGTATGA TTAAAGTCTT GATTTTATAA GTATAAGATC
2151 TTCATTTGTT AAGTTGCTAA TTGGTGTTC TTTTTTAAAT TGTTAAGCTT
2201 TTGTCTCTTT TGTAACAAAC TTTCAGCAAA GTCCTCTCAT TTTGTGAATG

2251 TATACTTTTG TGTCTCTTC TTTATTATTC TTTGTCTCCC TCTCTTTTTC
2301 GAAAAGATTA AAAAAAATCG TACCAAA

Appendix Figure B12. The complete coding sequence of gene encoding Gretchen Hagen 3.3 acyl acid amido synthetase (*AtGH3.17*; *At1g28130*) retrieved from *Arabidopsis thaliana* genome annotation version TAIR10 (<https://www.arabidopsis.org/>). Forward and reverse qPCR primers and probe binding sites are colored and underlined in green, red, and orange respectively.

```

1 ATGGCTTCAC TTCAATTTTC TTCTCAGTTT CTGGGCTCAA AACTAAAAC
51 ACACAGCTCT ATCATTTCCTA TCTCTCGTAG TTACTIONTCCA ACTCCATTCA
101 CTAGATTCTC CCGCAAGAAG TATGAGTCAT GTTCGATGTC TATGAATGGT
151 TGTGATGGAG ATTTCAAGAC GCCACTTGGT ACAGTGGAGA CAAGGACTAT
201 GACTGCTGTT TTATCTCCGG CAGCCGCCAC TGAAAGGCTA ATCTCCGCCG
251 TCTCTGAACT CAAATCTCAA CCTCCGTCGT TTTCCCTCCGG CGTCGTTCGG
301 TTACAGGTTT CAATTGACCA GCAAATCGGA GCAATTGATT GGCTTCAAGC
351 CCAGAATGAG ATTCAGCCTC GCTGTTTCTT CTCTCGTCGC AGTGACGTTG
401 GTCGTCCCGA TCTTCTTCTC GATCTAGCTA ACGAGAACGG AAACGGAAAC
451 GGAAACGGAA CAGTGTCAATC TGATCGTAAT CTGGTTAGCG TTGCTGGTAT
501 CGGCTCTGCA GTTTTCTTCC GTGACCTTGA TCCTTTCTCT CATGACGATT
551 GGAGATCCAT CAGAAGGTTT TTGTCTTCAA CGTCACCTCT GATTCTGTCC
601 TATGGTGGTA TCGTTTTTGA TCCTAATGGC AAGATCGCTG TTGAATGGGA
651 ACCTTTTGGT GCATTTTACT TTTTCTTCCC TCAGGTTGAG TTTAATGAGT
701 TTGGTGGAAG TTCAATGTTG GCTGCAACTA TTGCTTGGGA TGATGAACTC
751 TCTTGGACTC TGAAAATGC TATTGAAGCA CTCCAGGAGA CTATGCTTCA
801 AGTTTCTTCT GTTGTAATGA AGTTGAGAAA CAGATCTTTA GGAGTATCTG
851 TTTTAAGCAA GAATCATGTT CCTACCAAAG GAGCTTATTT CCCTGCTGTA
901 GAGAAGGCTT TAGAGATGAT TAACCAGAAA AGTTCACCCC TTAACAAGGT
951 TGTTCTTGCT CGTAACAGCA GGATAATTAC GGATACCGAC ATTGATCCCA
1001 TTGCTTGGCT AGCACAGTTA CAGCGTGAAG GGCATGATGC ATATCAGTTC
1051 TGTCTTCAAC CACCTGGTGC ACCAGCTTTT ATCGGAAACA CGCCTGAGAG
1101 ACTATTCCAA AGGACTCAAT TAGGTGTCTG CAGTGAAGCT TTGGCTGCAA
1151 CTAGGCCTAG AGCTGCTTCT AGTGCTCGTG ATATGGAGAT AGAGCGTGAC
1201 TTACTIONTCCA GTCCGAAAAGA CGACCTCGAG TTCTCTATCG TACGAGAGAA
1251 TATAAGAGAA AAGTTAAACG GTATATGTGA CAGAGTTGTT GTCAAGCCTC
1301 AAAAACTGT GAGGAAGCTT GCAAGAGTGC AACATCTATA TTCTCAATTG
1351 GCAGGGAGAC TTACGAAGGA AGATGATGAG TATAAAATAT TGGCTGCTCT
1401 GCATCCAACT CCAGCTGTTTT GTGGCTTCC AGCAGAAGA GCAAGGCTTT
1451 TGATTAAGGA GATAGAATCA TTCGATAGAG GAATGTATGC GGGACCTATT
1501 GGATTTTTTTG GTGGCGAGGA GAGTGAATTT GCAGTCGGGA TCAGATCAGC
1551 TCTAGTCGAA AAGGGTCTTG GGGCATTGAT CTATGCGGGG ACAGGGATAG
1601 TAGCTGGAAG TGACCCATCT TCAGAGTGGA ATGAGCTTGA TCTTAAGATA
1651 TCTCAGGTAC GAGCTTTTGT CCAGAAAATG TTTAGTGACA TCATGGTTCT
1701 CTGTTACCAA AATCCTAATT TTTATTCTCT CTTTTGTTGT TGTTTTTGCA
1751 GTTACCAAG TCAATTGAAT ATGAAGCAAC AACATCTCTA CAGGCGATTA
1801 ATTGAAGAAA GAGTAACATT TGTATTTGAT TGTTTTGTTT GTATGGGGGA
1851 TAAGGGGTTT TCACAATAA

```

Appendix Figure B13. The complete coding sequence of gene encoding isochorismate synthase 1 (*AtICS1*; *At1g74710*) retrieved from *Arabidopsis thaliana* genome annotation version TAIR10 (<https://www.arabidopsis.org/>). Forward and reverse qPCR primers and probe binding sites are colored and underlined in green, red, and orange respectively.

```

1 ATGGCAAATA TCTCCAGTAT TCACATTCTC TTCCTCGTGT TCATCACAAG
51 CGGCATTGCT GTTATGGCCA CAGACTTCAC TCTAAGGAAC AATTGCCCTA
101 CCACCCTCTG GGCCGGAAC CTCGCCGGTC AAGGACCCAA GCTCGGCGAT
151 GGAGGATTTG AATTGACTCC AGGTGCTTCC CGACAGCTCA CGGCTCCTGC
201 AGGATGGTCA GGCCGGTTCT GGGCTCGTAC AGGCTGCAAC TTTGACGCCT
251 CCGGAAACGG TAGATGTGTA ACCGGAGACT GTGGCGGTCT AAGATGTAA
301 GGCGGCGGAG TTCCTCCCGT CACTCTGGCT GAATTCACCT TAGTAGGCGA
351 TGGCGGCAAA GATTTCTACG ATGTGAGCCT CGTAGATGGT TACAATGTCA
401 AGCTGGGGAT AAGACCATCC GGAGGATCGG GAGATTGCAA ATACGCAGGC
451 TGTGTCTCTG ACCTCAACGC GGCTTGCCCC GACATGCTTA AGGTCATGGA
501 TCAGAACAAT GTCGTGGCCT GCAAGAGTGC CTGTGAGAGG TTTAATACGG
551 ATCAATATTG CTGCCGTGGA GCTAACGATA AGCCGGAAAC TTGTCCTCCC
601 ACGGACTACT CGAGGATTTT CAAGAACGCT TGCCCTGACG CCTATAGCTA
651 CGCTTATGAC GACGAAACGA GCACCTTCAC TTGTACCGGA GCTAACTACG
701 AAATCACTTT CTGCCCTTAA

```

Appendix Figure B14. The complete coding sequence of the pathogenesis related 5 (*AtPR5*; *At1g75040*) retrieved from *Arabidopsis thaliana* genome annotation version TAIR10 (<https://www.arabidopsis.org/>). Forward and reverse qPCR primers and probe binding sites are colored and underlined in green, red, and orange respectively.

1 TTATGTATTA TACATAAGCC CATTAGTTC TTATCTTTGA CAGGCCCAAT
51 TATATGGACA CAGCTTGAAG ATGGTTTAGC TGCTGCGAAA GACGAGCTCC
101 GGTCTCATTT CTCGTTCTTC TGATTGATAG ATCGCTCGGA ACTTGGAAG
151 CAGCGTAATC GGTAGGGAGT GATTTGAGTT TTGGTGAGGA TGTCTATGGT
201 TGATGAGCCT TTATAACCGA TTGCTGTGCT TATCGACGAG CTAAAAACG
251 ATGATATTCA GCGTAGATTG AACTCTATTA AACGGCTTTC TATCATTGCT
301 CGTGCTCTTG GAGAGGAGAG GACAAGAAAA GAGTTGATT CATTCTTAG
351 TGAGAACAAT GACGATGACG ATGAGGTGCT TTTGGCTATG GCGGAAGAGT
401 TGGGGGGTTT TATTCTGTAT GTAGGAGGGG TTGAGTATGC ATATGTTCTG
451 CTTCCACCTT TGGAGACTCT ATCCACTGTT GAGGAACTT GCGTGAGGGA
501 GAAAGCTGTG GATTCACTTT GTAGAATTGG TGCTCAGATG AGGGAGAGTG
551 ACTTGGTTGA GCATTTCACT CCTCTGGCTA AGCGACTTTC AGCTGGTGAA
601 TGGTTCACAG CCAGAGTATC AGCATGTGGG ATTTTCCATA TTGCATACCC
651 AAGTGCCCCA GATGTGCTAA AGACGGAGCT AAGATCAATA TATGGTCAGC
701 TTTGTCAAGA TGACATGCCA ATGGTGCGCA GAGCTGCAGC AACTAATTTG
751 GGAAGTTTG CTGCTACAAT TGAATCAGCT CATTTGAAGA CAGACATTAT
801 GTCCATGTTT GAGGATCTTA CGCAAGATGA TCAAGATTCG GTTAGATTAT
851 TGGCTGTTGA GGGTTGTGCT GCTCTTGGGA AATTGTTGGA GCCCCAGGAC
901 TGTGTTGCAC ACATTCTTCC TGTGATTGTC AATTTCTCGC AGGATAAGTC
951 CTGGCGTGTG CGTTATATGG TTGCAAATCA GCTCTATGAA CTTTGTGAAG
1001 CTGTAGGACC GGAGCCAAC AGGACGGATC TGGTGCCTGC ATATGCTCGT
1051 CTACTTTGTG ATAATGAGGC AGAAGTTCGG ATAGCAGCTG CTGGAAAAGT
1101 TACCAAGTTT TGTCGCATTT TAAACCCTGA ACTCGCTATC CAGCACATTC
1151 TTCCCTGTGT AAAGGAATTA TCATCAGACT CTTCTCAGCA CGTCAGATCT
1201 GCATTGGCAT CAGTTATAAT GGAATGGCT CCAGTCTTGG GTAAGGATGC
1251 AACAATTGAG CATCTTCTTC CAATCTTCTT TTCTCTATTG AAAGACGAAT
1301 TTCCTGATGT ACGCTTAAAC ATTATCAGCA AACTTGACCA AGTGAACCAG
1351 GTTATTGGGA TTGATCTACT ATCACAATCG TTAGTGCCAG CCATTGTAGA
1401 ACTTGCTGAA GACAGGCACT GGAGAGTACG TCTGGCTATA ATCGAGTATA
1451 TTCCCTTGTT GGCCAGTCAA TTAGGTGTAG GCTTCTTTGA TGAGAAGCTT
1501 GGTGCTCTTT GCATGCAATG GTTACAAGAC AAGGTTCACT CAATCCGTGA
1551 AGCTGCTGCA AACAATCTGA AGCGTCTTGC TGAAGAGTTT GGTCCGTAAT
1601 GGGCAATGCA GCATATAGTT CCTCAGGTT TAGAGATGAT TAACAACCCA
1651 CACTATCTAT ATCGGATGAC GATTCTTCGT GCAGTATCGC TTCTCGCTCC
1701 AGTAATGGGA TCCGAGATCA CATGTTCCAA ACTCTTACCT GCGGTAATAA
1751 CTGCATCTAA AGACAGAGTT CCAAACATCA AATTTAACGT GGCCAAAATG
1801 ATGCAATCTC TCATTCCGAT AGTCGACCAA GCGGTTGTGG AGAACATGAT
1851 ACGGCCATGC TTTGGTGGAGC TAAGTGAAGA CCCAGATGTT GATGTTCCGT
1901 ATTTTCGAAA TCAAGCTCTC CAATCTATTG ACAATGTGAT GATGTCTAGC
1951 TAAAAAAGG TAAAGAAGAC AGCAACGAAT TGTGTTTGGT TCTCATGAGA
2001 TTTTGTAAAC GATACTTTGT CGTGTGTTGT CTTTTACTTT ACACGTACGT
2051 GACCATTGTT TCTCTCTGCT ACTAATGTTA ATGTTGGCTT CATGTTTTCT
2101 GTGATTTGTT CGTTGGGCGT ATTTGCTTTT TGGTGCTTAA TTTTGTTTAG
2151 TCCAAATAAT TTA CTTATCA AGTGATTCGG CAACGTTTTT GCTCGAAGCA
2201 TGAGTG TACA ATTGGTC

Appendix Figure B15. The complete coding sequence of the PROTEIN PHOSPHATASE 2A SUBUNIT A3 (*AtPP2A43*; AT1G13320) retrieved from *Arabidopsis thaliana* genome

annotation version TAIR10 (<https://www.arabidopsis.org>). Forward and reverse qPCR primers and probe binding sites are colored and underlined in green, red, and orange respectively.

Appendix B Table B1. Primers used for PCR verification of auxin receptor *tir1-10* and *afb2-3* T-DNA insertions in Arabidopsis homozygous *tir1afb2* double mutant lines

Gene name	Primer sequence
<i>tir1-10</i> (SALK_090445)	LP: 5'-CACGTGTCATCATCAGAATCG-3'
	RP: 5'-ATTCCACCTCAGGAGATTC-3'
<i>afb2-3</i> (SALK_137151)	LP: 5'-TCAACGGTCAAGATCCATCTC-3'
	RP: 5'-CTGCAATTAGCGGCAATAGAG-3'
LBb1.3 (T-DNA border primer)	LB: 5'-ATTTTGCCGATTTCGGAAC-3'

LP: Left Primer, RP: Right Primer, LB: Left Border Primer

Appendix Table B2. The probability (P), degrees of freedom and F values for the relative transcript abundance of *PsAFB6* for comparisons among treatments (non-inoculated and clubroot-inoculated) and lines (*PsAFB6/+ 4-8 tir1afb2*, and *PsAFB6/+ 3-2 tir1afb245*), and the treatment x line interaction in the root tissue of 21 DAI seedlings using a two-way ANOVA analysis followed by mean separation using LSD post-hoc test (data presented in Figure 3.4).

Gene name	Treatments		Lines		Treatment x Line	
	F value	Pr(>F)	F value	Pr(>F)	F value	Pr(>F)
<i>PsAFB6</i>	14.8300	0.0023	230.8600	<0.0001	1.6800	0.2193
Degrees of freedom	1		1		1	

LSD post-hoc test (p values)	<i>PsAFB6/+ 4-8 tir1afb2</i> -non-inoculated	<i>PsAFB6/+ 4-8 tir1afb2</i> -clubroot-inoculated	<i>PsAFB6/+ 3-2 tir1afb245</i> -non-inoculated	<i>PsAFB6/+ 3-2 tir1afb245</i> -clubroot-inoculated
<i>PsAFB6/+ 4-8 tir1afb2</i> -non-inoculated	1			
<i>PsAFB6/+ 4-8 tir1afb2</i> -clubroot-inoculated	0.0034	1		
<i>PsAFB6/+ 3-2 tir1afb245</i> -non-inoculated	<0.0001	<0.0001	1	
<i>PsAFB6/+ 3-2 tir1afb245</i> -clubroot-inoculated	<0.0001	<0.0001	0.0959	1

Appendix Table B3. The probability (P), degrees of freedom and F values for clubroot disease index (DI) at 32 DAI for comparisons among lines (Set 1: WT, *tir1afb2C*, *tir1afb245*, *PsAFB6/+ 1-6 tir1afb245*, *PsAFB6/+ 3-2 tir1afb245*, and *PsAFB6/+ 5-9 tir1afb245*) using a one-way ANOVA analysis followed by mean separation using LSD post-hoc test (data presented in Figure 3.5A).

ANOVA	Lines	
	F value	Pr(>F)
Clubroot disease index	61.2413	<0.0001
Degrees of freedom	5	

LSD post-hoc test (P values)	WT	<i>tir1afb2C</i>	<i>tir1afb245</i>	<i>PsAFB6/+ 1-6 tir1afb245</i>	<i>PsAFB6/+ 3-2 tir1afb245</i>	<i>PsAFB6/+ 5-9 tir1afb245</i>
WT	1					
<i>tir1afb2C</i>	<0.0001	1				
<i>tir1afb245</i>	<0.0001	<0.0001	1			
<i>PsAFB6/+ 1-6 tir1afb245</i>	<0.0001	<0.0001	0.1616	1		
<i>PsAFB6/+ 3-2 tir1afb245</i>	<0.0001	<0.0001	0.0183	0.2708	1	
<i>PsAFB6/+ 5-9 tir1afb245</i>	<0.0001	<0.0001	0.0871	0.7307	0.4418	1

Appendix Table B4. The probability (P), degrees of freedom and F values for clubroot disease index (DI) at 32 DAI for comparisons among lines (Set 2: WT, *tir1afb2C*, *tir1afb2A2*, and *tir1afb2D1*) using a one-way ANOVA analysis followed by mean separation using LSD post-hoc test (data presented in Figure 3.5B).

ANOVA	Lines	
	F value	Pr(>F)
Clubroot disease index	8.5908	0.0007
Degrees of freedom	3	

LSD post-hoc test (P values)	WT	<i>tir1afb2C</i>	<i>tir1afb2A2</i>	<i>tir1afb2D1</i>
WT	1			
<i>tir1afb2C</i>	0.0001	1		
<i>tir1afb2A2</i>	0.0079	0.0483	1	
<i>tir1afb2D1</i>	0.0137	0.0291	0.8070	1

Appendix Table B5. The probability (P), degrees of freedom and F values for clubroot disease index (DI) at 32 DAI for comparisons among lines (Set 3: WT, *tir1afb2C*, *PsAFB6/+ 4-8 tir1afb2*, and *PsAFB6/+ 3-3 tir1afb2*) using a one-way ANOVA analysis followed by mean separation using LSD post-hoc test (data presented in Figure 3.5C).

ANOVA	Lines	
	F value	Pr(>F)
Clubroot disease index	18.5575	0.0006
Degrees of freedom	3	

LSD post-hoc test (P values)	WT	<i>tir1afb2C</i>	<i>PsAFB6/+ 4-8 tir1afb2</i>	<i>PsAFB6/+ 3-3 tir1afb2</i>
WT	1			
<i>tir1afb2C</i>	0.0049	1		
<i>PsAFB6/+ 4-8 tir1afb2</i>	0.0019	0.5001	1	
<i>PsAFB6/+ 3-3 tir1afb2</i>	0.0001	0.0065	0.0216	1

Appendix Table B6. The probability (P), degrees of freedom and F values on the average fresh weight of the root-shoot transition region at 32 DAI for comparisons among treatments (non-inoculated and clubroot-inoculated) and lines (Set 1: WT, *tir1afb2C*, *tir1afb245*, *PsAFB6/+ 1-6 tir1afb245*, *PsAFB6/+ 3-2 tir1afb245*, and *PsAFB6/+ 5-9 tir1afb245*) and the treatment x line interaction using a two-way ANOVA analysis followed by mean separation using LSD post-hoc test (data presented in Figure 3. 12A).

	Treatments		Lines		Treatment x Line	
	F value	Pr(>F)	F value	Pr(>F)	F value	Pr(>F)
Average fresh root weight	200.3400	<0.0001	97.9200	<0.0001	35.3900	<0.0001
Degrees of freedom	1		5		5	

LSD post-hoc test (P values)	WT-non-inoculated	WT-clubroot-inoculated	<i>tir1afb2C</i> -non-inoculated	<i>tir1afb2C</i> -clubroot-inoculated	<i>tir1afb245</i> -non-inoculated	<i>tir1afb245</i> -clubroot-inoculated	<i>PsAFB6/+ 1-6 tir1afb245</i> -non-inoculated	<i>PsAFB6/+ 1-6 tir1afb245</i> -clubroot-inoculated	<i>PsAFB6/+ 3-2 tir1afb245</i> -non-inoculated	<i>PsAFB6/+ 3-2 tir1afb245</i> -clubroot-inoculated	<i>PsAFB6/+ 5-9 tir1afb245</i> -non-inoculated	<i>PsAFB6/+ 5-9 tir1afb245</i> -clubroot-inoculated
WT-non-inoculated	1											
WT-clubroot-inoculated	<0.0001	1										
<i>tir1afb2C</i> -non-inoculated	0.2994	<0.0001	1									
<i>tir1afb2C</i> -clubroot-inoculated	<0.0001	<0.0001	<0.0001	1								
<i>tir1afb245</i> -non-inoculated	0.0080	<0.0001	0.0895	<0.0001	1							
<i>tir1afb245</i> -clubroot-inoculated	0.6328	<0.0001	0.4681	<0.0001	0.0091	1						
<i>PsAFB6/+ 1-6 tir1afb245</i> -non-inoculated	0.0139	<0.0001	0.1357	<0.0001	0.8289	0.0170	1					
<i>PsAFB6/+ 1-6 tir1afb245</i> -clubroot-inoculated	0.9768	<0.0001	0.2210	<0.0001	0.0023	0.5352	0.0046	1				
<i>PsAFB6/+ 3-2 tir1afb245</i> -non-inoculated	0.0181	<0.0001	0.1651	<0.0001	0.7459	0.0230	0.9139	0.0064	1			
<i>PsAFB6/+ 3-2 tir1afb245</i> -clubroot-inoculated	0.9951	<0.0001	0.2185	<0.0001	0.0020	0.5391	0.0040	0.9765	0.0057	1		
<i>PsAFB6/+ 5-9 tir1afb245</i> -non-inoculated	0.0088	<0.0001	0.0962	<0.0001	0.9713	0.0101	0.8571	0.0026	0.7733	0.0022	1	
<i>PsAFB6/+ 5-9 tir1afb245</i> -clubroot-inoculated	0.8024	<0.0001	0.3884	<0.0001	0.0093	0.8198	0.0166	0.7430	0.0220	0.7554	0.0103	1

Appendix Table B7. The probability (P), degrees of freedom and F values on the average fresh weight of the root-shoot transition region at 32 DAI for comparisons among treatments (non-inoculated and clubroot-inoculated) and lines (Set 2: WT, *tir1afb2C*, *tir1afb2A2*, and *tir1afb2D1*), and the treatment x line interaction using a two-way ANOVA analysis followed by mean separation using LSD post-hoc test (data presented in Figure 3.12B).

	Treatments		Lines		Treatment x Line	
	F value	Pr(>F)	F value	Pr(>F)	F value	Pr(>F)
Average fresh root weight	247.8830	<0.0001	39.2300	<0.0001	9.9560	<0.0001
Degrees of freedom	1		3		3	

LSD post-hoc test (P values)	WT-non-inoculated	WT-clubroot-inoculated	<i>tir1afb2C</i> -non-inoculated	<i>tir1afb2C</i> -clubroot-inoculated	<i>tir1afb2A2</i> -non-inoculated	<i>tir1afb2A2</i> -clubroot-inoculated	<i>tir1afb2D1</i> -non-inoculated	<i>tir1afb2D1</i> -clubroot-inoculated
WT-non-inoculated	1							
WT-clubroot-inoculated	<0.0001	1						
<i>tir1afb2C</i> -non-inoculated	0.6661	<0.0001	1					
<i>tir1afb2C</i> -clubroot-inoculated	0.0006	<0.0001	0.0001	1				
<i>tir1afb2A2</i> -non-inoculated	0.7299	<0.0001	0.9312	0.0002	1			
<i>tir1afb2A2</i> -clubroot-inoculated	<0.0001	0.0002	<0.0001	<0.0001	<0.0001	1		
<i>tir1afb2D1</i> -non-inoculated	0.6048	<0.0001	0.9312	0.0001	0.8628	<0.0001	1	
<i>tir1afb2D1</i> -clubroot-inoculated	<0.0001	<0.0001	<0.0001	<0.0001	<0.0001	0.2215	<0.0001	1

Appendix Table B8. The probability (P), degrees of freedom and F values on the average fresh weight of the root-shoot transition region at 32 DAI for comparisons among treatments (non-inoculated and clubroot-inoculated) and lines (WT, *tir1afb2C*, *PsAFB6/+ 4-8 tir1afb2*, and *PsAFB6/+ 3-3 tir1afb2*), and the treatment x line interaction using a two-way ANOVA analysis followed by mean separation using LSD post-hoc test (data presented in Figure 3.12C).

	Treatments		Lines		Treatment x Line	
	F value	Pr(>F)	F value	Pr(>F)	F value	Pr(>F)
Average fresh root weight	52.1000	<0.0001	22.9400	<0.0001	23.6500	<0.0001
Degrees of freedom	1		3		3	

LSD post-hoc test (P values)	WT-non-inoculated	WT-clubroot-inoculated	<i>tir1afb2C</i> -non-inoculated	<i>tir1afb2C</i> -clubroot-inoculated	<i>PsAFB6/+ 4-8 tir1afb2</i> -non-inoculated	<i>PsAFB6/+ 4-8 tir1afb2</i> -clubroot-inoculated	<i>PsAFB6/+ 3-3 tir1afb2</i> -non-inoculated	<i>PsAFB6/+ 3-3 tir1afb2</i> -clubroot-inoculated
WT-non-inoculated	1							
WT-clubroot-inoculated	<0.0001	1						
<i>tir1afb2C</i> -non-inoculated	0.9847	<0.0001	1					
<i>tir1afb2C</i> -clubroot-inoculated	0.0019	<0.0001	0.0017	1				
<i>PsAFB6/+ 4-8 tir1afb2</i> -non-inoculated	0.6607	<0.0001	0.6745	0.0005	1			
<i>PsAFB6/+ 4-8 tir1afb2</i> -clubroot-inoculated	0.0156	<0.0001	0.0147	0.2375	0.0042	1		
<i>PsAFB6/+ 3-3 tir1afb2</i> -non-inoculated	0.7891	<0.0001	0.8038	0.0008	0.8634	0.0071	1	
<i>PsAFB6/+ 3-3 tir1afb2</i> -clubroot-inoculated	0.1181	<0.0001	0.1131	0.0200	0.0404	0.2042	0.0626	1

Appendix Table B9. The probability (P), degrees of freedom and F values for the relative transcript abundance of *AtIAA9* in the root tissue of 21 DAI seedlings for comparisons among treatments (non-inoculated and clubroot-inoculated) and lines (WT, *tir1afb2C*, *tir1afb245*, *PsAFB6/+ 4-8 tir1afb2*, and *PsAFB6/+ 3-2 tir1afb245*), and the treatment x line interaction using a two-way ANOVA analysis followed by mean separation using LSD post-hoc test (data presented in Figure 3.13A).

Gene name	Treatments		Lines		Treatment x Line	
	F value	Pr(>F)	F value	Pr(>F)	F value	Pr(>F)
<i>AtIAA9</i>	140.7500	<0.0001	16.3200	<0.0001	17.1200	<0.0001
Degrees of freedom	1		4		4	

LSD post-hoc test (P values)	WT-non-inoculated	WT-clubroot-inoculated	<i>tir1afb2C</i> -non-inoculated	<i>tir1afb2C</i> -clubroot-inoculated	<i>tir1afb245</i> -non-inoculated	<i>tir1afb245</i> -clubroot-inoculated	<i>PsAFB6/+ 4-8 tir1afb2</i> -non-inoculated	<i>PsAFB6/+ 4-8 tir1afb2</i> -clubroot-inoculated	<i>PsAFB6/+ 3-2 tir1afb245</i> -non-inoculated	<i>PsAFB6/+ 3-2 tir1afb245</i> -clubroot-inoculated
WT-non-inoculated	1									
WT-clubroot-inoculated	0.7332	1								
<i>tir1afb2C</i> -non-inoculated	0.0003	<0.0001	1							
<i>tir1afb2C</i> -clubroot-inoculated	0.0315	0.0087	0.0545	1						
<i>tir1afb245</i> -non-inoculated	0.0001	<0.0001	0.7907	0.0307	1					
<i>tir1afb245</i> -clubroot-inoculated	0.0734	0.1129	<0.0001	0.0001	<0.0001	1				
<i>PsAFB6/+ 4-8 tir1afb2</i> -non-inoculated	<0.0001	<0.0001	0.1533	0.0016	0.2404	<0.0001	1			
<i>PsAFB6/+ 4-8 tir1afb2</i> -clubroot-inoculated	<0.0001	<0.0001	<0.0001	<0.0001	<0.0001	0.0027	<0.0001	1		
<i>PsAFB6/+ 3-2 tir1afb245</i> -non-inoculated	<0.0001	<0.0001	0.0044	<0.0001	0.0085	<0.0001	0.1155	<0.0001	1	
<i>PsAFB6/+ 3-2 tir1afb245</i> -clubroot-inoculated	0.0569	0.0177	0.0286	0.7667	0.0155	0.0003	0.0007	<0.0001	<0.0001	1

Appendix Table B10. The probability (P), degrees of freedom and F values for the relative transcript abundance of *AtIAA16* in the root tissue of 21 DAI seedlings for comparisons among treatments (non-inoculated and clubroot-inoculated) and lines (WT, *tir1afb2C*, *tir1afb245*, *PsAFB6/+ 4-8 tir1afb2*, and *PsAFB6/+ 3-2 tir1afb245*), and the treatment x line interaction using a two-way ANOVA analysis followed by mean separation using LSD post-hoc test (data presented in Figure 3.13B).

Gene name	Treatments		Lines		Treatment x Line	
	F value	Pr(>F)	F value	Pr(>F)	F value	Pr(>F)
<i>AtIAA16</i>	673.0700	<0.0001	23.6400	<0.0001	36.4300	<0.0001
Degrees of freedom	1		4		4	

LSD post-hoc test (P values)	WT-non-inoculated	WT-clubroot-inoculated	<i>tir1afb2C</i> -non-inoculated	<i>tir1afb2C</i> -clubroot-inoculated	<i>tir1afb245</i> -non-inoculated	<i>tir1afb245</i> -clubroot-inoculated	<i>PsAFB6/+ 4-8 tir1afb2</i> -non-inoculated	<i>PsAFB6/+ 4-8 tir1afb2</i> -clubroot-inoculated	<i>PsAFB6/+ 3-2 tir1afb245</i> -non-inoculated	<i>PsAFB6/+ 3-2 tir1afb245</i> -clubroot-inoculated
WT-non-inoculated	1									
WT-clubroot-inoculated	<0.0001	1								
<i>tir1afb2C</i> -non-inoculated	0.7097	<0.0001	1							
<i>tir1afb2C</i> -clubroot-inoculated	<0.0001	<0.0001	<0.0001	1						
<i>tir1afb245</i> -non-inoculated	0.0060	<0.0001	0.0091	<0.0001	1					
<i>tir1afb245</i> -clubroot-inoculated	<0.0001	<0.0001	<0.0001	0.0075	0.0001	1				
<i>PsAFB6/+ 4-8 tir1afb2</i> -non-inoculated	0.2663	<0.0001	0.4199	<0.0001	0.0578	<0.0001	1			
<i>PsAFB6/+ 4-8 tir1afb2</i> -clubroot-inoculated	<0.0001	<0.0001	<0.0001	0.0003	<0.0001	<0.0001	<0.0001	1		
<i>PsAFB6/+ 3-2 tir1afb245</i> -non-inoculated	0.1678	<0.0001	0.2711	<0.0001	0.1054	<0.0001	0.7636	<0.0001	1	
<i>PsAFB6/+ 3-2 tir1afb245</i> -clubroot-inoculated	<0.0001	<0.0001	<0.0001	0.5918	<0.0001	0.0267	<0.0001	0.0001	<0.0001	1

Appendix Table B11. The probability (P), degrees of freedom and F values for the relative transcript abundance of *AtIAA19* in the root tissue of 21 DAI seedlings for comparisons among treatments (non-inoculated and clubroot-inoculated) and lines (WT, *tir1afb2C*, *tir1afb245*, *PsAFB6/+ 4-8 tir1afb2*, and *PsAFB6/+ 3-2 tir1afb245*), and the treatment x line interaction using a two-way ANOVA analysis followed by mean separation using LSD post-hoc test (data presented in Figure 3.13C).

Gene name	Treatments		Lines		Treatment x Line	
	F value	Pr(>F)	F value	Pr(>F)	F value	Pr(>F)
<i>AtIAA19</i>	1233.1100	<0.0001	71.1400	<0.0001	50.7500	<0.0001
Degrees of freedom	1		4		4	

LSD post-hoc test (P values)	WT-non-inoculated	WT-clubroot-inoculated	<i>tir1afb2C</i> -non-inoculated	<i>tir1afb2C</i> -clubroot-inoculated	<i>tir1afb245</i> -non-inoculated	<i>tir1afb245</i> -clubroot-inoculated	<i>PsAFB6/+ 4-8 tir1afb2</i> -non-inoculated	<i>PsAFB6/+ 4-8 tir1afb2</i> -clubroot-inoculated	<i>PsAFB6/+ 3-2 tir1afb245</i> -non-inoculated	<i>PsAFB6/+ 3-2 tir1afb245</i> -clubroot-inoculated
WT-non-inoculated	1									
WT-clubroot-inoculated	<0.0001	1								
<i>tir1afb2C</i> -non-inoculated	0.0146	<0.0001	1							
<i>tir1afb2C</i> -clubroot-inoculated	<0.0001	0.0788	<0.0001	1						
<i>tir1afb245</i> -non-inoculated	0.0002	<0.0001	0.0814	<0.0001	1					
<i>tir1afb245</i> -clubroot-inoculated	<0.0001	<0.0001	<0.0001	<0.0001	<0.0001	1				
<i>PsAFB6/+ 4-8 tir1afb2</i> -non-inoculated	<0.0001	<0.0001	<0.0001	<0.0001	<0.0001	<0.0001	1			
<i>PsAFB6/+ 4-8 tir1afb2</i> -clubroot-inoculated	<0.0001	<0.0001	<0.0001	<0.0001	<0.0001	0.0177	<0.0001	1		
<i>PsAFB6/+ 3-2 tir1afb245</i> -non-inoculated	0.0001	<0.0001	0.0414	0.0001	0.7449	<0.0001	<0.0001	<0.0001	1	
<i>PsAFB6/+ 3-2 tir1afb245</i> -clubroot-inoculated	<0.0001	<0.0001	<0.0001	<0.0001	<0.0001	0.0557	<0.0001	0.0001	<0.0001	1

Appendix Table B12. The probability (P), degrees of freedom and F values for the relative transcript abundance of *AtARF3* in the root tissue of 21 DAI seedlings for comparisons among treatments (non-inoculated and clubroot-inoculated) and lines (WT, *tir1afb2C*, *tir1afb245*, *PsAFB6/+ 4-8 tir1afb2*, and *PsAFB6/+ 3-2 tir1afb245*), and the treatment x line interaction using a two-way ANOVA analysis followed by mean separation using LSD post-hoc test (data presented in Figure 3.14A).

Gene name	Treatments		Lines		Treatment x Line	
	F value	Pr(>F)	F value	Pr(>F)	F value	Pr(>F)
<i>AtARF3</i>	1029.7440	<0.0001	7.385	0.0003	27.1440	<0.0001
Degrees of freedom	1		4		4	

LSD post-hoc test (P values)	WT-non-inoculated	WT-clubroot inoculated	<i>tir1afb2C</i> -non-inoculated	<i>tir1afb2C</i> -clubroot inoculated	<i>tir1afb245</i> -non-inoculated	<i>tir1afb245</i> -clubroot inoculated	<i>PsAFB6/+ 4-8 tir1afb2</i> -non-inoculated	<i>PsAFB6/+ 4-8 tir1afb2</i> -clubroot inoculated	<i>PsAFB6/+ 3-2 tir1afb245</i> -non-inoculated	<i>PsAFB6/+ 3-2 tir1afb245</i> -clubroot inoculated
WT-non-inoculated	1									
WT-clubroot inoculated	<0.0001	1								
<i>tir1afb2C</i> -non-inoculated	0.0001	<0.0001	1							
<i>tir1afb2C</i> -clubroot inoculated	<0.0001	0.0003	<0.0001	1						
<i>tir1afb245</i> -non-inoculated	<0.0001	<0.0001	0.4770	<0.0001	1					
<i>tir1afb245</i> -clubroot inoculated	<0.0001	<0.0001	<0.0001	<0.0001	<0.0001	1				
<i>PsAFB6/+ 4-8 tir1afb2</i> -non-inoculated	0.0087	<0.0001	0.0628	<0.0001	0.0127	<0.0001	1			
<i>PsAFB6/+ 4-8 tir1afb2</i> -clubroot inoculated	<0.0001	<0.0001	<0.0001	0.0011	<0.0001	0.2278	<0.0001	1		
<i>PsAFB6/+ 3-2 tir1afb245</i> -non-inoculated	<0.0001	<0.0001	0.3571	<0.0001	0.8310	<0.0001	0.0076	<0.0001	1	
<i>PsAFB6/+ 3-2 tir1afb245</i> -clubroot inoculated	<0.0001	<0.0001	<0.0001	0.2436	<0.0001	0.0010	<0.0001	0.0216	<0.0001	1

Appendix Table B13. The probability (P), degrees of freedom and F values for the relative transcript abundance of *AtARF5* in the root tissue of 21 DAI seedlings for comparisons among treatments (non-inoculated and clubroot-inoculated) and lines (WT, *tir1afb2C*, *tir1afb245*, *PsAFB6/+ 4-8 tir1afb2*, and *PsAFB6/+ 3-2 tir1afb245*), and the treatment x line interaction using a two-way ANOVA analysis followed by mean separation using LSD post-hoc test (data presented in Figure 3.14B).

Gene name	Treatments		Lines		Treatment x Line	
	F value	Pr(>F)	F value	Pr(>F)	F value	Pr(>F)
<i>AtARF5</i>	372.5200	<0.0001	66.1800	<0.0001	33.3500	<0.0001
Degrees of freedom	1		4		4	

LSD post-hoc test (P values)	WT-non-inoculated	WT-clubroot-inoculated	<i>tir1afb2C</i> -non-inoculated	<i>tir1afb2C</i> -clubroot-inoculated	<i>tir1afb245</i> -non-inoculated	<i>tir1afb245</i> -clubroot-inoculated	<i>PsAFB6/+ 4-8 tir1afb2</i> -non-inoculated	<i>PsAFB6/+ 4-8 tir1afb2</i> -clubroot-inoculated	<i>PsAFB6/+ 3-2 tir1afb245</i> -non-inoculated	<i>PsAFB6/+ 3-2 tir1afb245</i> -clubroot-inoculated
WT-non-inoculated	1									
WT-clubroot-inoculated	<0.0001	1								
<i>tir1afb2C</i> -non-inoculated	<0.0001	<0.0001	1							
<i>tir1afb2C</i> -clubroot-inoculated	<0.0001	<0.0001	0.0001	1						
<i>tir1afb245</i> -non-inoculated	<0.0001	<0.0001	0.0197	<0.0001	1					
<i>tir1afb245</i> -clubroot-inoculated	<0.0001	<0.0001	0.0308	0.0309	0.0001	1				
<i>PsAFB6/+ 4-8 tir1afb2</i> -non-inoculated	<0.0001	<0.0001	0.0009	0.4119	<0.0001	0.1615	1			
<i>PsAFB6/+ 4-8 tir1afb2</i> -clubroot-inoculated	<0.0001	0.0004	<0.0001	<0.0001	<0.0001	<0.0001	<0.0001	1		
<i>PsAFB6/+ 3-2 tir1afb245</i> -non-inoculated	0.0012	<0.0001	0.0001	<0.0001	0.0624	<0.0001	<0.0001	<0.0001	1	
<i>PsAFB6/+ 3-2 tir1afb245</i> -clubroot-inoculated	<0.0001	<0.0001	0.0853	0.0100	0.0002	0.6287	0.0640	<0.0001	<0.0001	1

Appendix Table B14. The probability (P), degrees of freedom and F values for the relative transcript abundance of *AtARF19* in the root tissue of 21 DAI seedlings for comparisons among treatments (non-inoculated and clubroot-inoculated) and lines (WT, *tir1afb2C*, *tir1afb245*, *PsAFB6/+ 4-8 tir1afb2*, and *PsAFB6/+ 3-2 tir1afb245*), and the treatment x line interaction using a two-way ANOVA analysis followed by mean separation using LSD post-hoc test (data presented in Figure 3.14C).

Gene name	Treatments		Lines		Treatment x Line	
	F value	Pr(>F)	F value	Pr(>F)	F value	Pr(>F)
<i>AtARF19</i>	1.9570	0.1720	39.2610	<0.0001	29.1540	<0.0001
Degrees of freedom	1		4		4	

LSD post-hoc test (P values)	WT-non-inoculated	WT-clubroot-inoculated	<i>tir1afb2C</i> -non-inoculated	<i>tir1afb2C</i> -clubroot-inoculated	<i>tir1afb245</i> -non-inoculated	<i>tir1afb245</i> -clubroot-inoculated	<i>PsAFB6/+ 4-8 tir1afb2</i> -non-inoculated	<i>PsAFB6/+ 4-8 tir1afb2</i> -clubroot-inoculated	<i>PsAFB6/+ 3-2 tir1afb245</i> -non-inoculated	<i>PsAFB6/+ 3-2 tir1afb245</i> -clubroot-inoculated
WT-non-inoculated	1									
WT-clubroot-inoculated	<0.0001	1								
<i>tir1afb2C</i> -non-inoculated	0.9266	<0.0001	1							
<i>tir1afb2C</i> -clubroot-inoculated	0.0083	<0.0001	0.0037	1						
<i>tir1afb245</i> -non-inoculated	0.7984	<0.0001	0.7076	0.0094	1					
<i>tir1afb245</i> -clubroot-inoculated	0.1461	<0.0001	0.1411	0.0001	0.0686	1				
<i>PsAFB6/+ 4-8 tir1afb2</i> -non-inoculated	0.3354	<0.0001	0.3462	0.0003	0.1918	0.5830	1			
<i>PsAFB6/+ 4-8 tir1afb2</i> -clubroot-inoculated	<0.0001	<0.0001	<0.0001	<0.0001	<0.0001	0.0001	<0.0001	1		
<i>PsAFB6/+ 3-2 tir1afb245</i> -non-inoculated	0.1110	<0.0001	0.0707	0.2088	0.1451	0.0020	0.0083	<0.0001	1	
<i>PsAFB6/+ 3-2 tir1afb245</i> -clubroot-inoculated	0.8285	<0.0001	0.8930	0.0026	0.6108	0.1790	0.4178	<0.0001	0.0536	1

Appendix Table B15. The probability (P), degrees of freedom and F values for the relative transcript abundance of *AtGH3.3* in the root tissue of 21 DAI seedlings for comparisons among treatments (non-inoculated and clubroot-inoculated) and lines (WT, *tir1afb2C*, *tir1afb245*, *PsAFB6/+ 4-8 tir1afb2*, and *PsAFB6/+ 3-2 tir1afb245*), and the treatment x line interaction using a two-way ANOVA analysis followed by mean separation using LSD post-hoc test (data presented in Figure 3.15A).

Gene name	Treatments		Lines		Treatment x Line	
	F value	Pr(>F)	F value	Pr(>F)	F value	Pr(>F)
<i>AtGH3.3</i>	9959.2300	<0.0001	80.0600	<0.0001	50.4400	<0.0001
Degrees of freedom	1		4		4	

LSD post-hoc test (P values)	WT-non-inoculated	WT-clubroot-inoculated	<i>tir1afb2C</i> -non-inoculated	<i>tir1afb2C</i> -clubroot-inoculated	<i>tir1afb245</i> -non-inoculated	<i>tir1afb245</i> -clubroot-inoculated	<i>PsAFB6/+ 4-8 tir1afb2</i> -non-inoculated	<i>PsAFB6/+ 4-8 tir1afb2</i> -clubroot-inoculated	<i>PsAFB6/+ 3-2 tir1afb245</i> -non-inoculated	<i>PsAFB6/+ 3-2 tir1afb245</i> -clubroot-inoculated
WT-non-inoculated	1									
WT-clubroot-inoculated	<0.0001	1								
<i>tir1afb2C</i> -non-inoculated	<0.0001	<0.0001	1							
<i>tir1afb2C</i> -clubroot-inoculated	<0.0001	0.0010	<0.0001	1						
<i>tir1afb245</i> -non-inoculated	0.0105	<0.0001	<0.0001	<0.0001	1					
<i>tir1afb245</i> -clubroot-inoculated	<0.0001	<0.0001	<0.0001	0.0073	<0.0001	1				
<i>PsAFB6/+ 4-8 tir1afb2</i> -non-inoculated	<0.0001	<0.0001	<0.0001	<0.0001	<0.0001	<0.0001	1			
<i>PsAFB6/+ 4-8 tir1afb2</i> -clubroot-inoculated	<0.0001	<0.0001	<0.0001	<0.0001	<0.0001	<0.0001	<0.0001	1		
<i>PsAFB6/+ 3-2 tir1afb245</i> -non-inoculated	0.0007	<0.0001	<0.0001	<0.0001	0.2683	<0.0001	<0.0001	<0.0001	1	
<i>PsAFB6/+ 3-2 tir1afb245</i> -clubroot-inoculated	<0.0001	<0.0001	<0.0001	<0.0001	<0.0001	0.0046	<0.0001	0.0032	<0.0001	1

Appendix Table B16. The probability (P), degrees of freedom and F values for the relative transcript abundance of *AtGH3.17* in the root tissue of 21 DAI seedlings for comparisons among treatments (non-inoculated and clubroot-inoculated) and lines (WT, *tir1afb2C*, *tir1afb245*, *PsAFB6/+ 4-8 tir1afb2*, and *PsAFB6/+ 3-2 tir1afb245*), and the treatment x line interaction using a two-way ANOVA analysis followed by mean separation using LSD post-hoc test (data presented in Figure 3.15B).

Gene name	Treatments		Lines		Treatment x Line	
	F value	Pr(>F)	F value	Pr(>F)	F value	Pr(>F)
<i>AtGH3.17</i>	7.0320	0.0128	112.0550	<0.0001	71.9080	<0.0001
Degrees of freedom	1		4		4	

LSD post-hoc test (P values)	WT-non-inoculated	WT-clubroot-inoculated	<i>tir1afb2C</i> -non-inoculated	<i>tir1afb2C</i> -clubroot-inoculated	<i>tir1afb245</i> -non-inoculated	<i>tir1afb245</i> -clubroot-inoculated	<i>PsAFB6/+ 4-8 tir1afb2</i> -non-inoculated	<i>PsAFB6/+ 4-8 tir1afb2</i> -clubroot-inoculated	<i>PsAFB6/+ 3-2 tir1afb245</i> -non-inoculated	<i>PsAFB6/+ 3-2 tir1afb245</i> -clubroot-inoculated
WT-non-inoculated	1									
WT-clubroot-inoculated	<0.0001	1								
<i>tir1afb2C</i> -non-inoculated	0.5477	<0.0001	1							
<i>tir1afb2C</i> -clubroot-inoculated	<0.0001	<0.0001	<0.0001	1						
<i>tir1afb245</i> -non-inoculated	<0.0001	0.0383	<0.0001	<0.0001	1					
<i>tir1afb245</i> -clubroot-inoculated	<0.0001	<0.0001	0.0001	0.0716	<0.0001	1				
<i>PsAFB6/+ 4-8 tir1afb2</i> -non-inoculated	0.8256	<0.0001	0.6798	<0.0001	<0.0001	<0.0001	1			
<i>PsAFB6/+ 4-8 tir1afb2</i> -clubroot-inoculated	0.1236	<0.0001	0.0247	<0.0001	<0.0001	<0.0001	0.0605	1		
<i>PsAFB6/+ 3-2 tir1afb245</i> -non-inoculated	<0.0001	0.7374	<0.0001	<0.0001	0.0180	<0.0001	<0.0001	<0.0001	1	
<i>PsAFB6/+ 3-2 tir1afb245</i> -clubroot-inoculated	<0.0001	0.5249	<0.0001	<0.0001	0.0087	<0.0001	<0.0001	<0.0001	0.7624	1

Appendix Table B17. The probability (P), degrees of freedom and F values for the relative transcript abundance of *AtICS1* in the root tissue of 21 DAI seedlings for comparisons among treatments (non-inoculated and clubroot-inoculated) and lines (WT, *tir1afb2C*, *tir1afb245*, *PsAFB6/+ 4-8 tir1afb2*, and *PsAFB6/+ 3-2 tir1afb245*), and the treatment x line interaction using a two-way ANOVA analysis followed by mean separation using LSD post-hoc test (data presented in Figure 3.16A).

Gene name	Treatments		Lines		Treatment x Line	
	F value	Pr(>F)	F value	Pr(>F)	F value	Pr(>F)
<i>AtICS1</i>	220.3800	<0.0001	21.5400	<0.0001	29.0000	<0.0001
Degrees of freedom	1		4		4	

LSD post-hoc test (P values)	WT-non-inoculated	WT-clubroot-inoculated	<i>tir1afb2C</i> -non-inoculated	<i>tir1afb2C</i> -clubroot-inoculated	<i>tir1afb245</i> -non-inoculated	<i>tir1afb245</i> -clubroot-inoculated	<i>PsAFB6/+ 4-8 tir1afb2</i> -non-inoculated	<i>PsAFB6/+ 4-8 tir1afb2</i> -clubroot-inoculated	<i>PsAFB6/+ 3-2 tir1afb245</i> -non-inoculated	<i>PsAFB6/+ 3-2 tir1afb245</i> -clubroot-inoculated
WT-non-inoculated	1									
WT-clubroot-inoculated	0.0422	1								
<i>tir1afb2C</i> -non-inoculated	<0.0001	0.0013	1							
<i>tir1afb2C</i> -clubroot-inoculated	0.0671	0.8114	0.0007	1						
<i>tir1afb245</i> -non-inoculated	<0.0001	<0.0001	0.0001	<0.0001	1					
<i>tir1afb245</i> -clubroot-inoculated	0.1050	0.6290	0.0004	0.8062	<0.0001	1				
<i>PsAFB6/+ 4-8 tir1afb2</i> -non-inoculated	<0.0001	0.0003	0.6140	0.0002	0.0002	0.0001	1			
<i>PsAFB6/+ 4-8 tir1afb2</i> -clubroot-inoculated	0.0001	<0.0001	<0.0001	<0.0001	<0.0001	<0.0001	<0.0001	1		
<i>PsAFB6/+ 3-2 tir1afb245</i> -non-inoculated	<0.0001	<0.0001	<0.0001	<0.0001	0.7573	<0.0001	0.0001	<0.0001	1	
<i>PsAFB6/+ 3-2 tir1afb245</i> -clubroot-inoculated	0.7340	0.0640	<0.0001	0.1028	<0.0001	0.1614	<0.0001	<0.0001	<0.0001	1

Appendix Table B18. The probability (P), degrees of freedom and F values for the relative transcript abundance of *AtPR5* in the root tissue of 21 DAI seedlings for comparisons among treatments (non-inoculated and clubroot-inoculated) and lines (WT, *tir1afb2C*, *tir1afb245*, *PsAFB6/+ 4-8 tir1afb2*, and *PsAFB6/+ 3-2 tir1afb245*), and the treatment x line interaction using a two-way ANOVA analysis followed by mean separation using LSD post-hoc test (data presented in Figure 3.16B).

Gene name	Treatments		Lines		Treatment x Line	
	F value	Pr(>F)	F value	Pr(>F)	F value	Pr(>F)
<i>AtPR5</i>	39.5450	<0.0001	4.5490	0.0057	2.0430	0.1145
Degrees of freedom	1		4		4	

LSD post-hoc test (P values)	WT-non-inoculated	WT-clubroot-inoculated	<i>tir1afb2C</i> -non-inoculated	<i>tir1afb2C</i> -clubroot-inoculated	<i>tir1afb245</i> -non-inoculated	<i>tir1afb245</i> -clubroot-inoculated	<i>PsAFB6/+ 4-8 tir1afb2</i> -non-inoculated	<i>PsAFB6/+ 4-8 tir1afb2</i> -clubroot-inoculated	<i>PsAFB6/+ 3-2 tir1afb245</i> -non-inoculated	<i>PsAFB6/+ 3-2 tir1afb245</i> -clubroot-inoculated
WT-non-inoculated	1									
WT-clubroot-inoculated	0.8326	1								
<i>tir1afb2C</i> -non-inoculated	0.2847	0.1698	1							
<i>tir1afb2C</i> -clubroot-inoculated	0.0478	0.0548	0.0019	1						
<i>tir1afb245</i> -non-inoculated	0.0009	0.0002	0.0082	<0.0001	1					
<i>tir1afb245</i> -clubroot-inoculated	0.6376	0.4625	0.5124	0.0103	0.0015	1				
<i>PsAFB6/+ 4-8 tir1afb2</i> -non-inoculated	0.0494	0.0208	0.3081	0.0001	0.0821	0.0997	1			
<i>PsAFB6/+ 4-8 tir1afb2</i> -clubroot-inoculated	0.7956	0.9589	0.1551	0.0610	0.0002	0.4322	0.0184	1		
<i>PsAFB6/+ 3-2 tir1afb245</i> -non-inoculated	0.0059	0.0018	0.0513	<0.0001	0.4271	0.0116	0.3278	0.0016	1	
<i>PsAFB6/+ 3-2 tir1afb245</i> -clubroot-inoculated	0.4441	0.5482	0.0532	0.1740	<0.0001	0.1868	0.0048	0.5827	0.0004	1